Exxon Valdez Oil Spill
Restoration Project Final Report

2004-2005 LTEMP Oil Monitoring Report
Restoration Project 040724

James R. Payne, Ph.D.
Payne Environmental Consultants, Inc.
1991 Village Park Way, Suite 206 B
Encinitas, CA 92024
760-942-1015
jrpayne@sbcglobal.net

William B. Driskell
6536 20th Avenue NE
Seattle, WA 98115
206-522-5930
bdriskell@comcast.net

Jeffrey W. Short, Ph.D. and Marie L. Larsen
NOAA/NMFS Auke Bay Laboratory
11305 Glacier Highway
Juneau, AK 99801
907-789-6065
jeff.short@noaa.gov
Marie.Larsen@noaa.gov

Prepared for
Lisa Ka'aihue
Project Manager
Prince William Sound Regional Citizens' Advisory Council
3709 Spenard Road
Anchorage, Alaska 99503
907/277-7222 or 273-6225
kaaihue@pwsrcac.org

November 2006

Exxon Valdez Oil Spill
Restoration Project Final Report

2004-2005 LTEMP Oil Monitoring Report
Restoration Project 040724

James R. Payne, Ph.D.
Payne Environmental Consultants, Inc.
1991 Village Park Way, Suite 206 B
Encinitas, CA 92024
760-942-1015
jrpayne@sbcglobal.net

William B. Driskell
6536 20th Avenue NE
Seattle, WA 98115
206-522-5930
bdriskell@comcast.net

Jeffrey W. Short, Ph.D. and Marie L. Larsen
NOAA/NMFS Auke Bay Laboratory
11305 Glacier Highway
Juneau, AK 99801
907-789-6065
jeff.short@noaa.gov
Marie.Larsen@noaa.gov

Prepared for
Lisa Ka'aihue
Project Manager
Prince William Sound Regional Citizens' Advisory Council
3709 Spenard Road
Anchorage, Alaska 99503
907/277-7222 or 273-6225
kaaihue@pwsrcac.org

November 2006

2nd cover page

Study History

Preceding EVOS Trustees Restoration Project 040724, the Long Term Environmental Monitoring Program (LTEMP) began in 1993 as a mandate in the charter of the Prince William Sound Regional Citizen's Advisory Council (PWS RCAC). Aspects of the monitoring program have changed through the years, but mussel tissues are still being sampled biannually at ten fixed locations in Port Valdez, Prince William Sound, and along the outer coast from Seward to Kodiak in addition to subtidal sediments from two sites within Port Valdez. In 2004, joint funding was acquired from the Trustees along with an expansion in program objectives in 2005/2006 to include sampling at random locations of EVOS impact (in addition to the original ten fixed LTEMP sites) to assess lingering oil and exploration of human habitation sites and extent of Monterey formation residues (from the 1964 earthquake). Annual reports, datasets, and program reviews can be obtained from the PWS RCAC with the most recent publications available on their website, *www.pwsrcac.org.*

Abstract

The Long Term Environmental Monitoring Program (LTEMP) has been sampling mussels (and some sediments) twice annually at ten sites in Port Valdez, Prince William Sound, and nearby Gulf of Alaska sites since 1993. Samples are analyzed primarily for polycyclic aromatic and saturated hydrocarbons (PAH and SHC). New indices have been developed to quantify the proportions of a hydrocarbon signal into dissolved, particulate/oil, and pyrogenic phases. After 1999, a decreasing trend appears in total PAH (TPAH) with current values below 100 ng/g dry weight (and many below 50 ng/g). Most currently measured samples reflect a predominantly dissolved-phase signal. This new low in TPAH likely represents ambient background levels. Furthermore, peaks and lows in total PAH trends and the similarities of the hydrocarbon signatures portray regional-scale dynamics. The five inner Prince William Sound sites have similar composition and behave similarly and yet are different from the three Gulf of Alaska sites. The two Port Valdez sites are primarily influenced by the treated ballast water discharge from the Alyeska Marine Terminal. An unreported diesel spill was detected in 2004 at Gold Creek, Port Valdez.

Key Words

Alaska
Exxon Valdez oil spill
oil monitoring
PAH
Prince William Sound
Northern Gulf of Alaska
intertidal
marine
Mytilus trossulus
sediments
hydrocarbon chemistry

Project data

Current and historical data for this program are maintained by the PWS RCAC LTEMP contractors and supplied along with metadata to the EVOS Trustees. Annual reports and the data are available on request and generally carried on the website, *www.pwsrcac.org*.

Citation

Payne, James R., William B. Driskell, Jeffrey W. Short, Marie L. Larsen 2006. 2004-2005 LTEMP Oil Monitoring Report, Exxon Valdez Oil Spill Restoration Project Final Report (Restoration Project 040724), Prince William Sound Regional Citizen's Advisory Council, Anchorage, Alaska. 149 pp.

PRINCE WILLIAM SOUND RCAC
LONG-TERM ENVIRONMENTAL MONITORING PROGRAM

2004-2005 LTEMP Monitoring Report

Photo by William Driskell, 2004

James R. Payne, Ph.D.

William B. Driskell

Jeffrey W. Short, Ph.D.

Marie L. Larsen

November 2006

PWSRCAC Contract 951.05.1

TABLE OF CONTENTS

LIST OF FIGURES

LIST OF TABLES

LIST OF ABBREVIATIONS

Stations:

AMT	Alyeska Marine Terminal, Port Valdez
AIB	Aialik Bay, west of Seward
DII	Disk Island, Knight Island Group, western PWS
GOC	Gold Creek, Port Valdez
KNH	Knowles Head, eastern PWS
SHB	Sheep Bay, eastern PWS
SHH	Shuyak Harbor, Kodiak
SLB	Sleepy Bay, LaTouche Island, western PWS
WIB	Windy Bay, Outer Kenai Peninsula
ZAB	Zaikof Bay, Montague Island, central PWS

ABL	NOAA/NMFS Auke Bay Laboratory, Juneau AK
AHC	aliphatic hydrocarbons
ANS	Alaskan North Slope
BWTF	Alyeska Terminal's Ballast Water Treatment Facility
DSI	Dissolved Signal Index
EVOS	*Exxon Valdez* oil spill
EVTHD	*Exxon Valdez* Trustees Hydrocarbon Database
EMAP	US EPA Environmental Monitoring and Assessment Program
FFPI	fossil fuel pollution index
GC/FID	gas chromatography/flame ionization detector
GC/MS	gas chromatography/mass spectrometry
GERG	Geochemical and Environmental Research Group, Texas A&M
HAZMAT	NOAA Hazardous Materials Response Branch (now Office of Response and Restoration (OR&R) – Emergency Response Division (ERD)
KLI	Kinnetic Laboratories, Inc., Anchorage AK
MDL	analytic method detection limit
NIST	National Institute of Standards and Technology
NMFS	National Marine Fisheries Service
NOAA	National Oceanographic and Atmospheric Administration
PAH	polycyclic (or polynuclear) aromatic hydrocarbons
PECI	Payne Environmental Consultants, Inc., Encinitas, CA
PGS	particle grain size
PSI	Particulate Signal Index
PWS	Prince William Sound
SHC	saturated hydrocarbons (same as AHC: n-alkanes + pristane and phytane)
SIM	selected ion monitoring
SRM	NIST standard reference material
TAHC	total AHC
TALK	total n-alkanes
TIC	total inorganic carbon
TOC	total organic carbon
TPAH	total PAH
TSHC	total saturated hydrocarbons (same as TALK)
UCM	unresolved complex mixture

1 Executive Summary

Readers unfamiliar with hydrocarbon chemistry may refer to Appendix A for a primer on basic hydrocarbon chemistry, weathering patterns, and using mussels as indicator organisms.

In this, the twelfth year of the LTEMP monitoring program, our approach to evaluating the new and historic data has taken an interesting turn. While working on a review of EVOS chemistry data for the NOAA HAZMAT group, new methods were developed for quantifying the dissolved- and particulate-oil phase of an oil signature (from the profile plot of measured analytes). With a bit more refinement, we were able to apply these methods to LTEMP data and noticed for the first time that the nearly synchronous rise and fall of total polycyclic aromatic hydrocarbons (TPAH) in LTEMP stations was also being reflected by changes in the separate-phase components. In brief, we found that while TPAH is decreasing at all locations to unprecedented low levels (in LTEMP data), the relative proportion from soluble-phase constituents is increasing, and regional trends have begun to appear.

One of the factors that has confounded our interpretations in the past has been the issue of how to use the lower-concentration pre-1997 data from the more pristine sites. Often these data are not comparable with data generated by newer instrumentation and modern standards, and many early results definitely included laboratory procedural artifacts. In addition, there were unexpected TPAH peaks between 1997 and 2001, which also had credibility issues. Once again, we delved into the details of each individual LTEMP sample (n=886) and concluded that many of the early (1993-1997) low-level data should, for our purposes, be ignored rather than propagating further misinterpretations. For this report, adjustments were made where appropriate and the unusable data are graphically distinguished from useful data. On a positive note, we have now concluded that the previously-questioned, post-1997 series of peaks in TPAH concentrations actually show unique regional patterns that are both credible and add significant information to the interpretations.

From these filtered results, the data since 1999 are tracking a trend of decreasing TPAH outside of Port Valdez. Most stations are now showing *Mytilus* tissues with less than 100 ng/g TPAH (many less than 50 ng/g) and mostly as a dissolved–phase hydrocarbon signal from an unknown source(s). The synchrony of TPAH highs and lows plus the similarity of signatures also tell us that the inner Prince William Sound sites are collectively experiencing one low-level source of hydrocarbons while the outer coastal stations are exposed to different sources. The two Port Valdez stations, being mainly influenced by the treated ballast water discharge from the Alyeska Marine Terminal, are independent of the trends at the regional sites.

One significant event this year was detecting an unreported diesel spill at Gold Creek within Port Valdez. Monitoring works again! Mussels at the site were contaminated by diesel fuel sometime in late summer 2004 with residues still detected at the site in March 2005. At the Alyeska Terminal site, conditions are improving; after a prior two-year

plateau at already low TPAH levels, subtidal sediments have dropped to even lower levels but still show the weathered ballast oil signature. Mussel tissues at the Terminal have dropped and then maintained steady concentrations within a range of 55-70 ng/g of the weathered ballast-water signature for the last three years. These trends most likely reflect the decreased ballast-water throughput from the facility (currently down to 9 million gallons/day) as double-hulled tankers (carrying segregated ballast not requiring treatment) come into use and Alaska North Slope crude oil flow through the pipeline drops in volume.

In summary, the LTEMP program is in a very interesting phase; most stations are showing extremely clean results. Using the current highly-sensitive methods, even slight deviations in what now appear to be the ambient background amounts of hydrocarbons can be detected, fingerprinted, and perhaps identified to source. For example, at the current levels of sensitivity and under near-pristine conditions, the Gold Creek diesel spill appears as a monumental spike in the trend line, a jump from 42 to 835 ng/g and a shift to a strongly particulate/oil-phase signal. For perspective, in some urban harbors, this spike would barely rise above background levels. And then there is the background signal itself; what is the source(s) and what drives the regional similarities, and what oceanographic–scale process would make them all peak and fall together?

2 Introduction

The primary objective of the ongoing Long-Term Environmental Monitoring Program (LTEMP) is to collect "…standardized measurements of hydrocarbon background in the EVOS region as long as oil flows through the pipeline." Under Federal and State statutes, the unregulated release of oil into the environment is strictly prohibited; the LTEMP data serve as a sentinel indicator and independent quality control check for Alyeska Marine Terminal and tanker operations throughout the region.

Currently measured variables include polycyclic (or polynuclear) aromatic and saturated (or aliphatic) hydrocarbon levels (PAH and SHC) in mussel (*Mytilus trossulus*) tissues from ten stations between Valdez and Kodiak and sediments from two stations in Port Valdez. The Port Valdez sediment samples are also analyzed for particle grain size and total organic carbon content. Sampling and analytical methods are patterned after the protocols developed by the National Oceanic and Atmospheric Administration (NOAA) Status and Trends Mussel Watch Program as fully detailed in the annual Monitoring Reports prepared by Kinnetic Laboratories, Inc. (KLI) and the Geochemical and Environmental Research Group (GERG).

With the program's inception in 1993, LTEMP samples were collected by KLI and analyzed by GERG. In 1998, the LTEMP results were reviewed in a synthesis paper (Payne et al. 1998) covering the 1993-97 results. At that time, background oil levels were higher, hot spots were identified, large and small spill events were visible in the data set, and identification of weathered sources was important. The authors of the 1998 review recommended several changes to the existing program at that time, including:

- adjusting the sampling plan to include more sites,
- modifying the statistical criteria,
- adding intertidal sediment samples,
- rectifying method detection limit (MDL) problems in the laboratory analyses,
- paying closer attention to field and procedural blank contamination problems,
- reinstating aliphatic hydrocarbon analyses in mussel tissue samples,
- tightening field sample procedures regarding sampling depth and mussel size,
- dropping lipid corrections, seasonal sampling, and unnecessary shell measurements from the mussel sampling, and
- sampling and analyzing potential background sources with common laboratory methods.

The PWSRCAC subsequently made several changes reducing the scope of the program and resulting in the current biannual sampling program of regional mussel tissues and Port Valdez sediments. In recent years, in addition to the early spring and mid-summer samplings, another set of mussel samples, taken in the fall just in Port Valdez (Alyeska Marine Terminal and Gold Creek), was added to the sample design. Analyses of aliphatic hydrocarbons in mussel tissues, dropped from the original program in 1995 due to results confounded from lipid interference, were reinstated in 1998.

In 2001, another data evaluation and synthesis review was completed on just the LTEMP results from the Port Valdez sites (Payne et al., 2001). Review of the data from Alyeska Marine Terminal and the Gold Creek control site suggested Alaska North Slope (ANS) crude oil residues from the terminal's ballast water treatment facility (BWTF) had accumulated in the intertidal mussels within the port. Payne et al. (2001) concluded, however, that the PAH and SHC levels measured in sediments and mussel tissues (and the estimated water-column levels) were very low and unlikely to cause deleterious effects. From the signature of analytes, however, they were able to discriminate between particulate- (oil droplet) and dissolved-phase signals in the water column and then correlate those signals with seasonal uptake of hydrocarbons in mussels and with absorption in herring eggs (from other studies). These findings give new insight into the transport and exposure pathways in Port Valdez. The results also suggested a surface microlayer mechanism may be responsible for seasonal transport of ANS weathered oil residues from the BWTF diffuser to intertidal zones to the north and west of the terminal. Payne et al. (2001) concluded that the possibility of concentrated contaminants in a surface microlayer combined with the potential for photo-enhanced toxicity should be considered in future investigations of potential impacts in Port Valdez.

In July 2002, Payne Environmental Consultants, Inc (PECI) and the NOAA/NMFS Auke Bay Laboratory (ABL) began conducting the Long Term Environmental Monitoring Program. Detailed discussions of the 2002/2003 LTEMP samples and interlaboratory comparisons of split samples and Standard Reference Materials (SRMs) supplied by the National Institute of Standards and Technology (NIST) analyzed by both GERG and ABL are presented in Payne et al. (2003a). The results from the 2003/2004 LTEMP and a comprehensive review and synthesis of all analyses completed since the beginning of the program are available in Payne et al. (2005a).

3 Objectives

This report examines the 2004/2005 samples and trend analyses of over 748 tissue and 138 sediment samples collected historically within Prince William Sound and the surrounding region (Figure 1) in addition to the laboratory quality control results. The report also contains the results of intertidal sediment and mussel samples collected after a May 2004 diesel fuel spill in Jack Bay (Figure 1), located outside of Port Valdez (Appendix D). Where possible, this year's report also compares the LTEMP results with those from related studies, chiefly, Alyeska's Environmental Monitoring Program (EMP) (Blanchard et al. 2005), 2002 regional Environmental Protection Agency EMAP data, and the results of detailed investigations of the biodegradation of PAH and SHC of treated ballast water discharged into Port Valdez by the Alyeska Marine Terminal BWTF (Payne et al., 2005b,c).

4 Methods

4.1 Sampling Design

For both the tissue and sediment collections, the current sample design followed the previous years' efforts (KLI 2002) with slight modifications. As noted above, mussel

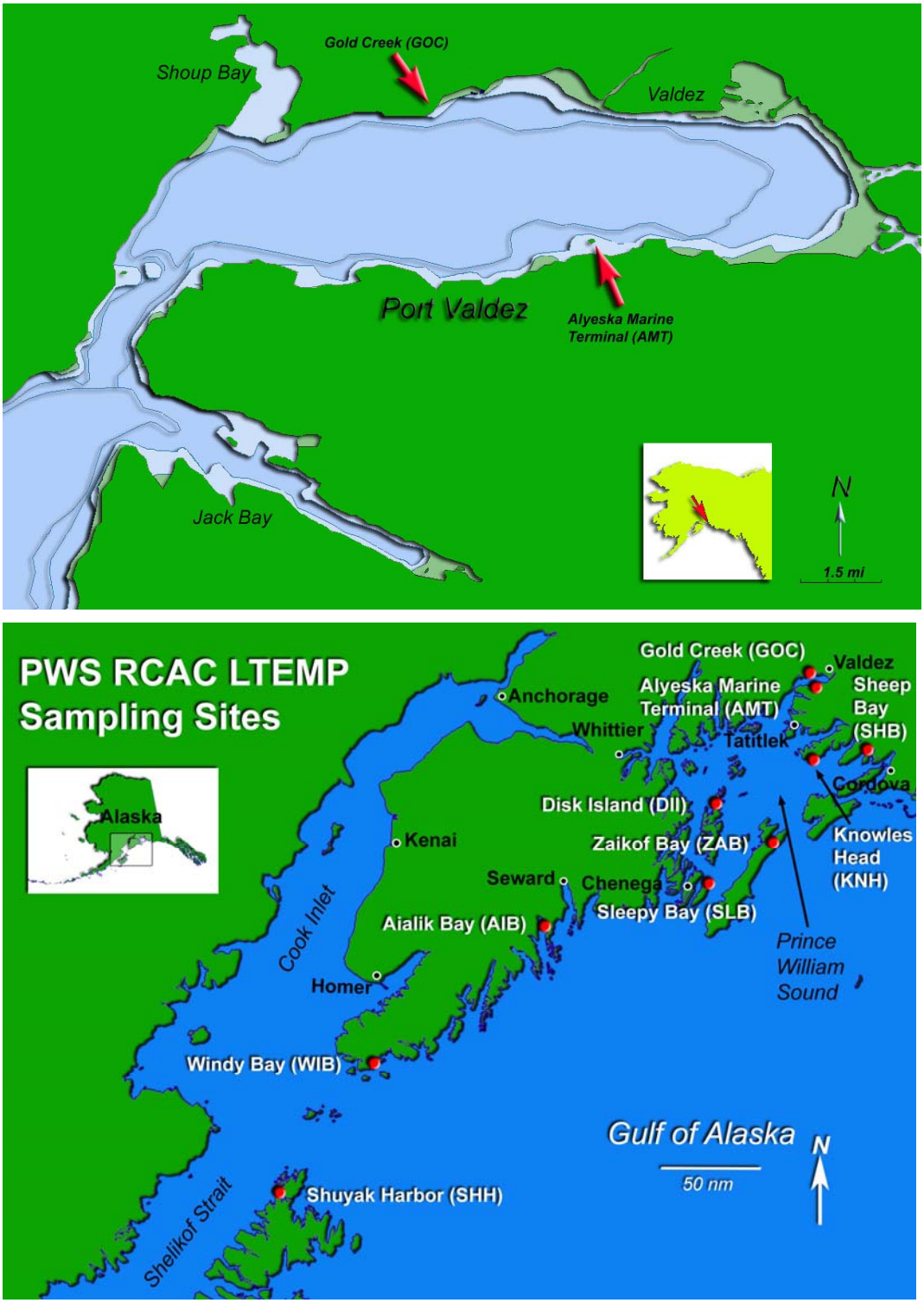

Figure 1 Map of LTEMP sites with close-up of Port Valdez.

tissues are sampled at ten sites and sediments from two sites in Port Valdez on a biannual basis (March-April and July-August) (lower Figure 1). Mussel tissues are also collected from the two Port Valdez sites in October (upper Figure 1).

For tissues, three replicates were typically taken from random locations between the transect end-markers at each site. At Sleepy Bay, the absence of mussels along portions of the transect necessitated off-transect sampling. Each replicate of 25-30 mussels was collected by hand using Nitrile gloves, wrapped in aluminum foil, Ziplock® bagged, labeled, double-bagged and kept chilled until reaching the nearest freezer. The collection site was photographed and GPS coordinates recorded for chain-of-custody documentation. The entire trip collection was eventually air-freighted frozen to the NOAA/NMFS Auke Bay Laboratory in Juneau.

Subtidal sediments were collected from the *M/V Auklet* support vessel using a modified Van Veen grab sampler, i.e., the standard pincer-jawed, bucket grab augmented with an encircling stabilization frame to ensure vertical penetration. Upon retrieval, only the top centimeter of undisturbed sediment was collected from the center of each sample (away from the edges of the grab), scooping with a pre-cleaned spoon into a sterile, contaminant-free, glass jar. An additional sample was also taken from each grab for particle-grain-size analysis. Water depth and GPS location were recorded for each sample. Prior to sampling at each station, the grab was scrubbed with Alconox® detergent, rinsed with a previously tested, seawater deck hose, dunked overboard, and the drippings collected as a rinsate blank. The deck hose was also used for rinsing the grab between samples. The sediment samples are immediately frozen onboard and eventually air-freighted to Auke Bay Laboratory in Juneau.

A combination of vessel and float plane is used to access the sampling sites (Table 1). Typically, during PECI field efforts, the *M/V Auklet* is used for the Port Valdez and Knowles Head stations and a float plane to sample all other sites.

Table 1. LTEMP Stations 2004-2005.

Station Location	Station Code	Sample Type	Sampling Date	Average Station Depth	Global Positioning System (GPS) Coordinates Latitude (N)	Longitude (W)
Aialik Bay	AIB-B	Intertidal Mussel	7/30/04		59° 52.786'	149° 39.467'
			3/7/05		59° 52.785'	149° 39.462'
Alyeska Marine Terminal	AMT-B	Intertidal Mussel	7/28/04		61° 5.445'	146° 24.381'
			10/13/04		61° 5.499'	146° 24.382'
			3/4/05		61° 5.449'	146° 23.381'
	AMT-S	Subtidal Sediment	7/28/04	68.3 m	61° 5.400'	146°23.673'
			3/4/05	67.8 m	61° 5.429'	146°23.558'
Disk Island	DII-B	Intertidal Mussel	7/30/04		60° 29.937'	147° 39.515'
			3/7/05		60° 29.938'	147° 39.510'
Gold Creek	GOC-B	Intertidal Mussel	7/28/04		61° 7.472'	146° 29.651'
			10/13/04		61° 7.441'	146° 29.649'
			3/4/05		61° 7.454'	146° 29.763'
	GOC-S	Subtidal Sediment	7/28/04	30.9 m	61° 7.455'	146°29.591'
			3/4/05	31.5 m	61° 7.468'	146°29.469'

Knowles Head	KNH-B	Intertidal Mussel	7/29/04 3/14/05	60° 41.469' 60° 41.472'	146° 35.011' 146° 35.017'
Sheep Bay	SHB-B	Intertidal Mussel	7/29/04 3/14/05	60° 38.795' 60° 38.795'	145° 59.726' 145° 59.772'
Shuyak Harbor	SHH-B	Intertidal Mussel	8/1/04 3/15/05	58° 30.123' 58° 30.125'	152° 37.520' 152° 37.521'
Sleepy Bay	SLB-B	Intertidal Mussel	7/30/04 3/17/05	60° 4.071' 60° 4.082'	147° 49.997' 147° 49.861'
Windy Bay	WIB-B	Intertidal Mussel	8/1/04 3/15/05	59° 13.136 59° 13.133'	151° 31.102' 151° 31.000'
Zaikof Bay	ZAB-B	Intertidal Mussel	7/30/04 3/7/05	60° 15.942' 60° 15.943'	147° 4.997' 147° 4.994'

4.2 Analytic Methods

Sediment samples (50 g wet weight) or mussel samples (10 g wet weight) were spiked with a suite of 5 aliphatic and 6 aromatic perdeuterated hydrocarbon surrogate standards (identified in Table 2) and then extracted with dichloromethane at 100°C and 2,000 psi for 10 min in a Dionex ASE 200 accelerated solvent extractor. The dichloromethane solutions were exchanged with hexane over steam, and separated into aliphatic and aromatic fractions by column chromatography (10 g 2%-deactivated alumina over 20 g 5%-deactivated silica gel; columns for sediments also contained 20 g granular elemental copper and 8 g anhydrous sodium sulfate for removal of sulfur and water, respectively). Aliphatics eluting with 50 mL pentane were analyzed by gas chromatography with a flame ionization detector (GC/FID) following concentration to ~ 1 mL hexane over steam and addition of dodecylcyclohexane as an internal standard to evaluate recoveries of the surrogate standards. PAH constituents from the sample extracts were further purified by gel-permeation high performance liquid chromatography (HPLC). The injection volume was 0.5 mL into dichloromethane flowing at 7 mL/min through two size-exclusion gel columns (Phenomenex, phenogel, 22.5 mm x 250 mm, 100 Å pore size) connected sequentially. The initial 110 mL eluate was discarded, and the following 50 mL was concentrated over a 60–70^{o} C water bath and exchanged with hexane to a final volume of *ca*. 1 mL, then spiked with hexamethylbenzene as an internal standard for estimating recoveries of the initially added perdeuterated aromatic hydrocarbon surrogate standards.

PAHs in extracts were separated and analyzed with a Hewlett-Packard 6890 gas chromatograph equipped with a 5973 mass selective detector (MSD). The injection volume was 1 µL into a splitless injection port at 300° C. The initial oven temperature was 60° C, increasing at 10° C per minute immediately following injection to a final temperature of 300° C, then held for 12 min. The chromatographic column was a 25 m fused silica capillary (0.20 mm ID) coated with 5% phenyl methyl silicone. The helium carrier gas was maintained at 70 kPa inlet pressure. The gas chromatographic column was eluted into the 70 eV electron impact MSD through a 240° C transfer line. The ionizer temperature and pressure were 240° C and 10^{-5} torr, respectively. The MSD was

Table 2. Polycyclic aromatic hydrocarbon (PAH) and saturated hydrocarbon (SHC) analytes measured in this study, along with analyte abbreviations, internal and surrogate standards.

Analytes	Abbreviation	Internal Standard	Surrogate Standard
PAH			
Naphthalene	N	A	1
C1-Naphthalene	N1	A	1
C2-Naphthalene	N2	A	2
C3-Naphthalene	N3	A	2
C4-Naphthalene	N4	A	2
Biphenyl	BI	A	2
Acenaphthylene	AC	A	2
Acenaphthene	AE	A	2
Fluorene	F	A	2
C1-Fluorenes	F1	A	2
C2-Fluorenes	F2	A	2
C3-Fluorenes	F3	A	2
Dibenzothiophene	D	A	3
C1-Dibenzothiophene	D1	A	3
C2-Dibenzothiophene	D2	A	3
C3-Dibenzothiophene	D3	A	3
C4-Dibenzothiophene	D4	A	3
Anthracene	A	A	3
Phenanthrene	P	A	3
C1-Phenanthrene/Anthracene	P/A1	A	3
C2-Phenanthrene/Anthracene	P/A2	A	3
C3-Phenanthrene/Anthracene	P/A3	A	3
C4-Phenanthrene/Anthracene	P/A4	A	3
Fluoranthene	FL	A	3
Pyrene	PYR	A	3
C1-Fluoranthene/Pyrene	F/P1	A	3
C2-Fluoranthene/Pyrene	F/P2	A	3
C3-Fluoranthene/Pyrene	F/P3	A	3
C4-Fluoranthene/Pyrene	F/P4	A	3
Benzo(a)Anthracene	BA	A	4
Chrysene	C	A	4
C1-Chrysenes	C1	A	4
C2-Chrysenes	C2	A	4
C3-Chrysenes	C3	A	4
C4-Chrysenes	C4	A	4
Benzo(b)fluoranthene	BB	A	5
Benzo(k)fluoranthene	BK	A	5
Benzo(e)pyrene	BEP	A	5
Benzo(a)pyrene	BAP	A	5
Perylene	PER	A	6
Indeno(1,2,3-cd)pyrene	IP	A	5

Dibenzo(a,h)anthracene	DA	A	5
Benzo(g,h,i)perylene	BP	A	5
Total PAH	TPAH		5

n-Alkanes

n-Decane	C10	B	7
n-Undecane	C11	B	7
n-Dodecane	C12	B	7
n-Tridecane	C13	B	7
n-Tetradecane	C14	B	8
n-Pentadecane	C15	B	8
n-Hexadecane	C16	B	8
n-Heptadecane	C17	B	8
Pristane	Pristane	B	8
n-Octadecane	C18	B	9
Phytane	Phytane	B	9
n-Nonadecane	C19	B	9
n-Eicosane	C20	B	9
n-Heneicosane	C21	B	9
n-Docosane	C22	B	10
n-Tricosane	C23	B	10
n-Tetracosane	C24	B	10
n-Pentacosane	C25	B	10
n-Hexacosane	C26	B	10
n-Heptacosane	C27	B	10
n-Octacosane	C28	B	10
n-Nonacosane	C29	B	11
n-Triacontane	C30	B	11
n-Hentriacontane	C31	B	11
n-Dotriacontane	C32	B	11
n-Tritriacontane	C33	B	11
n-Tetratriacontane	C34	B	11
Total n-Alkanes	TALK		

Calibrated analytes are identified by boldface. Internal standards:
A = hexamethylbenzene; B = dodecylcyclohexane.
Surrogate standards: 1 = naphthalene-d8, 2 = acenaphthene-d10,
3 = phenanthrene-d10, 4 = chrysene-d12, 5 = benzo[a]pyrene-d12,
6 = perylene-d12, 7 = dodecane-d26, 8 = hexadecane-d34, 9 = eicosane-d42,
10 = tetracosane-d50, and 11 = triacontane-d62.

operated in the selected-ion-monitoring (SIM) mode. The MSD was tuned with mass 69, 102, and 512 fragments of perfluorotributylamine before each batch of samples was analyzed.

Calibrated PAHs were identified based on retention time and ratio of two mass fragment ions characteristic of each hydrocarbon. Calibrated PAHs are identified by bold typeface in Table 2, and include dibenzothiophene and the aromatic hydrocarbons in SRMs

supplied by NIST. Chromatographic peaks were identified as a calibrated aromatic hydrocarbon if both ions were co-detected at retention times within ±0.15 minutes (9 seconds) of the mean retention time of the hydrocarbon in the calibration standards, and if the ratio of the confirmation ion to the quantification ion was within ±30% of the expected ratio.

Uncalibrated PAHs include the alkyl-substituted isomers of naphthalene (except the 1- and 2-methyl-substituted homologues), fluorene, dibenzothiophene, phenanthrene/ anthracene, fluoranthene/pyrene, and chrysene (Table 2). Uncalibrated PAHs were identified by the presence, within a relatively wide retention time window, of a single mass fragment ion that is characteristic of the uncalibrated PAH sought. Wider retention time windows were necessary for the uncalibrated PAH because of the range of retention times of the various isomers that are included in an uncalibrated PAH homologue grouping (e.g. C3-phenanthrene).

Concentrations of calibrated PAHs in extracts were estimated by a method employing multiple internal standards and a five-point calibration curve for each calibrated PAH. The deuterated surrogate standards that were initially spiked into each sample are treated as internal standards, where each surrogate compound is associated with one or more calibrated PAHs (see Table 2). A calibration curve for each calibrated PAH and batch of samples analyzed was based on five different hexane dilutions of the PAH standard run before each sample batch or "laboratory string." Each calibration curve was derived from linear regression of (1) the ratio of MSD/SIM quantification ion response of the calibrated PAH and the associated deuterated surrogate standard and (2) the ratio of the amount of calibrated PAH and the amount of deuterated surrogate in the calibration standards. This approach effectively means that all reported analytes are corrected for the appropriate surrogate recoveries.

Concentrations of uncalibrated PAHs in extracts were determined with calibration curves and procedures for the most similar calibrated PAH. The MSD/SIM response to the quantification ion of each uncalibrated PAH homologue isomer were summed; this sum was used in place of the calibrated PAH response in the procedure described above for calculating concentrations of calibrated PAHs. For example, the fluorene calibration curve and procedure was used for all the alkyl-substituted fluorenes identified, but 2,6-dimethylnaphthalene, 2,3,5-trimethylnaphthalene and 1-methylphenanthrene calibration curves were used for C2-naphthalenes, C3-naphthalenes, and for all the alkyl-substituted phenanthrenes, respectively.

Alkanes in extracts were separated and analyzed with a Hewlett-Packard 5890 gas chromatograph equipped with a flame ionization detector (FID). The injection volume was 1 µL into a splitless injection port at 300° C. The 60° C initial oven temperature was maintained for 1 minute, then increased at 6° C per minute to a final temperature of 300° C, then held for 25 min. The detector temperature was 320° C. The chromatographic column was the same as that used for PAH analysis (see above). The helium carrier gas flow rate was 0.80-2.0 mL per minute, and the column effluent was combined with 34 mL per minute nitrogen make-up gas before entering the FID. The

FID was operated with hydrogen- and air-flow rates of approximately 33 and 360-410 mL per minute, respectively. Alkane hydrocarbons were identified based on their retention times. Any peak detected above the integrator threshold within ±0.25% of the mean retention time of the alkane in the calibration standards was identified and quantified as that alkane.

Concentrations of calibrated alkanes (Table 2) were determined by an internal-standard method employing a five-point calibration curve for each alkane. The deuterated surrogate standards that were initially spiked into each sample were treated as internal standards, where each surrogate compound was associated with a group of calibrated alkanes (see Table 2). A calibration curve for each calibrated alkane and batch of samples analyzed was based on five different hexane dilutions of the alkane standards. Each calibration curve was derived from linear regression of (1) the ratio of FID response of the alkane and the associated deuterated surrogate standard, and (2) the ratio of the amount of calibrated alkane and the amount of deuterated surrogate in the calibration standards. As with quantitation of the PAH, this approach means that reported concentrations for all n-alkanes are surrogate-recovery corrected.

Amounts of uncalibrated alkane hydrocarbons and the cumulative amount of hydrocarbons in the unresolved complex mixture (UCM) were based on detector responses and the calibration curve for hexadecane. Flame ionization detector response due to the UCM was determined as the difference of the total FID response and the response due to distinguishable peaks using valley-to-valley baseline integrations.

4.3 Quality Assurance

Quality control samples were analyzed with each batch of 12 samples to assess the accuracy and precision of the analysis, and to verify the absence of laboratory contaminants introduced during analysis. Two quality control samples for accuracy assessment were prepared from hydrocarbon standards prepared by NIST (for PAH) or by ABL (for aliphatics), and run with each batch. Precision was assessed by analysis of two NIST standard reference material (SRM) samples analyzed with each batch: SRM 1974a for mussels and SRM 1944 for sediments. The mussel reference is especially appropriate for these analyses because the PAH concentrations are quite low, with many of the PAH analytes present at concentrations near the method detection limits (MDLs). Absence of laboratory contaminants was verified by analysis of one method blank sample with each batch.

Method detection limits (MDLs) were estimated for each calibrated alkane and PAH analyte following the procedure described in Appendix B, 40 Code of Federal Regulations, Part 136. Method detection limits for uncalibrated PAHs were not experimentally determined. Consequently, detection limits for these analytes were arbitrarily assumed as the MDL of the most closely related calibrated PAH analyte. MDLs for all components presented in bar chart plots throughout this report are depicted by a dashed blue line with blue diamonds. This reminds the reader of the incredibly low concentrations observed and provides a caveat or framework for assessing the

significance of any given peak in a sample. We report individual analytes measured below the statistically-defined MDL because the consistently-observed patterns within a given site are useful for source characterization (dissolved- vs. particulate/oil-phase) and many of the samples exhibit such low concentrations that the majority of observed components are in fact below the MDL. If those components were not included, there would be little or no data to evaluate.

4.4 Determination of Moisture Content

Weighed aliquots of wet mussel homogenates or of sediments were dried at 100^{o} C for 24 h and re-weighed to determine the moisture content, and the ratio of these wet and dry weights was used to convert PAH and SHC concentrations to a dry weight basis.

4.5 Particle Grain Size Determination

Determination of the distribution of particle grain sizes in the sediment samples was determined by a combination of sieving and pipette methods based on the procedures given by Folk (1974). Implementation of these procedures at ABL (Larsen and Holland 2004) is almost identical with the method described in SOP-8908 at GERG. The ABL procedure differs from the GERG procedure in the sample pre-treatment. At ABL, a somewhat smaller sample aliquot is used (8 – 12 g instead of 15 – 20 g sediment), the minimum amount of hydrogen peroxide is used to oxidize organic matter (typically 30 – 60 mL of 30% H_2O_2 instead of 50 – 100 mL), the sample is not washed with distilled water to remove soluble salts at ABL because of the risk of loosing sediment fines, and only ~ 100 mL of sodium hexametaphosphate solution is used to disperse the sample at ABL instead of 400 mL at GERG. These changes were implemented at ABL because they were specifically optimized for the samples analyzed for the LTEMP program. The effects of these minor procedural differences on the estimates of particle grain size distributions in comparison with results produced at GERG are almost certainly negligible.

4.6 Determination of Total Organic and Total Carbon

Analytical measurements of total organic and total carbon are determined on oven dried and pulverized sediment samples using a Dohrmann DC-85A TOC catalytic combustion (oxygen at 200 mL/min and cobalt oxide on alumina) furnace. The carbon dioxide produced is passed through an acidified liquid sparger (scrubs out entrained water vapor and corrosive species), two scrubbers (copper and tin) and linearized non-dispersive infrared detection, by comparison with results from a calibration curve based on potassium acid phthalate. Total organic carbon (TOC) and total carbon (TC) are determined on samples treated with and without 10% HCl in methanol. Total inorganic carbon is calculated as the difference between TC and TOC.

4.7 Data Analysis

The original LTEMP program was designed to use inferential statistics to respond to questions of changing trends in various indices. This suite of statistical questions became less germane when our team was able to extract more in-depth source identification information from the data. For example, simplistic tests for assessing the statistical

significance of increasing or decreasing TPAH values were less relevant than understanding the changing nature of the source, the state of weathering, and dissolved/particulate phase composition of the profile. A more cogent story could be told by subjectively assessing the chemical composition and levels of the analytes than could be garnered from inferentially testing means and variances. Except for occasional regression lines or correlation coefficients to explore data relationships, pattern recognition expertise has resulted in a paucity of inferential testing for this project.

A somewhat contentious technique we use in pattern recognition is accepting and interpreting hydrocarbon data that fall below EPA-defined laboratory method detection limits (MDLs). MDLs result from a rigorous, repeated, analytic laboratory process statistically summarized into a minimum acceptable value for a single analyte (Federal Register 1986). But for pattern recognition, statistical confidence increases due to familiar co-occurring analytes (primarily PAH). If a familiar or expected pattern is present below MDLs, we have little anxiety in accepting it. In this report, we do reach new extremely low levels of dissolved patterns of unrecognized sources where we do qualify the interpretations. Fortunately, these qualified identifications do not compromise any of the issues of concern for the LTEMP project goals but are simply trends of interest.

4.7.1 Hydrocarbon Indices

Over the past eight years, we have developed new analytic tools and insights into the behavior and fate of oil in the regional environment (Payne et al., 1998, 2001, 2003a, 2005a,b,c). This year, the analyses and interpretations focused on trends in the oil signatures. In prior LTEMP studies, several indices, both published and *ad hoc*, have been used with varying degrees of utility to describe LTEMP data trends. However, in recent months we also have been actively engaged in testing, modifying, and applying weathering models to various PWS oil chemistry datasets, including EVTHD, NOAA HAZMAT, and EMAP. From these efforts, we developed a new interest in quantifying the various portions of a PAH oil signature (Driskell et al., 2005), and we realized that several of the more traditional indices either needed adjustment or were simply not fulfilling our analytic needs. As a result, we subsequently formulated two new indices and modified a third (Table 3) which quantify the dissolved-, particulate/oil-phase, and pyrogenic-source signals in a sample signature.

Table 3. Hydrocarbon Parameters Used in the LTEMP Data Analysis.

Parameter	**Relevance**
DSI (mussel tissues and sediments)	Dissolved Signal Index sums the soluble PAH fractions of an oil signature (see accompanying text) DSI = dissolved (naphthalenes + fluorene + C1-fluorene) + dissolved (phenanthrenes) + dissolved (dibenzothiophenes)

PSI (mussel tissues and sediments)	Particulate Signal Index sums the less soluble PAH fractions plus any water-washed groups (see accompanying text) PSI = (C2- + C3-fluorene) + particulate (anthracenes & phenanthrenes) + particulate (dibenzothiophenes) + particulate (fluoranthene/pyrenes) + particulate (chrysenes)
Pyrogenic index (mussel tissues and sediments)	Pyrogenic Index = pyrogenic fraction + pyrogenic (phenanthrenes) + pyrogenic (dibenzothiophenes) + pyrogenic (fluoranthene/pyrenes) + pyrogenic (chrysenes) Where: Pyrogenic fraction = benzo(a)anthracene + benzo(b)fluoranthene + benzo(k)fluoranthene + benzo(e)pyrene + benzo(a)pyrene + indeno(1,2,3-cd)pyrene + dibenzo(a,h)anthracene + benzo(g,h,i)perylene
TPAH (mussel tissue and sediments)	Total PAH as determined by high resolution GC/MS with quantification by selected ion monitoring; defined as the sum of 2- to 5-ring polycyclic aromatic hydrocarbons: Naphthalene + fluorene + dibenzothiophene + phenanthrene/anthracene + chrysene, and their alkyl homologues + other PAHs (excluding perylene); useful for determining TPAH contamination and the relative contribution of petrogenic, pyrogenic, and diagenic sources
TSHC (sediments)	Total Saturated Hydrocarbons quantifies the total n-alkanes (n-C_{10} to n-C_{34}) + pristane and phytane; represents the total resolved hydrocarbons as determined by high resolution gas chromatography with flame ionization detection (GC/FID); includes both petrogenic and biogenic sources
UCM (sediments)	Unresolved Complex Mixture – petroleum compounds represented by the GC-FID signal for total resolved peaks plus unresolved area under the peaks minus the total area of the resolved peaks quantified with valley-to-valley baseline integration; a characteristic of some fresh oils and most weathered oils.

In water, oil partitions by physical equilibrium into two phases, the dissolved phase and the particulate or whole-oil droplet phase. During a 2004/2005 study of the Alyeska Marine Terminal Ballast Water Treatment Facility (BWTF), Payne et al. (2005b,c) utilized a Portable Large Volume Water Sampling System (PLVWSS) to separate (via

filtration through a 0.7 µm glass fiber filter) the dissolved- and particulate/oil-phase fractions (Payne et al., 1999) in a sample of the BWTF effluent just before discharge into Port Valdez.

The less water-soluble higher-molecular-weight PAH (Figure 2 top) and SHC (Figure 3 top) components are readily apparent in the fine particulate phase and finite oil droplets trapped on the glass-fiber filter of the PLVWSS. In the dissolved phase (filtrate – Figure 2 bottom) sample, however, the naphthalenes clearly predominate over all the other PAH, and the presence of the declining but slightly water-soluble C1- and C2-alkylated homologues is in direct contrast to the water-washed pattern (see Appendix A) obtained for the higher-molecular-weight particulate/oil phase PAH trapped on the filter. Also, almost all of the n-alkanes (Figure 3 bottom) are just barely above (or in most cases below) the MDL in the filtrate (dissolved phase) because of their limited water solubility.

This partitioning behavior is controlled by the concentration (mole-fraction) of a given component in the starting oil phase as well as the solubility of that component in both the oil and water phases (i.e., the oil/water partition coefficient). The kinetics of this partitioning is controlled by the oil droplet surface-area-to-volume ratio, the interphase mass-transfer coefficient, and the distance from equilibrium concentrations of a given water-soluble component in the oil and water phases (Payne et al., 1984; NRC 1985, 2003, 2005). When oil is spilled at sea, a true equilibrium of oil and water-column concentrations is rarely attained because of continuing dilution of dissolved components due to mixing with fresh seawater, and at any given moment a dynamic (rather than static) equilibrium exists between the oil and water phases.

When filter-feeding indicator organisms (in this case, mussels) are exposed to water containing oil, the resulting PAH profile of the mussel tissue extracts will reflect the physical state of the oil in the water (dissolved- versus particulate/oil-phase) plus any non-soluble pyrogenic (combustion) products (Baumard et al., 1998; Payne and Driskell 2003; also see Appendix A). These signatures are easily differentiated by their plots (examples in Figure 4) although mixtures can be tricky to tease out. To more clearly illustrate a pyrogenic source, we have included an LTEMP sediment sample in Figure 4. Combustion products generally make up only 20% or less of the total PAH signal in most LTEMP mussel samples (i.e., there are other components present at higher concentrations).

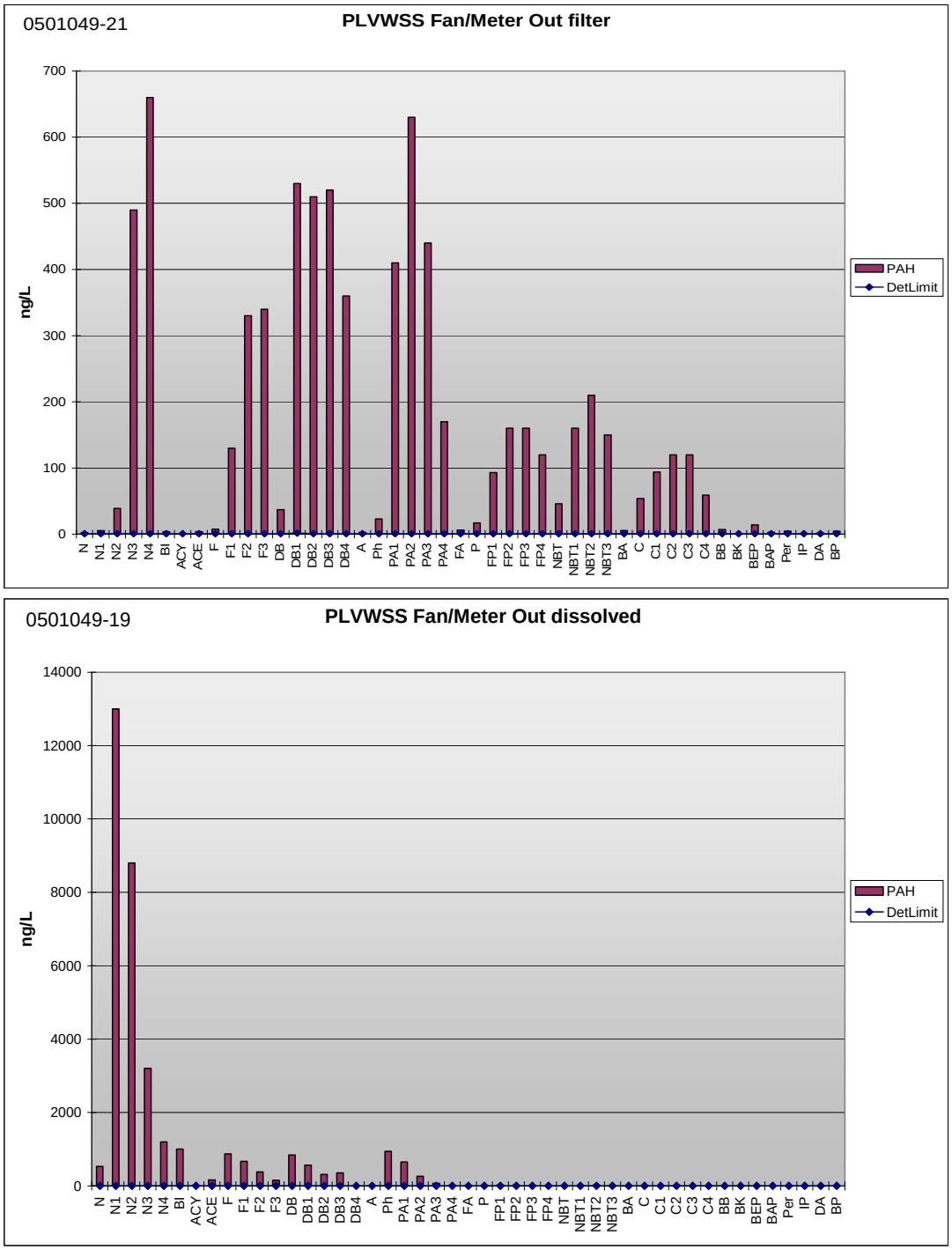

Figure 2 PAH profiles of oil droplets removed by filtration (upper) and the dissolved-phase (lower) of the AMT BWTF effluent, January 2005 (from Payne et al. 2005b).

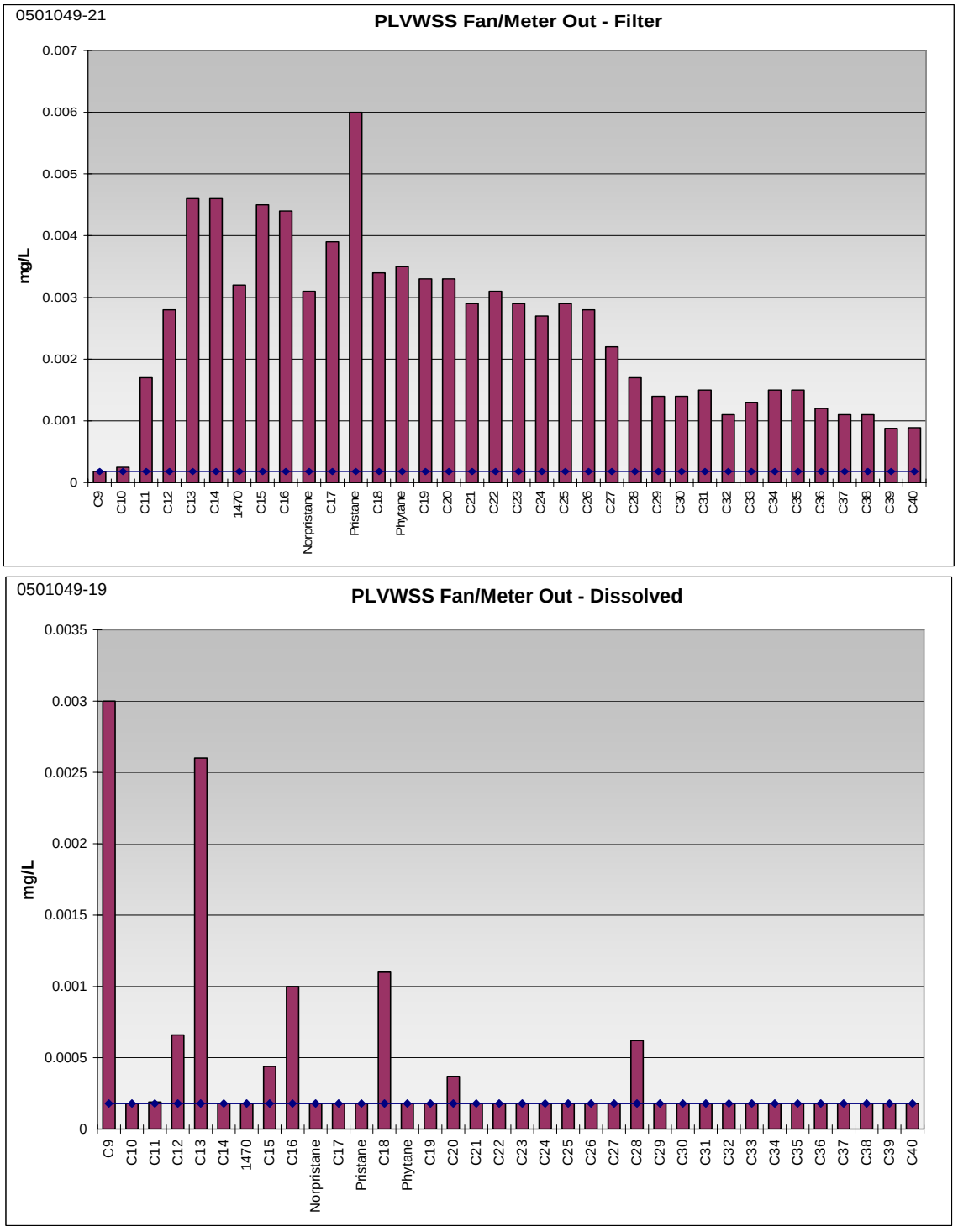

Figure 3 SHC profiles of oil droplets removed by filtration (upper) and the dissolved-phase (lower) of the AMT BWTF effluent, January 2005 (from Payne et al. 2005b).

So with any given PAH pattern, how might one quantify the oil-state? In previous years, we have relied on a series of indices from other authors and have even created a few as needed. Most recently, we meticulously designed a combination of weighting factors and logic statements to mimic, in an artificial intelligence manner, the subjective expertise of an experienced oil chemist (Driskell et al. 2005). A similar pattern-scoring approach was formulated by Carls' PSCORE (2006). In our early approach, we formulated a Dissolved Signal Index (DSI) to assess specific diagnostic portions of a sample's PAH signature and calculate a value quantifying its degree of likeness to a pure dissolved phase signal (e.g., Figure 2 bottom). A Particulate Signal Index (PSI) did the same, quantifying the likeness to a whole-oil droplet signal (e.g., Figure 2 top). We also found it useful to quantify the pyrogenic portion using a weighted pyrogenic index. Unfortunately, the inclusion of logic scalars (bonus weighting if a portion of the signal matched its expected form) also introduced a non-linear scoring scheme that was difficult to evaluate. For this LTEMP study, we reexamined the earlier formulations in Driskell et al. (2005) and found most of the logic scalars unnecessary; a clearer perspective was gained using just the summed concentrations of the respective analytes characteristic for each solubility grouping. The tricky part is that some analytes can be present as a dissolved, particulate, or pyrogenic signal. Logic statements were thus designed to allocate specific analytes to their respective fractions based on their relative concentration patterns versus their expected solubility patterns for each fraction.

For example, a dissolved naphthalene pattern will have the characteristic solubility-driven, descending stair-step pattern plus the more-soluble naphthalene family will dominate over the less-soluble phenanthrenes (Figure 2 bottom and Figure 4 top) or in some cases, the naphthalenes are hyper-dominant (>3.25 times larger than the phenanthrenes) but may not show the stair-step pattern. If none of these patterns are present, then naphthalenes are considered to be part of a particulate/oil-phase signal.

The advantages of these new indices are that they behave in an essentially linear manner, are easy to interpret, and can be normalized to total PAH (TPAH) for between-sample comparisons. We find these indices to be powerful tools in understanding the character of oil in environmental samples and in tracking trends over time. But be advised, these formulations still require chemistry expertise for interpretation and validation. These indices are just mathematical formulations and are not robust to laboratory artifacts or very noisy, low-level results (see discussion below following the DSI, PSI, and Pyro Index definitions).

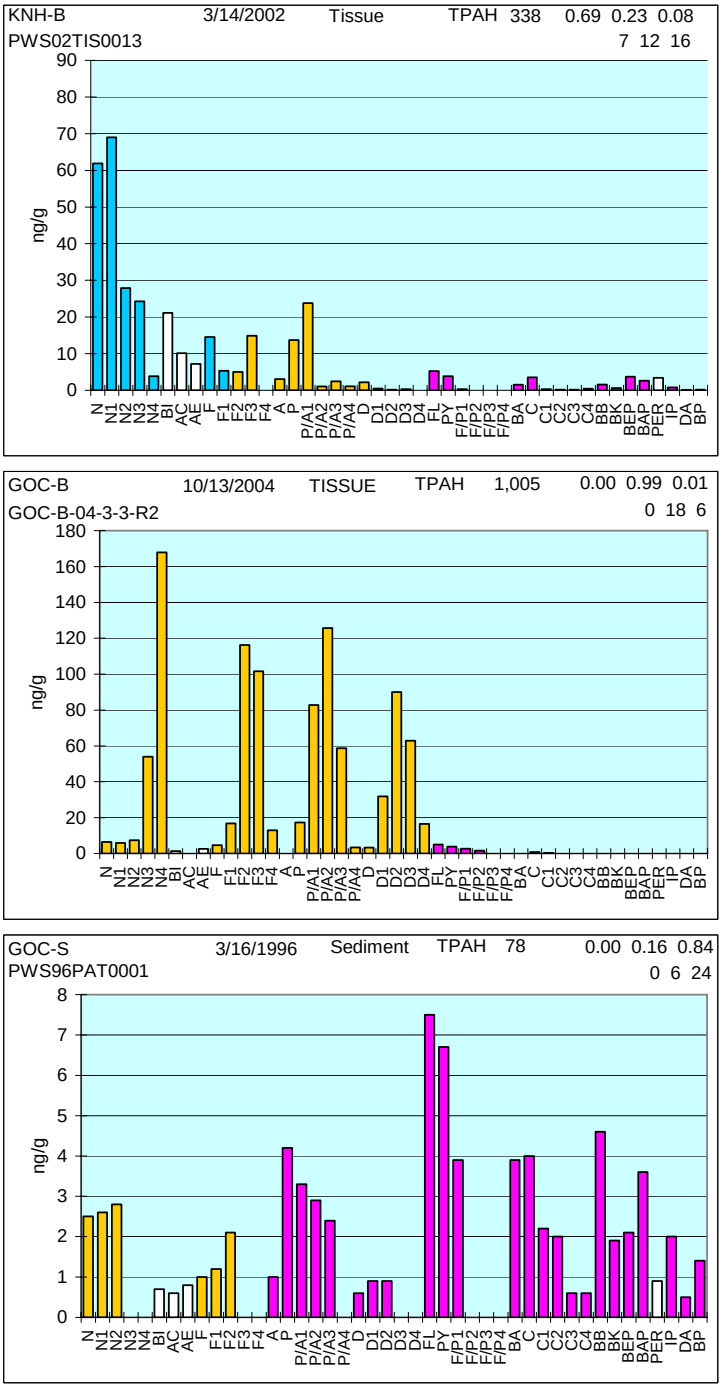

Figure 4 Examples of PAH profiles from LTEMP mussels containing primarily background dissolved-phase components (analytes colored turquoise; top – Knowles Head) and particulate/oil-phase components from a diesel spill (colored gold; middle – Gold Creek), and LTEMP sediments containing primarily low-level combustion products (colored fuchsia; bottom – Gold Creek). The fractional proportions of each phase (soluble, particulate/oil, and pyrogenic) are shown by the numbers in the upper right-hand corner of each plot with the number of analytes assigned to each group just below (e.g., the bottom replicate was 84% pyrogenic from the 24 fuchsia-coded analytes).

The dissolved-signal value (DSI) is formulated using the PAH analytes that display water-soluble patterns, which primarily comprise the lighter-molecular-weight analytes found on the left side of the PAH profiles plots.

Dissolved Signal Index =

Dissolved (naphthalenes + fluorene + C1-fluorene) + dissolved phenanthrenes + dissolved dibenzothiophenes

The particulate index (PSI) is similarly formulated using less-water-soluble, mid-molecular-weight PAH.

Particulate Signal Index =

(C2- + C3-fluorene) + particulate (anthracenes & phenanthrenes) + particulate dibenzothiophenes + particulate fluoranthene/pyrenes + particulate chrysenes

A pyrogenic signal is characterized by the higher-molecular-weight PAH plus the suites of middle (3-4 ringed) PAH when they display descending stair-step patterns and are not part of the dissolved signal. This index is modified from the pyrogenic index developed last year (Payne et al., 2005a) by the contributions from the pyrogenic mid-weight PAH.

Pyrogenic Index =

Pyrogenic fraction + pyrogenic phenanthrenes + pyrogenic dibenzothiophenes + pyrogenic fluoranthene/pyrenes + pyrogenic chrysenes

Where:

Pyrogenic fraction = benzo(a)anthracene + benzo(b)fluoranthene + benzo(k)fluoranthene + benzo(e)pyrene + benzo(a)pyrene + indeno(1,2,3-cd)pyrene + dibenzo(a,h)anthracene + benzo(g,h,i)perylene

Algorithms for assigning the five multi-state PAH families to their appropriate dissolved, particulate, or pyrogenic fraction are described below as general logic statements. The logic was reformulated into Excel formulas for batch processing of the PAH data.

Naphthalenes and fluorene + C1-fluorene are allocated as a group to dissolved or particulate fractions by:

IF

(C1-naphthalene > C2-naphthalene > C3-naphthalene)
or
Sum (all naphthalenes) > sum (all phenanthrenes + anthracenes) and
sum (all fluorenes) > sum (all phenanthrenes + anthracenes)
Or
Sum (all naphthalenes) > 3.25 x sum (all phenanthrenes + anthracenes)

THEN

Dissolved naphthalenes = sum (all naphthalenes + fluorene + C1-fluorene)

ELSE

Particulate naphthalenes = sum (all naphthalenes + fluorene + C1-fluorene)

For tissues, phenanthrenes are allocated as dissolved, particulate, or pyrogenic by:

IF

Tissue phenanthrene > max (phenanthrene homologues)

THEN

IF

Naphthalenes are dissolved (see above)

THEN

Dissolved phenanthrenes = sum (all phenanthrenes + anthracene)

ELSE

IF

Pyrogenic fraction > 0
or
Fluoranthene or pyrene or chrysene are pyrogenic (see below)

THEN

Pyrogenic phenanthrenes = sum (all phenanthrenes + anthracene)

ELSE

Particulate phenanthrenes = sum (all phenanthrenes + anthracene)

ELSE

Particulate phenanthrenes = sum (all phenanthrenes+ anthracene)

Dissolved phenanthrenes are unlikely to occur in sediments, so sediment phenanthrenes and fluorenes are only attributed as pyrogenic or particulate based on:

IF

Sediment phenanthrene > max (phenanthrene homologues)
and
(Pyrogenic fraction > 0
or
Fluoranthene or pyrene or chrysene are pyrogenic) (see below)

THEN

Pyrogenic phenanthrenes = sum (all phenanthrenes + anthracene)

ELSE

Particulate phenanthrenes = sum (all phenanthrenes+ anthracene)

Dibenzothiophenes, similar in solubility to the phenanthrenes, are allocated into dissolved, particulate, and pyrogenic fractions by matching the assignment of the phenanthrenes.

For tissues or sediments, fluoranthene/pyrenes are allocated as pyrogenic or particulate by:

IF

Pyrene > max (fluoranthene/pyrene homologues)
or
Fluoranthene = sum (all fluoranthene/pyrenes)

THEN

Pyrogenic fluoranthene/pyrenes = sum (all fluoranthene/pyrenes)

ELSE

Particulate fluoranthene/pyrenes = sum (all fluoranthene/pyrenes)

Chrysenes are allocated as pyrogenic or particulate by:

IF

(Chrysene $\geq$ sum (all chrysenes)
or
(Chrysene > max (chrysene homologues)
or
(Chrysene = 0 and C1-chrysene > C2-chrysene > 0)

THEN

Pyrogenic chrysene = sum (all chrysenes)

ELSE

Particulate chrysene = sum (all chrysenes)

Note that four of the PAHs, biphenyl, acenaphthene, acenaphthylene and perylene, are not predictably assignable to the three phases and are thus excluded from the calculations. TPAH is adjusted accordingly for the proportional fractions.

We acknowledge that these indices may seem slightly arbitrary, but they actually encode a substantial amount of knowledge regarding PAH solubilities, source fingerprinting, and hydrocarbon weathering and, most importantly, appear to be qualitatively effective. For the current report, we have found that plotting a joint time series of DSI, PSI, Pyro, and TPAH gives a very comprehensive look at the trend of oiling at a given station. Spikes and dips in the trend lines suggest places that should be more closely investigated. At times, aberrant quantities for example, of naphthalene or fluorene, have spiked a series but more often a change in trends tracks a change in signal.

4.7.2 Data Anomalies

One very important caveat that should be recognized in examining the LTEMP PAH indices time-series plots relates to our treatment of early program data where laboratory artifacts were inadvertently reported as real PAH components in exceptionally clean or low-PAH level tissue samples. Fortunately, this issue does not appear to be a problem with sediment chemistry data or with mussel tissue results from later (post 1997) years of the program.

In our initial LTEMP synthesis/review (Payne et al., 1998) and in two previous LTEMP reports (Payne et al., 2003a, 2005a), we documented the problem of reporting laboratory artifacts as measured PAH components in tissue samples. The issue arose during the

early years of the LTEMP program when the software for the GC/MS instrumentation used by the analytical laboratory did not automatically integrate all the alkylated PAH homologues (08/07/03 personal communication with Dr. Guy Denoux, GERG Laboratory Director). Most parent PAH components (and methylnaphthalenes) were automatically integrated, but quantification of the remaining C_2-, C_3-, and C_4-alkylated homologues had to be done manually by the GC/MS operator, and then only when a recognizable signal was observed first. As a result, PAH patterns identical to those shown in Figure 5 were often obtained on tissue samples from the cleaner areas and in many of the laboratory procedural blanks.

By design, the GC/MS integrator in selected-ion-monitoring mode was gated to measure the signal for a specific ion only during an expected retention time window, and any signal (including electronic noise) measured during that interval was automatically included as a measured PAH component. Because this automated integration only occurred for the specific retention times and ions selected for analyses, the observed pattern shown in Figure 5 was routinely obtained for cleaner samples. Reported values of individual components (in ng/g dry weight) would then depend on the stochastic intensity of the integrated signal (including noise) and a multiplier based on the dry weight of the tissue sample initially extracted. When significant oil contamination was present (such as at the Alyeska Marine Terminal and Gold Creek sites after the *T/V Eastern Lion* oil spill in 1994), the instrument was sensitive enough to detect the signal for the remaining alkylated homologues, and they were then manually integrated. The rest of the time, however, less useful profiles similar to those shown in Figure 5 were consistently generated in 145 of the 246 tissues analyzed between March 1993 and March 1997. They suggest the samples contained low level concentrations of hydrocarbons, but there is little to no information as to exactly how much or what the true profile looked like.

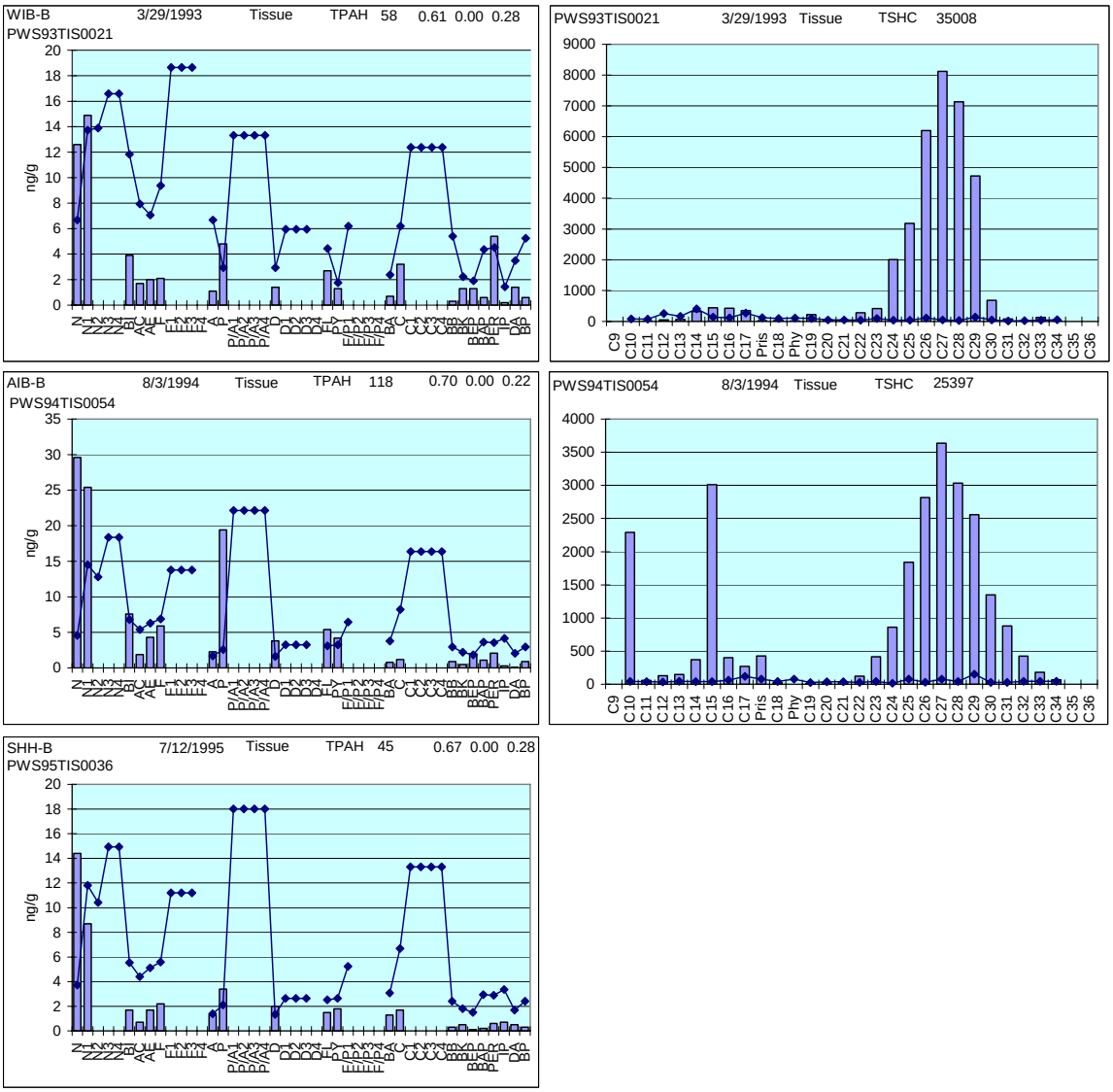

Figure 5 PAH procedural artifact patterns (left graphs) common in early LTEMP samples and procedural blanks between March 1993 and March 1997. For these samples, homolog data are incomplete. The overlaying solid lines with the blue diamonds represent reported MDLs. SHC analyses (right graphs) were discontinued between 1995 and 1998 due to lipid interference problems.

Another procedural artifact that we discussed at length in the 2002-2003 LTEMP report (Payne et al., 2003a) was from anomalously high fluorene and alkylated-fluorene (F, F1, F2, F3) concentrations being reported as a result of incomplete sample cleanup and lipid interference. This was particularly problematic in tissue samples analyzed by GERG from the July 1994, July 1996, and July 1999 sample collections (Figure 6). The possibility of an anomalous fluorene signal was first noted in our 2001 synthesis report on potential PAH toxicity issues in Port Valdez LTEMP samples (Payne et al., 2001), but it wasn't identified as a confirmed problem until the analyses of split samples run as part of an inter-laboratory intercalibration program involving GERG, the NOAA Auke Bay Laboratory, and the NOAA Montlake Facility (Northwest Science Center – National Marine Fisheries Services) (Payne et al., 2003a). Total fluorenes reported by GERG were between ten and two hundred times higher than values from the other laboratories analyzing mussel tissue splits from Alyeska Marine Terminal (AMT) and Gold Creek (GOC), and individual fluorene homologue concentrations were two-to-six times higher for GERG compared to the other labs after the analyses of National Institute of Standards and Technology (NIST) standard reference materials. In our 2002-2003 LTEMP report, we proportionally reduced the fluorene contributions in samples that showed the anomalous pattern (Figure 6). But for this report, we elected to simply drop the fluorene contribution to the TPAH and other diagnostic indices (DSI and PSI) for the July 1994, July 1996, and July 1999 tissue samples based on the reasoning that it would eliminate the megaspikes and where there was a significant real signal from other PAH, the loss would be minimal and characterization mostly unaffected.

Finally, in the July 1997 samples from Disk Island (DII), Gold Creek (GOC), Knowles Head (KNH), Sheep Bay (SHB), and Sleepy Bay (SLB), we noticed that the PAH patterns were remarkably similar (if not identical) and that they were characterized by one or two additional naphthalenes at higher concentrations plus all the other procedural artifacts identified in Figure 5. In these instances, there were no other alkylated components detected (except for the extra naphthalenes) to suggest that the observed patterns were in fact real (Figure 7), and we concluded that the laboratory had again erroneously reported concentrations for procedural artifacts plus additional naphthalenes that were manually integrated. As will be discussed later under site-specific considerations of tissue-sample trends, these elevated naphthalenes lead to an apparent region-wide spike in TPAH levels in 1997 with major contributions from the dissolved phase. However, we have little confidence in those data and suspect instead that this apparent trend is really nothing more than an anomaly introduced by changing laboratory integration procedures.

Because of these problems with potential analytical artifacts, for this report, we once again re-examined <u>all</u> the historic tissue data and flagged those samples that were characterized by one of the three patterns discussed above. Then, to avoid propagating questionable data, we decided to exclude any questionable data points in our PAH time series plots. For these plots, values in which we have confidence are represented by symbols on the connecting lines; questionable data have dashed connecting lines between

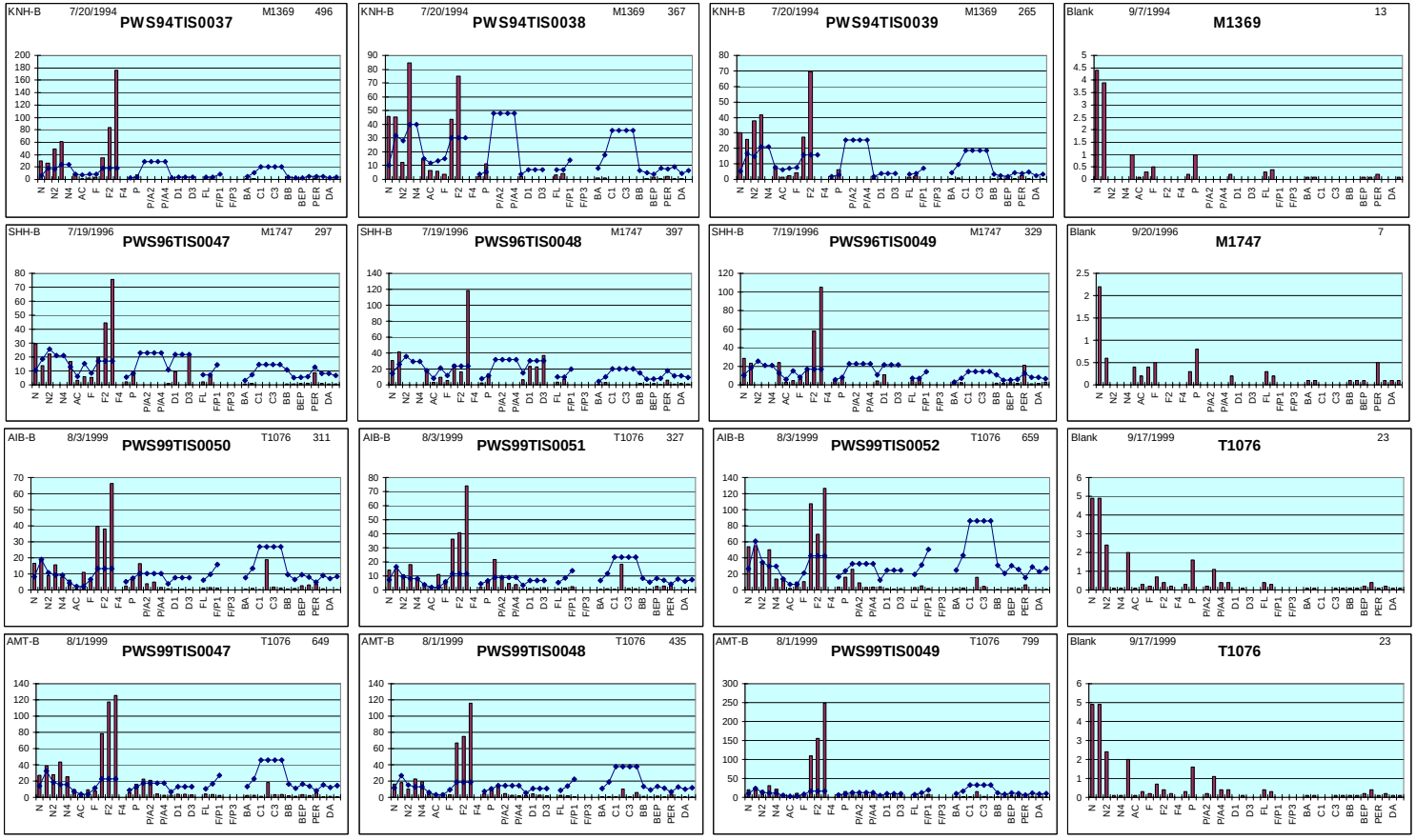

Figure 6 Representative PAH plots showing fluorene/lipid interference in July 1994, July 1996, and August 1999 tissue samples analyzed by GERG (from Payne et al., 2003a). Presented horizontally are three replicate samples plus the respective lab blank.

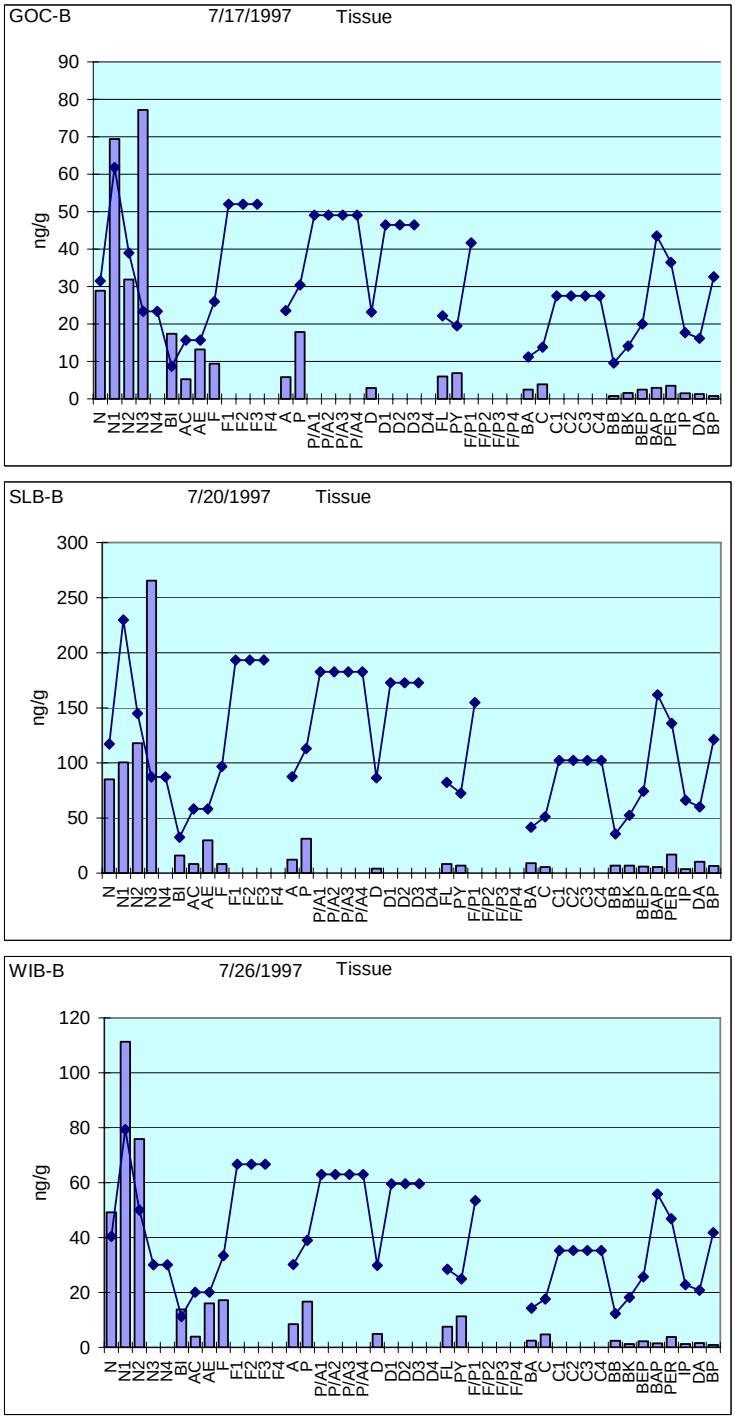

Figure 7 Representative PAH profiles and method detection limits (solid lines with blue diamonds) from July 1997 tissue samples showing highly similar procedural patterns (GC/MS integration artifacts – see Figure 5) plus additional naphthalenes.

sampling intervals but no symbols. With this approach, legitimate data are easily identified while questionable values are only presented in the context of general trends within the complete data set.

4.7.3 Data Reduction

Data analysis for this project relies heavily on pattern recognition in which the bar chart plot of each sample is scrutinized for relevant details. To facilitate this effort, an Excel application was developed to plot each sample from a station in replicate groups (by station and sampling date) with lab method detection limits (MDLs) superimposed on the plot and the relevant lab method blank adjacent to the group. For more detailed comparisons, another Excel application could graph both PAH and SHC analytes with relevant indices from any three samples plus a reference standard (e.g., BWTF outfall, ANS crude, dissolved-, particulate-, or pyrogenic-dominated profiles, etc.). For evaluating time trends, graphs of select indices' averages or groupings of indices were used.

When reviewing the replicate bar charts, we prefer looking at single replicates as the best method to maximize the information about the sample profile. The alternative is to average each analyte using TPAH standardized samples or to composite samples. On various projects, we have encountered replicates with wholly different signatures (reflecting different sources) that when averaged, display an undifferentiated amalgam of mixed sources and hence, a confounded interpretation. Because for this project, understanding the source and fate of the waterborne oil is more relevant in developing the site scenarios than is knowing the statistical variance of the samples, obtaining maximum information from the profiles is of prime interest. Furthermore, considering the data anomalies discussed above, only by looking at each replicate alone, can the investigator be confident of the underlying data quality. We have encountered analytic results that fully met laboratory QC requirements but simply did not make sense; reanalyzing the samples confirmed our suspicions. For statistical purposes, we subsequently reduce the data and average any derived index, e.g., TPAH, or the phase compositions, in order to look at trends and comparisons.

4.8 Data Management

Two years ago, data received in spreadsheet format from ABL were combined with historic data from KLI Microsoft Access database archives. Slight modifications were made to the historic data to standardize chemical compound names and abbreviations. This year's data will be amended to the same database, metadata updated, and the product delivered to the EVOS Trustees data archives. Microsoft Excel pivot tables were used for most data compilations. Graphing and data processing routines (described above) were custom programmed for Excel using Microsoft Visual Basic for Applications (VBA) code.

5 Results and Discussion

5.1 Sampling and Data Quality

5.1.1 ABL Quality Assurance Chemistry Results

The 2004-2005 field samples were processed with a set of quality assurance samples designed to verify analytical accuracy, precision, method cleanliness, and method efficiency. Analysis of the twenty accuracy-check samples (i.e. SRM 1491 or the ABL aliphatic standard) indicated that accuracy for the calibrated compounds ranged from 89% to 107% of certified or expected values in these samples. The median precision of the PAH (including the uncalibrated PAH) in the nine SRM 1974b samples analyzed for the mussel batches, expressed as the coefficient of variation, was 29%. The precision ranged from 10% to 139%, and was less than 36% for all but nine analytes, which included naphthalene, biphenyl, acenaphthylene, C-4 fluorenes, C-2, C-3 and C-4 phenanthrenes/anthracenes, C-4 fluoranthenes/pyrenes, and C-3 chrysenes, most of which (C-2 and C-3 phenanthrene/anthracenes excepted) are present in this SRM at concentrations that are near or below their detection limits. The median precision of the PAH (including the uncalibrated PAH) in the two SRM 1944 samples analyzed for the sediment batches, expressed as the coefficient of variation, was 7%. The precision ranged from 0.3% to 20.5% for all analytes. The method blanks analyzed with each batch of samples for this report were lower than or near respective MDLs for analytes listed in Table 2 verifying the absence of positive interferences introduced at the laboratory.

Recoveries of surrogate standards were between 30% and 111% for 98.5% of all surrogate hydrocarbons. These values are within the accepted ranges published in the standard operating procedures (SOP's) for the ABL laboratory and those recommended in NOAA Status and Trends protocols. In accordance with those protocols and to be consistent with procedures utilized at GERG, all individual and total PAH and SHC concentrations have been corrected for surrogate recoveries and are reported on a dry weight basis.

5.1.2 Mussel Populations

One issue of moderate concern is the availability of mussels at some of the sites (Table 4). Some locations have but patchy remnants of former colonies so boldly obvious in earlier KLI photos. At most sites, there is normal attrition in the dominant 6-7 year old mussel age class (based on growth rings) with a 3-4 year old class maturing to fill the space. There are also new 0-3 year old recruits at most locations. The size and robustness of mussels differ substantially among the sampling sites, most likely natural variation from available food resources and predation. The Sleepy Bay site is the most impoverished location and is definitely in a transition state. Recruitment is poor and

Table 4. Field notes on mussel populations.

Station	Field notes – March 2005
Aialik Bay	Very good population. Dense, 5-6 yr old, plump and healthy crop of recruits. No predators visible.
Alyeska Marine Terminal	Denser population and not as patchy as Gold Creek.
Disk Island	Healthy, plump, vivid blue shells. No mussels in mid-transect swale. Normally abundant mussels at left end of transect have been mostly stripped; only bysuss threads remain. Otter predation??
Gold Creek	Colony in eroded patchy strips, slippery, silt-covered with reduced shell volume. Suboptimal niche?
Knowles Head	Mussels dense but small. Good crop of 3-4 yr old recruits. *[In July 2006, they were completely removed by Pisaster predation.]*
Sheep Bay	Harvestable mussels discontinuous in mid transect. Shells small (<2 cm) but still 6-7 yr old. Distinct zone in KLI photos no longer visible. 3-4 yr old recruits appearing on upper surfaces.
Shuyak Harbor	Mussels patchy near right end. But healthy and aged 5-6 yr old. Less patchy near left end but slightly smaller. Good recruitment.
Sleepy Bay	Mussels are only in broken shale above the marker and at left end beyond marker. Mostly very small 3-5 yr olds. No mussels in mid-section. Small healthy group found on back side of outcrop beyond left end marker. This site may be in jeopardy. *[Almost completely removed by Nucella predation in July 2006.]*
Windy Bay	Good site. Beds dense and continuous. Mussels healthy, plump and aged. Good recruitment. No visible predators.
Zaikof Bay	Dense, medium-sized population but more patchy than previous year. *Pisaster* starfish common in low intertidal (see cover photo). *[By March 2006, this colony had been completely stripped; sampling was shifted slightly off-site.]*

adults are mostly scattered or absent along the transect. If current trends persist, sampling at this site may be relocated to nearby off-transect populations. Disk Island and Zaikof Bay populations are also under heavy pressure, presumably from predation.

5.2 Port Valdez Sediments

The primary purpose of the Port Valdez sites is to monitor the regulated discharges (or accidental spills) from the tanker operations at the Alyeska Marine Terminal (AMT), the terminus of the Trans-Alaska oil pipeline. From one nearby site, mussels and subtidal sediments are sampled that are chronically exposed to the diluted discharge of the Alyeska Ballast Water Treatment Facility (BWTF). A reference station, across the port at Gold Creek (GOC), is also sampled for mussels and subtidal sediments.

The BWTF currently treats and discharges an average of nine million gallons per day (MGD) of oil-contaminated ballast water offloaded from the tankers prior to refilling them with Alaska North Slope (ANS) crude oil. The ballast-water treatment uses both physical and biological methodologies, which remove most of the BTEX and partially degrade the PAH and SHC components. The treated ballast water is released through a 63 m-long diffuser, approximately 400 m offshore at a depth of 62-82 m.

During warmer months, SHC biodegradation within the facility is very rapid while PAH biodegradation is only partially complete before the effluent is discharged into Port Valdez. During colder months, the biodegradation process is less efficient for both SHC and PAH (Payne et al., 2005b,c). In both seasons, the effluent signature is low level (usually < 300 ppb), but PAH and SHC constituents still appear in local sediments within the mixing zone sampled by the Alyeska Environmental Monitoring Program (EMP) (Blanchard et al., 2005; Shaw et al., 2005) and in mussel and sediment samples historically collected by LTEMP and other PWS RCAC studies (KLI, 2000 and references therein; Payne et al., 2001, 2003a,c,d, 2005a; Salazar et al., 2002). Despite the excellent processing efficiency at the BWTF, the sheer volume processed results in an estimated 0.5-1.4 barrels of highly diluted oil (both as finely dispersed free oil-droplet and dissolved phases – Figure 2 and Figure 3) being discharged daily into the port, with 10-20% of the PAH contributed by the oil-droplet phase (Payne et al., 2005c).

5.2.1 Sediment Particle Grain Size

Sediment grain size plots (Figure 8) show that sediment compositions from the last two samplings are within the range of previous years. The 2003 LTEMP report (Payne et al. 2003a) discusses sources and relevance of this variance. To summarize, the PGS data serve two main purposes to the LTEMP program. First, they ensure that the monitored location has not undergone drastic changes, e.g., slope failures, dredge spoils deposits, etc. Secondly, the silt + clay value allows a rough confirmation or calibration of TPAH levels should it ever become necessary.

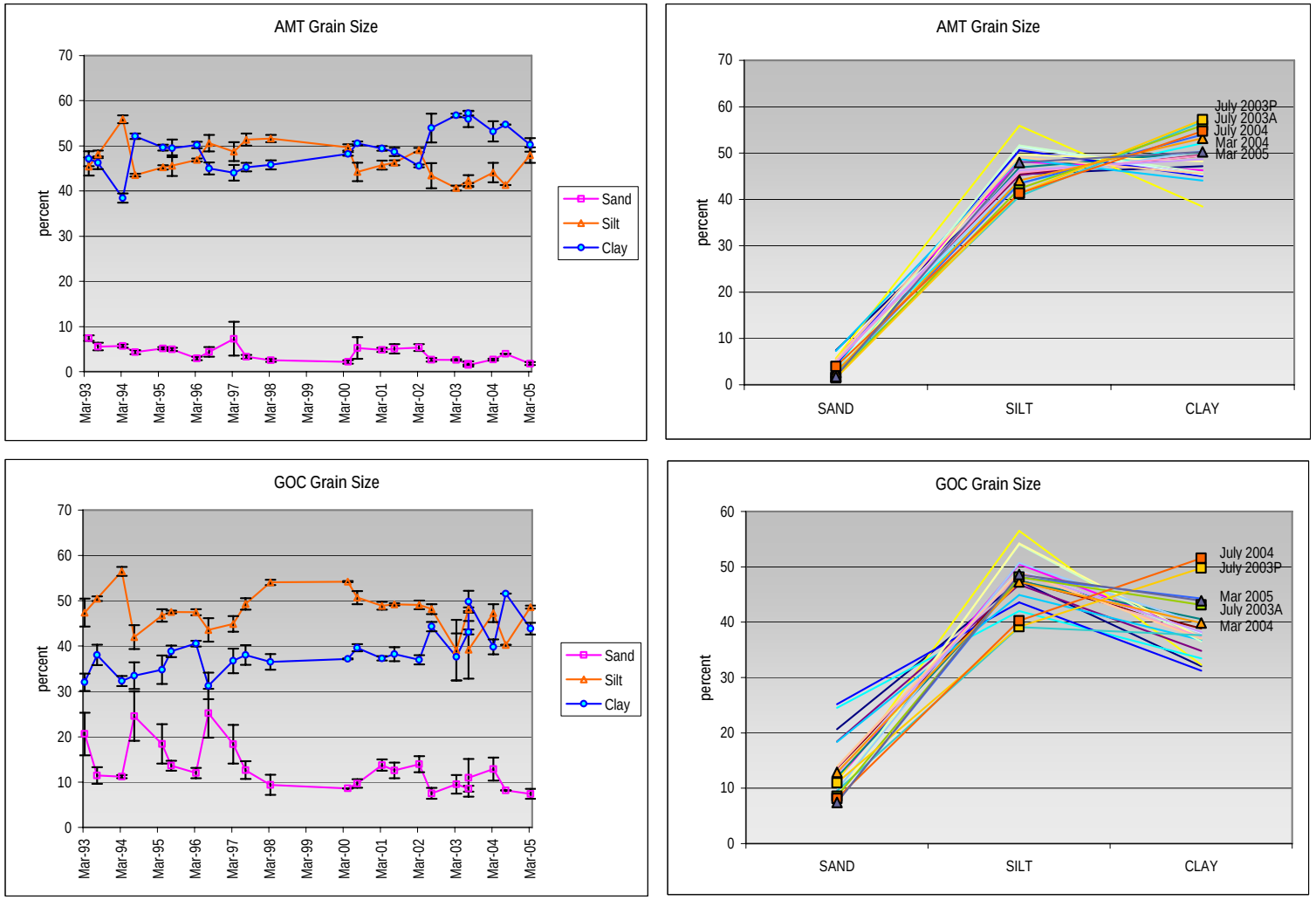

Figure 8 Time series and time overlays of grain size composition at Alyeska Marine Terminal and Gold Creek, 1993-2005. Sediments were not collected in 1998-99.

From the past and current data, we have noted outlier samples and their effect on the chemistry data but conclude that the outliers represent spatial heterogeneity rather than site changes and more importantly, have not affected the trends nor the interpretation of results. Note the recent cyclic trend of fines at GOC (Figure 9) seem to reflect seasonal silt deposition. This phenomenon is also observed in the intertidal; at times, the GOC intertidal site becomes slippery with a noticeable cover of silt. Examining the total fines (silt + clay), there appear to be increasing trends over time at both sites (Figure 9) but the sampling design is too confounded to draw any real conclusions (e.g., variance in site location, change in soil labs, consistency in obtaining surface pgs sample). Results do suggest that AMT is a less dynamic regime than GOC but the sites have always yielded similar soft fines at every sampling and thus represent a good comparative site pairing.

5.2.2 Total Organic and Inorganic Carbon

Although suspended sediment loads are visibly high in the eastern portion of the Port Valdez basin, the carbon contents (Table 5 and Figure 10) are typical of the predominate, organically-poor glacial flour common throughout the Port Valdez and Prince William Sound Basin.

Table 5 Total organic and inorganic carbon in sediment replicates at Port Valdez stations.

Station Replicates	TC (ppm)	TOC (ppm)	TIC (ppm)	TC (%)	TOC (%)	TIC (%)
Jul-04						
AMT-S-04-2-1	7188	6960	228	0.72	0.7	0.02
AMT-S-04-2-2	6832	6797	35	0.68	0.68	0
AMT-S-04-2-3	6403	6361	42	0.64	0.64	0
AMT mean	6808	6706	102	**0.68**	**0.67**	**0.01**
AMT std dev	393	310	109	0.04	0.03	0.01
GOC-S-04-2-1	6820	6324	496	0.68	0.63	0.05
GOC-S-04-2-2	6213	6179	34	0.62	0.62	0
GOC-S-04-2-3	5795	5808	-13	0.58	0.58	0
GOC mean	6276	6104	172	**0.63**	**0.61**	**0.02**
GOC std dev	515	266	281	0.05	0.03	0.03
Mar-05						
AMT-S-05-1-1	6165	5946	219	0.62	0.59	0.02
AMT-S-05-1-2	6019	6042	-23	0.6	0.6	0
AMT-S-05-1-3	5863	5779	84	0.59	0.58	0.01
AMT mean	6016	5922	93	**0.6**	**0.59**	**0.01**
AMT std dev	151	133	121	0.02	0.01	0.01
GOC-S-05-1-1	5791	5729	62	0.58	0.57	0.01
GOC-S-05-1-2	6083	5765	318	0.61	0.58	0.03
GOC-S-05-1-3	6369	6329	40	0.64	0.63	0
GOC mean	6081	5941	140	**0.61**	**0.59**	**0.01**
GOC std dev	289	336	155	0.03	0.03	0.02

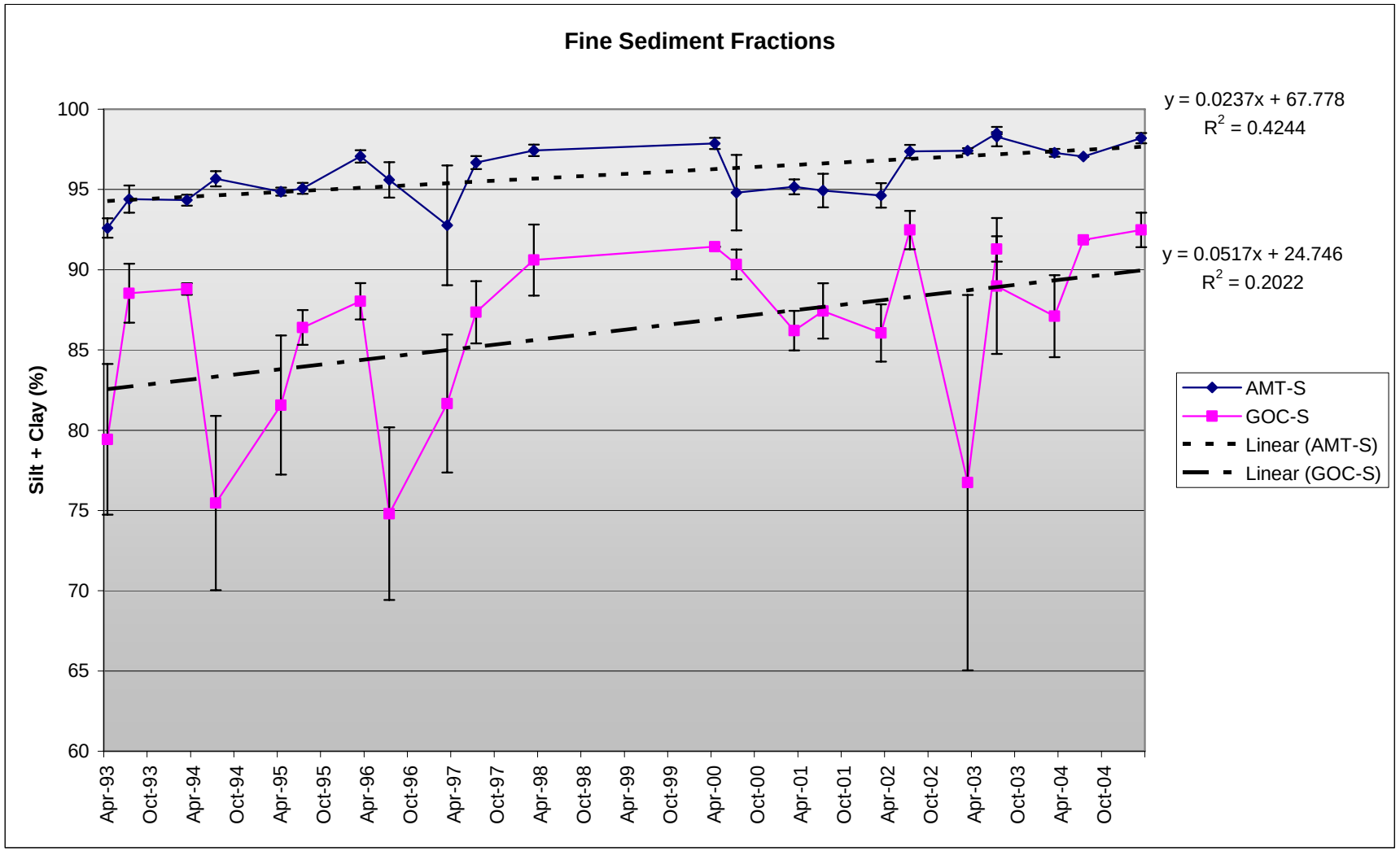

Figure 9 Average fine sediment fractions (silt + clay) time series trends (±standard error of means) from GOC and AMT surficial sediment grabs. Note y-axis scale has been clipped for detailed viewing. Sediments were not collected in 1998-99.

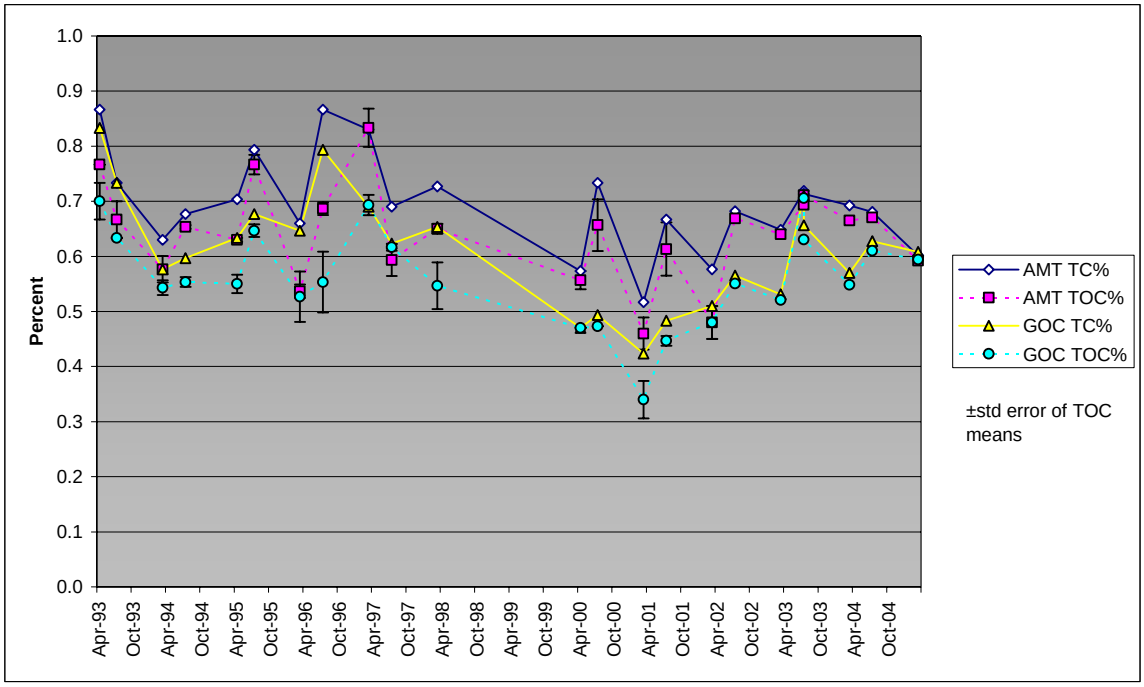

Figure 10 Time series of total carbon and total organic carbon in AMT and GOC sediment.

5.2.3 Sediment Chemistry

For a historic recap of all the sediment chemistry data, Appendix B-1 tabulates the total SHC and PAH values of individual samples, seasonal averages, and the associated coefficients of variation for the replicate measurements completed between 1993 and 2005. Using the recently developed dissolved-, particulate-, and combustion indices described in Section 4.7, we developed a graphic style (Figure 11), which presents the sediment time series data for Alyeska Marine Terminal (top) and Gold Creek (bottom). The dual-axis data in the left-hand panels show the relative percentages of the TPAH from the soluble, particulate (oil phase), and pyrogenic fractions (left axis) as well as the TPAH value (on a logarithmic scale – right axis), while the right-hand panels present the same data simply as total concentrations (ng/g dry weight on a linear scale) for each fraction. In the right-hand panels, the sum of the soluble, particulate, and pyrogenic fractions equals the total PAH (TPAH – dark fuchsia-colored circles). This dual-presentation format allows overall trends to be easily identified with the absolute magnitude of each fraction shown in the right-hand panels, while finer details on relative contributions from the different fractions can be tracked in the left-hand panels. In the following sections, these data are discussed for each site separately and compared with Alyeska Environmental Monitoring Program data where appropriate.

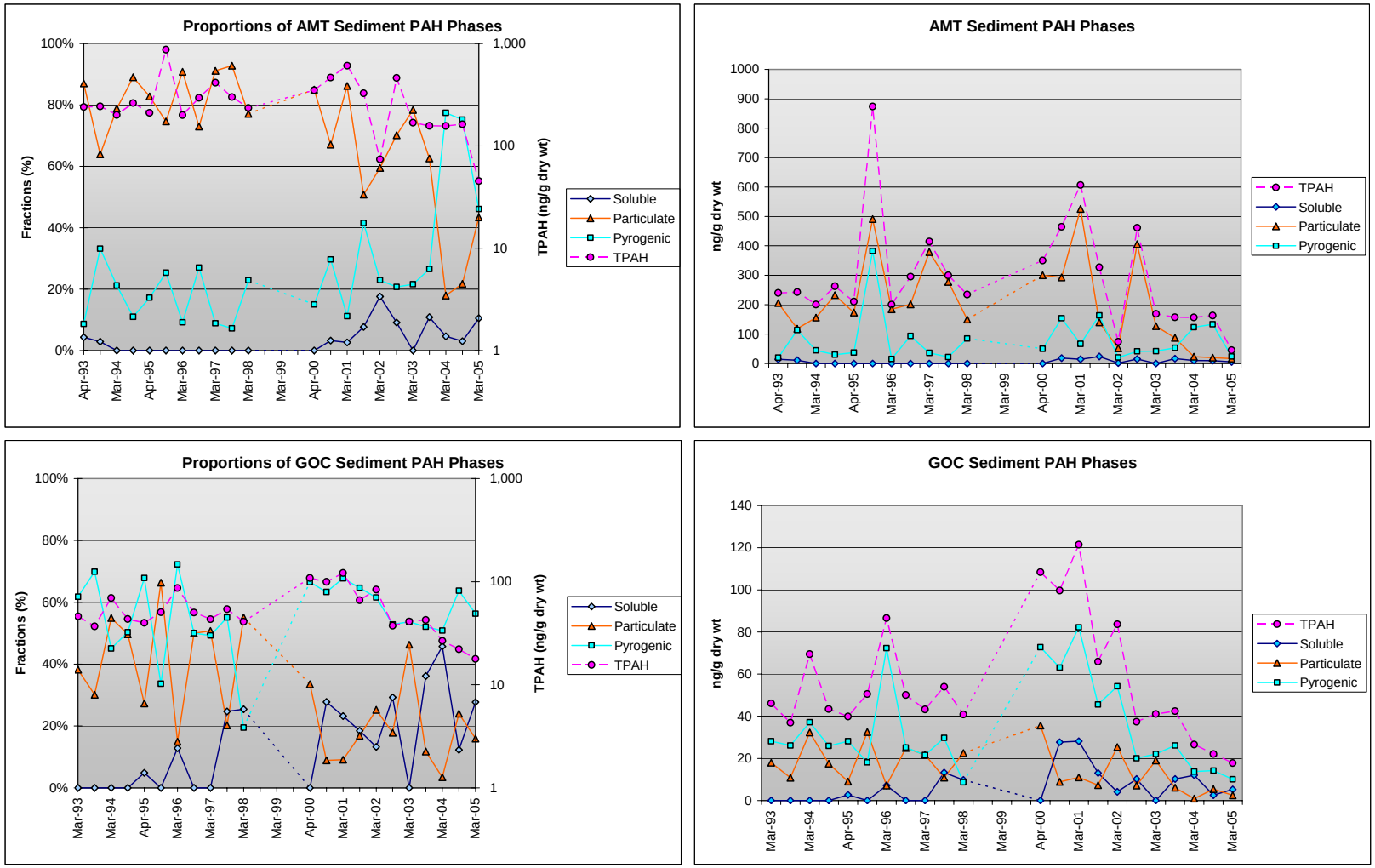

Figure 11 Time series TPAH and relative proportional make up of PAH profiles in AMT and GOC sediment samples. Sediments were not collected in 1998-99.

5.2.3.1 Alyeska Marine Terminal

While there has historically been a lot of variability in the triplicate sediment TPAH values at this site (top panels in Figure 11), the concentrations have been less variable over the last three years (since March 2003), and they have significantly declined compared to the historical range. Also, it is clear that until recently, the majority of the TPAH signal has been associated with the particulate/oil-droplet phase with lesser contributions from pyrogenic components (upper right Figure 11). This is probably the result of free oil droplets from the diffuser interacting with suspended particulate material (SPM) followed by near-field sedimentation (Payne et al. 2003b).

Yet while the overall TPAH concentrations are declining, the relative contribution of TPAH from the particulate/oil-phase fraction also may be dropping (from around 80-90% historically to ~40% in March 2005 with only ~20% contributions in March and July 2004—upper left Figure 11). This may reflect lower levels of free oil droplets in the BWTF discharge from reduced discharge volumes, or improvements in the ballast water treatment process efficiency at removing free oil droplets, or both. Conversely, the relative contribution from combustion-sourced (pyrogenic) PAH appears to be increasing (from around 20-30% historically to over 75% in March and July 2004 and ~46% in March 2005). Contributions from soluble constituents have historically been negligible (0 to 5%); however, it appears that more soluble-phase components (up to 18%) have been observed intermittently since July 2000. While the naphthalene (and fluorine) components identified as the soluble fraction encompass individual compounds that are generally associated with the aqueous phase in oil/water partitioning experiments (and in the BWTF effluent – see Figure 2 bottom), we cannot tell from these data if this soluble fraction is truly in solution (i.e., in the interstitial water associated with the sediments) or simply lower-molecular-weight PAH bound up in the sediment phase. Furthermore, upon closer examination of the individual plot profiles for these more recent samples, usually only one of the three replicates showed a significant dissolved-phase fraction with the other two represented primarily by particulate/oil-phase and pyrogenic components.

The increase in the pyrogenic fraction in the sediments collected in 2004 is worthy of note, and this is reflected in the LTEMP PAH and SHC plots from AMT sediment samples collected in July 2003 and July 2004 (Figure 12). The most striking difference between the samples is the predominance of the parent PAH (phenanthrene, fluoranthene, pyrene, and chrysene) relative to their respective alkylated homologues (“descending steps”) in the July 2004 sample compared to the more water-washed petrogenic profile (“ascending steps”) in July 2003. It is these features that contribute to the relative proportional increase in the pyrogenic fractions noted in Figure 11.

Also, in the July 2003 sample, the SHC profiles contain significant contributions from pristane (present in ANS oil but more likely from copepod and zooplanktivore feces – Blumer et al., 1964; Short 2005) and phytane (from whole oil droplets – NRC 1985) in addition to the higher-molecular-weight n-C30 to n-C35 alkanes from heavily degraded petroleum (NRC 1985). In the July 2004 sample, the pristane and phytane levels are

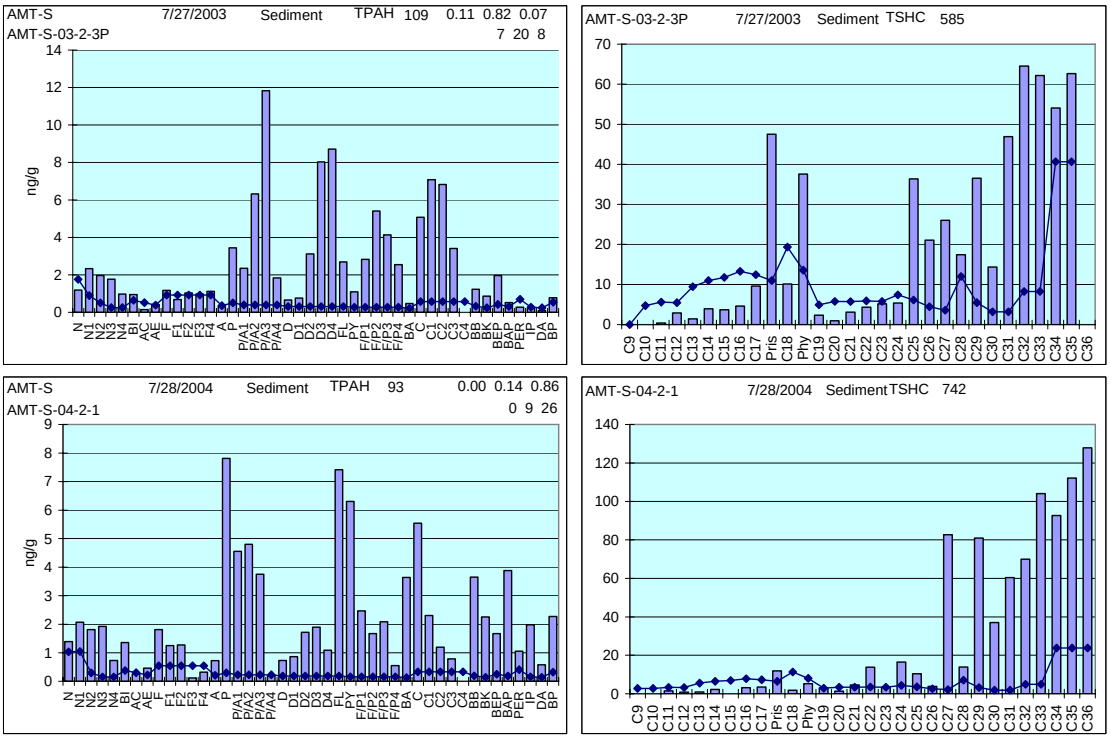

Figure 12 PAH and SHC profiles from representative AMT sediments in July 2003 and July 2004 illustrating the relative increase in pyrogenic components in 2004.

much lower, while the higher-molecular-weight residual n-alkanes are still very persistent. In addition, the relative abundance of n-C27 and n-C29 is more apparent suggesting accumulation of terrestrial detritus as well.

While the LTEMP sediment sampling program at the Alyeska Marine Terminal (AMT) site is limited to one location, the Alyeska Environmental Monitoring Program (EMP) involves (among other tasks) sediment sampling at numerous locations within Port Valdez by a team from the University of Alaska Fairbanks. The design include six sites within and five sites around the perimeter of the NPDES-defined mixing zone and four additional stations along an east-west trending transect in the center of the fjord from east of the Terminal to west of Shoup Bay (Figure 13; Blanchard et al., 2005; Shaw et al., 2005). But only one of these sites, D51, is located near enough to AMT to provide a point of comparison between the programs.

And yet, direct comparisons of PAH profiles between EMP and LTEMP are difficult at best since the EMP primarily just analyzes EPA's PAH priority pollutants, an abbreviated analytic suite designed more to regulate the discharge of hazardous pollutants than to monitor and identify oil contaminants. Numerous analytes are not analyzed in the EMP data that are reported by the LTEMP program (notably the alkylated homologues, which are in fact the dominant PAH constituents in crude oil and refined petroleum products). For source characterization, the extra detail in the LTEMP data (Figure 14) allows us to see that one of the three sediment replicates from the July 2004 sampling (Rep. 3)

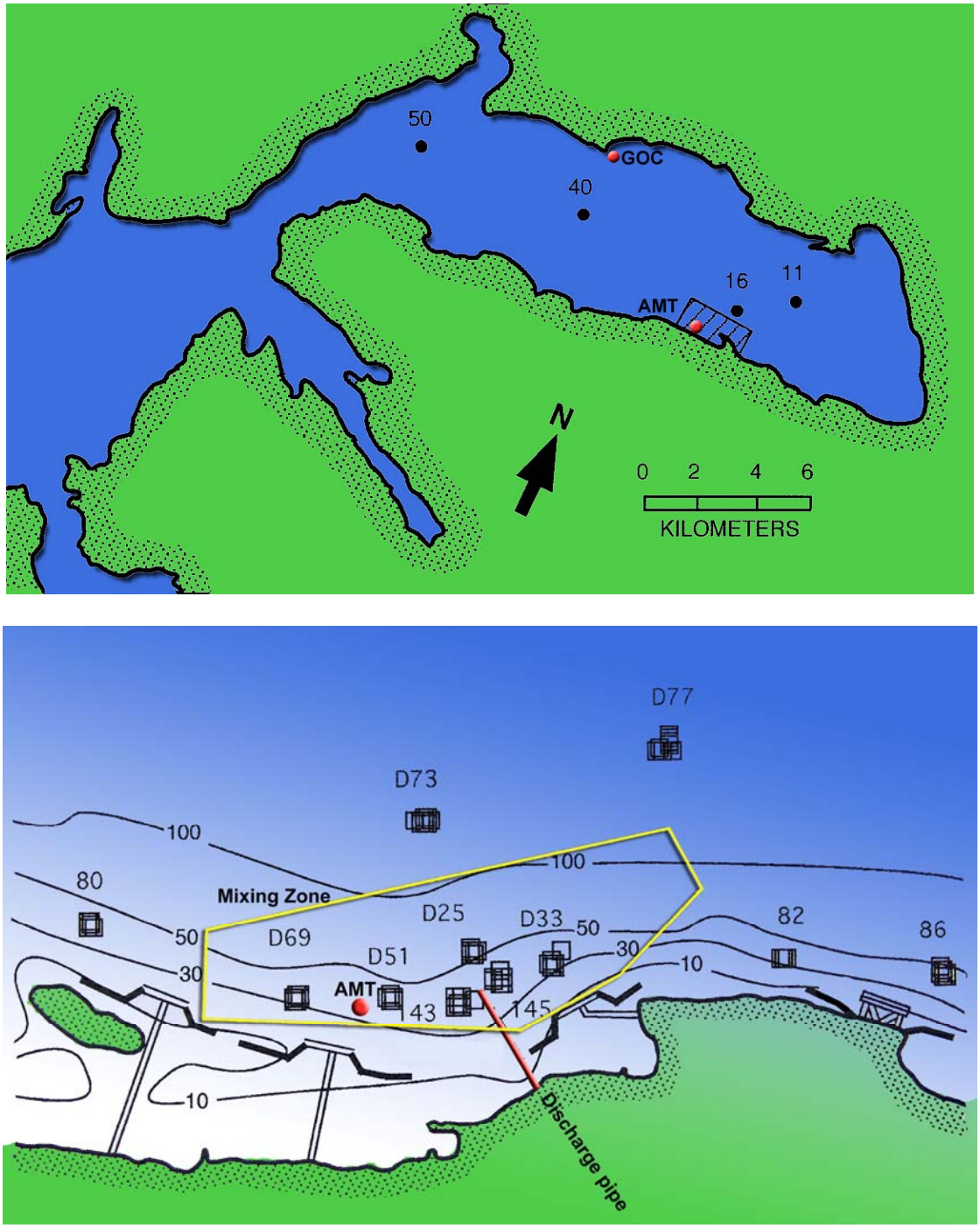

Figure 13 Alyeska Environmental Monitoring Program (EMP) sampling station locations in Port Valdez (upper) and surrounding the BWTF diffuser at the Alyeska Marine Terminal (lower). The irregular hexagon shown in yellow depicts the mixing zone defined by EPA Permit for BWTF effluent discharges; the red dots are LTEMP sites. (Graphics adapted from Shaw et al. 2005.)

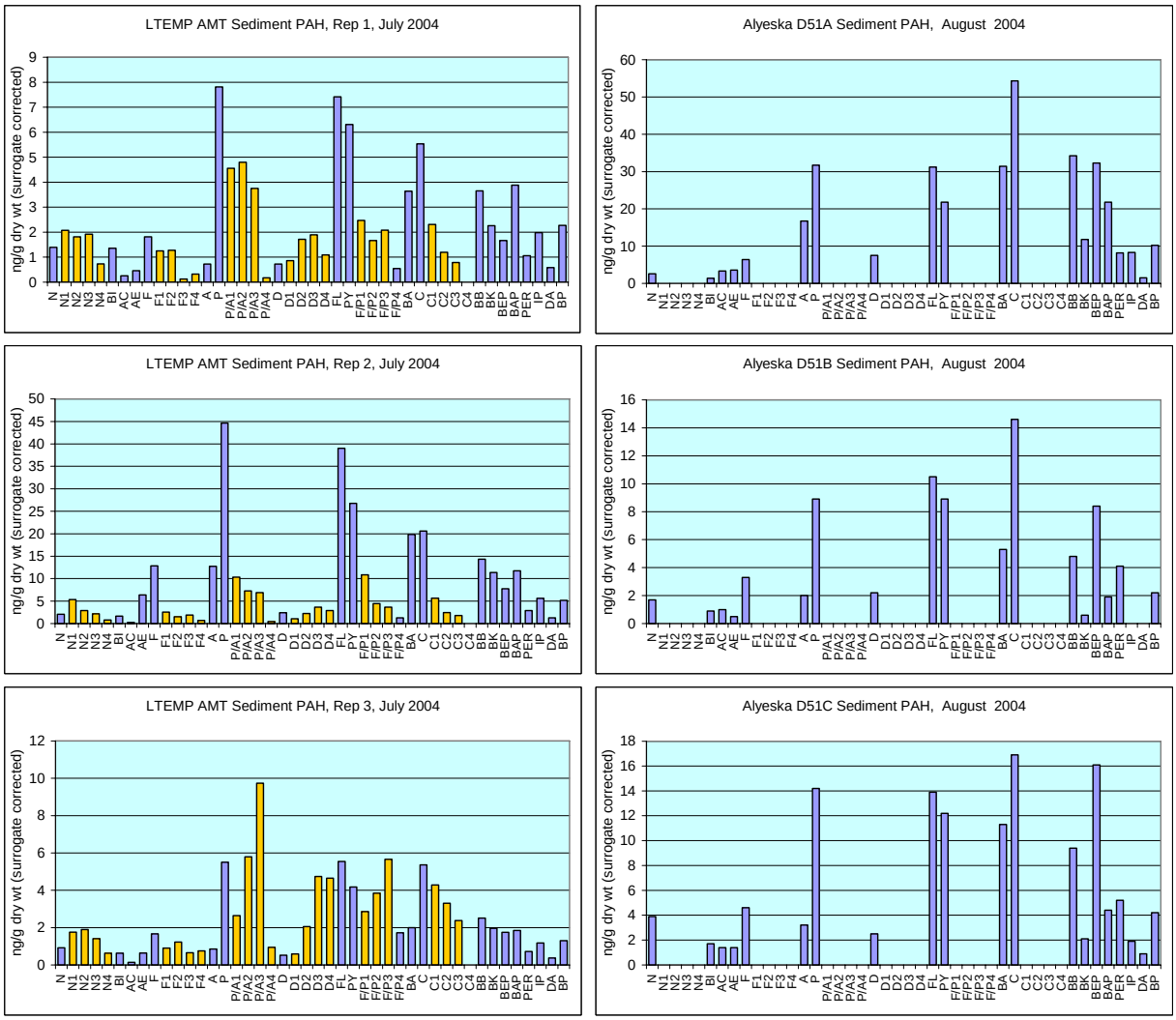

Figure 14 Comparison of LTEMP (left) and Alyeska EMP (right) sediment data from summer 2004 replicate samples obtained at the Alyeska Marine Terminal (AMT). The alkylated components shown in gold in the LTEMP samples are not reported in the EMP.

contains more petrogenic components compared to the other two replicates. Note that we prefer to do source characterization on each sample without averaging the data into a potentially hybrid signature (discussed above). The LTEMP Rep. 3 petrogenic signal is indicated by the increasing concentrations (ascending steps) of higher-alkylated phenanthrenes/anthracenes (P/As), dibenzothiophenes (Ds), and fluoranthenes/pyrenes (F/Ps), in addition to the combustion products discussed above. These components may suggest the inclusion of a free oil droplet in that sample, thus creating more of a mixed petrogenic and combustion-derived profile. In summary, the data averages in Figure 11 indicate 75% of the PAH were derived from combustion products with 22% coming from

the particulate/oil-droplet phase. In contrast, without the alkylated homologues, the sparser data of the three Alyeska EMP samples (Figure 14) can only be interpreted as possessing a pyrogenic pattern.

To better equate comparisons between the two programs, we re-graphed the LTEMP AMT data (Figure 15) using just those analytes measured in the Alyeska EMP program. With this adjustment, both programs' samples display similar results (phenanthrene, fluoranthene, pyrene, and chrysene predominate) but there are still differences in the relative abundance of these constituents. Also, as noted above, this particular analyte

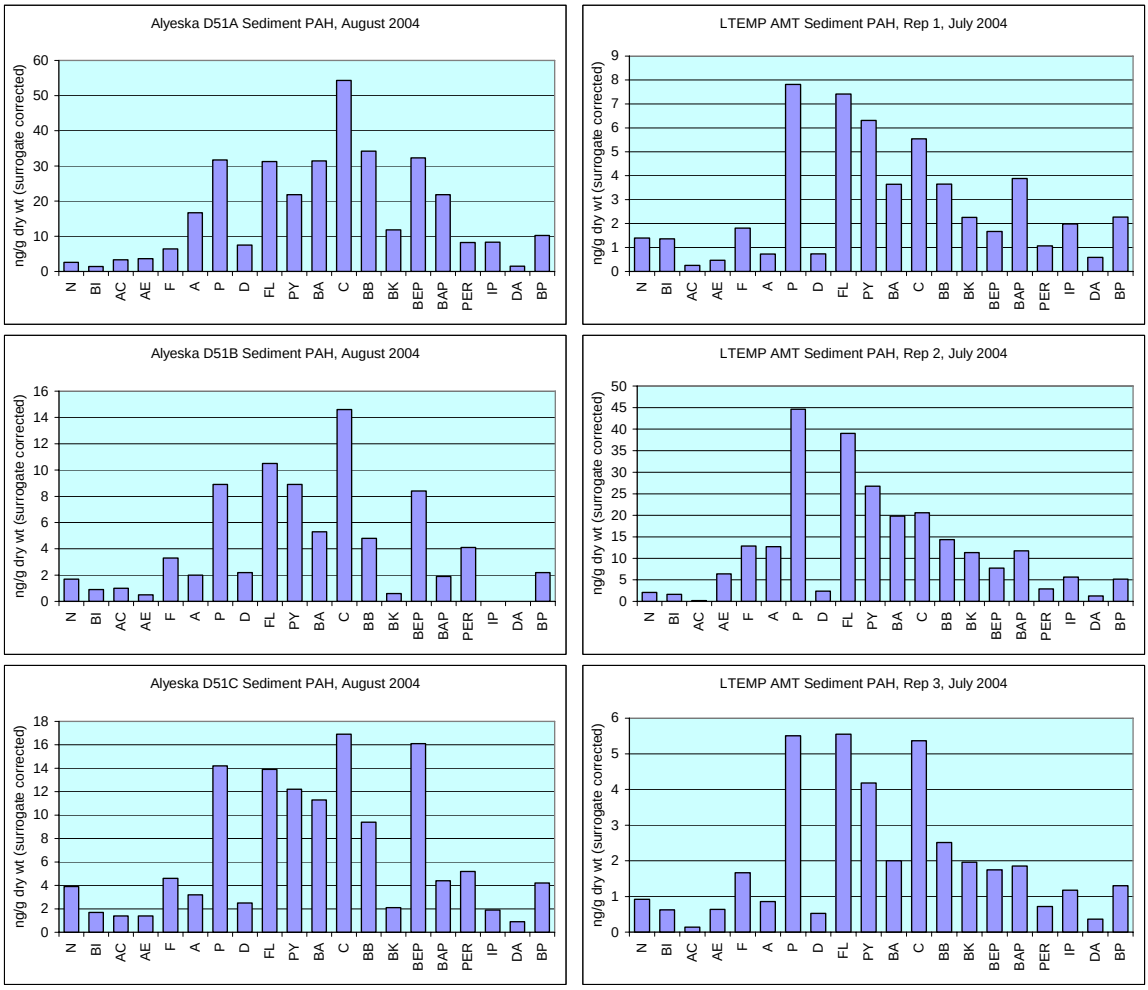

Figure 15 EMP sediment D51 (Aug. 31, 2004) PAH profiles compared to the abbreviated LTEMP sediment plots (July 28, 2004).

suite biases the data by diminishing the petrogenic signal and emphasizing the contribution from pyrogenic components. Nevertheless, based on all the EMP data, including the definitive hopane biomarkers, we concur with the EMP findings that the

AMT signal from the diffuser source is being detected in most of the shallower sediment samples below the irregularly shaped mixing zone (Figure 13) and to a more limited extent elsewhere in deeper Port Valdez sediments (Blanchard et al., 2005; Shaw et al., 2005). The AMT signal did not appear at EMP stations 11 or 16, but traces of the signal at decreasing concentrations with increasing distance from the diffuser could be observed as far away as EMP sites 40 and 50 (Figure 13).

5.2.3.2 Gold Creek

Just as in the sediment samples from the Alyeska Marine Terminal, there has been considerable variability in the TPAH values at GOC in the past, but the overall TPAH concentrations are generally five-to-ten times lower at GOC (lower panels Figure 11). And just like AMT, the GOC sediments show declining TPAH levels since July 2003 (right-hand graphs Figure 11); however, the overall TPAH levels appear to track primarily with the pyrogenic (combustion) fraction whereas they were almost exclusively driven by the particulate/oil-phase at AMT. The relative composition data (lower right Figure 11) show that while the combustion- and particulate/oil-derived constituents in Gold Creek sediments appear to be declining since March 2002, the relative contributions from more soluble, lower-molecular-weight constituents, are higher in July 2003 and March 2004 (36 to 46%). Even with this apparent increase, however, it is important to note that the overall TPAH levels are very low (< 50 ng/g dry weight since July 2002), and in that context we should caution that at very low levels the relative proportional signals can become pretty noisy.

As with the AMT results, we cannot tell from these data if the water-soluble constituents are truly dissolved, i.e., in interstitial water and therefore, more readily bioavailable, or bound up with the sediments themselves. Based on the bar plots (Figure 16), the more water-soluble naphthalenes (shown in turquoise) are present at higher concentrations in March 2004, but even in March 2005 (where they are generally at or just below the MDL), they still constitute a major fraction of the identified PAH. Dominant naphthalenes have been observed elsewhere throughout Prince William Sound (EMAP data; Susan Saupe, 2006) and in eroding coal and source rock (Short et al. 1999, Boehm et al. 2001) so they are most likely associated with the solid sediment particles and not present as a truly dissolved phase. The prominent phenanthrene, fluoranthene, pyrene, and chrysene compared to their respective alkylated homologues (shown in fuchsia) also confirm the presence of combustion products as reflected by their 51-57% contributions (bottom left-hand graph Figure 11).

The SHC profiles (Figure 16) show significant contributions from terrestrial detritus and odd-carbon-number vascular plant waxes (n-C25, n-C27, n-C29, n-C31) in addition to minor (below MDL) even- and odd-carbon numbered n-alkanes between n-C16 and n-C22 plus phytane, which reflect low-level petrogenic input, and n-C15 and pristane from marine phytoplankton and copepods (Blumer et al., 1964; NRC 1985; Short 2005).

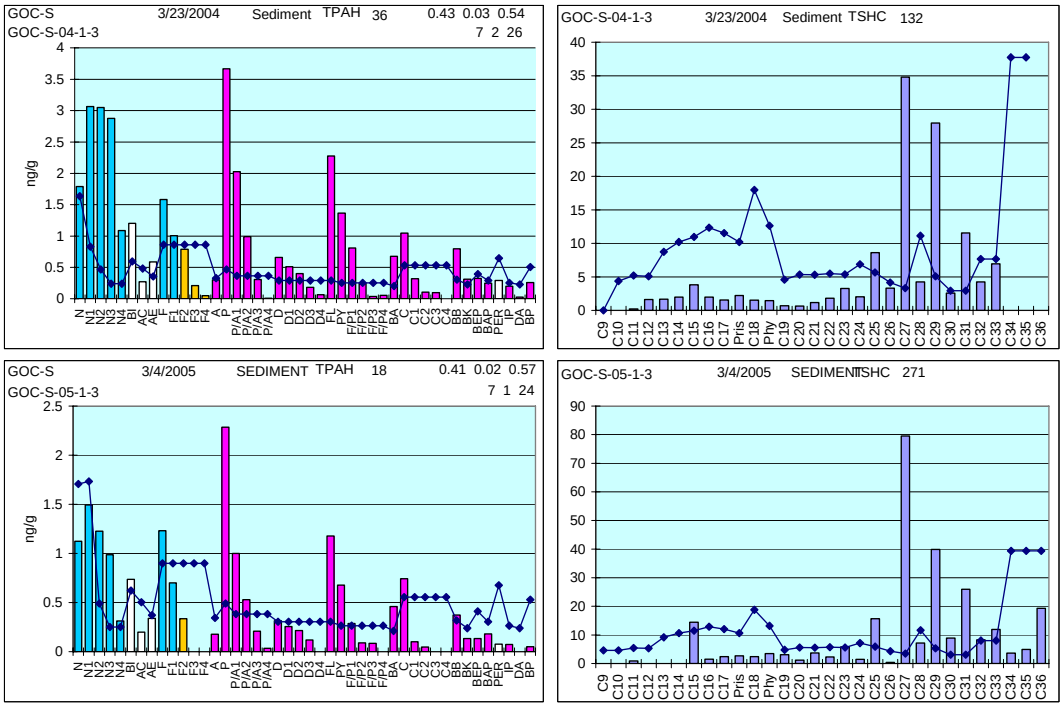

Figure 16. Bar plots of PAH and SHC data for March 2004 and March 2005 Gold Creek sediments. More water soluble constituents are shown in turquoise while pyrogenic (combustion) products are shown in fuchsia.

Without additional sterane and triterpane data, it is impossible to determine if the very minor petrogenic signal observed in the sediments at Gold Creek can be attributed to input from the Alyeska Marine Terminal; however, as noted above, Shaw et al. (2005) concluded from their triterpane data that the sediment profiles at EMP Stations 40 and 50 (Figure 13) contained petrogenic components derived from Alaska North Slope crude oil.

As before, it is difficult to directly compare EMP and LTEMP data because of the different number of analytes considered in the two programs, but data from September 2004 EMP station 40 (the closest to the LTEMP Gold Creek site but at greater depth) and the average PAH profiles from GOC collected in July 2004 show similarities (Figure 17) using either the reduced LTEMP analyte suite (left panels) or the full suite (right panels).

While there are some subtle differences in the abbreviated LTEMP and EMP plots (left panels Figure 17), they are similar enough to demonstrate that comparable data are being obtained by the two programs, and to confirm the minor presence of ANS oil in the GOC sediments. Based on the relative proportions (Figure 11), we estimate that less than 25% of the total PAH signal in the July 2004 GOC sediments may be derived from petrogenic sources. In addition to ANS crude oil from the BWTF, other possible sources include marine vessel traffic in Port Valdez (tankers, fishing vessels and recreational boaters), snow removal, street runoff and treated sewage discharges from the city of Valdez, and petrogenic components in eroded sediments from Mineral Creek and Gold Creek.

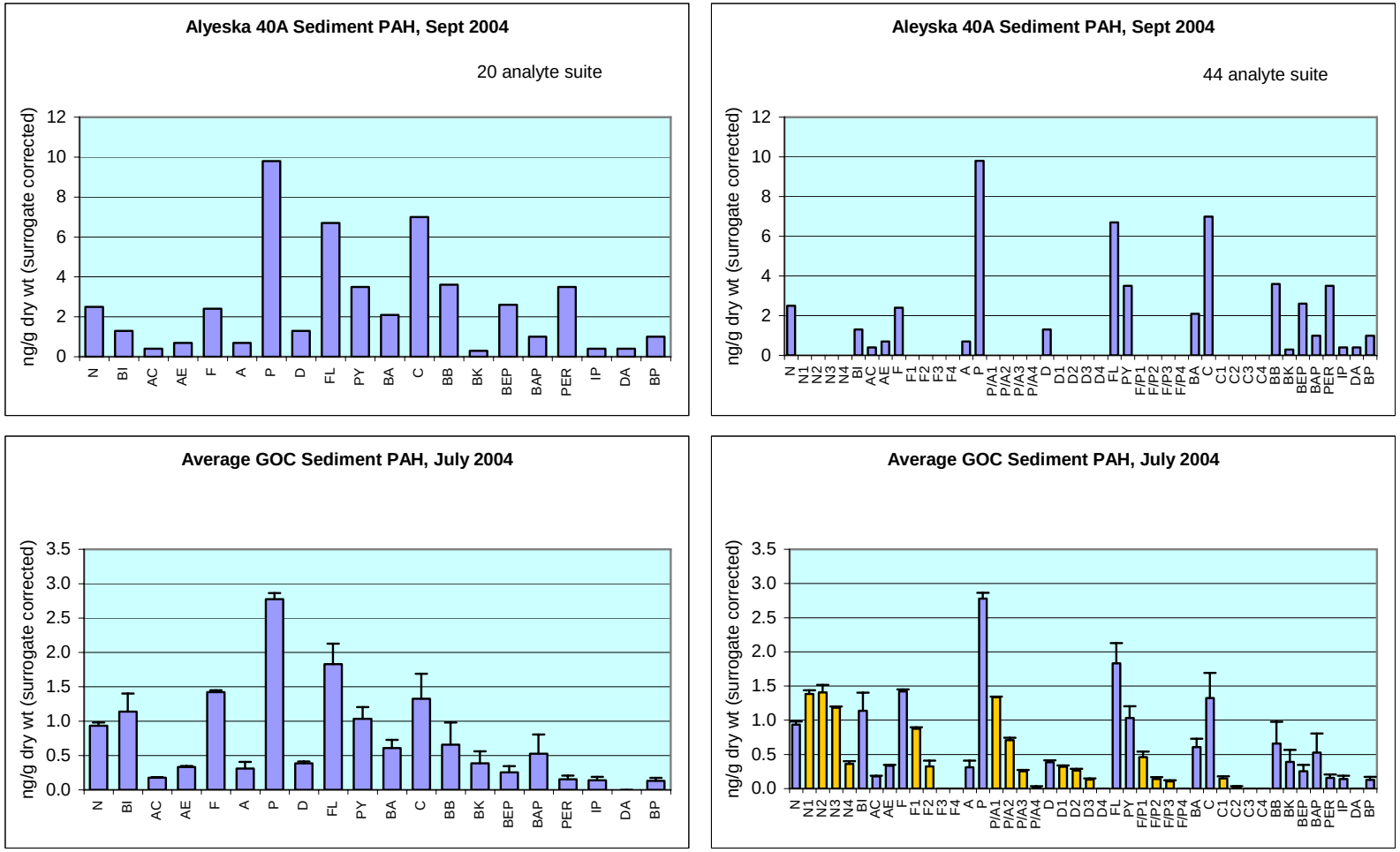

Figure 17. PAH profiles from Alyeska's EMP Sediment Station 40 compared to the same analytes from LTEMP's Gold Creek site (left). On the right, the same samples, using the LTEMP analyte suite, present a more detailed signature and highlight data not reported by EMP (shaded in gold). From this signature, the PAH show a dissolved oil source mixed with combustion products.

5.2.4 Broader Findings from the Alyeska EMP Program

The Alyeska EMP findings put the LTEMP Port Valdez results into a larger perspective. EMP time series of infauna data and hydrocarbon levels suggest local impacts occurred directly around the diffuser, but further from the source they see only natural variation in infauna and background hydrocarbons (Blanchard et al. 2005). Additional findings include:

> "Hydrocarbon concentrations in shallow water sediments near the Marine Terminal are greater than those in sediments in deeper water distant from the terminal."
>
> "Statistical analyses indicate that higher concentrations of hydrocarbons occur in sediments near the effluent discharge but since 1989, the magnitude of the increase in concentration has become smaller. This is supported by the trends in geostatistical and contrast analyses. Significant relationships of PAH summary measures to TOC and depth suggest that accumulations in sediments are directly related to these variables. Comparisons between years and the geostatistical analysis also suggest that hydrocarbons are not high in 2004 compared to previous years studied."
>
> "Factors such as bottom topography and currents lead to complex sedimentation patterns in Port Valdez. In addition, the variation in PAH concentrations in sediments is influenced by the fact that sedimentation rates are higher in eastern Port Valdez than in the west. This natural sedimentation of glacial material, which is very low in TOC and PAH, acts to selectively lower PAH and TOC concentrations in sediments of the eastern Port. Hydrocarbon concentrations often show a significant relationship with sediment grain size with finer grained sediments having greater hydrocarbon concentrations. The failure to detect *[this expected]* significant relationship between summary measures of PAH concentration and grain size parameters in Port Valdez sediments probably reflects the narrow range of sediment grain size distributions in the sediments sampled."
>
> "The faunal community near the diffuser demonstrates ecologically minor adjustment in the presence of residual hydrocarbons in effluents. The minor adjustment of two sensitive polychaete worms provides evidence that effluents may be directly or indirectly influencing fauna, but overall, the faunal variations are small and driving factors are not fully understood. Other factors important to the distribution of fauna in Port Valdez include depth and TOC. Considering the decreasing concentrations of sediment hydrocarbons over time and the increasing percentages of sensitive taxa on the shelf (as shown by the inverse relationship of TARO and percent sensitive species in the plots from the geostatistical analysis), it appears that the influence of hydrocarbons on fauna near the diffuser is small and decreasing."

5.2.5 Sediment Chemistry Summary

From examination of all the PAH data from both sediment-sampling sites, it is clear that the Alyeska Marine Terminal subtidal sediments are primarily contaminated by a weathered ANS oil signal, which would be consistent with BWTF-diffuser-sourced, dispersed oil-droplet/suspended-particulate-material (SPM) interactions and resulting sedimentation (Payne et al. 1989; 2003a,b). The Gold Creek sediments, on the other hand, show PAH contamination from combustion (pyrogenic) sources with lesser contributions from low-level petrogenic sources. It is not possible to tell from LTEMP data alone if the low-level petroleum source in the subtidal sediments at Gold Creek is from the BWTF and other activities at Alyeska Marine Terminal, or other sources (boat traffic, sewage and wastewater discharges from the City of Valdez). It may be possible to identify this source through sterane/triterpane analyses of Gold Creek sediments and comparisons to Alyeska Marine Terminal sediments and Alyeska BWTF discharges as part of future LTEMP or other PWS RCAC research activities. Triterpane data from the Alyeska EMP indicate that PAH from their station 40 (deeper and further offshore from the LTEMP GOC station) are consistent with weathered Alaska North Slope crude oil released from the terminal (Shaw et al., 2005).

The SHC patterns observed for the subtidal sediments at Alyeska Marine Terminal (Figure 12) show a combination of biogenic and very weathered ANS oil signals, again consistent with terrestrial and marine copepod fecal-pellet sources along with substantial oil-droplet/SPM interactions given the elevated levels of dispersed oil droplets introduced to the region from the BWTF diffuser (Payne et al. 2001; 2003a,b; 2005b,c; Salazar et al. 2002; Short 2005). In contrast, the SHC profiles from the subtidal sediments at Gold Creek (Figure 16) show a combination of marine and terrestrial biogenic input, with very little weathered-oil signal in keeping with the extremely low TPAH values observed at the site.

5.3 Mussel Tissue Chemistry

5.3.1 Regional Trends and Approaches

The time series of TPAH data (Figure 18) using the consistently reliable post-1997 data shows generally decreasing trends with a subseries of somewhat synchronous peaks along the timeline. The generally simultaneous TPAH maxima occurred in July 1999, March 2001 (excluding Aialik Bay, Shuyak Harbor, and Windy Bay), March 2002 (again except for Shuyak Harbor and Windy Bay), and July 2002 (for Aialik Bay and Windy Bay only – all the other sites are dropping). These events have been discussed in previous reports couched as possibly ambiguous results or perhaps laboratory artifacts. Using the recently-developed PAH indices, however, we have noted that not only were there synchronous peaks, but in many of the stations, the composition of the signatures were also similar. After further exploration, three regional patterns became apparent; the Port Valdez, Prince William Sound, and Gulf of Alaska regional stations were each trending in similar fashion (Figure 19) and often with regionally similar, low-level

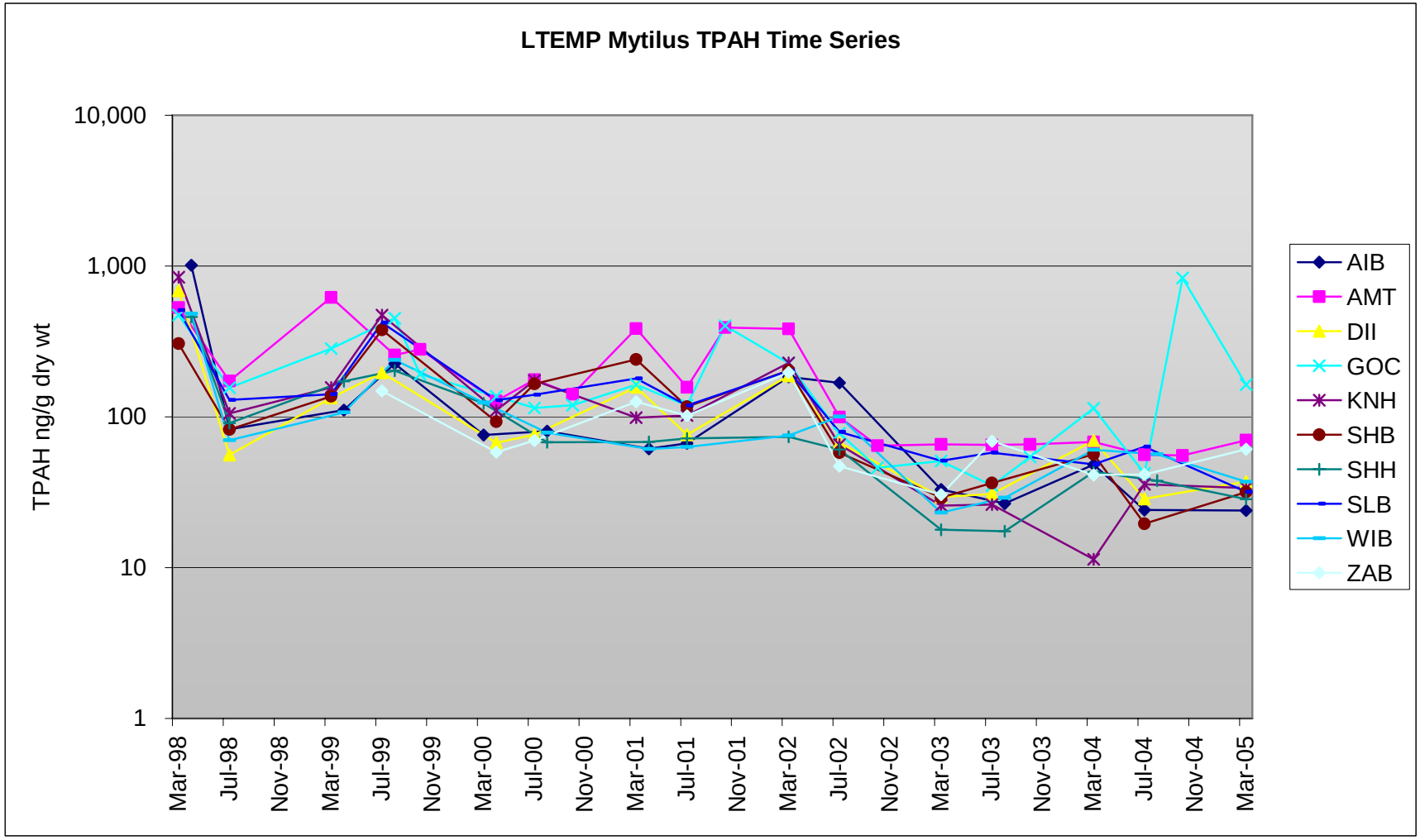

Figure 18 Mytilus TPAH time series (triplicate averages) for all LTEMP stations, 1998-2005.

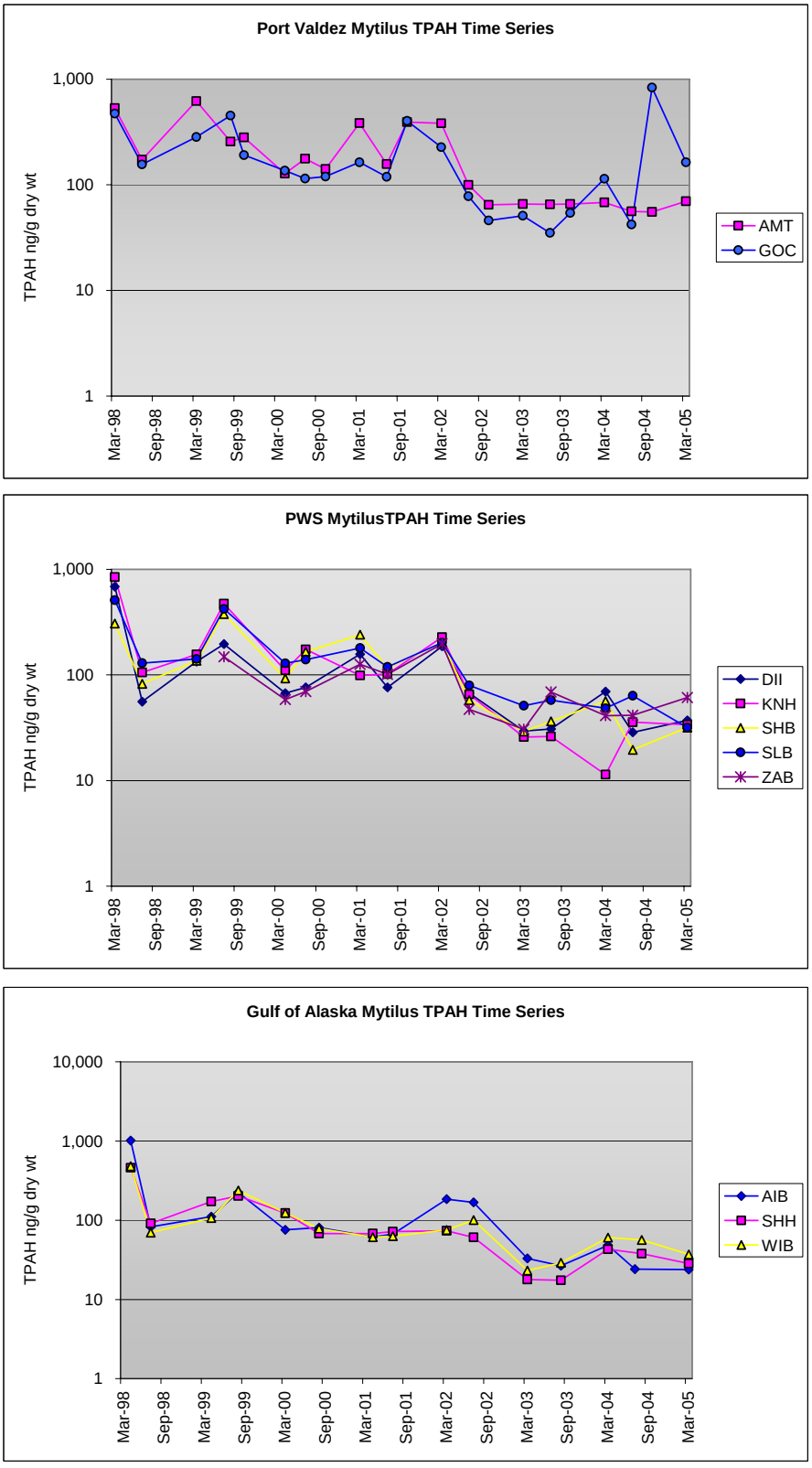

Figure 19 Regional LTEMP Mytilus TPAH time series, 1998-2005.

dissolved signals (Table 6). These trends and similarities will be discussed further below, but their discovery prompted us to organize the following sections on mussel tissue chemistry by regions (Figure 19).

This report greatly expands on our previous approach of examining the TPAH data from the perspective of dissolved- and particulate/oil-phase signals. Specifically, when analyzing the LTEMP mussel tissue samples, it is important to recognize that as filter feeders, mussels can accumulate an oil signature from both the dissolved- and particulate/oil-droplet phases, in addition to combustion products (soot) present as finely suspended pyrogenic particles in the water column (Baumard et al. 1998; Payne and Driskell 2003). Using the recently developed dissolved-, particulate-, and pyrogenic indices described in Section 4.7.1, we graphically review in this section the mussel-tissue, time-series trends for each site (as shown in Figure 20 for Alyeska Marine Terminal and Gold Creek), and augment that discussion with PAH and SHC graphs to further elucidate source signatures as necessary. Recall from Section 4.7.2, data in which we have confidence are represented by solid symbols, while the early samples where procedural artifacts are suspected (1993-1997) are left in context but represented only by finely-dashed lines.

The dual-axis data in the left-hand panels (Figure 20) show the relative percentages of the total PAH (TPAH) from the soluble, particulate (oil phase), and pyrogenic fractions (left axis) as well as the TPAH value (on a logarithmic scale – right axis). The right-hand panels present the same data simply as total concentrations (ng/g dry weight on a linear scale) for each fraction. In the right-hand panels, the sum of the soluble, particulate, and pyrogenic fractions equals the total PAH (dark fuchsia-colored circles). This dual-presentation format allows overall trends to be easily identified with the absolute magnitude of each fraction shown in the right-hand panels, while finer details on relative contributions from the different fractions can be tracked in the left-hand panels.

In our report for the 2003-2004 program (Payne et al., 2005a), a complete review and detailed discussion of the tissue chemistry data from all stations sampled over the first eleven years of the program was presented in Appendix A-3 – Station Accounts for Tissue Samples; the interested reader is directed to that report for additional information. Appendix B-1 of this document tabulates the total SHC and PAH values of individual tissue samples, sampling averages, and the associated coefficients of variation for the replicate measurements completed between 1993 and 2005. Appendix B-2 does the same for the PAH indices. The following three sections briefly consider the time-series trends noted for the three regions depicted in Figure 19 and Table 6. Section 5.3.2 presents the mussel tissue chemistry results for Port Valdez, including Alyeska Marine Terminal (AMT) and Gold Creek (GOC). Section 5.3.3 presents the mussel tissue chemistry results for inner Prince William Sound, including Disk Island (DII), Knowles Head (KNH), Sheep Bay (SHB), Sleepy Bay (SLB) and Zaikof Bay (ZAB). Section 5.3.4 presents the mussel tissue chemistry results from the outermost Gulf of Alaska stations, including Aialik Bay (AIB), Shuyak Harbor (SHH), and Windy Bay (WIB).

Table 6 Time series TPAH peaks at LTEMP regional stations showing similarity of local signals

	Jul-99	Mar-01	Mar-02	Jul-02	Jul-04
PWS Stations					
Disk Island (DII)	Peak Dissolved	Peak Dissolved	Peak Dissolved	Peak Dissolved	Low Level Particulate
Knowles Head (KNH)	Peak Dissolved		Peak Dissolved	Peak Dissolved	Low Level Particulate
Sheep Bay (SHB)	Peak Dissolved	Peak Dissolved	Peak Dissolved	Peak Dissolved	Low Level Particulate
Sleepy Bay (SLB)	Peak Dissolved	Peak Dissolved	Peak Dissolved	Peak Dissolved	Low Level Particulate
Zaikof Bay (ZAB)	?	Peak Dissolved	Peak Dissolved	Peak Dissolved	Low Level Particulate
Gulf of Alaska Stations					
Aialik Bay (AIB)	Peak Dissolved	Low	Peak Dissolved closer to SLB	Peak Dissolved	Low Level Particulate
Shuyak Bay (SHH)	Peak Dissolved	Low Dissolved	Low Dissolved		Low Level Particulate
Windy Bay (WIB)	Peak Dissolved	Low Dissolved	Low Dissolved	Peak Dissolved	Low Level Particulate
Port Valdez Stations					
Gold Creek (GOC)	Peak Particulate				
Alyeska Marine Terminal (AMT)			Peak Particulate	Peak Particulate	

Peaks and lows from Figure 19. Dominant PAH phase is identified by Dissolved or Particulate.

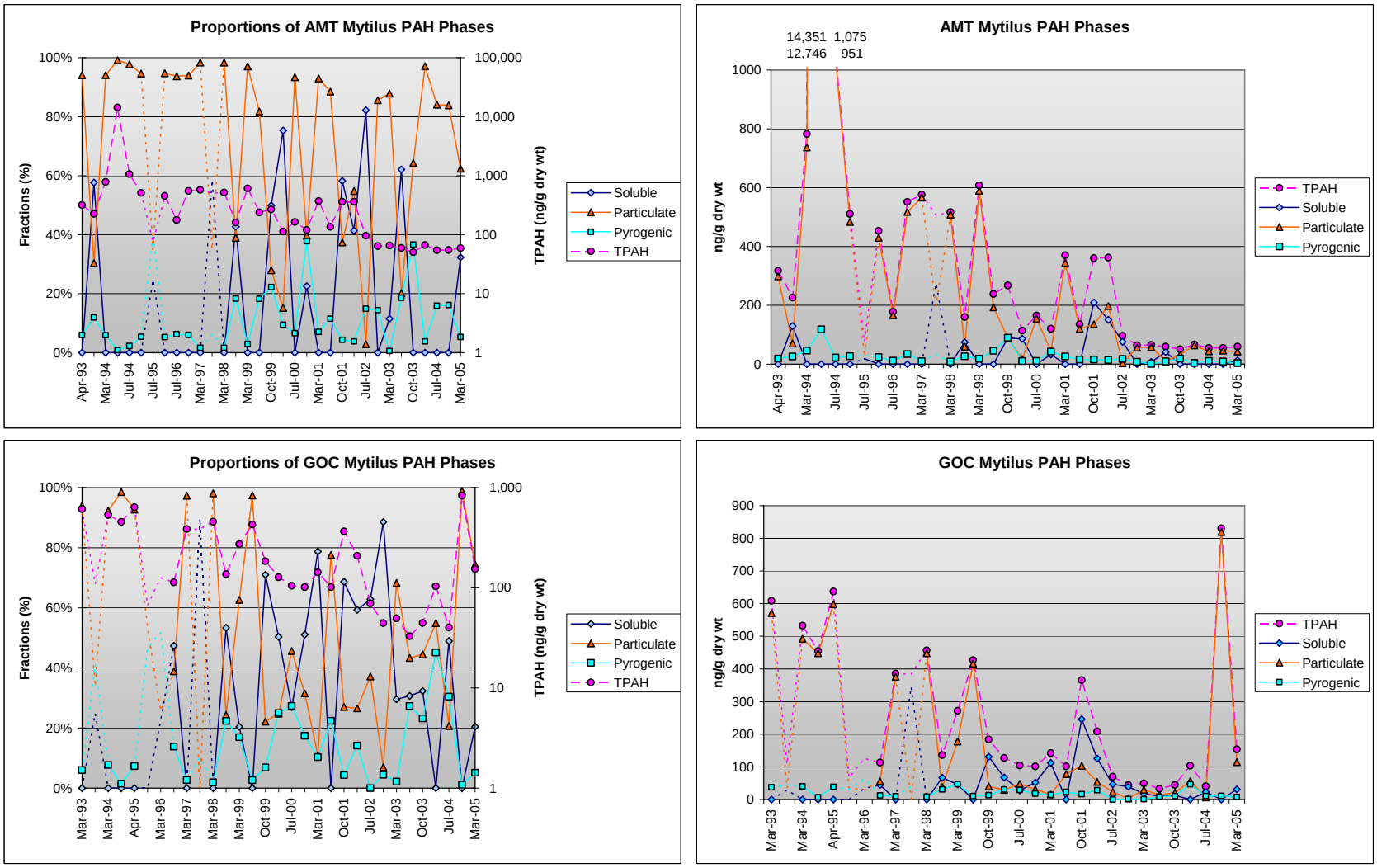

Figure 20 Time series trends of PAH indices from AMT and GOC Mytilus tissues. Dotted connecting lines without symbols indicate questionable data.

5.3.2 Port Valdez Stations

5.3.2.1 Alaska Marine Terminal Mussel Tissue Chemistry

Mussels collected from Saw Island, adjacent to berth 5 at the Alyeska Marine Terminal (AMT), have historically contained the highest and most variable TPAH concentrations of any site in the program (top Figure 20). These values reflect input from the daily discharge of treated ballast water from the terminal as well as known spill events, such as the *T/V Eastern Lion* oil spill in May 1994 and the BWTF spill/sheening event in January 1997. Immediately after the May 1994, *Eastern Lion* oil spill, extremely high TPAH levels in excess of 14,300 ng/g dry weight were measured with >99% derived from the particulate/whole-oil droplet phase. By July 1994, the TPAH level dropped to 1,075 ng/g, with the particulate/oil-phase still contributing >98% of the total. Elevated TPAH values were still observed in April 1995 (511 ng/g) with 95% of the PAH signal from the particulate/oil-phase and 5% from combustion products (Figure 21). The oil signal then disappeared by July 1995 with only a soluble fraction and combustion products inferred from the PAH profiles. These data probably were procedural (laboratory) artifacts (represented by the dashed lines in top panels of Figure 20), but they do suggest that only a low-level signal was present.

Reliable data from March 1996 indicated that the TPAH level had stabilized around 430 ng/g with the majority of the TPAH derived from the particulate/oil-phase, and in July 1996, the particulate/oil-phase-dominated TPAH signal dropped to 166 ng/g. In January 1997 after the BWTF spill/sheening incident, a spike in the TPAH (551 ng/g) was observed which persisted through March 1997 with 94-98% particulate/oil-phase signal over that time frame. In July 1997, the TPAH level appeared to remain around 500 ng/g, but the PAH patterns suggested only contributions from dissolved-phase naphthalenes plus procedural artifacts. As such, the July 1997 data are not plotted in Figure 20, but it is clear from the profile data, that the dominant particulate-phase pattern from the preceding samples had disappeared. PAH profiles reflect the transition from the low-level background particulate-phase signal before the sheening event, to the distinctive PAH signature from the heavily-weathered BWTF sheen, to the dissolved-phase/procedural artifact pattern observed in July 1997 (Figure 22).

By March 1998, the TPAH levels were still around 500 ng/g, but the particulate/oil-phase signal dominated again. After that, an alternating pattern of low-high-low TPAH levels was observed through August and October 1999 (the first time fall collections at the terminal and Gold Creek were completed), and then the TPAH levels dropped to less than 200 ng/g through October 2000. Several more spikes in TPAH levels (driven almost exclusively by particulate/oil-phase signals) were observed in March 1999 and March 2001, and then after a soluble-phase spike in October 2001 and a particulate/oil-phase dominated spike in July 2002, the TPAH concentrations dropped significantly to extremely low levels (<100 ng/g) where they have consistently remained at around 60 ng/g for the last two and one-half years.

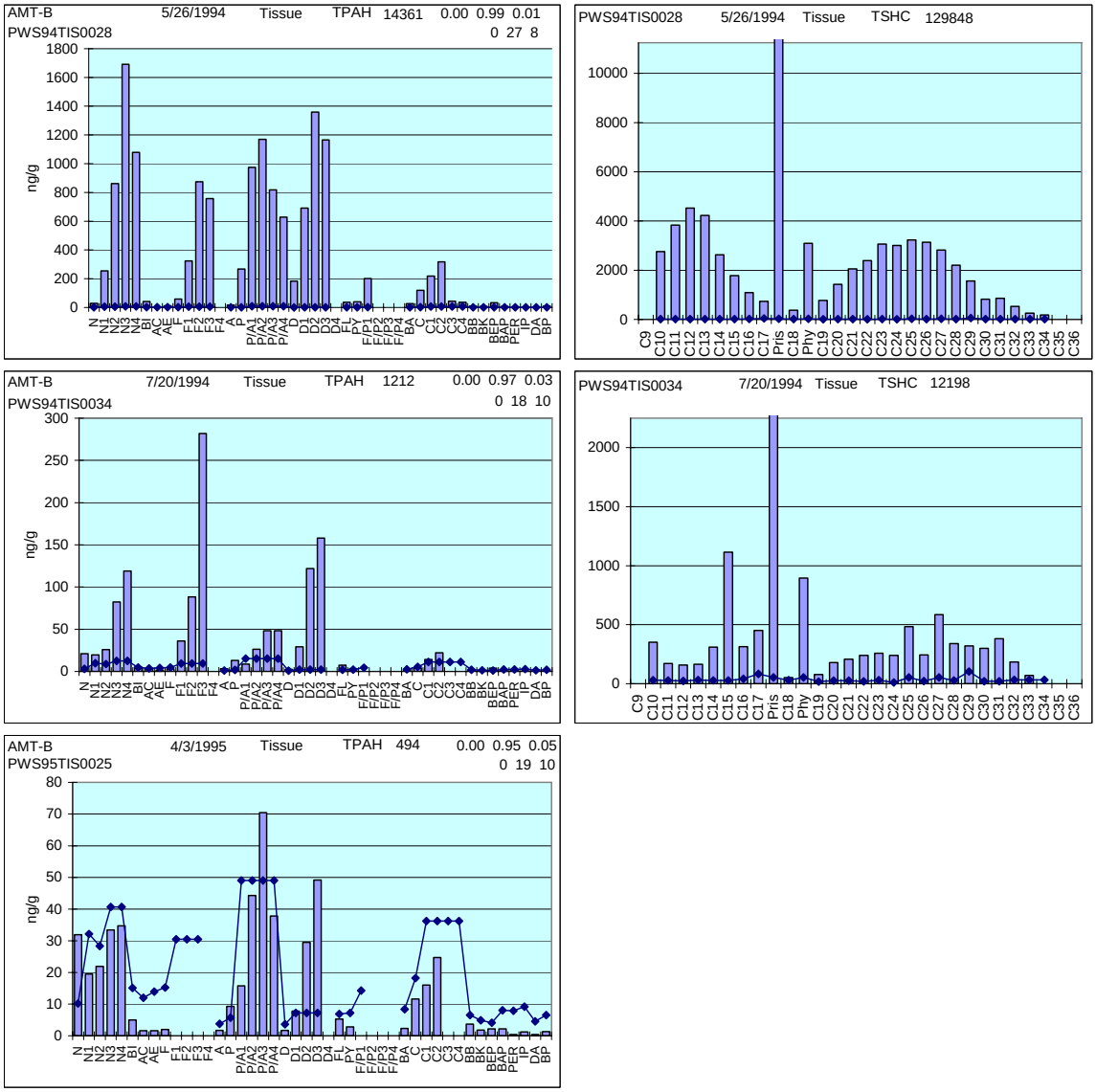

Figure 21 Representative PAH and SHC plots from May 1994, July 1994, and April 1995 AMT tissue samples illustrating the immediate and lingering signal from the *T/V Eastern Lion* oil spill. SHC analyses were discontinued in April 1995.

Soluble constituents dominated in April 2000, July 2002 and July 2003, but the particulate/oil-phase signal has made up the majority of the extremely low-level TPAH observed in all the other samples examined since October 2003 (Figure 23). Combustion products (Figure 20) have been relatively low (generally <20%) and variable over the duration of the program, although they do appear to be slighter higher during summer and fall collections. Two samples with elevated combustion-product signals (approaching 40%) were observed in October 2000 and October 2003.

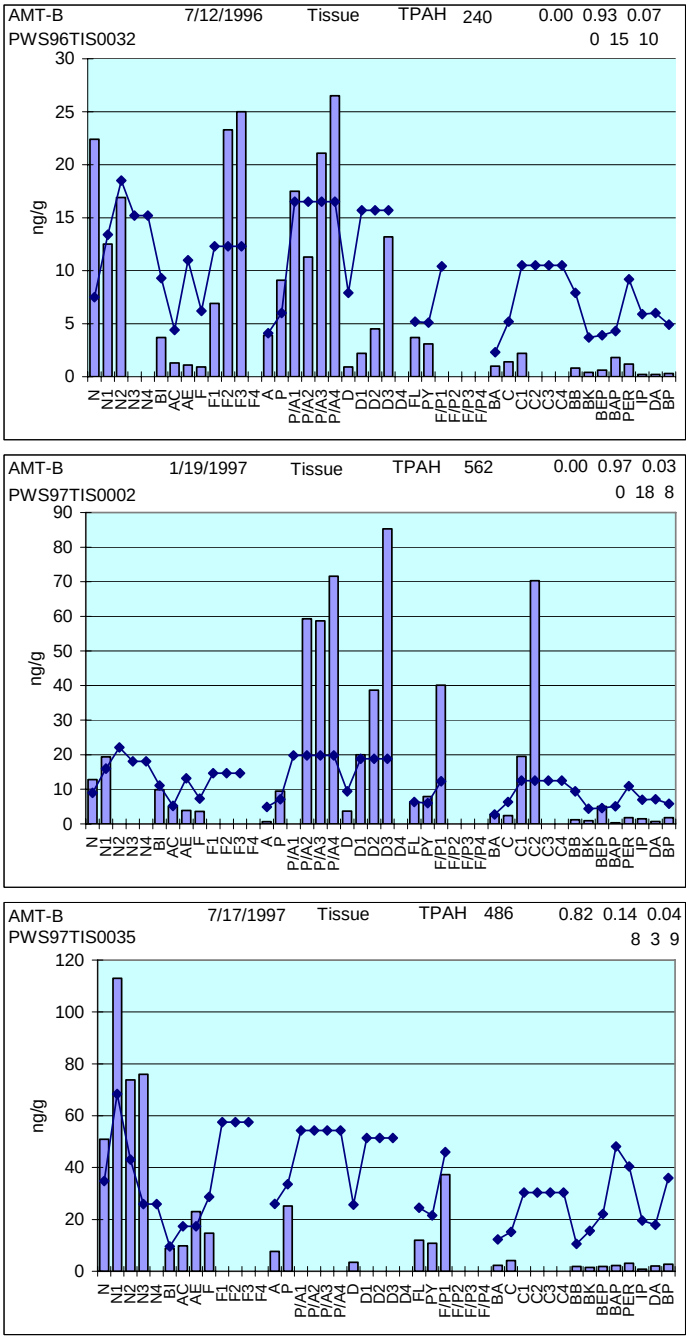

Figure 22 PAH profiles before and after the January 1997 sheening event at the AMT BWTF, and in July 1997 illustrating the dissolved-phase/procedural artifact pattern (also see Figure 5 and Figure 7).

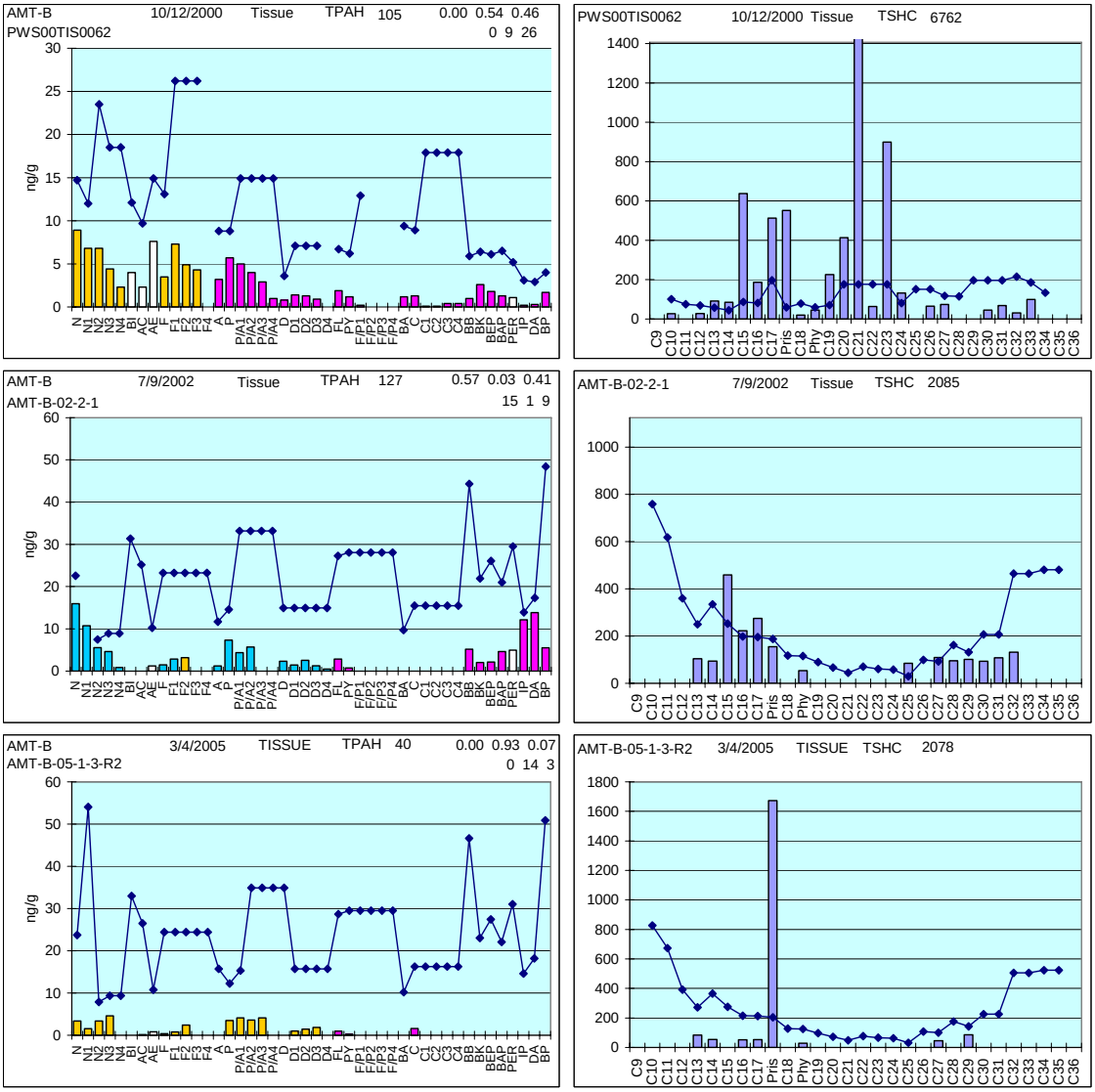

Figure 23 PAH and SHC plots of very low contaminant-level (below MDL) AMT tissue samples showing mixed-phase contributions in October 2000, primarily dissolved-phase components in July 2002, and a particulate/oil-phase contribution in March 2005. Phase coding: turquoise = dissolved, gold = particulate/oil-phase, fuchsia = pyrogenic. The SHC fractions (on the right) reflect contributions from oil droplets, marine phytoplankton, and zooplankton.

One of the most striking features of the data in Figure 20 is the alternating saw-tooth pattern for the particulate/oil phase dominating in the spring, and the soluble phase in the summer. Excluding the data from the *Eastern Lion* oil spill (which contributed higher particulate/oil-phase signals in the summer of 1994), the soluble-phase constituents were dominant in the July/August or October samples in 1993, 1995, 1997, 1998, 1999 (October only), 2001 (October only), 2002, and 2003. The particulate/oil-phase signal on the other hand, was dominant in the March/April samples from 1993, 1994 (before the *Eastern*

Lion), 1996, 1997, 1998, 1999, 2001, and 2003. The samples from April and July 2000 then reversed the pattern but switched to a pyrogenic and dissolved signal in October 2000, and the March/April particulate/oil-phase dominance re-emerged in 2001 and continued through the 2004 collections. Since March 2004, a low-level particulate/oil-phase signal has dominated in all the AMT mussel collections.

This alternating pattern of particulate/oil-phase signals being high in the spring and low in the summer/fall, led us to earlier hypothesize a seasonally-controlled entrapment of particulate/oil-phase components from the BWTF diffuser by water-column stratification during the warmer summer months allowing only water-soluble fractions to eventually reach the surface and intertidal mussel populations (Payne et al., 2001, 2003d). Relative to the receiving seawater, the BWTF effluent is warmer and less saline, so its behavior and dilution are controlled by the physical oceanography and water-column structure in the Port (Colonell 1980a,b; Woodward Clyde Consultants and ENTRIX 1987). During the period of stable water-column stratification in the Port (late spring, summer, and fall), we believe that the dispersed oil droplets released from the BWTF effluent are primarily entrained beneath the pycnocline (stratified layer) in the middle-water-column regions where they are advected and diluted into the receiving waters of Port Valdez without ever reaching the upper water column and surface layer to any significant extent. As a result, a predominantly dissolved-phase signal (Figure 20) is observed in the AMT intertidal mussels collected in the summer period. During the winter and early spring, however, when the water column is not stratified, the warmer and less-saline BWTF effluent can reach the water surface where it is likely to form a surface microlayer (Hardy 1982; Hardy et al., 1987a,b, 1990; Cross et al., 1987) containing higher levels of weathered oil-droplet-phase SHC and PAH components. Since mussels feed from the surface and upper few meters of the water column, this effect results in the predominance of the particulate/oil-phase signals observed in the intertidal mussels at Alyeska Marine Terminal and (to a lesser extent) the Gold Creek (GOC) reference station 6 km across the port during the spring LTEMP collections.

Another feature that emerges from the data in Figure 20 (particularly the upper right-hand panel) is the precipitous drop in the overall TPAH values along with significantly reduced seasonal and interannual variability beginning in July 2002. This is also coincidently when the NOAA Auke Bay Laboratory began the hydrocarbon analyses for the program. This coincidence appeared initially suspicious but the continued seasonal alteration in particulate/oil-phase and dissolved-phase signals, and equivalent or even increased TPAH levels in July 2002 samples from Aialik Bay, Shuyak Harbor, and Windy Bay compared to March 2002 data generated by GERG (discussed in Section 5.3.4) seem to rule out a systematic bias or laboratory artifact as the reason for the observed decrease in TPAH values. Also, as discussed in Section 5.1.1 on Auke Bay Laboratory quality assurance results, surrogate recoveries have been consistently very good at ABL, further reducing the probability of poor extraction efficiencies or lipid mitigation being a contributing cause.

Similar declines in sediment TPAH burdens over the last three years were discussed in Section 5.2.3.1, and although the sediment PAH profile at AMT is dominated by a particulate/oil-phase signal (presumably from whole oil droplet/SPM interactions), we also

noted an increase in the relative proportion of combustion products (also possibly suggested in the July and October 2004 mussel-tissue data shown in Figure 20). We do not know if the observed decreases in tissue and sediment TPAH burdens reflect reduced BTWF discharge volumes as more double-hulled tankers are brought into the tanker fleet, or improved BWTF efficiency at removing particulate/oil-phase PAH, or a combination of these factors.

5.3.2.2 Gold Creek Mussel Tissue Chemistry

In general, the overall levels of TPAH measured at GOC (Figure 20, bottom graphs) are slightly lower than those at AMT, but the observed peaks and valleys (concentration maxima) track with those at AMT, particularly during the early years of the program when spills or other discharges from the terminal were more frequent. Also, the same seasonally-dependent, saw-tooth pattern of alternating soluble- and particulate/oil-phase signals observed at AMT is apparent, although to a lesser extent. While many of the lower-TPAH level samples (July 1993, July 1995, March 1996, and July 1997) were subject to the procedural artifact issues discussed in Section 4.7.2 (shown as dashed lines without solid data points in Figure 20), the data for the elevated PAH levels were judged to be of good quality and appear to be related to the known spill events at the terminal.

The elevated TPAH values in March 1993 and March 1994 are due primarily to particulate/oil-phase constituents and track with similar TPAH and compositional spikes observed at the same time at the Alyeska Marine Terminal. The elevated TPAH in July 1994 and April 1995 are most certainly associated with weathered oil residues from the *Eastern Lion* oil spill with over 90% of the signal derived from the particulate/oil-phase (Figure 24). The lighter-molecular-weight constituents are subsequently lost to weathering, but the residues from the spill are still apparent in April 1995 (Figure 24).

The next elevated spike in TPAH levels at GOC occurred in March 1997 (376 ng/g and 97% particulate/oil-phase), and here again, nearly identical PAH profiles were obtained at AMT and GOC suggesting residual oil from the BWTF sheening incident as the source (Figure 25). This parallel trend between the two stations generally appears to continue through October 2001 (Figure 20) when another spike in TPAH was noted at both AMT and GOC, but in this case, the signal appears to be primarily derived from the soluble phase (Figure 26). Perhaps this reflects an increased BWTF discharge event.

After October 2001, the TPAH levels at GOC are observed to uniformly decrease to extremely low levels (Figure 20), and notwithstanding the aforementioned spikes associated with specific pollution events at the terminal, the overall trend at GOC appears to be to lower and lower levels through July 2004. In October 2004, however, the TPAH concentration spikes to the highest levels ever recorded at GOC (830 ng/g), due to a diesel spill which occurred sometime between the July and October 2004 samplings. One possible source might be fishing vessels, which before openings, anchor at GOC instead of Valdez Harbor; in July 2005, fishing vessels were anchored in the bight east of GOC Point.

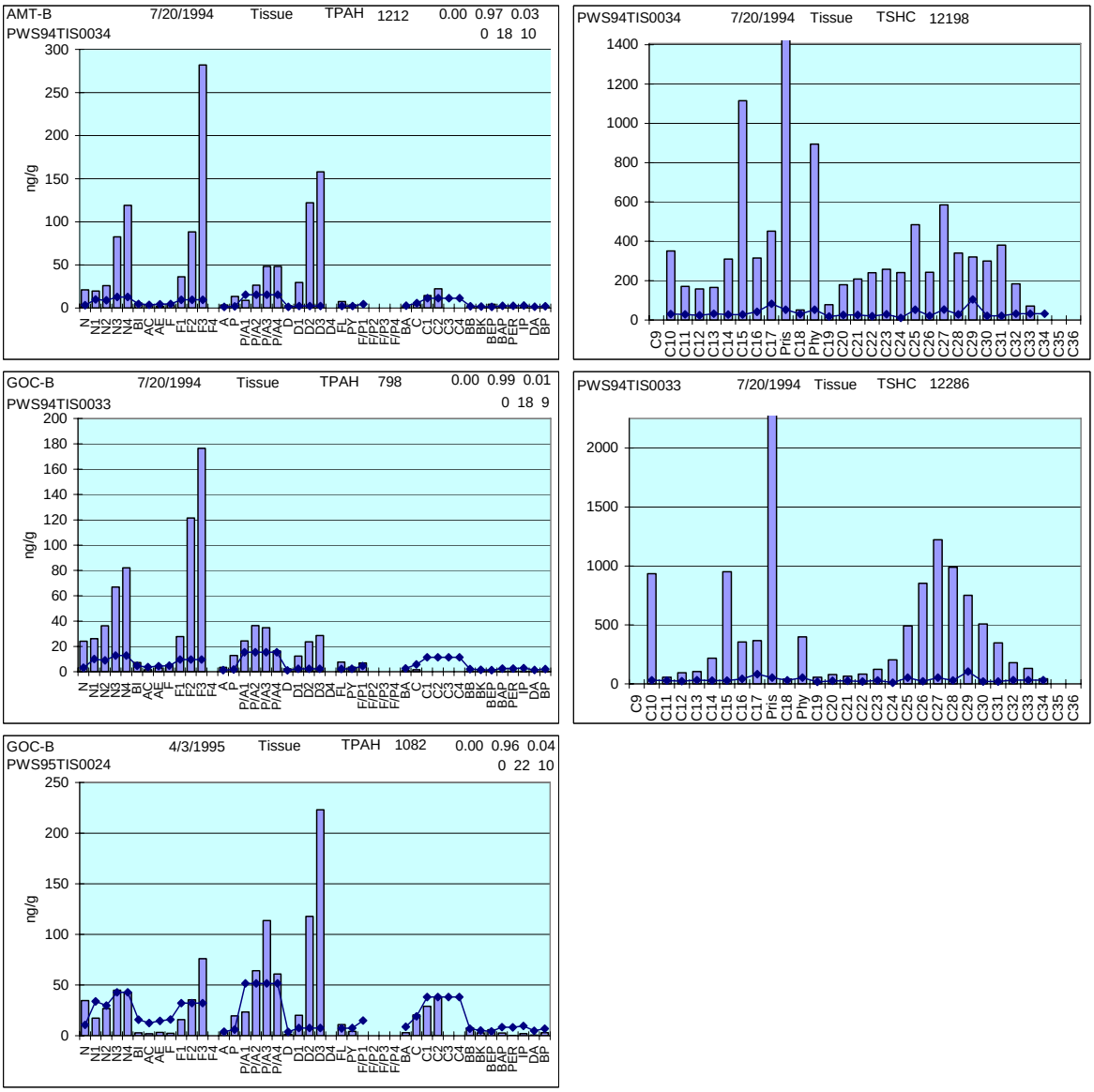

Figure 24 PAH and SHC profiles showing residues from the *Eastern Lion* oil spill at AMT and GOC in July 1994 and GOC in April 1995. SHC analyses were discontinued in 1995.

Evidence of the residual diesel signal was observed to persist through the sample collections in March 2005 (Figure 27). Pre-spill, GOC TPAH levels were extremely low (Figure 27), essentially a below-MDL level soluble-phase background signal (which we also observe at numerous remote locations within Prince William Sound – see Section 5.3.3). The pre-spill SHC profile includes n-C15 and n-C17 from marine plants and phytoplankton and pristane from copepods. After the spill, the PAH profile is dominated by particulate/oil-phase components, which show evidence of some water washing and evaporation weathering by the loss of the naphthalenes (N, N1, and N2). The SHC profile is characterized primarily by pristane and phytane (the latter only found in oil and refined petroleum products) and below-MDL traces of other n-alkanes. Usually, SHC profiles

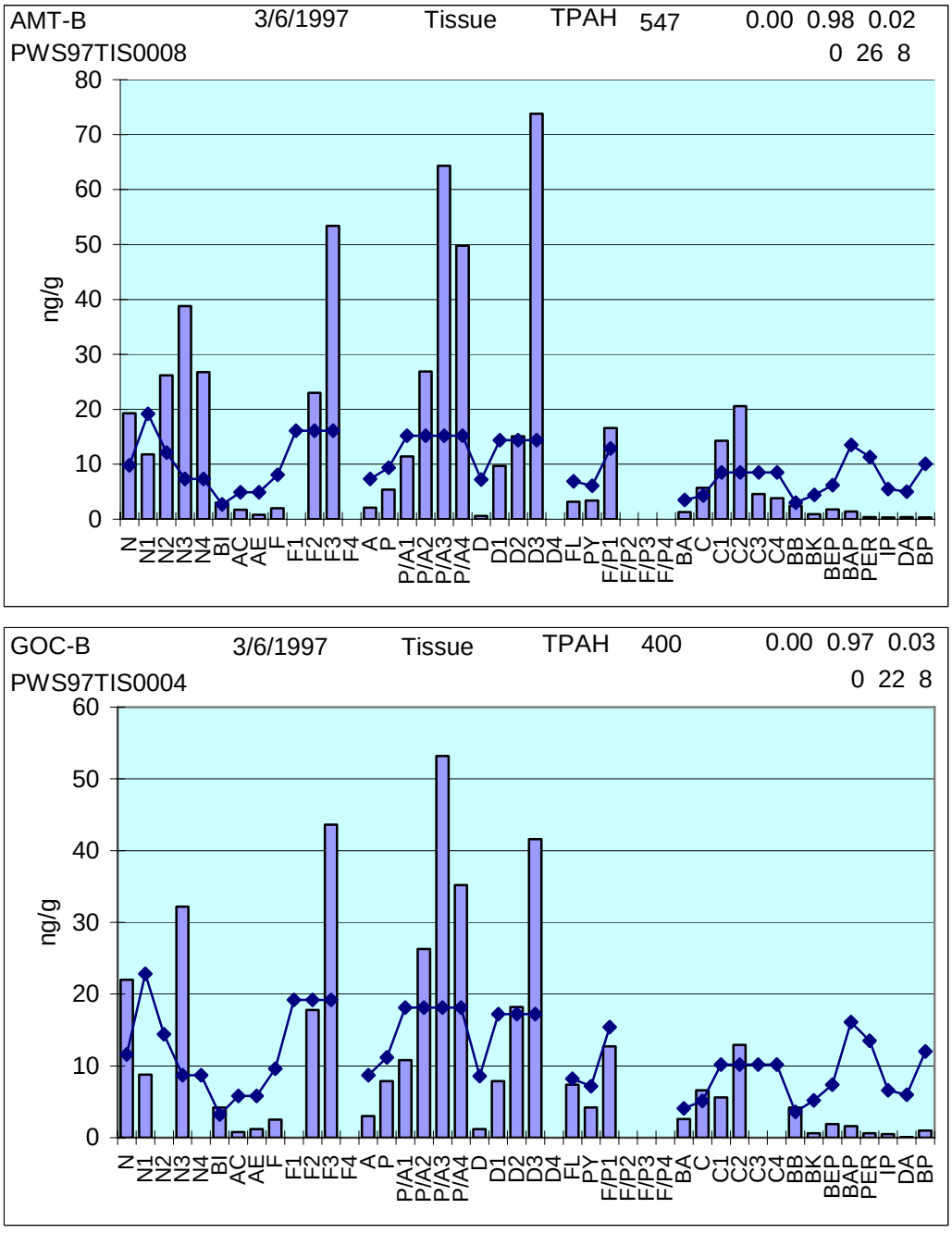

Figure 25 PAH profiles from March 1997 tissue samples at AMT and GOC showing the residual oil pattern from the January 1997 BWTF sheening incident in both locations.

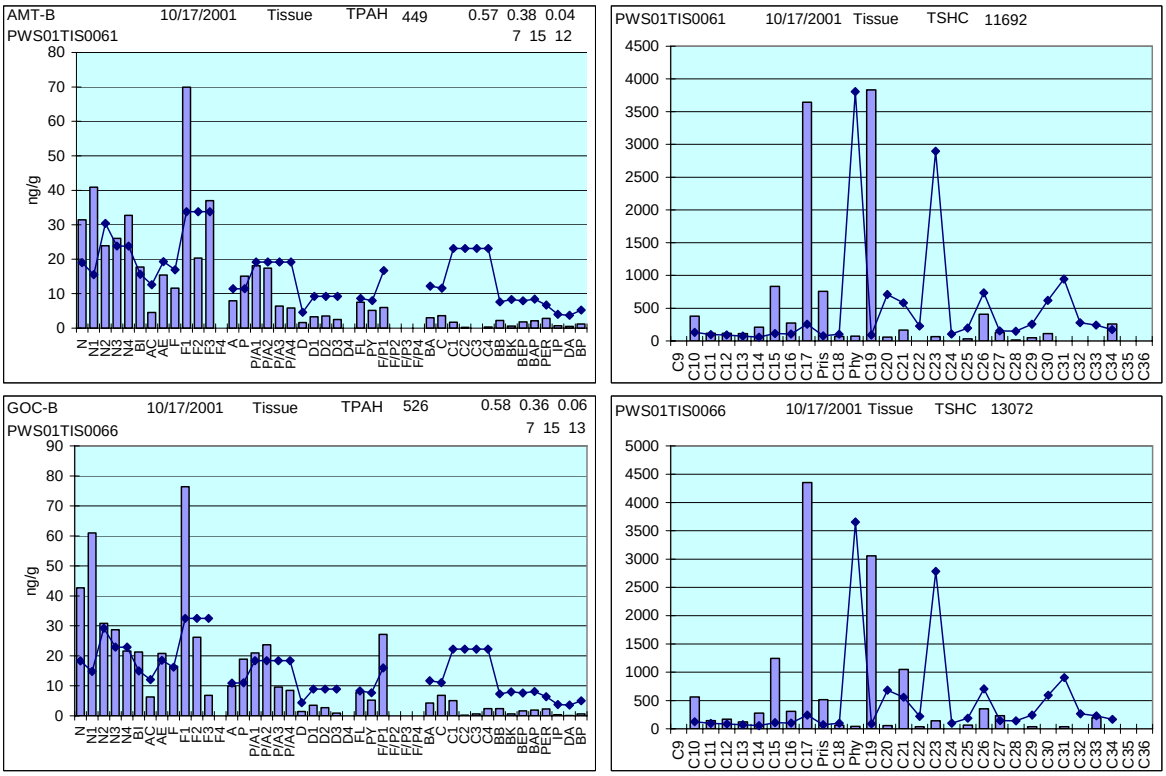

Figure 26 PAH and SHC profiles from October 2001 tissue samples at AMT and GOC showing the similarity in soluble-phase signatures associated with a TPAH spike at both stations.

from fresh diesel contain an evenly repeating series of even- and odd-carbon number n-alkanes from n-C14 through n-C22 (see Appendix D), and their absence here suggests extensive microbial degradation either before or after uptake by the mussels. Microbial and physical weathering behavior of diesel in sub-arctic intertidal regimes is discussed further in Appendix D, which presents the results from intertidal sediment and mussel analyses after an unrelated diesel spill in Jack Bay that occurred in May 2004. We know that the two diesel spills are unrelated because the PAH signatures are different – even allowing for weathering – and none of the May 2004 Jack Bay diesel signal was observed in either the GOC (Figure 27) or AMT (Figure 28) mussel samples collected in July 2004.

Based on the observed PAH and SHC profiles for the Gold Creek mussels collected in October 2004 (and the changes in PAH patterns discussed in Appendix D where we know the date and time of the release), we estimate that the diesel spill at Gold Creek probably occurred several weeks to a month before the samples were collected. There was no evidence of the diesel spill in any of the AMT mussel samples collected in July or October 2004, and there was no evidence of the diesel signal in the subtidal sediments collected at Gold Creek in March 2005 (Figure 28). This latter finding should not be a surprise, because very little evidence of oil transfer to near-shore subtidal sediments has been observed in numerous other spills, including the *Exxon Valdez* oil spill in 1989.

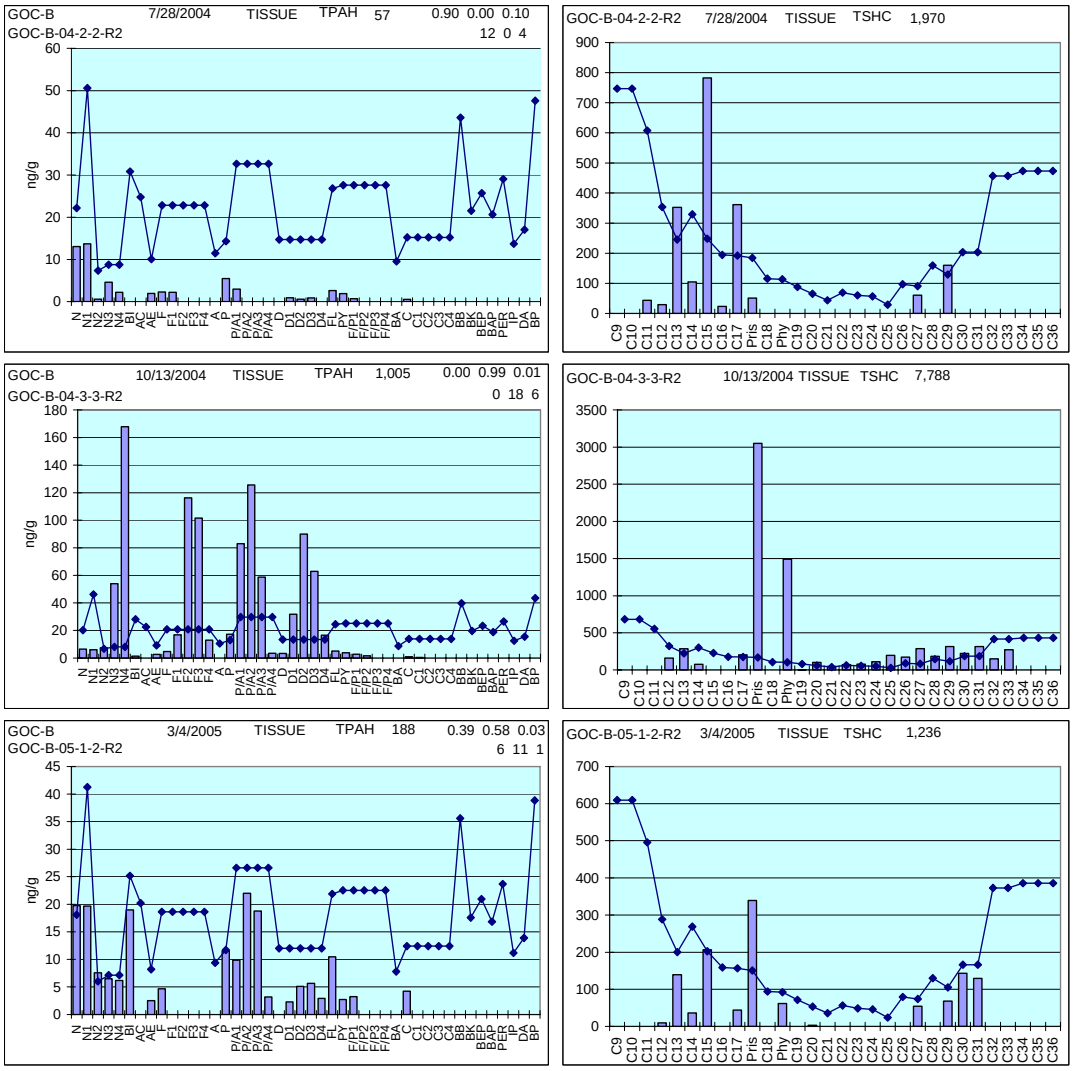

Figure 27 PAH and SHC profiles from GOC showing below MDL background-level soluble-phase constituents in July 2004, the impact of a diesel spill in October 2004 samples, and the residual diesel signal still apparent five months later in March 2005.

The AMT 2004-05 tissue plots (Figure 28) in no way resemble the unmistakable diesel signal shown for the October 2004 tissue sample from GOC (Figure 27), and the GOC sediment sample (bottom panels, Figure 28) reflects only trace-level (22 ng/g dry weight) concentrations of a mixed signal from soluble-, particulate/oil-phase, and pyrogenic components at 42, 2, and 56%, respectively. As in the other SHC profiles from Gold Creek, the aliphatic constituents primarily reflect higher-molecular-weight n-alkanes from terrestrial plant waxes and perhaps a trace of refined petroleum residues suggested by the below MDL phytane.

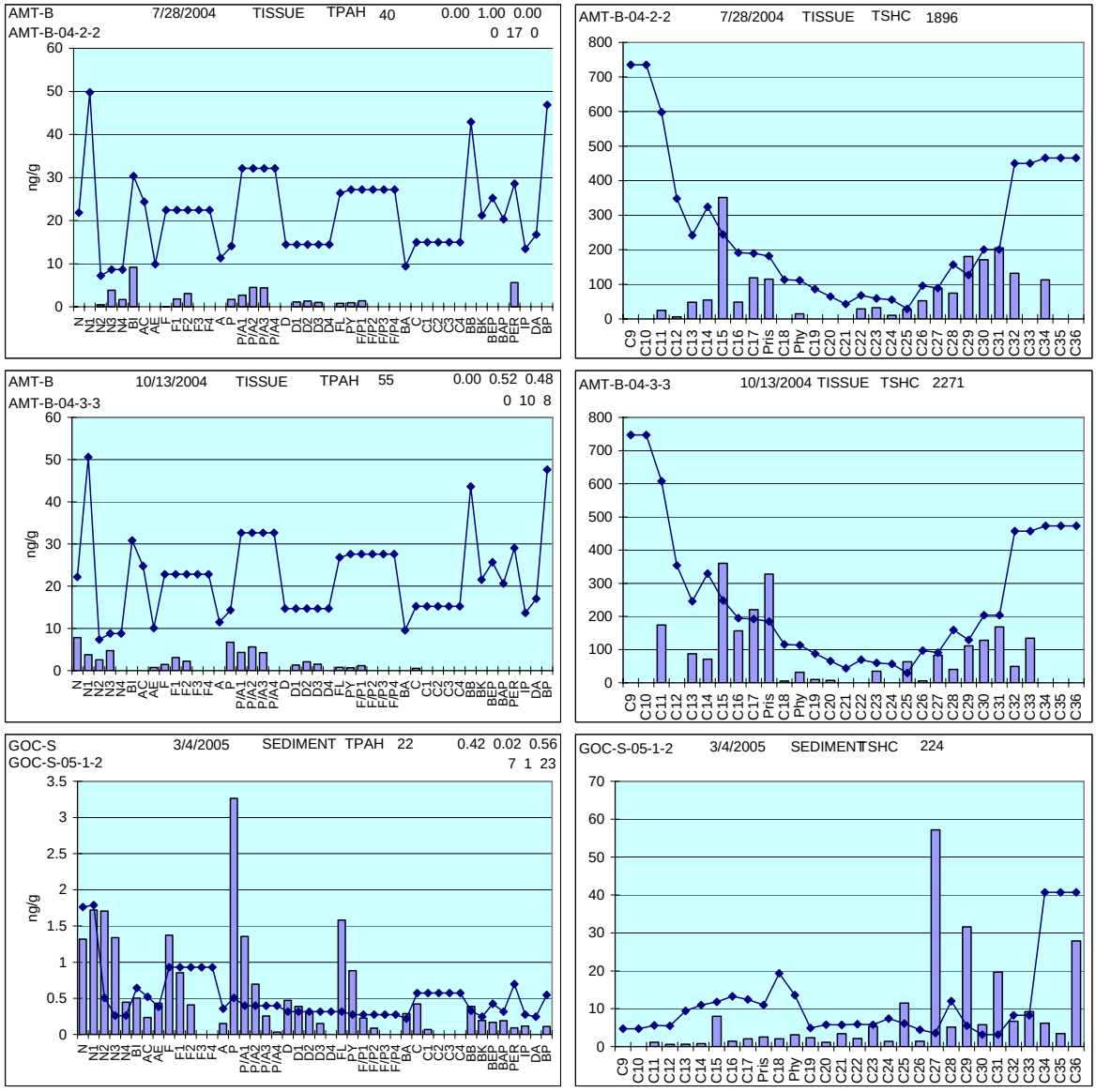

Figure 28 PAH and SHC profiles from AMT mussels collected in July and October 2004 and GOC subtidal sediments collected in March 2005 showing no evidence of the diesel signal observed in the GOC intertidal mussels collected in October 2004.

5.3.3 Prince William Sound Stations

This section presents the 1993–2005 tissue chemistry data from the LTEMP stations within Prince William Sound. As with the Port Valdez samples, we first present the PAH time series plots for each station to illustrate any trends followed by plots for individual samples to explain anomalies or specific features noted in the trend-lines. The Prince William Sound stations are arranged alphabetically as: Disk Island, Knowles Head, Sheep Bay, Sleepy Bay, and Zaikof Bay.

5.3.3.1 Disk Island Mussel Tissue Chemistry

Only a few of the early Disk Island samples were low-level and thereby dominated by the procedural artifacts patterns discussed in Section 4.7.2. Because of its history of EVOS oiling and occasional post-spill cleanup activities liberating buried oil, hydrocarbon concentrations at this site were higher (facilitating GC/MS peak integration) and thus, measurable and reliable for a most of the 1993-1997 samples (Figure 29).

Elevated TPAH signals derived almost exclusively from the particulate/oil-phase (Figure 30) were observed in March and July 1994 with the latter believed to be from beach cleaning operations active at that time. By March 1995, TPAH levels had dropped again, but still reflected a primarily particulate/oil-phase signal, presumably from residues liberated by winter/spring storm events. The elevated TPAH levels observed in March 1997 and March 1998 were somewhat enigmatic, with the majority of the earlier sample generated from a particulate/oil-phase (72%) and the later sample showing mixed-phase composition with 53% from the soluble fraction (Figure 31). Over the next four months, there was a significant drop in TPAH, and by July 1998, only below-MDL levels of primarily soluble-phase constituents remained (Figure 31). This soluble-phase dominance then persisted in most of the samples collected between March 1998 and July 2003 (Figure 29 left panel), including the TPAH maxima noted in March 2001 and March 2002 (Figure 32). The data in Figure 32 also illustrate several other features worthy of note: First, the July 1999 PAH profile, which reflects a slight particulate/oil-phase dominance, contains anomalously high fluorenes and although these procedural artifacts are not included in the TPAH time series values shown in Figure 29 (see Section 4.7.2), there is lingering uncertainty as to the potential for correlated peaks in other components, and they can sway dissolved- vs. particulate-phase assignments. Second, the SHC plots for both August 1999 and March 2002 contain excessively high n-C21, n-C22, and n-C23 levels that are also believed to be artifacts associated with incomplete lipid removal again adding uncertainty as to the true magnitude of these peaks. These elevated concentrations of higher-molecular-weight n-alkanes are most certainly of biogenic origin and not from exposure to oil. SHC Patterns closer to the one observed for the March 2001 sample (Figure 32 middle) would normally be expected in a sample containing primarily soluble-phase hydrocarbons.

The SHC profiles shown for the March and July 1994 Disk Island samples (Figure 30) contain n-C15, n-C17, and pristane from marine plankton and copepods (NRC 1985) plus a higher-molecular-weight suite of even and odd n-alkanes between n-C24 and n-C33.

Although it is surprising that the data do not show more evidence of microbial degradation, these profiles are more in line with what might be expected in mussels exposed to buried particulate-phase oil after its release from storm events and shoreline cleaning activities. Alternatively, this suite of higher-molecular-weight n-alkanes might simply represent another manifestation of the early laboratory issues, namely, incomplete lipid removal (see discussion in Payne et al., 2003a), because the absence of significant levels of phytane, which would be expected in buried oil, is somewhat suspicious.

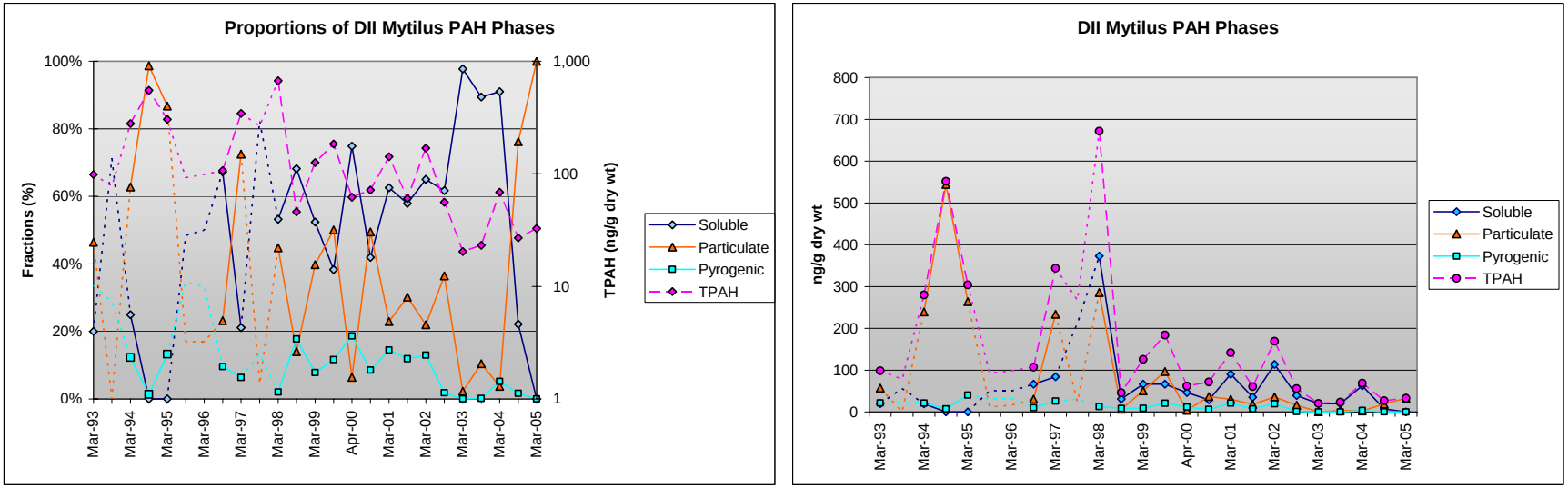

Figure 29 Time series of PAH indices for Disk Island *Mytilus* tissues, 1993-2005. Dotted connecting lines without symbols indicate questionable data.

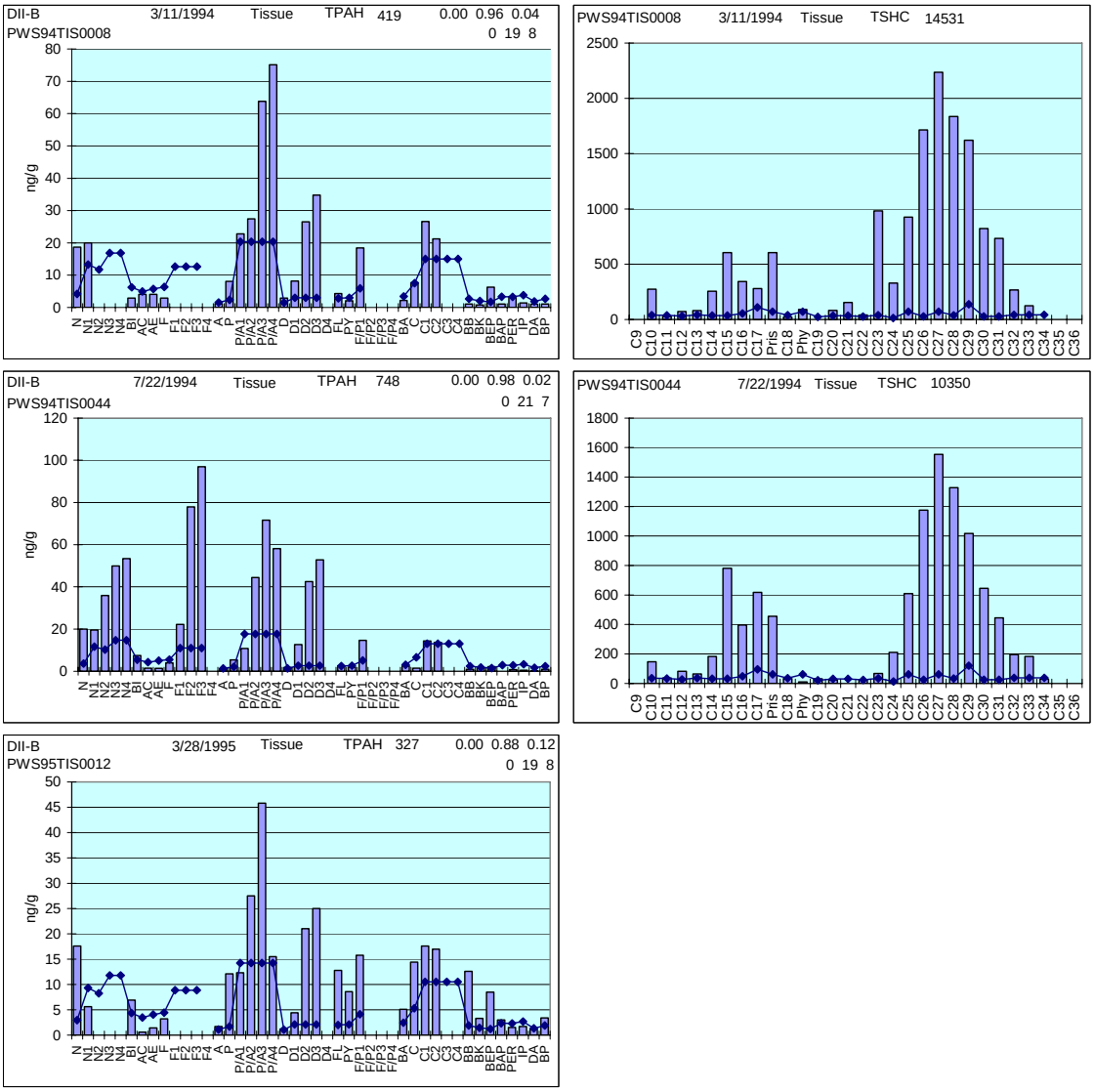

Figure 30 Representative PAH and SHC plots from Disk Island (March 1994, July 1994, and March 1995) showing particulate-phase EVOS oil residues released from winter/spring storms and beach cleaning activities undertaken during the summer.

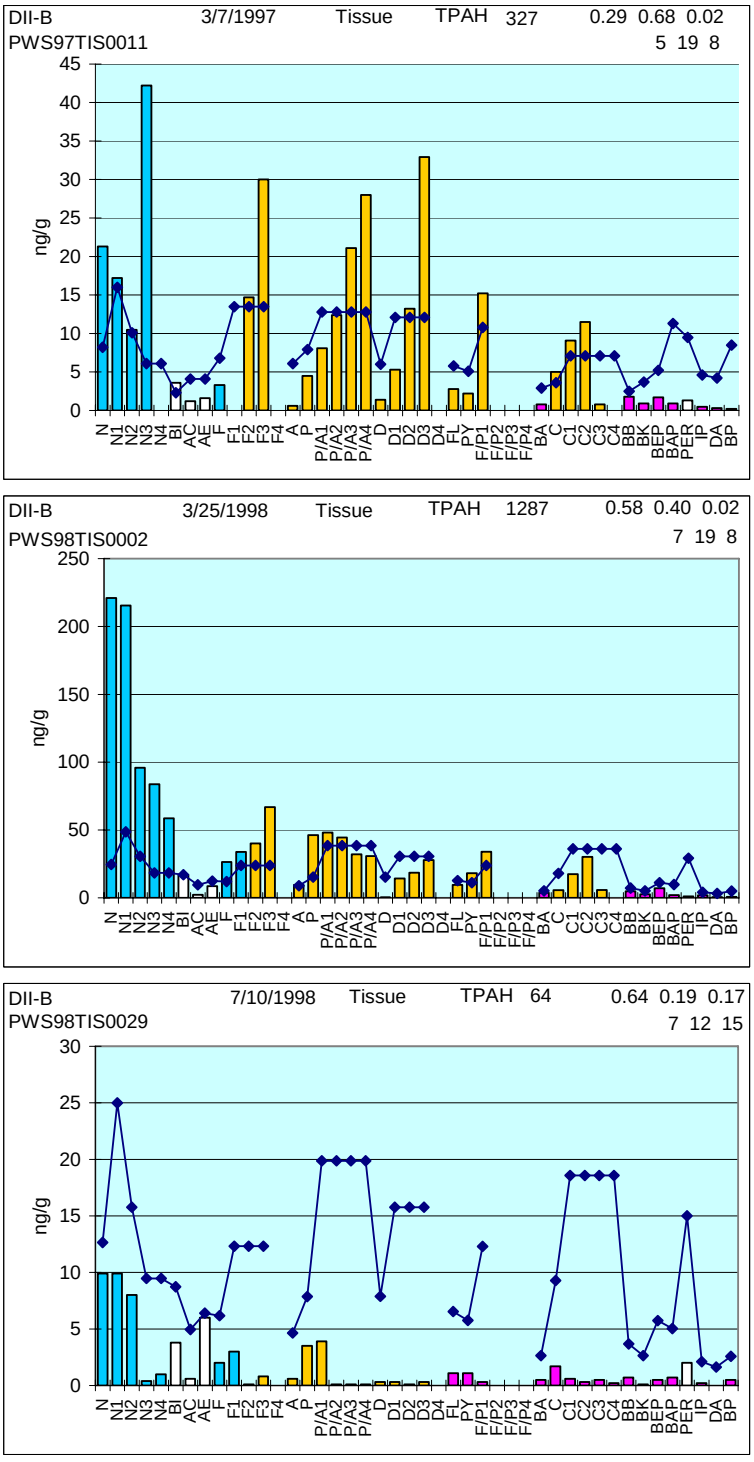

Figure 31 Representative Disk Island PAH plots from March 1997, March 1998, and July 1998 showing the transition from a moderate-level particulate/oil-phase signal to an exceptionally high-concentration primarily soluble-fraction signal, to the background-level pattern typical of most low (< 100 ng/g) level profiles from this site. Phase coding: turquoise = dissolved, gold = particulate/oil-phase, fuchsia = pyrogenic.

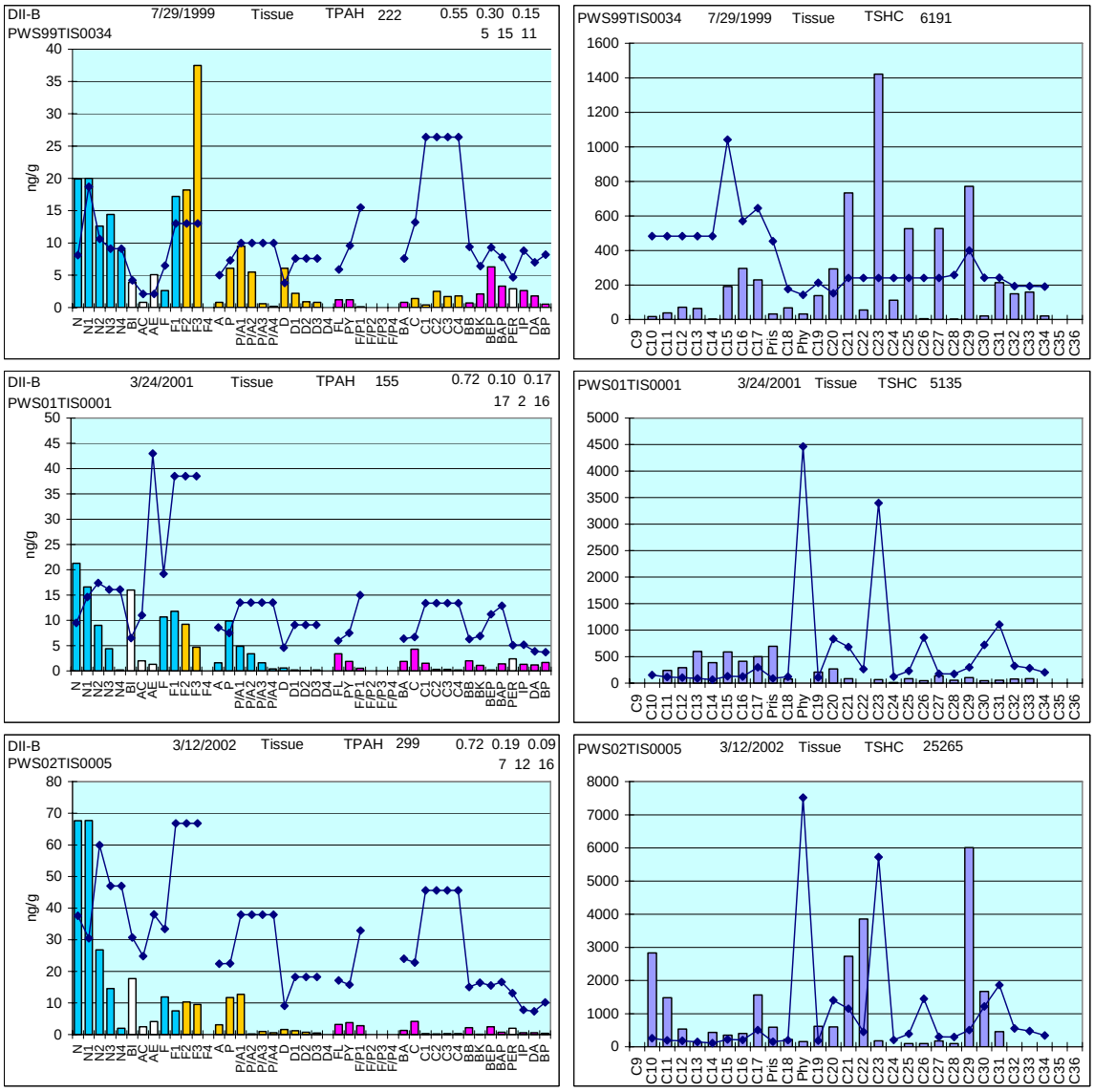

Figure 32 Representative Disk Island PAH and SHC patterns observed in samples reflecting the TPAH maxima (all still <200 ng/g) noted in July 1999, March 2001, and March 2002. Note, the anomalous fluorene pattern observed in July 1999 is not included in the TPAH value shown in Figure 29, but setting the fluorenes to zero caused the naphthalene phase assignment to switch from dissolved to particulate in one of the three replicates. Phase coding: turquoise = dissolved, gold = particulate/oil-phase, fuchsia = pyrogenic.

After March 2002, the TPAH levels at Disk Island declined to values consistently below 100 ng/g, and in fact, the data (left panel Figure 29) suggest an overall decline in TPAH values over the twelve years of LTEMP measurements with steadily increasing contributions from the soluble phase through March 2004. The PAH-phase trend lines from March 2004 through March 2005 (Figure 29) show a switch in the pattern of soluble- and particulate/oil-phase constituents, but it should be noted that as the TPAH levels drop

to extremely low levels (<100 ng/g), the corresponding PAH and SHC profiles are so low, that all analytes are well below the MDL (Figure 33), and the assignment of soluble- versus particulate/oil-phase fractions, although methodically calculated, gets to be fairly subjective.

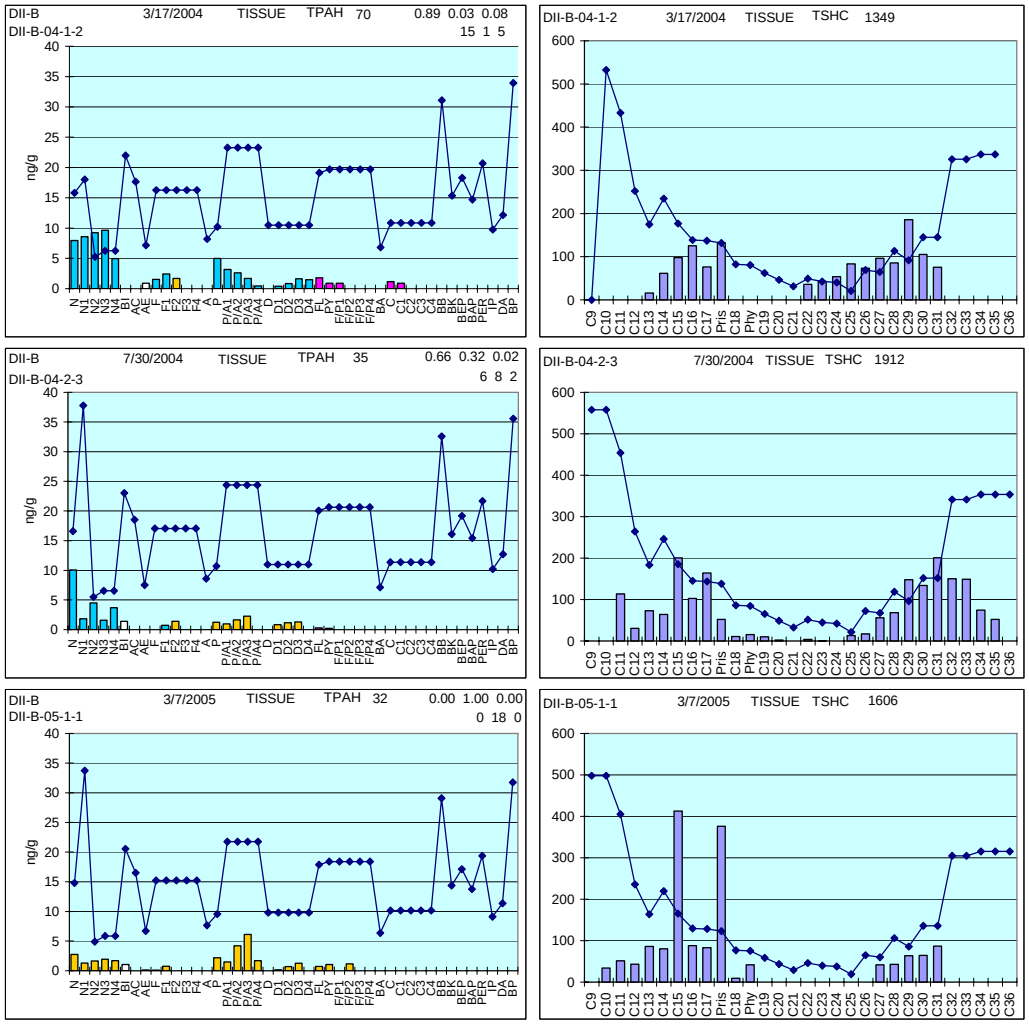

Figure 33 Representative Disk Island PAH and SHC profiles from March 2004, July 2004, and March 2005 showing the extremely low levels of measured constituents and the difficulty in definitively assigning soluble- and particulate/oil-phase fractions at these (<70 ng/g) concentrations. Phase coding: turquoise = dissolved, gold = particulate/oil-phase, fuchsia = pyrogenic.

For example, the March 2004 sample (reported to contain a 89% dissolved-phase fraction – Figure 33 top) may also be interpreted to reflect a predominantly particulate/oil-phase signal because N1<N2<N3. However, the total naphthalenes are greater than three times the total phenanthrenes and the phenanthrenes show a descending stair-step pattern. As such, both the naphthalenes and phenanthrenes are assigned to the soluble phase (see Section 4.7.1). In this instance, phase assignment for the naphthalenes could go either way with a particulate/oil-phase assignment supported by the presence of increasing

dibenzothiophenes (D1<D2<D3) and the below MDL-level higher-molecular-weight n-C22 to n-C34 n-alkanes. However, there is no phytane present, so another scenario is that these n-alkanes may also be due to bacteria associated with the mussel tissues (Davis, 1968; Han and Calvin, 1969), and therefore, the dissolved-phase assignment is correct. These are the types of issues that can make these low-TPAH level phase assignments so difficult, but it is precisely because of these factors (N1<N2<N3, total naphthalenes < total phenanthrenes, and the presence of phytane in the SHC profile), that gives us confidence in the assignment of the particulate/oil-phase signature to the March 2005 sample. The lipid interference problems in earlier samples were largely eliminated with the change to Auke Bay Laboratory in July 2002, and subsequently, the SHC fractions for most samples have exhibited only a marine biogenic profile with prominent n-C15, n-C17, and pristane. Therefore, when higher-molecular-weight n-alkanes are observed, it is possible to place a little more credence in the aliphatic data.

Notwithstanding all the above discussion about soluble- versus particulate/oil-phase distinctions, the take-home message for Disk Island is that these concentration values are extremely low, and they reflect the extremely pristine nature of the site at the time of the 2004/2005 collections.

5.3.3.2 Knowles Head Mussel Tissue Chemistry

From this historically clean site near the Prince William Sound tanker anchorage, much of the earlier (1993-1997) data appears to be confounded by procedural and laboratory artifacts (Figure 34). Also, as described in detail in Appendix A-3.5 of our 2003/2004 LTEMP Final Report (Payne et al., 2005a), there was often no agreement between PAH and SHC data (when available) to confirm any petroleum hydrocarbon contamination at this site over the first eleven years of LTEMP.

As noted in Section 5.3.1 and Figure 19 there is an apparent synchronicity in TPAH maxima for the Prince William Sound regional stations, and the PAH profiles (Figure 35) for the elevated TPAH values suggested in March 1998 (84% particulate/oil-phase), July 1999 (51% particulate/oil-phase) and March 2002 (67% soluble phase) are in fact nearly identical to the complementary PAH patterns discussed above for Disk Island samples collected at the same time (Figure 31 and Figure 32). As indicated in Figure 19 and discussed further below, we also observed similar TPAH maxima and PAH profiles at the same times (July/August 1999, March 2001, and March 2002) at Sheep Bay, Sleepy Bay, and Zaikof Bay.

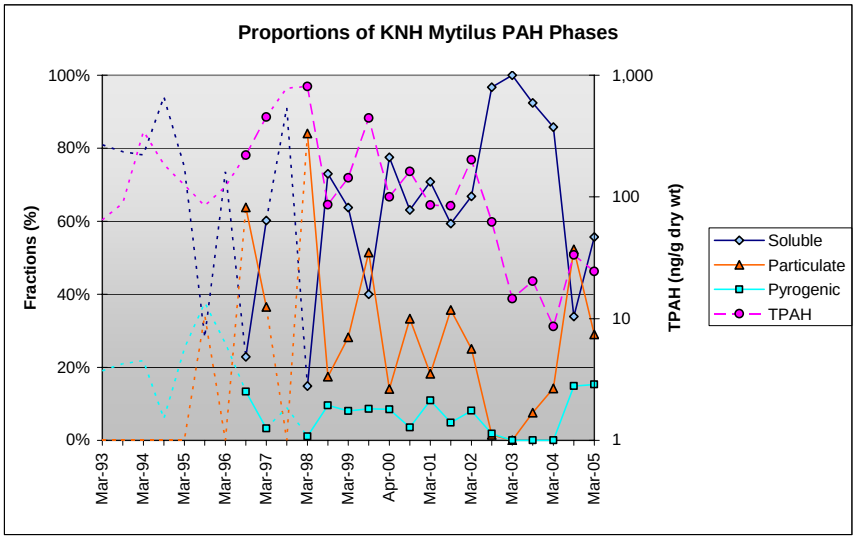

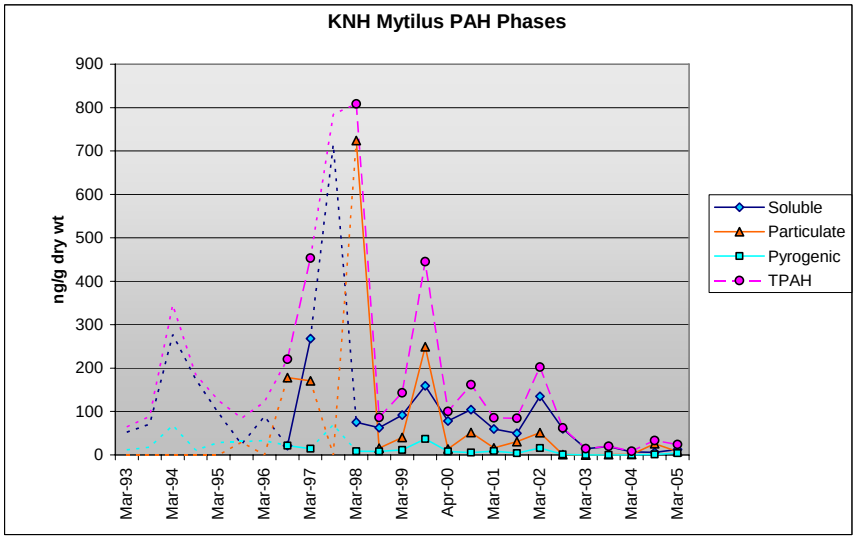

Figure 34 Time series of PAH indices for Knowles Head *Mytilus* tissues, 1993-2005. Dotted connecting lines without symbols indicate questionable data.

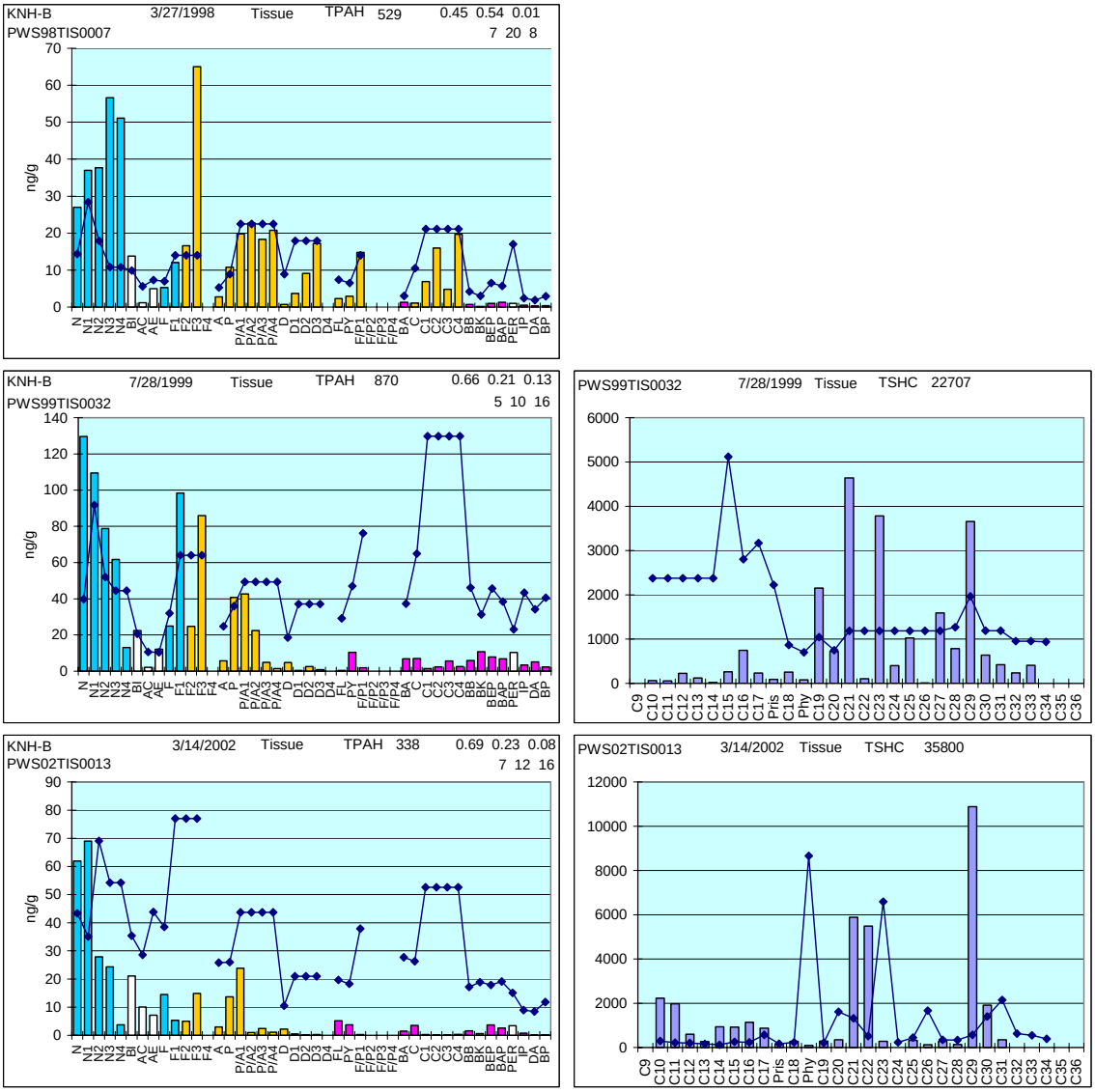

Figure 35 Representative PAH and SHC plots for Knowles Head tissue samples from March 1998, July 1999, and March 2002 showing nearly identical patterns to complementary samples collected at the same times (corresponding to observed elevated TPAH levels) at Disk Island (Figure 19, Figure 31, and Figure 32). Phase coding: turquoise = dissolved, gold = particulate/oil-phase, fuchsia = pyrogenic.

With the available data, however, it is not possible to determine if this was due to some region-wide perturbation (*El Nino, La Nina*, or other oceanographic phenomena) or some other unknown factor associated with the Prince William Sound stations during these times. While we had previously attributed this pattern to possible procedural artifacts (Payne et al., 2005a), careful analyses of individual PAH profiles and the synchrony of the region-specific trends (Figure 19) have led us to conclude that the increased TPAH levels and PAH profiles accurately reflect field conditions.

The data from March and July 2004 and March 2005 indicate that this site continues to be extremely pristine with individual PAH analytes consistently below the MDL and with TPAH values consistently less than 40 ng/g (Figure 36). As noted for Disk Island, however, assignment of soluble- versus particulate/oil-phase source identifications at these extremely low TPAH values is extremely difficult, and subtle differences between these two phases suggested in recent years (Figure 34) should be interpreted with caution.

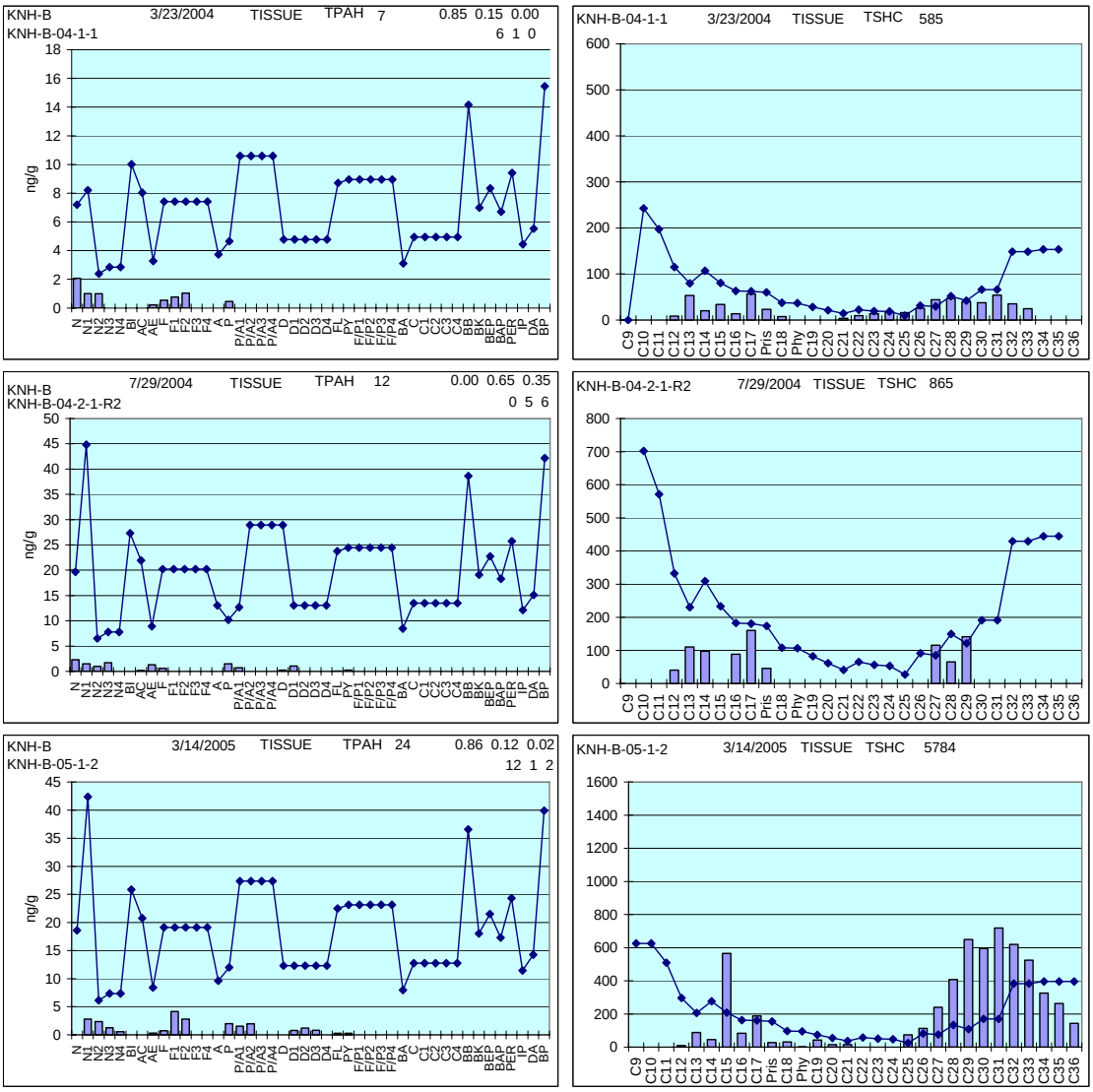

Figure 36 Representative PAH and SHC Knowles Head tissue-sample profiles from March and July 2004 and March 2005 showing TPAH levels so low that soluble- versus particulate/oil-phase discrimination cannot be reliably made.

Again, taken together, all these data indicate that the Knowles Head site is extremely pristine, and that measured PAH components, from whatever source, have been steadily declining since March 1998 (Figure 34, right panel).

5.3.3.3 Sheep Bay Mussel Tissue Chemistry

The PAH time-series for Sheep Bay mussels (Figure 37) show that all of the early (March 1993 – March 1996) low-PAH-level samples were compromised by procedural artifacts as described in Section 4.7.2. Presumably reliable data, obtained in July 1996 and March 1997 (Figure 38 top and middle), suggested noteworthy alternating accumulations of soluble- and particulate/oil-phase components, but the soluble-phase maxima suggested in July 1997 (shown by the dotted lines in Figure 37) was characterized as questionable because the sample contained only procedural artifacts plus additional naphthalene (Figure 38 bottom). A predominantly particulate/oil-phase pattern was noted again in March 1998 (Figure 37), and reliable PAH profiles essentially identical to those obtained in March 1997 (Figure 38 middle) were obtained. A very low (<100 ng/g TPAH) soluble-phase profile was then observed in July 1998, and this was followed by a mixed-phase and two soluble-phase TPAH maxima in July 1999, March 2001, and March 2002 (Figure 37). Similar TPAH maxima were observed at Disk Island and Knowles Head (Figure 19), and the PAH and SHC profiles for the Sheep Bay samples (Figure 39) are also very similar to the corresponding samples for the TPAH maxima at the other stations(Figure 32 and Figure 35). As will be discussed further below, similar TPAH maxima and PAH profiles were also observed for Sleepy Bay and Zaikof Bay at these times.

Since July 2002, the TPAH concentrations at Sheep Bay have been extremely low (<60 ng/g), and with the exception of July 2004, they have been consistently characterized by a soluble-phase signal (Figure 40). Note the increasing naphthalene series (N<N1<N2<N3), the higher total phenanthrenes compared to the total naphthalenes, and the trace of phytane in the July 2004 sample profile that taken together help to define the particulate/oil-phase signal. As noted before, however, the individual constituents in recent years are at such low levels that assigning an accurate source-signal phase is extremely tentative.

Notwithstanding the temporal maxima in July 1999, March 2001, and March 2002, the overall TPAH levels appear to be trending lower each year (at least since more reliable data have been collected after March/July 1998 – Figure 19) as observed at the other Prince William Sound regional stations.

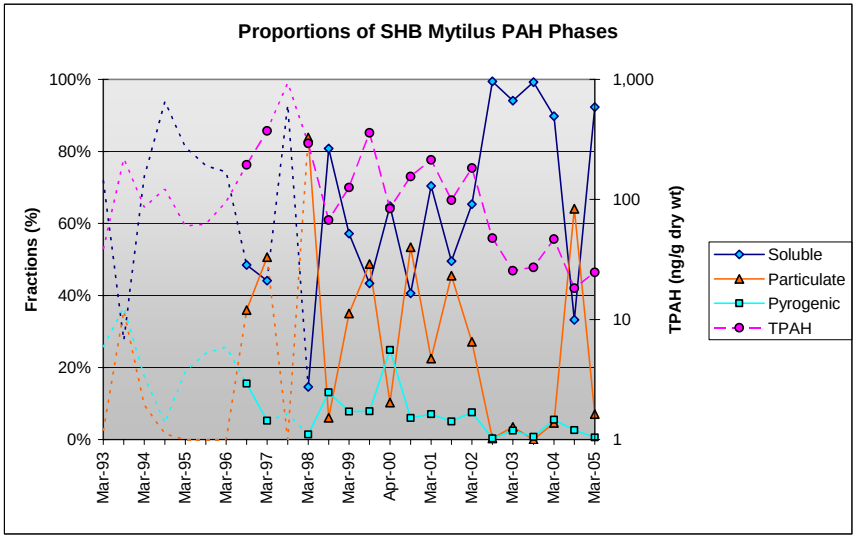

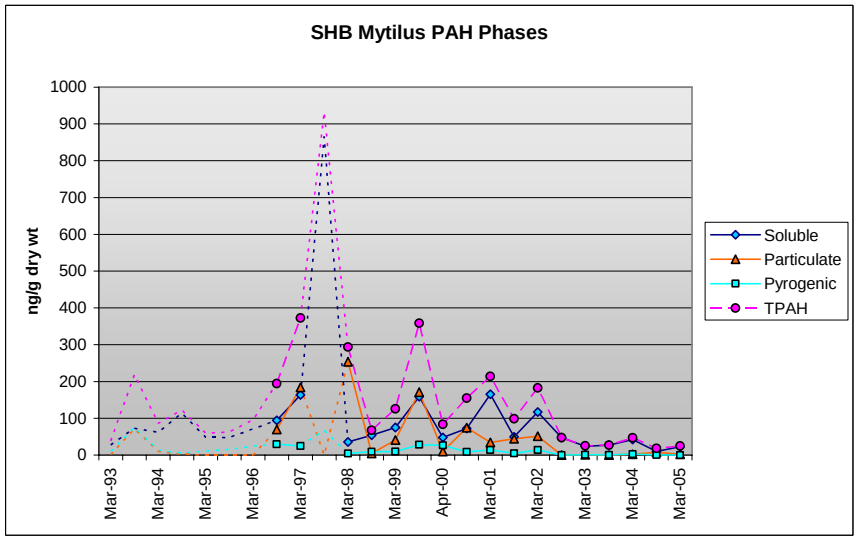

Figure 37 Time series of PAH indices for Sheep Bay *Mytilus* tissues, 1993-2005. Dotted connecting lines without symbols indicate questionable data.

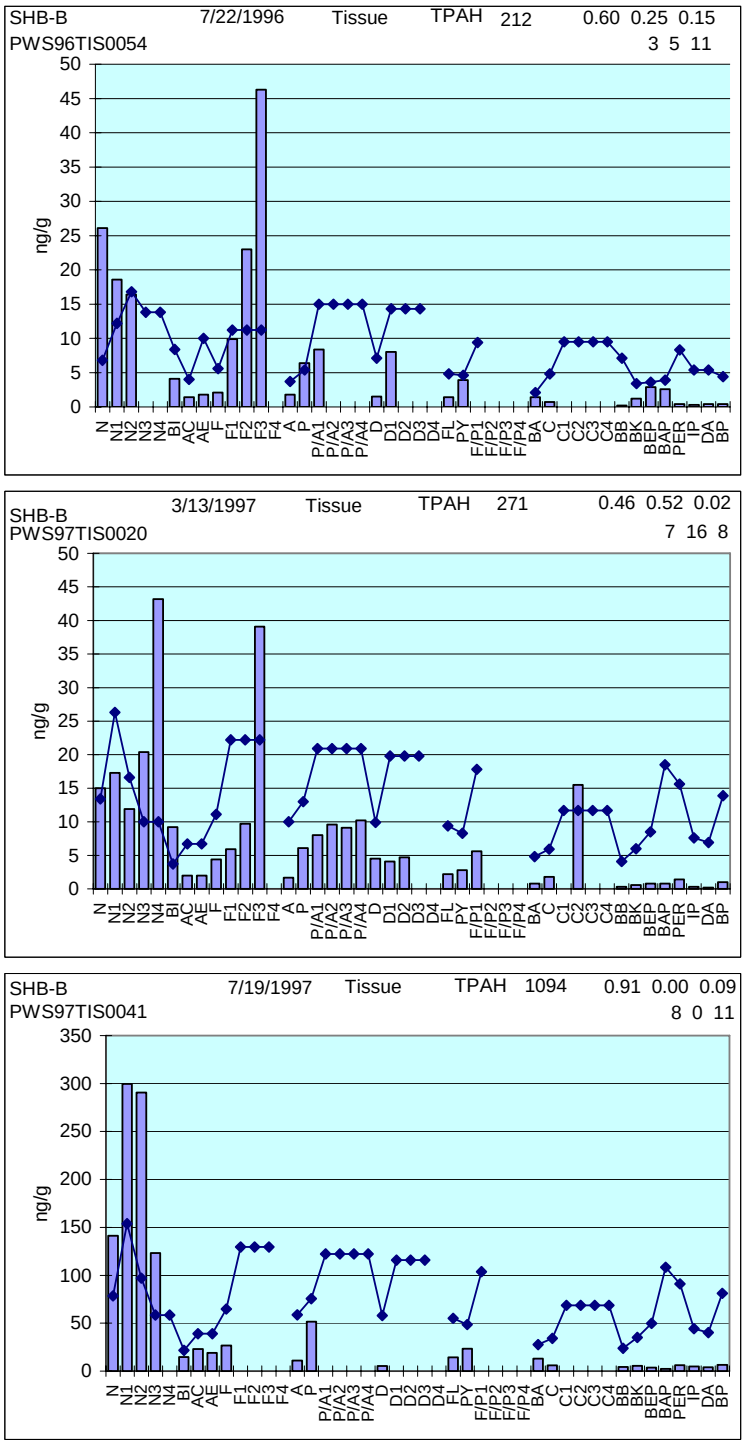

Figure 38 Representative PAH plots of Sheep Bay tissue samples from July 1996 and March 1997 showing mixed-signal composition and July 1997 characterized as questionable due to the procedural artifact pattern plus extra naphthalenes (see Section 4.7.2).

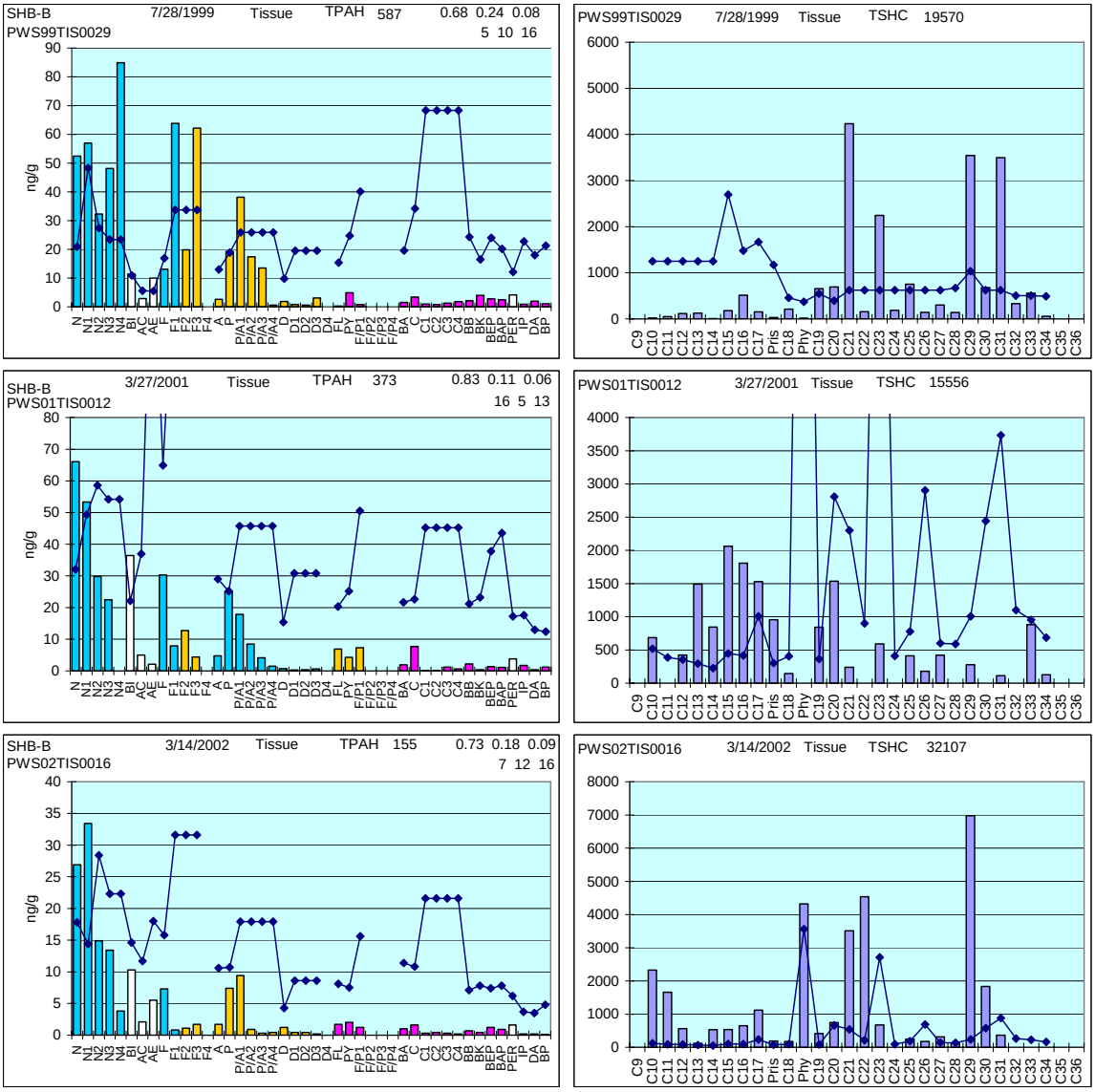

Figure 39 Representative PAH and SHC plots from the Sheep Bay PAH maxima observed in July 1999, March 2001, and March 2002 (see Figure 37) showing similar patterns to the corresponding maxima for Disk Island and Knowles Head (see Figure 32 and Figure 35, respectively). Phase coding: turquoise = dissolved, gold = particulate/oil-phase, fuchsia = pyrogenic.

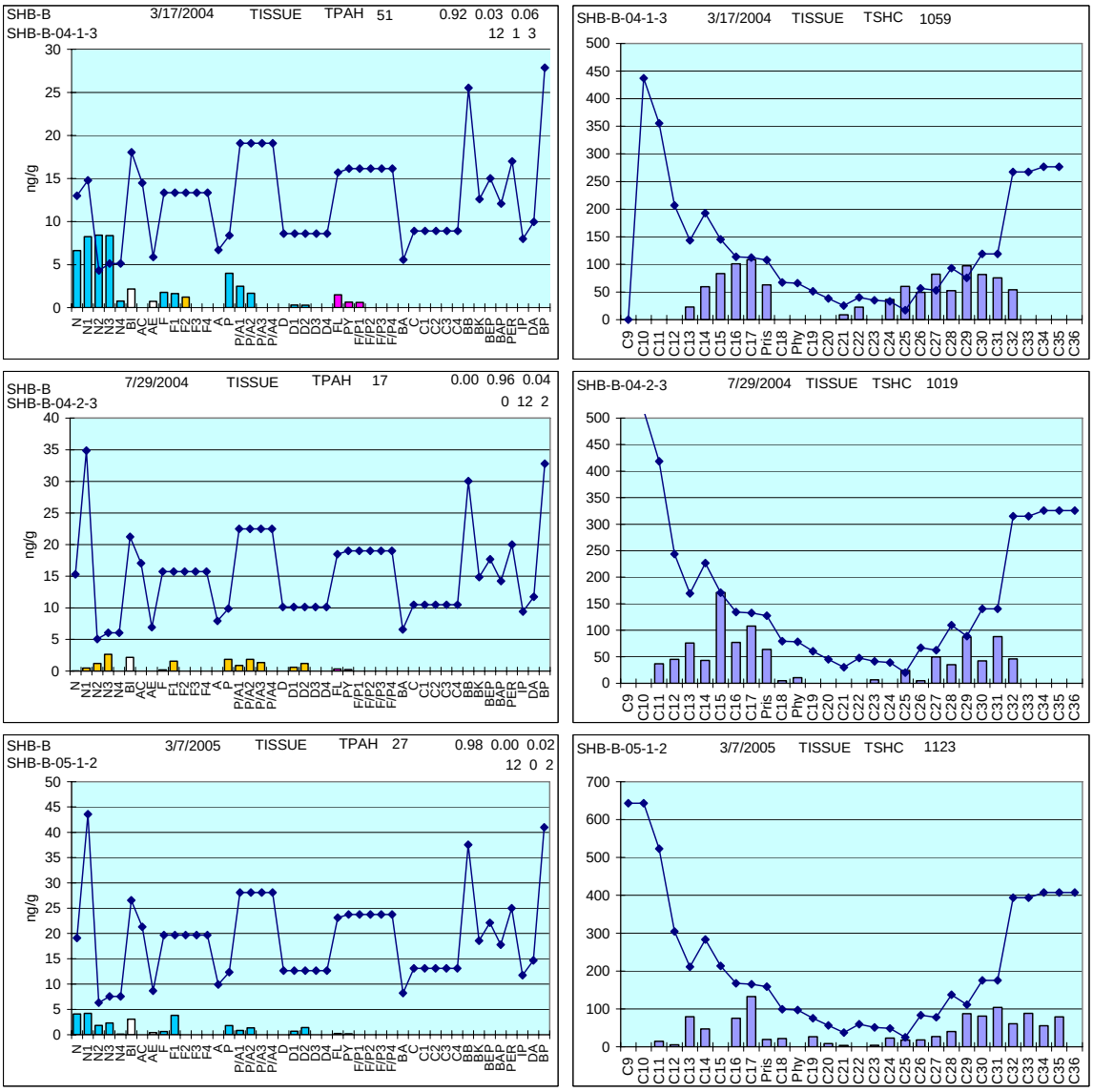

Figure 40 Representative PAH and SHC plots of Sheep Bay mussel tissue extracts from March 2004, July 2004, and March 2005 showing extremely low and possibly alternating soluble- and particulate/oil-phase signals. Phase coding: turquoise = dissolved, gold = particulate/oil-phase, fuchsia = pyrogenic.

5.3.3.4 Sleepy Bay Mussel Tissue Chemistry

Like Disk Island, the history of EVOS oiling and subsequent releases of buried oil from winter/spring storms and beach-cleaning events have resulted in higher TPAH concentrations in the mussel-tissue extracts at Sleepy Bay. As a result, more accurate GC/MS integration of parent and alkylated homologues has been possible, and more reliable data for trend analyses during the early years of the program have been generated (Figure 41).

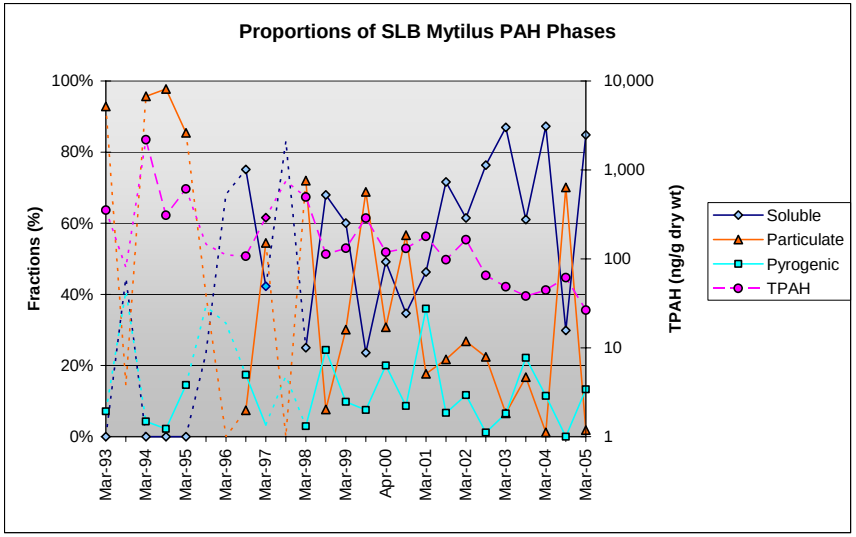

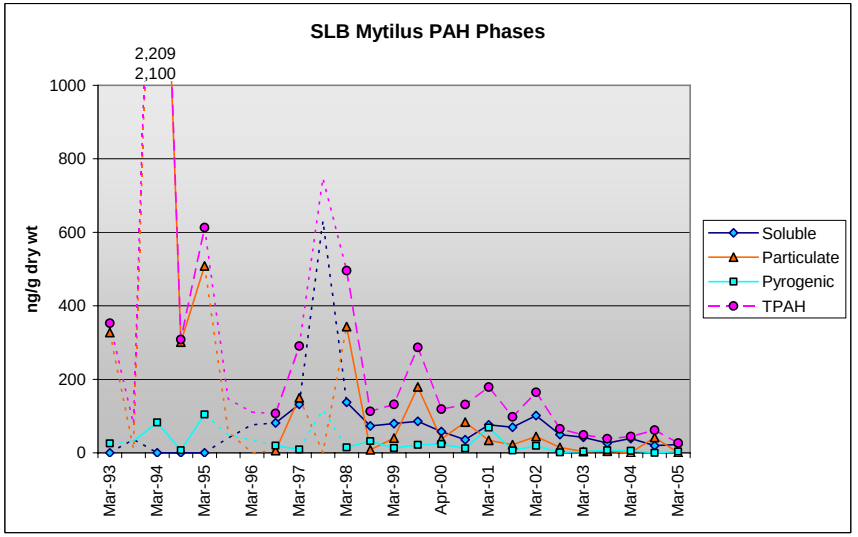

Figure 41 Time series of PAH indices for Sleepy Bay *Mytilus* tissues, 1993-2005. Dotted connecting lines without symbols indicate questionable data.

Very high TPAH levels were noted in March collections during the first three years of the program, and exceptionally high TPAH levels (>2,200 ng/g) were observed in March 1994, in particular. The March 1994 TPAH concentrations are second only to the levels measured in the mussels collected at the Alyeska Marine Terminal immediately after the *Eastern Lion* oil spill (see Section 5.3.2.1). In the March 1993 and 1994 samples from Sleepy Bay, the particulate/oil-phase signals constituted over 90% of the total PAH (Figure 42) with significantly lower contributions from soluble-phase and pyrogenic constituents. By March 1995, however, continued weathering of the subsurface oil had further removed more of the lower-molecular-weight constituents, and the pyrogenic fraction had increased proportionally (Figure 41 and Figure 42).

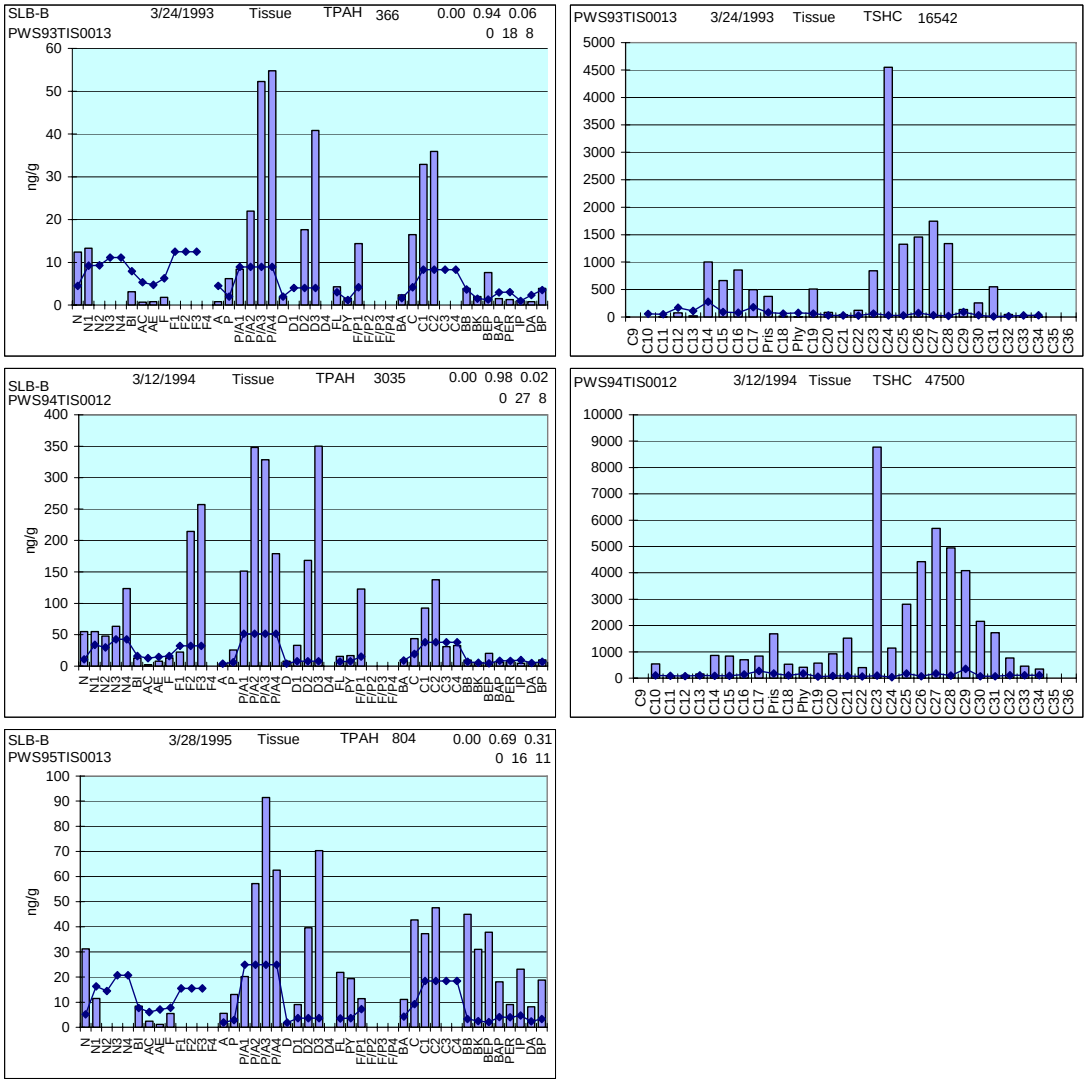

Figure 42 Representative PAH and SHC plots from Sleepy Bay mussel tissue samples collected in March 1993, March 1994, and March 1995. Note SHC analyses were discontinued in 1995.

These exceptionally high particulate/oil-phase concentrations are believed to have been liberated from buried EVOS oil residues after severe winter- and spring-storm events (Payne et al., 2005a). Sleepy Bay is exposed to extensive open water to the northeast (east of Knight Island), and as such, it is subject to a considerable fetch of storm activity and wave turbulence from northerly spring winds. These events are quite likely responsible for the release of buried oil that was observed in the tissue samples collected at those times (Figure 42). In contrast, most of the summer samples collected between 1993 and 1996 were very low (Figure 41), and they were characterized as only low-level procedural artifacts or a possible low-level (107 ng/g) dissolved-phase signal in July 1996 (Figure 43).

The exception to these low-level summer-time samples occurred in July 1994 when intermediate-level TPAH concentrations (308 ng/g) were accurately quantified (Figure 41 and Figure 43). Unfortunately, we are unaware of any correlating activities responsible for these elevated levels. In contrast, the PAH profiles in July 1993 reflect only procedural artifacts (see Section 4.7.2), and the July 1996 pattern suggests a very low-level soluble-phase signal possibly confounded by procedural artifacts (Figure 43).

As observed at several other Prince William Sound regional stations (Disk Island, Knowles Head, and Sheep Bay), the possibility of a July 1997 soluble-phase TPAH spike is suggested in the PAH time-series plot (Figure 41) for Sleepy Bay (also see Figure 29, Figure 34, and Figure 37). Although another beach-cleaning event with PES-51 occurred just 18 days prior to sampling, we are not convinced that this is a real signal, and instead believe that it is due to exceptionally high naphthalenes (possibly due to laboratory contamination) with no other PAH except for integration artifacts (Figure 44). In two of the replicates (PWS97TIS0043 and PWS97TIS0045), two extra naphthalene peaks are noted (N2 and N3), and in the third replicate (PWS97TIS0044), these two additional naphthalenes (N2 and N3) are joined by chrysene (C); however, we believe that these signals are only due to probable contamination and integration artifacts (as discussed in Section 4.7.2). This same pattern was responsible for the July 1997 spikes in TPAH observed at the other regional sites, and while it may represent a region-wide spike in soluble naphthalenes, we are highly dubious because the naphthalenes do not show a descending pattern as one would expect for a water-soluble fraction, and there are no other PAH which would be expected given such a high naphthalene signal (see Figure 2). In that naphthalene can often be introduced as a laboratory contaminant, we have elected to take a conservative stance and dismiss the signal in our treatment of the July 1997 data for this and the other Prince William Sound Regional stations.

Reliable signals begin to appear again in March 1998 (Figure 41), and what we believe to be real particulate/oil-phase and soluble-phase maxima are observed in July 1999, March 2001, and March 2002 just as they were at Disk Island, Knowles Head, and Sheep Bay. The PAH profiles observed for most of these samples (Figure 45) appear to be real

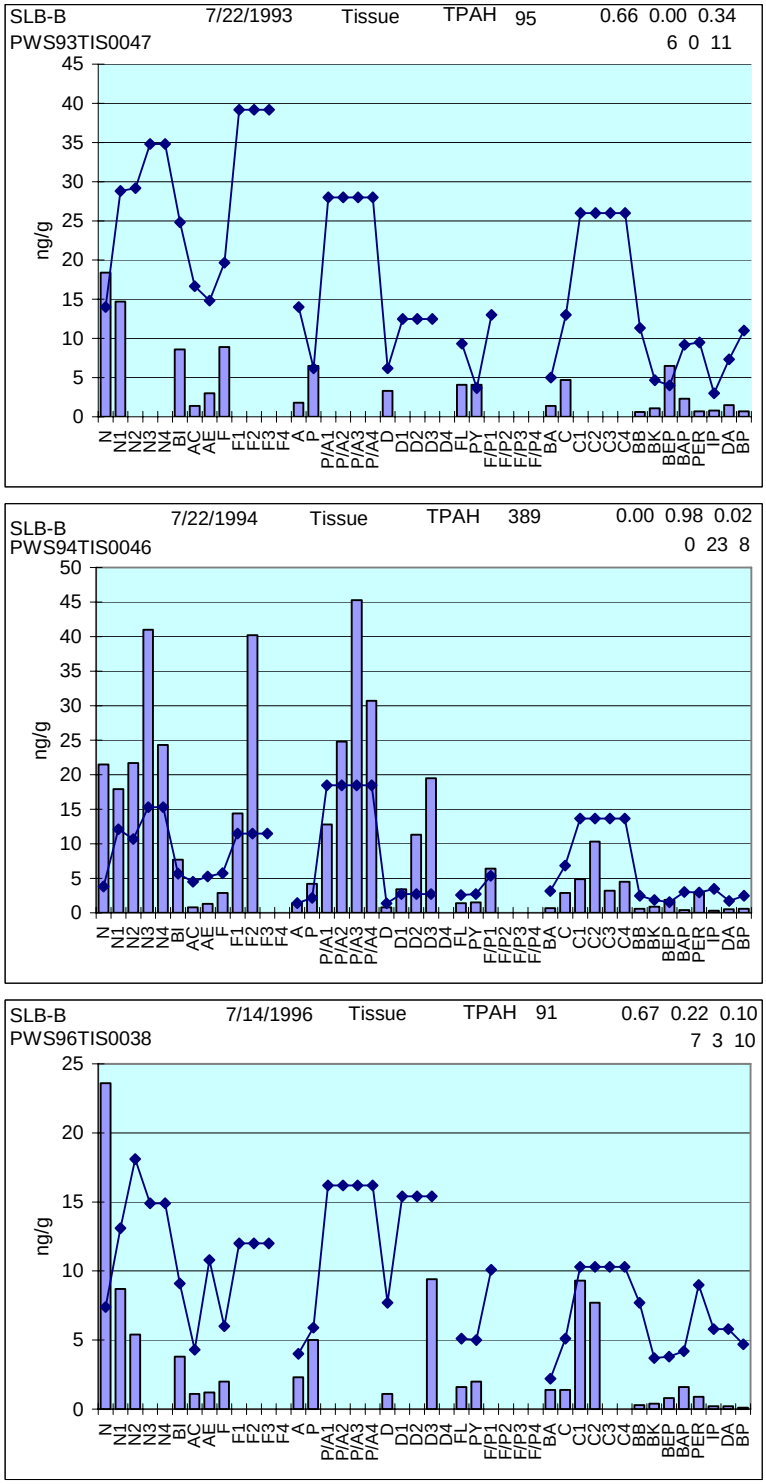

Figure 43 Representative PAH plots from Sleepy Bay mussel tissue samples collected in July 1993, 1994, and 1996. The July 1993 signal is due to procedural artifacts, the July 1994 signal reflects buried EVOS oil released by unknown events, and the July 1996 signal reflects a very low-level mixed soluble- and particulate/oil-phase signal confounded by procedural artifacts.

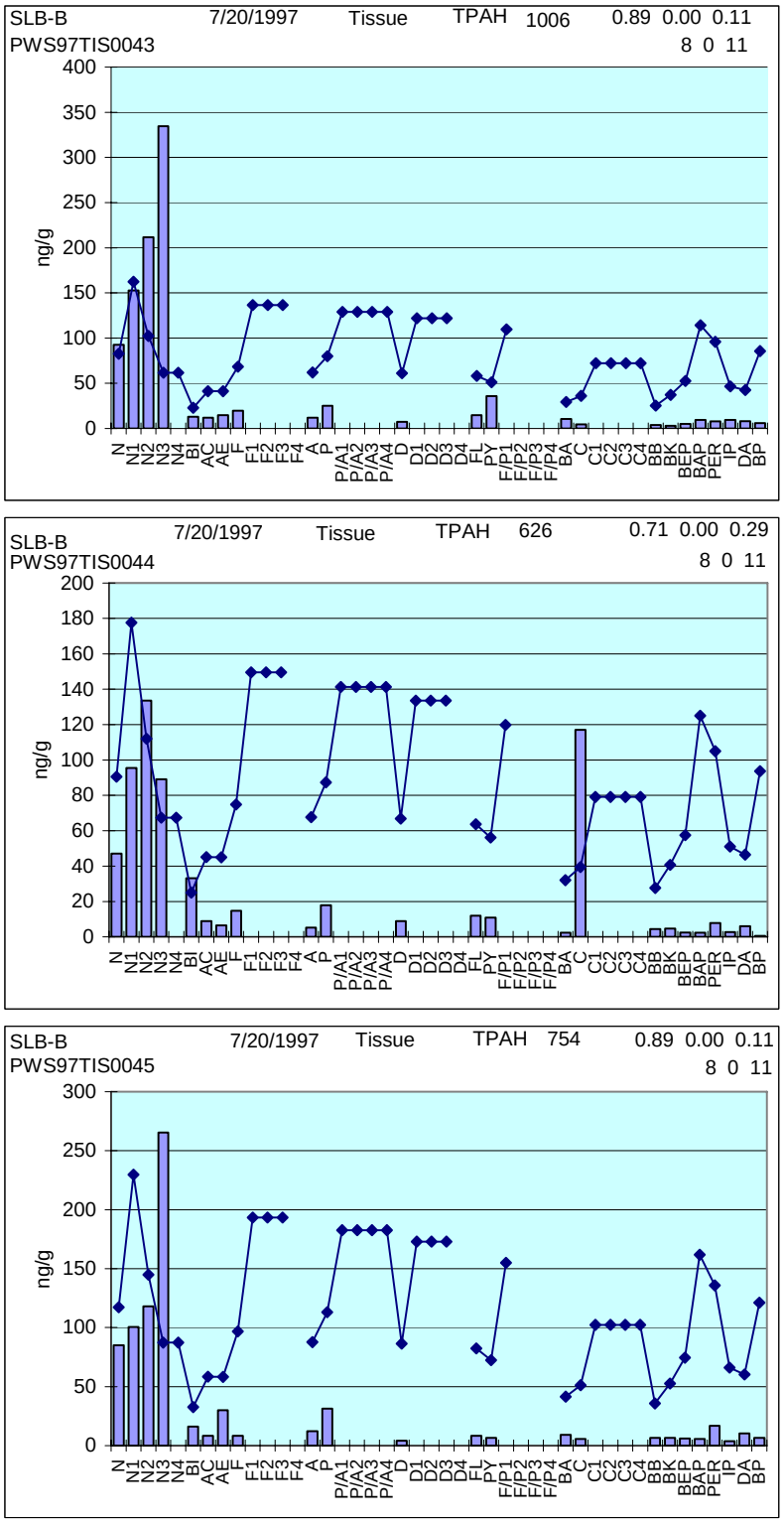

Figure 44 Suspected procedural artifact signal in triplicate Sleepy Bay mussel tissue samples from July 1997.

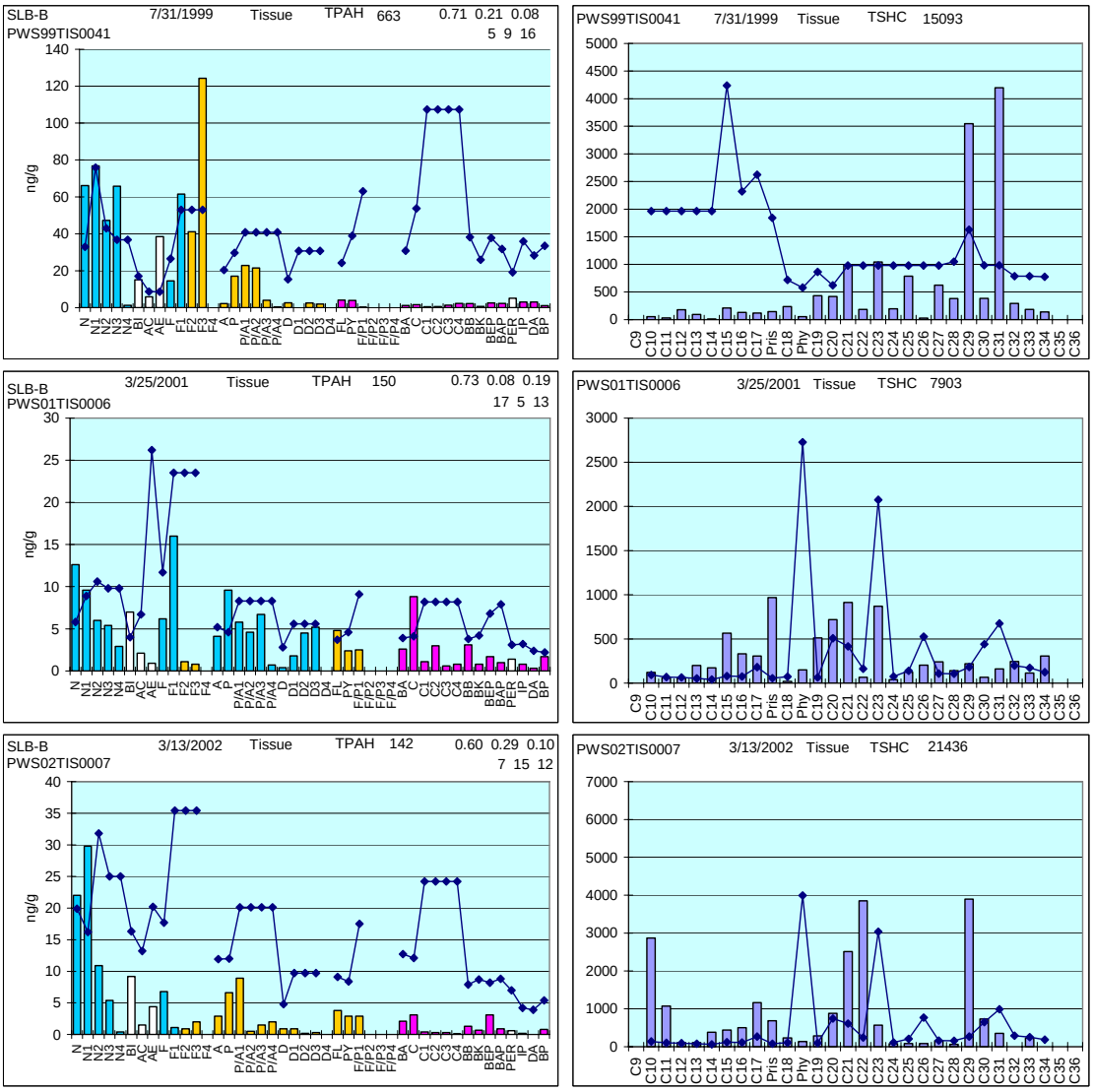

Figure 45 Representative Sleepy Bay PAH and SHC patterns observed in samples reflecting the TPAH maxima noted in July 1999, March 2001, and March 2002. Note, the anomalous fluorene pattern observed in July 1999 is not included in the TPAH value shown in Figure 41. Phase coding: turquoise = dissolved, gold = particulate/oil-phase, fuchsia = pyrogenic.

because they contain a more representative suite of soluble-phase constituents, and they are similar to the corresponding time-series samples from the other PWS regional sites (with just enough differences to convince us that the signal is real and not due to some ubiquitous laboratory or field contamination problem – see Figure 32, Figure 35, and Figure 39).

After the series of three TPAH maxima in July 1999, March 2001, and March 2002, the TPAH values at Sleepy Bay dropped in July 2002 to less than 100 ng/g, and they have remained at these low levels through March 2005 (Figure 41). In July 2004, the signal

appeared to be derived from particulate/oil-phase components, but the rest of the time, a predominantly soluble-phase signal was suggested by the extremely low-level PAH profiles (Figure 46). The phase assignments in July 2004 resulted from the fact that N1<N2 and the total naphthalenes were not three times greater than the phenanthrenes. Also, the phenanthrenes, dibenzothiophenes, and fluoranthene/pyrenes all showed increasing (stepped up) concentrations with higher degrees of alkylation (see Section 4.7.1).

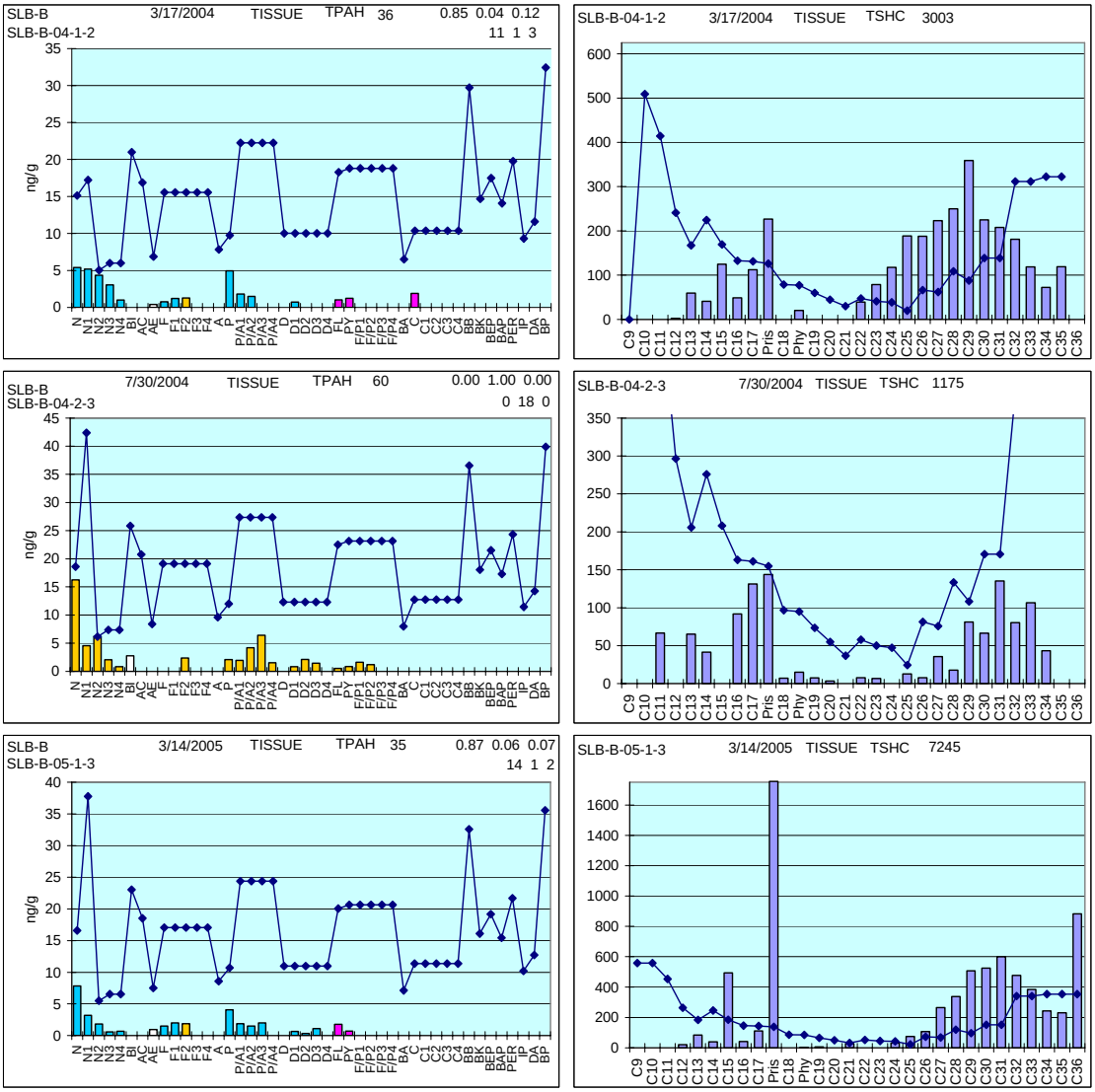

Figure 46 Representative PAH and SHC plots of Sleepy Bay mussel tissue extracts from March and July 2004 and March 2005 showing alternating signals derived primarily from dissolved- and particulate/oil-phase components. Phase coding: turquoise = dissolved, gold = particulate/oil-phase, fuchsia = pyrogenic.

The above MDL levels of higher-molecular-weight n-alkanes (between n-C22 and n-C34) and the trace of phytane in March 2004 are at odds with the PAH soluble-phase assignment (Figure 46 top and bottom). But at these low PAH concentrations (well below the MDL), the levels of any associated higher-molecular-weight PAH (which are several orders of magnitude lower in concentration than the aliphatics) are not detected even by selected ion monitoring GC/MS. It is also possible that the higher-molecular-weight n-alkanes could be from bacterial sources associated with the mussel tissues (Davis 1968; Han and Calvin 1969). The absence of phytane in the March 2005 sample supports the soluble-phase assignment.

In summary, like others in the Sound, this site has settled into a background pattern of extremely-low TPAH levels. The site appears pristine even though there are known deposits of residual EVOS oil at the head of the bay.

5.3.3.5 Zaikof Bay Mussel Tissue Chemistry

Zaikof Bay was only added to the LTEMP program in July 1999, and since that time all collections have shown very low TPAH concentrations (<200 ng/g) (Figure 47). Because of the delayed start, it is impossible to tell if the initial July 1999 TPAH level of 135 ng/g represents a peak in TPAH concentrations, but it is clear that low-level peaks were observed in March 2001 (113 ng/g) and March 2002 (176 ng/g), similar to the maxima observed at the other Prince William Sound regional stations (Figure 19 middle panel). In addition, there appears to be a very low-level TPAH spike (52 ng/g) at Zaikof Bay in July 2003 that was not observed in the other PWS stations. As at the other PWS regional stations, the PAH profiles for these maxima suggest a mixed-phase signal in July 1999 and a dominant soluble-phase signal in all of the other samples (Figure 48). In this regard, the PAH profiles appear very similar but not identical to, the patterns observed at the other stations within the Sound (Figure 32, Figure 35, Figure 39, and Figure 45).

The PAH profiles for the exceptionally low levels observed since the TPAH peak in March 2002 (Figure 47), suggest a predominantly soluble-phase pattern except possibly for July 2004, when an increase in the particulate/oil-phase pattern generated more of a mixed-phase signal (Figure 49). Traces of phytane and higher-molecular-weight n-alkanes in the SHC profiles from July 2004 and March 2005 also support the slight increase in the particulate/oil-phase signature, but again it should be stressed that these overall levels are extremely low, consistently below the laboratory MDL, and subject to interference from potential laboratory artifacts. Nevertheless, the suggested phase assignments do agree with the qualitative appearance of the plots even at these low levels. Furthermore, an increase in the particulate/oil-phase signal was observed in the July 2004 samples at all of the other Prince William Sound regional stations.

Like the other regional Prince William Sound stations, Zaikof Bay is exceptionally clean and shows no evidence of any recent oil contamination.

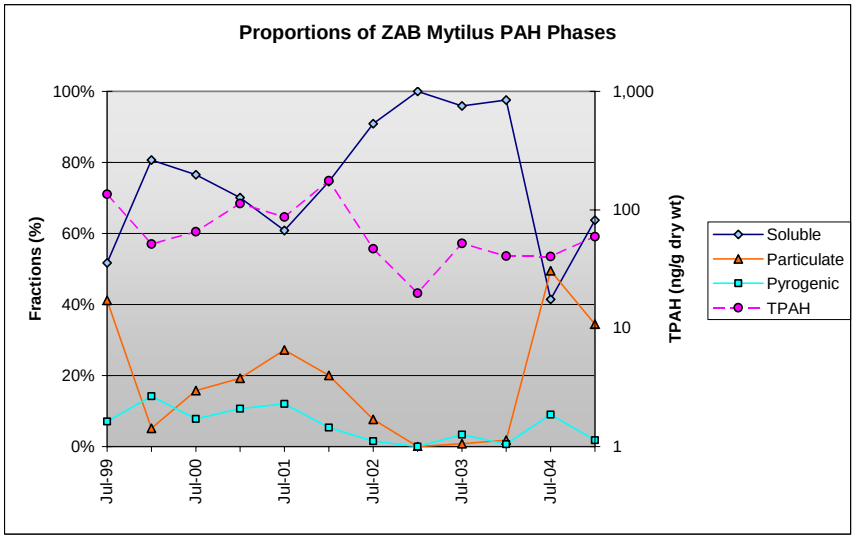

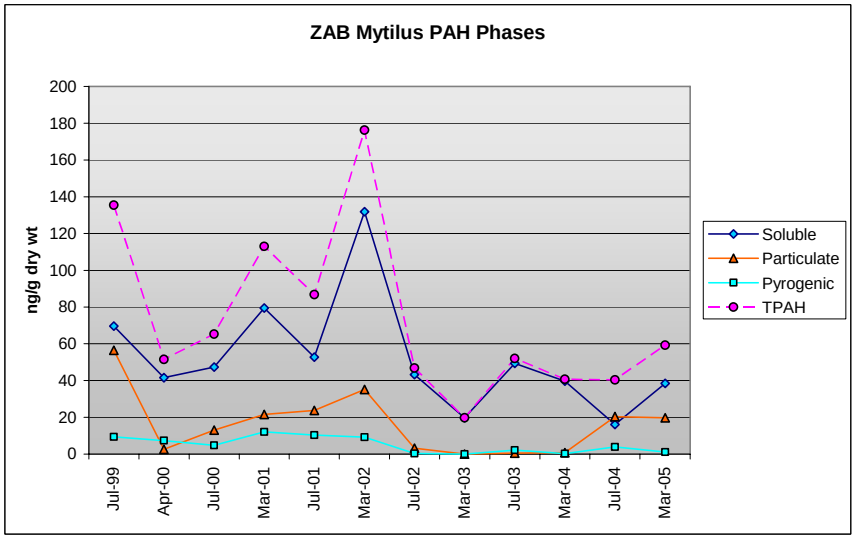

Figure 47 Time series of PAH indices for Zaikof Bay *Mytilus* tissues, 1993-2005.

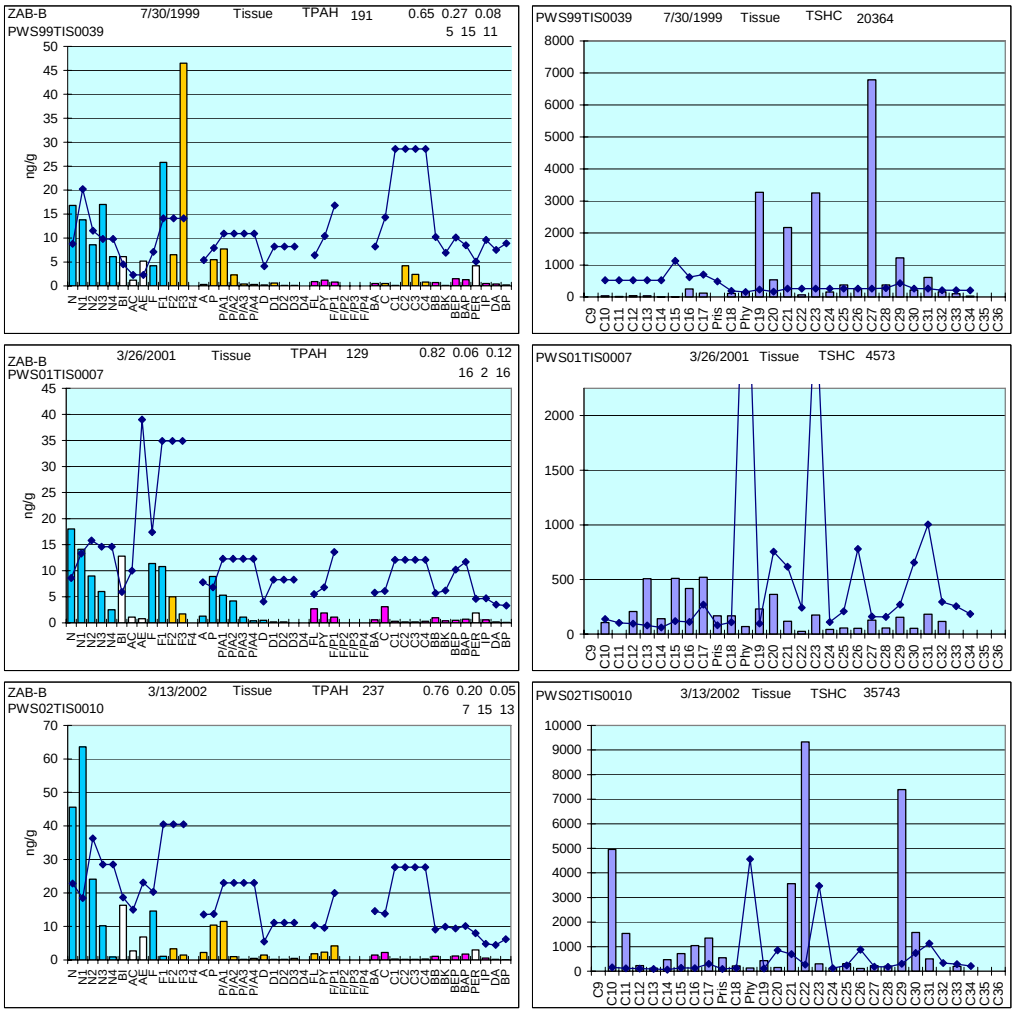

Figure 48 Representative Zaikof Bay PAH and SHC patterns observed in samples reflecting the TPAH maxima noted in July 1999, March 2001, and March 2002. Note, the anomalous fluorene pattern observed in July 1999 is not included in the TPAH value shown in Figure 47. Phase coding: turquoise = dissolved, gold = particulate/oil-phase, fuchsia = pyrogenic.

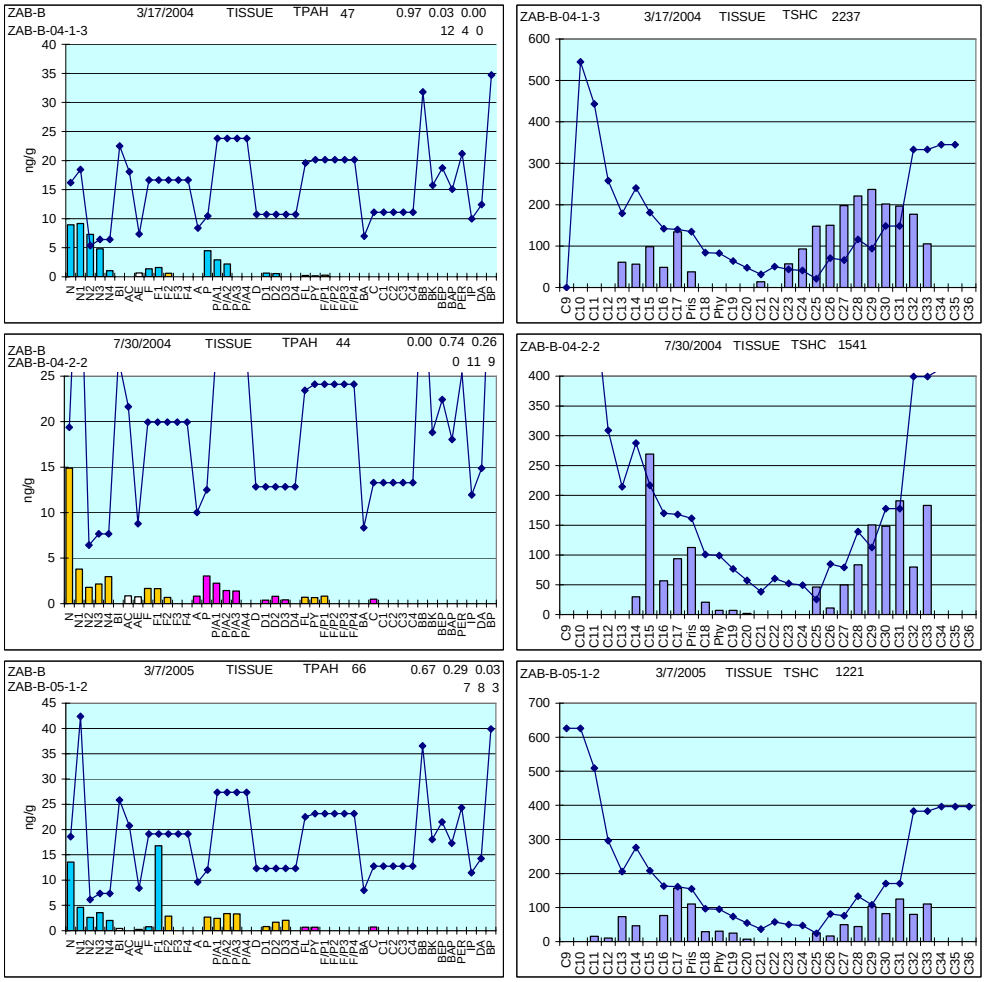

Figure 49 Representative PAH and SHC plots of Zaikof Bay mussel tissue extracts from March and July 2004 and March 2005. Phase coding: turquoise = dissolved, gold = particulate/oil-phase, fuchsia = pyrogenic.

5.3.4 Gulf of Alaska Stations

This section presents the tissue chemistry data from the Gulf of Alaska LTEMP stations, and includes: Aialik Bay (AIB), Shuyak Harbor (SHH), and Windy Bay (WIB). As in Sections 5.3.2 and 5.3.3, we first present the PAH index time-series plots to illustrate trends for each station followed by profiles for individual samples to examine specific features or explain anomalies noted in the trend-lines.

5.3.4.1 Aialik Bay Mussel Tissue Chemistry

All of the early LTEMP tissue data from Aialik Bay (AIB) appear compromised (Figure 50) due to the procedural artifact patterns associated with extremely-low-PAH-level samples (discussed in Section 4.7.2). Starting in July 1996, however, the data are

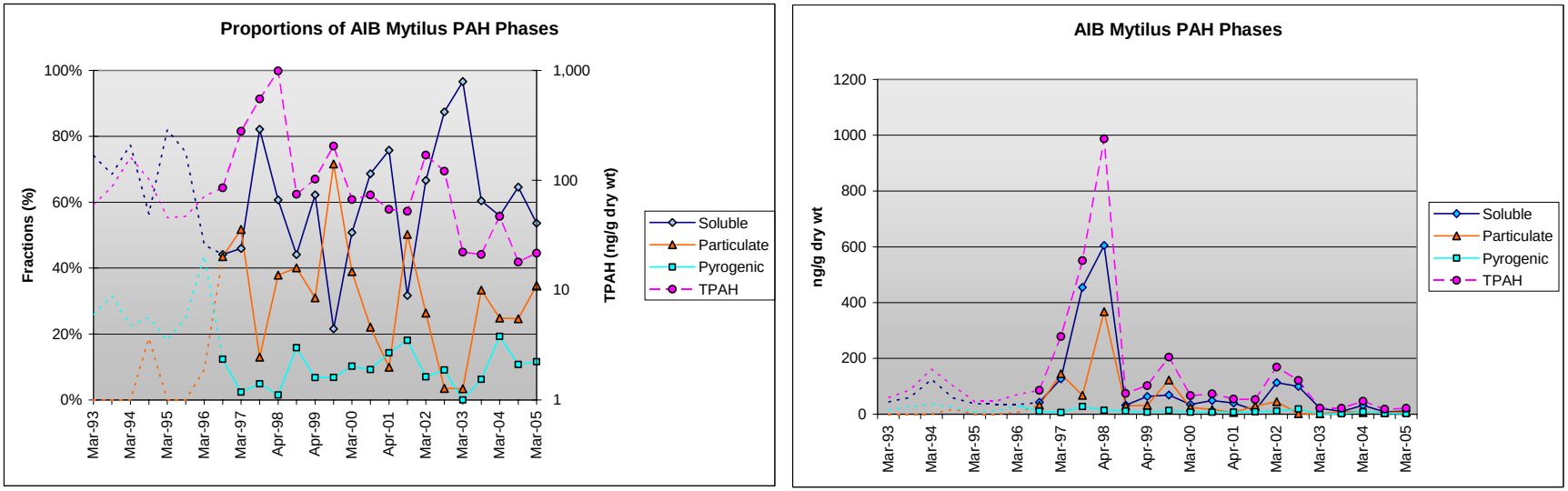

Figure 50 Time series of PAH indices for Aialik Bay *Mytilus* tissues, 1993-2005. Dotted connecting lines without symbols indicate questionable data.

believed to be more reliable, and they show three events with possibly elevated PAH concentrations. The first was a significant increase in TPAH concentrations starting in March 1997 that culminates in extremely high levels (978 ng/g dry weight) in April 1998. Enigmatically, the particulate and dissolved phases both contribute to the TPAH shift in March 1997, but as the peak builds through July 1997, the soluble-phase dominates, only to be joined again with an increase in the particulate/oil-phase at the peak in April 1998, suggesting unknown changing sources of hydrocarbons (Figure 51).

The TPAH slightly spikes again in August 1999 and in both March and July sample sets from 2002 (as do the within-PWS regional stations), but there is no corresponding TPAH peak in April 2001 compared to the PWS stations (Table 6). Similar time-series TPAH concentration maxima (and more importantly the missing TPAH spike in April 2001) were also observed at the two other Gulf of Alaska Stations (Shuyak Harbor and Windy Bay) (Figure 18, Figure 19 bottom graph, and Table 6). With the first of these low-level (<250 ng/g) TPAH spikes, a mixed-phase source is suggested, while the soluble-fraction makes up the majority of the PAH signal with variable contributions from the particulate/oil-phase and pyrogenic components in the subsequent peaks in March and July 2002 (Figure 50).

The data (Figure 52) for the TPAH spike in August 1999 show the same fluorene/lipid interference patterns and SHC anomalies discussed earlier for other samples collected at that time and analyzed at GERG (see Figure 32, Figure 35, Figure 39, Figure 45 and Figure 48). The July 2002 sample (Figure 52) is important to compare to the March 2002 sample, because it was part of the first sample set analyzed for this program by the Auke Bay Laboratory (ABL). On such an occasion, there might be concern if reported levels differed significantly from the previous sampling/analysis, but from supporting evidence, the ABL data seem reliable. While the TPAH level is slightly lower (121 ng/g) than GERG's March 2002 sample (169 ng/g), the overall TPAH values are both in the same range, and the PAH patterns are comparable (both showing a predominately dissolved-phase signal). The July 2002 SHC profile generated by ABL also shows a marine biogenic pattern (free of particulate/oil-phase components) without interfering lipids.

As noted above, the Aialik Bay, Shuyak Harbor and Windy Bay samples from April 2001 did not show the TPAH maxima observed at the PWS regional sites (Table 6 and Figure 19), and while they had similar PAH profiles among themselves (Figure 53), they were different from the corresponding samples measured in Prince William Sound (compare the data in Figure 53 with the March 2001 PWS data in Figure 32, Figure 39, Figure 45 and Figure 48). Because all of these samples were analyzed at the same time, we attribute the observed differences to actual differences in the field as opposed to laboratory or systematic bias or error.

After July 2002, the TPAH levels at Aialik Bay have all been extremely low (< 50 ng/g) with the overall trend since 1998 decreasing (Figure 50 left panel) and the majority of PAH components usually contributed from the soluble fraction. The PAH and SHC plots for March 2004, July 2004, and March 2005 (Figure 54) show a change in this overall

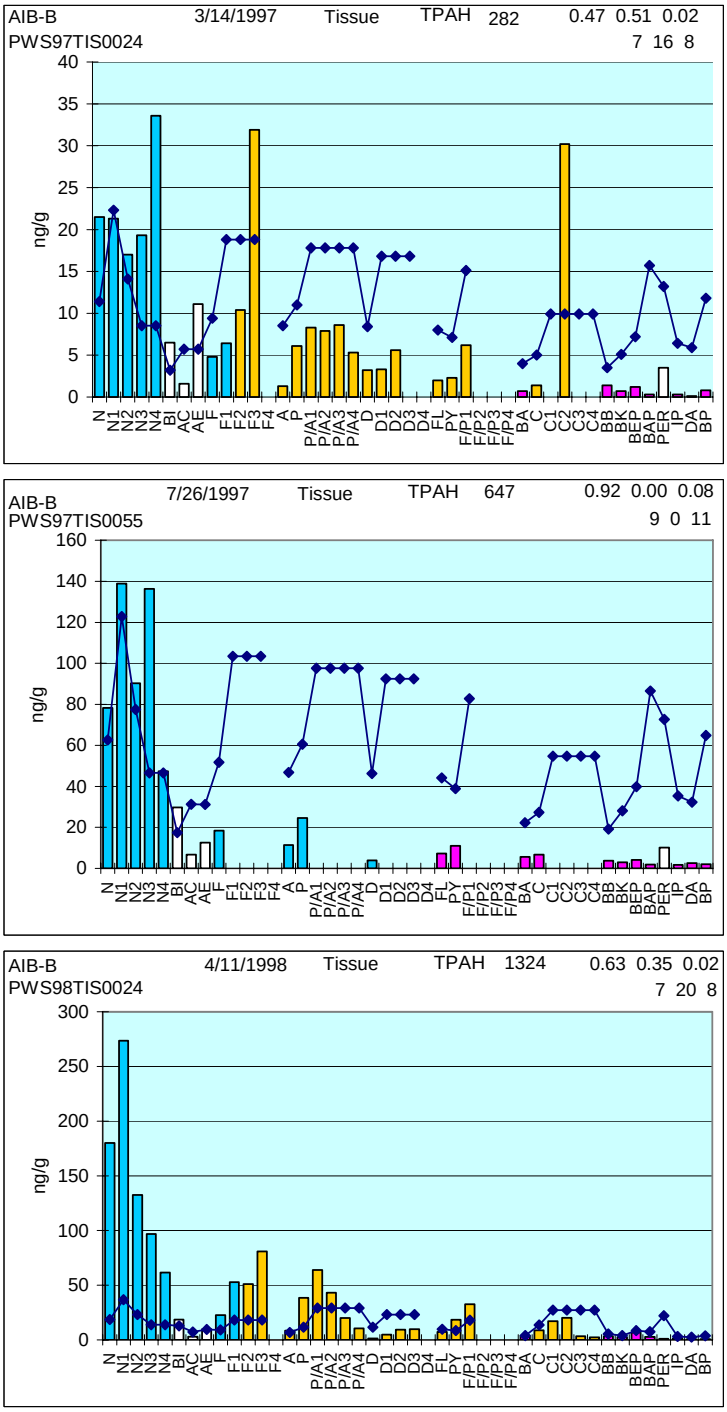

Figure 51 Representative PAH plots from the elevated TPAH levels observed between March 1997 and April 1998 at Aialik Bay. Phase coding: turquoise = dissolved, gold = particulate/oil-phase, fuchsia = pyrogenic.

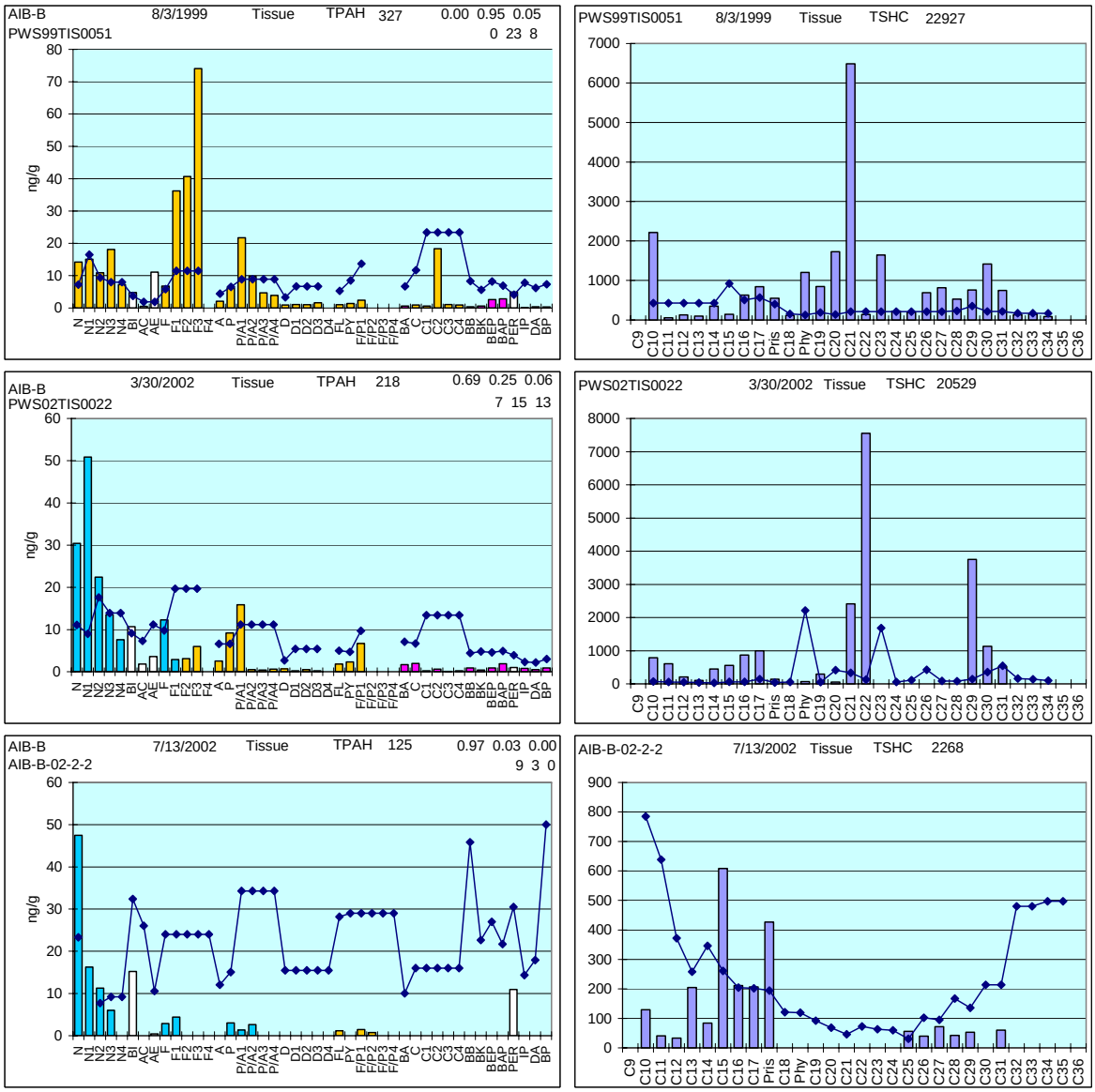

Figure 52 Representative profiles of *Mytilus* tissue extracts from Aialik Bay in August 1999, March 2002, and July 2002. The 1999 and March 2002 samples were analyzed by GERG, and the July 2002 sample was among the first to be analyzed by ABL (see text for discussion). Phase coding: turquoise = dissolved, gold = particulate/oil-phase, fuchsia = pyrogenic.

pattern, with a relative decline in the soluble-phase (from March 2004) and concomitant increases in the pyrogenic- and particulate/oil-phase fractions in July 2004 and March 2005, respectively. Again, however, the overall TPAH levels are extremely low (all < 50 ng/g) and, as such, these phase-fraction assignments are made with less confidence.

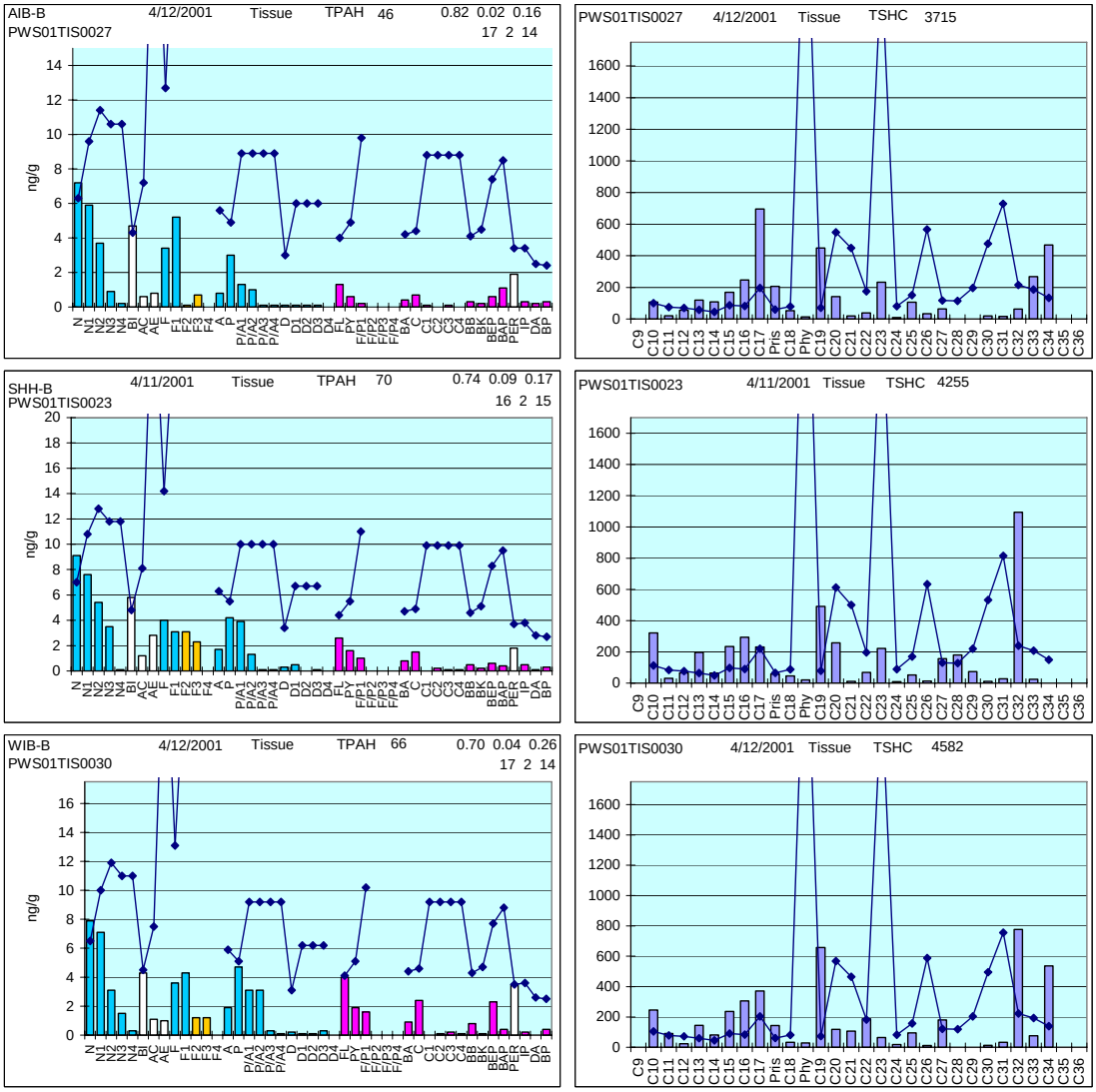

Figure 53 Representative *Mytilus* tissue PAH and SHC profiles from April 2001, Gulf of Alaska regional stations (AIB, SHH, and WIB) showing similarity in low-level TPAH. Contrast these patterns with those from PWS regional stations in March 2001 showing increased TPAH levels (Figure 32, Figure 39, Figure 45 and Figure 48). Phase coding: turquoise = dissolved, gold = particulate/oil-phase, fuchsia = pyrogenic.

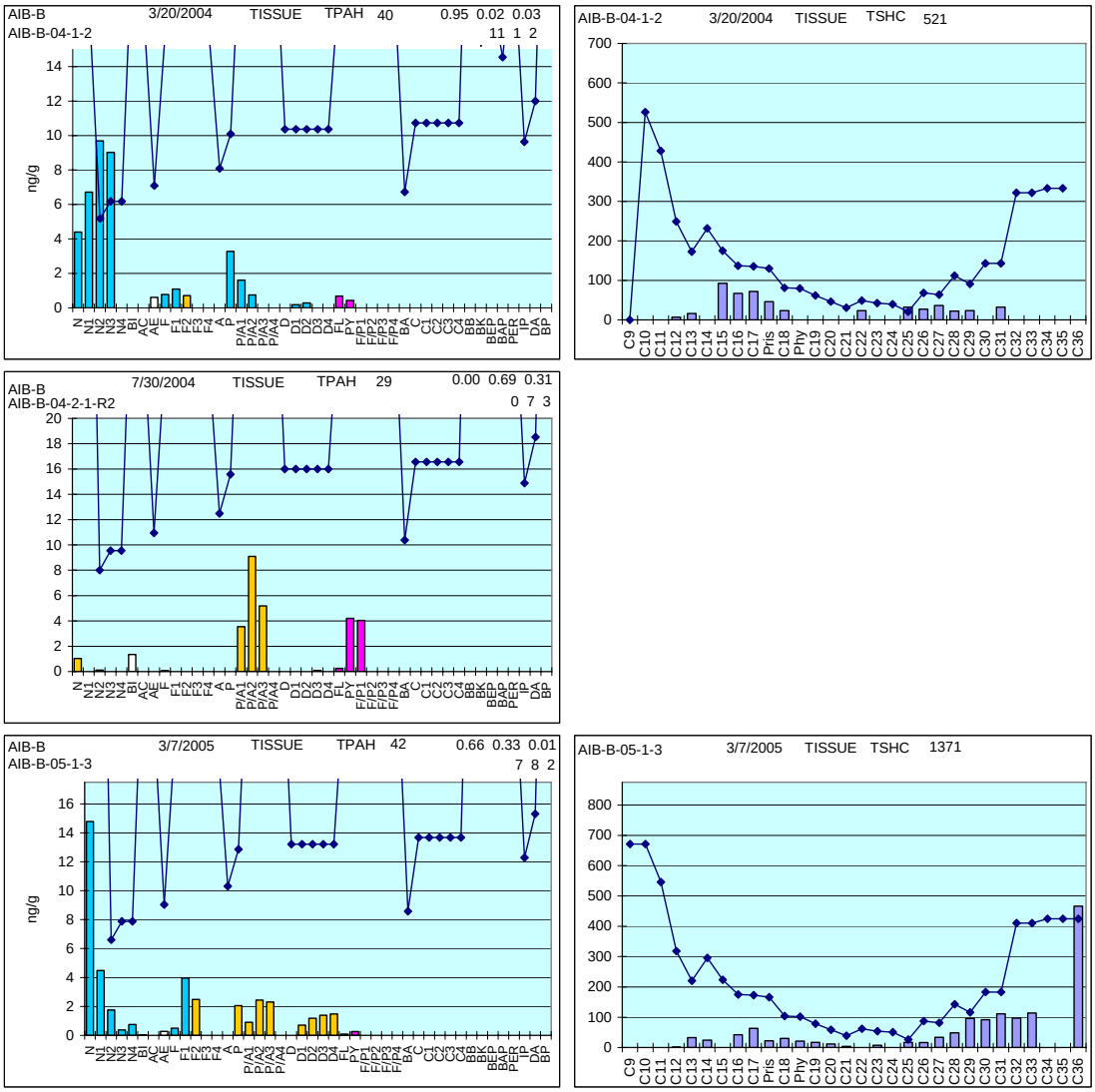

Figure 54 Representative PAH and SHC profiles from extremely low-level Aialik Bay *Mytilus* tissue extracts collected in March 2004, July 2004, and March 2005 showing variable contributions from soluble-, pyrogenic-, and particulate/oil-phase fractions. The SHC fraction from July 2004 was lost during sample workup. Phase coding: turquoise = dissolved, gold = particulate/oil-phase, fuchsia = pyrogenic.

5.3.4.2 Shuyak Harbor Mussel Tissue Chemistry

As at all other remote and more pristine LTEMP stations, all of the early (March 1993 – March 1996) tissue data from Shuyak Harbor were compromised (Figure 55) due to the procedural artifact patterns associated with extremely-low-PAH-level samples (discussed in Section 4.7.2). More reliable data were generated starting with the July 1996 samples, and since that time, two events with elevated TPAH levels were observed.

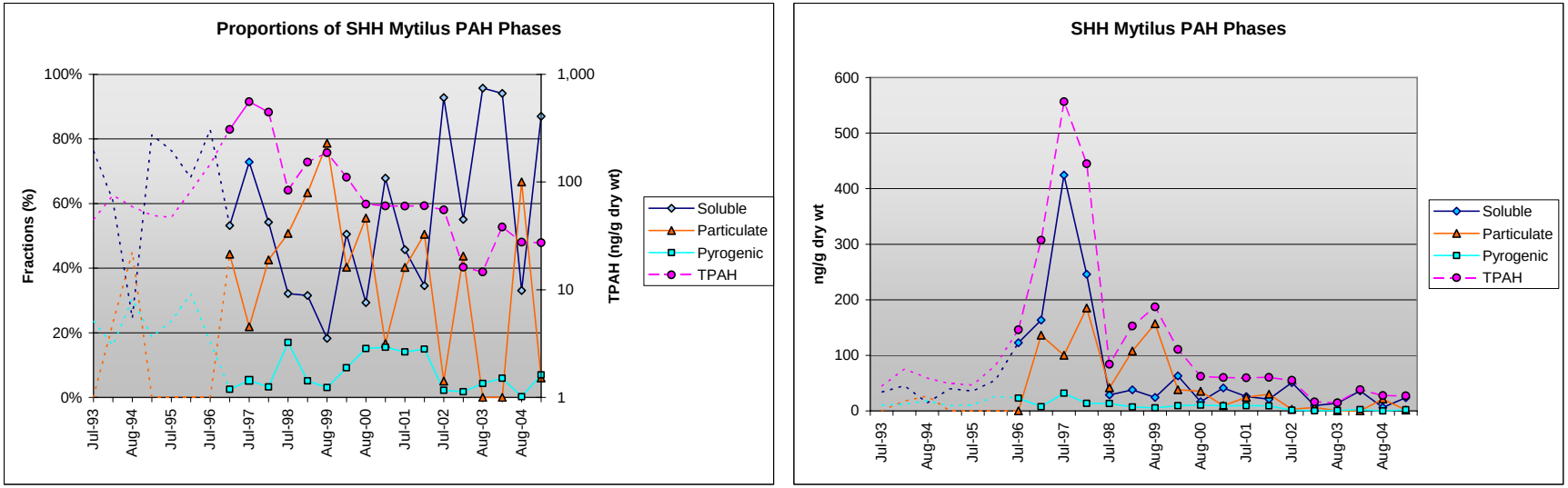

Figure 55 Time series of PAH indices for Shuyak Harbor *Mytilus* tissues, 1993-2005. Dotted connecting lines without symbols indicate questionable data.

Similar to the trend observed at Aialik Bay, there was a significant increase in PAH concentrations starting in July 1996, but at Shuyak Harbor it spiked early in July 1997 at 557 ng/g rather than the following April. However, two of the three April 1998 replicate levels were still elevated (445 ng/g mean), and this was followed by another secondary TPAH maxima in August 1999 (187 ng/g). Throughout the 1996-1998 interval, the TPAH maxima were primarily derived from a combination of soluble- and particulate/oil-phase signals (Figure 56) with the soluble phase dominating. The smaller, secondary maxima observed in August 1999 (Figure 55) showed greater contributions from the particulate/oil-phase with the soluble-phase constituents becoming slightly more important in March 2000 (Figure 57). The peak in August 1999 corresponded with similar TPAH maxima at Aialik Bay and Windy Bay (Figure 19**)**, the other two Gulf of Alaska regional stations. As in all the other July/August 1999 LTEMP samples, the fluorenes shown in the plot are not included in the TPAH values shown in Figure 55.

TPAH levels then leveled out at around 60 ng/g in August 2000, and unlike the other two Gulf of Alaska regional stations that showed elevated TPAH levels again in July 2002, no further TPAH maxima have been observed. To allow direct comparisons with the other GOA regional stations, Figure 58 presents representative Shuyak Harbor PAH and SHC profiles for March and July 2002 and July 2004 (see Figure 52 and Figure 54).

In April 2001, the three Gulf of Alaska sites did not show the TPAH maxima observed at the PWS regional sites (Table 6 and Figure 19). While they had similar PAH profiles among themselves (Figure 53), they were different from the corresponding samples measured in Prince William Sound (Figure 53 versus March 2001 data in Figure 32, Figure 39, Figure 45 and Figure 48). Because both the Gulf and PWS samples were analyzed in the same batch, we attribute the observed differences to actual differences in the samples as opposed to laboratory or systematic bias.

After March 2003, the TPAH levels at Shuyak Harbor were all extremely low (< 40 ng/g) with the overall trend decreasing since 1997 (Figure 55), and the majority of PAH components usually contributed from the soluble fraction. The one possible exception to this pattern occurred in August 2004 (Figure 55 and Figure 58), when there was a shift to the particulate/oil-phase. Interestingly, this same phase shift was also observed at Aialik Bay and Windy Bay, the other two GOA regional stations, as well as most of the Prince William Sound regional stations. In the past, elevated particulate/oil-phase contributions have been observed at Shuyak Harbor in August 1999 (Figure 57) and March 2002 (Figure 58). In all cases, the PAH contributions from pyrogenic products have been low (<20%) and variable (Figure 55); however, at these very low overall TPAH levels, quantitative assignment of phase-fractions is very tenuous. Nevertheless, the TPAH levels measured at Shuyak Harbor over the last six years are extremely low and reflect the pristine nature of the site.

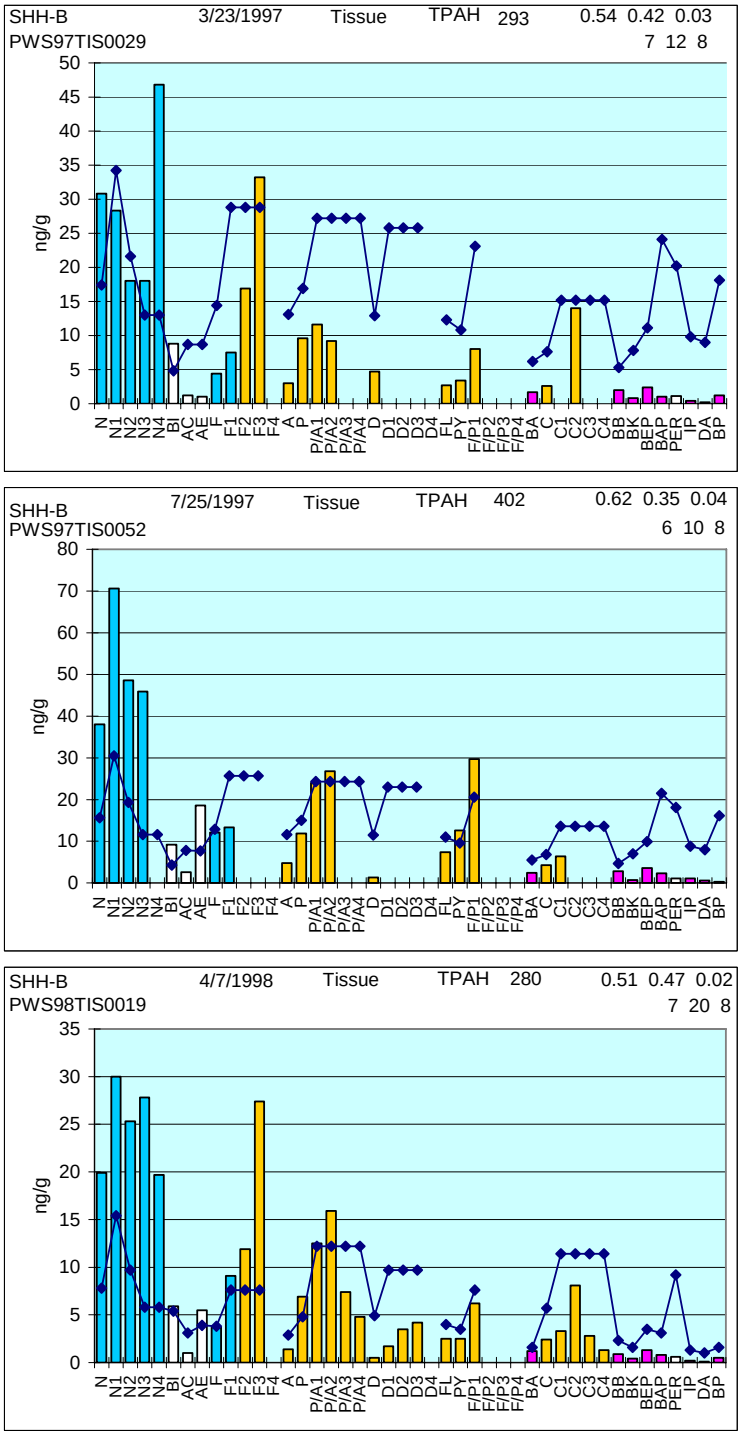

Figure 56 Representative PAH profiles from the TPAH maxima observed at Shuyak Harbor in March 1997, July 1997, and April 1998. Phase coding: turquoise = dissolved, gold = particulate/oil-phase, fuchsia = pyrogenic.

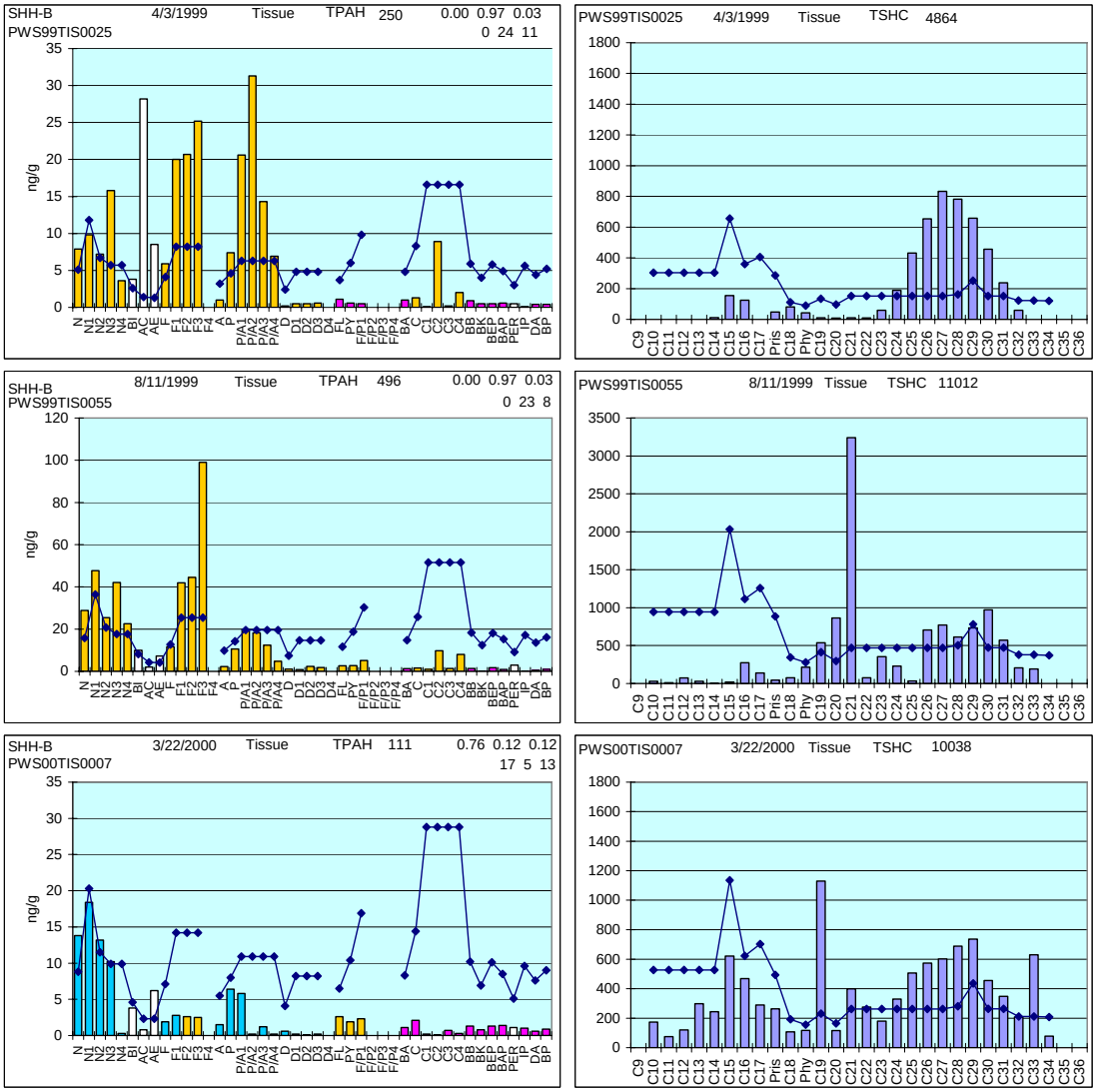

Figure 57 Representative PAH profiles from the secondary TPAH maxima observed at Shuyak Harbor in April 1999, August 1999, and March 2000. Phase coding: turquoise = dissolved, gold = particulate/oil-phase, fuchsia = pyrogenic.

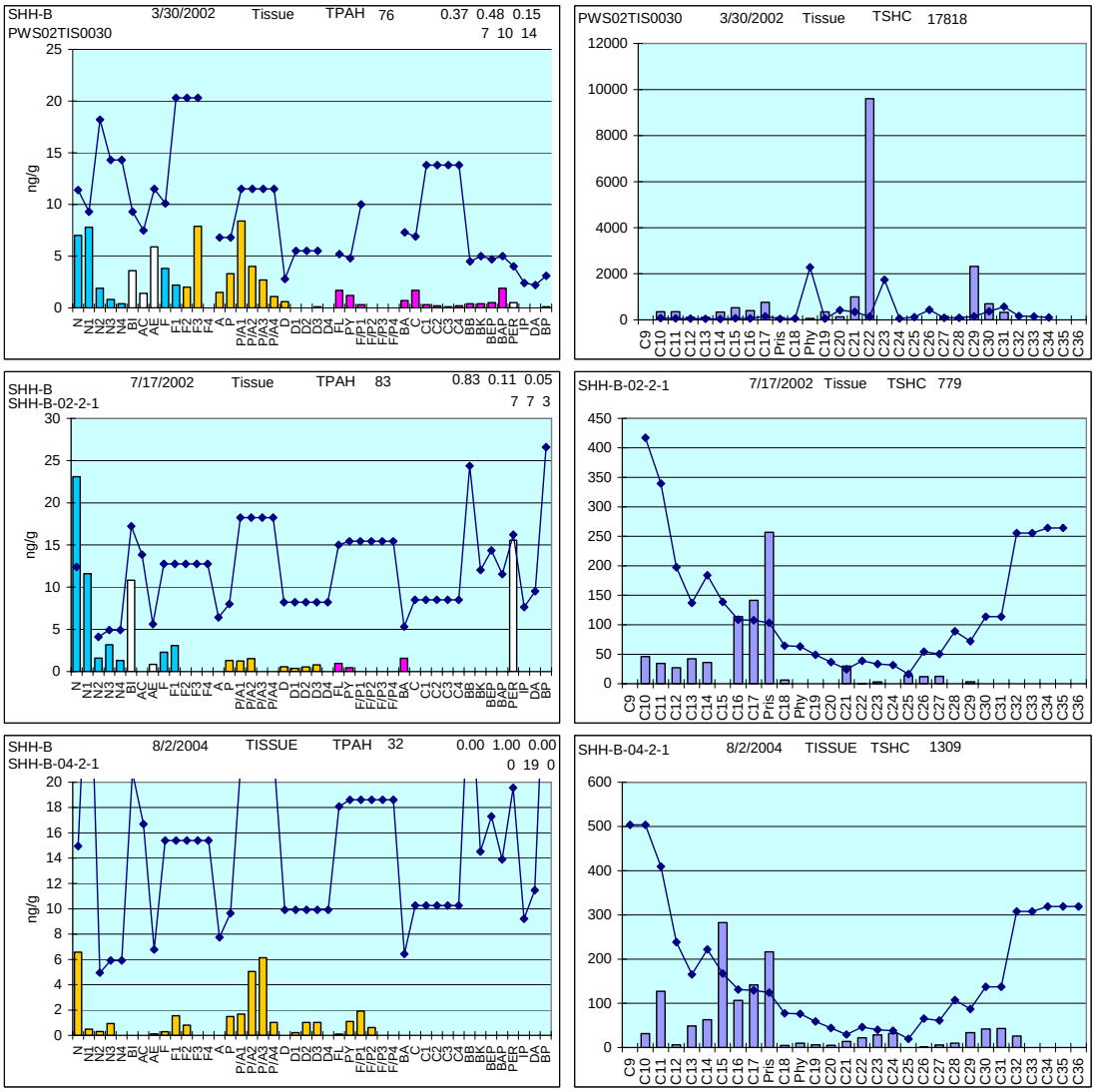

Figure 58 Representative profiles of *Mytilus* tissue extracts from Shuyak Harbor in March 2002, July 2002, and August 2004. Phase coding: turquoise = dissolved, gold = particulate/oil-phase, fuchsia = pyrogenic.

5.3.4.3 Windy Bay Mussel Tissue Chemistry

The time-series of PAH Indices at Windy Bay (Figure 59) suggest an overall decreasing trend of TPAH values since March 1997, and as was the case at most of the other cleaner LTEMP sites, all of the early data from March 1993 to July 1996 appear compromised by procedural artifacts. The mixed-phase sourced TPAH maxima at 539 ng/g in March 1997 is unique to this station; however, the predominantly soluble-phase sourced TPAH peaks at 501 ng/g in July 1997 and 469 ng/g in April 1998, corresponds to similar maxima (or elevated TPAH levels) at Aialik Bay and Shuyak Harbor, the other two regional Gulf of Alaska stations.

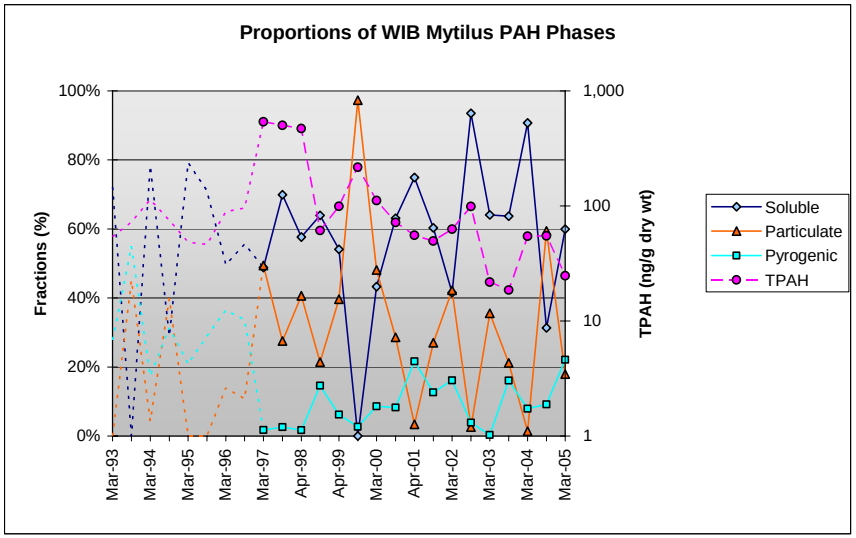

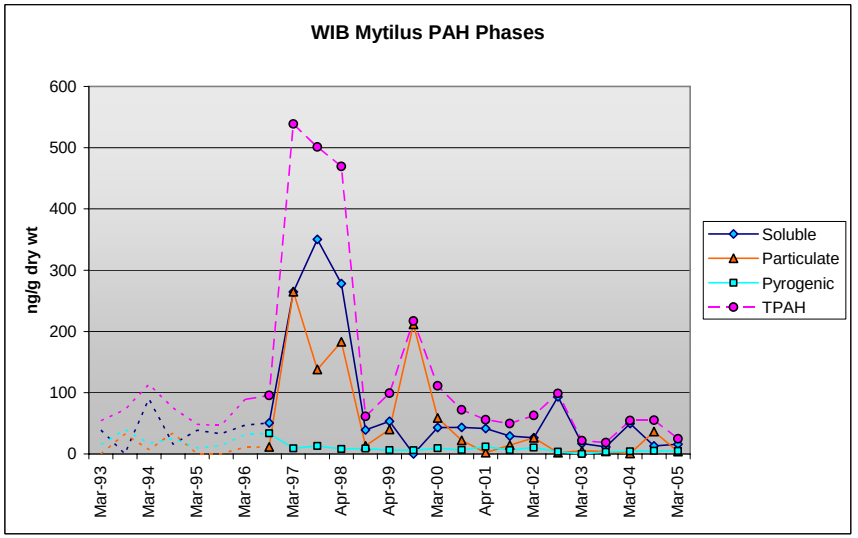

Figure 59 Time series of PAH indices for Windy Bay *Mytilus* tissues, 1993-2005. Dotted connecting lines without symbols indicate questionable data.

The PAH profiles for the elevated TPAH samples collected in March and July 1997 and April 1998 (Figure 60) show the relative transition from a mixed-phase sourced signal to a dominant soluble-phase and then back to a mixed signal with relatively higher contributions from the soluble phase. This is the only site in the LTEMP program where these three sequentially elevated TPAH levels and source-signatures were observed; however, it is possible to see the similarity in the PAH profiles for the April 1998 data from this site with those from Aialik Bay and Shuyak Harbor (compare Figure 60 with Figure 51 and Figure 56). The data for April 1998 suggest a common mixed-phase source at all three sites.

Following these TPAH maxima in the July 1997 – April 1998 period, the TPAH levels at Windy Bay dropped significantly (Figure 59) only to show two lower-level maxima in August 1999 and July 2002. The August 1999 TPAH peak corresponds to similar maxima at the other two Gulf of Alaska stations, but in July 2002 a similar peak was only observed at Aialik Bay and not Shuyak Harbor (Figure 19 bottom). The PAH profiles from the August 1999, March 2002, and July 2002 samples from Windy Bay (Figure 61) allow comparisons with Aialik Bay (Figure 52) and Shuyak Harbor (Figure 57 and Figure 58). Based on the similar TPAH levels and the comparative PAH signatures, we concluded that the three stations were subject to similar soluble-phase and particulate/oil-phase sources at these times.

As noted above, the samples from the three April 2001 Gulf of Alaska sites did not show the TPAH maxima observed at the PWS regional sites (Table 6 and Figure 19). In particular, the TPAH levels at Windy Bay in April 2001 were at a minimum (Figure 59), and while they had similar PAH profiles among themselves (Figure 53), they were different from the corresponding samples measured in Prince William Sound (compare the data in Figure 53 with the March 2001 data in Figure 32, Figure 39, Figure 45 and Figure 48). These comparisons further support the hypothesis that the outer Gulf of Alaska regional stations were receiving hydrocarbon sources different from the stations within Prince William Sound.

Since March 2003, the TPAH levels at Windy Bay have been very low (< 60 ng/g), and the PAH and SHC profiles suggest a predominant soluble-phase signal with the possible exception of August 2004 when a particulate/oil-phase signal was suggested in two of the three replicates (Figure 59 and Figure 62). A similar particulate/oil-phase signal was also observed in the July/August 2004 samples from Aialik Bay and Shuyak Harbor (Figure 54 and Figure 58) and all of the Prince William Sound regional stations.

Overall, the TPAH levels at Windy Bay appear to be continuing to decline (Figure 59), and at this time, there is no evidence of any significant hydrocarbon contamination at this site.

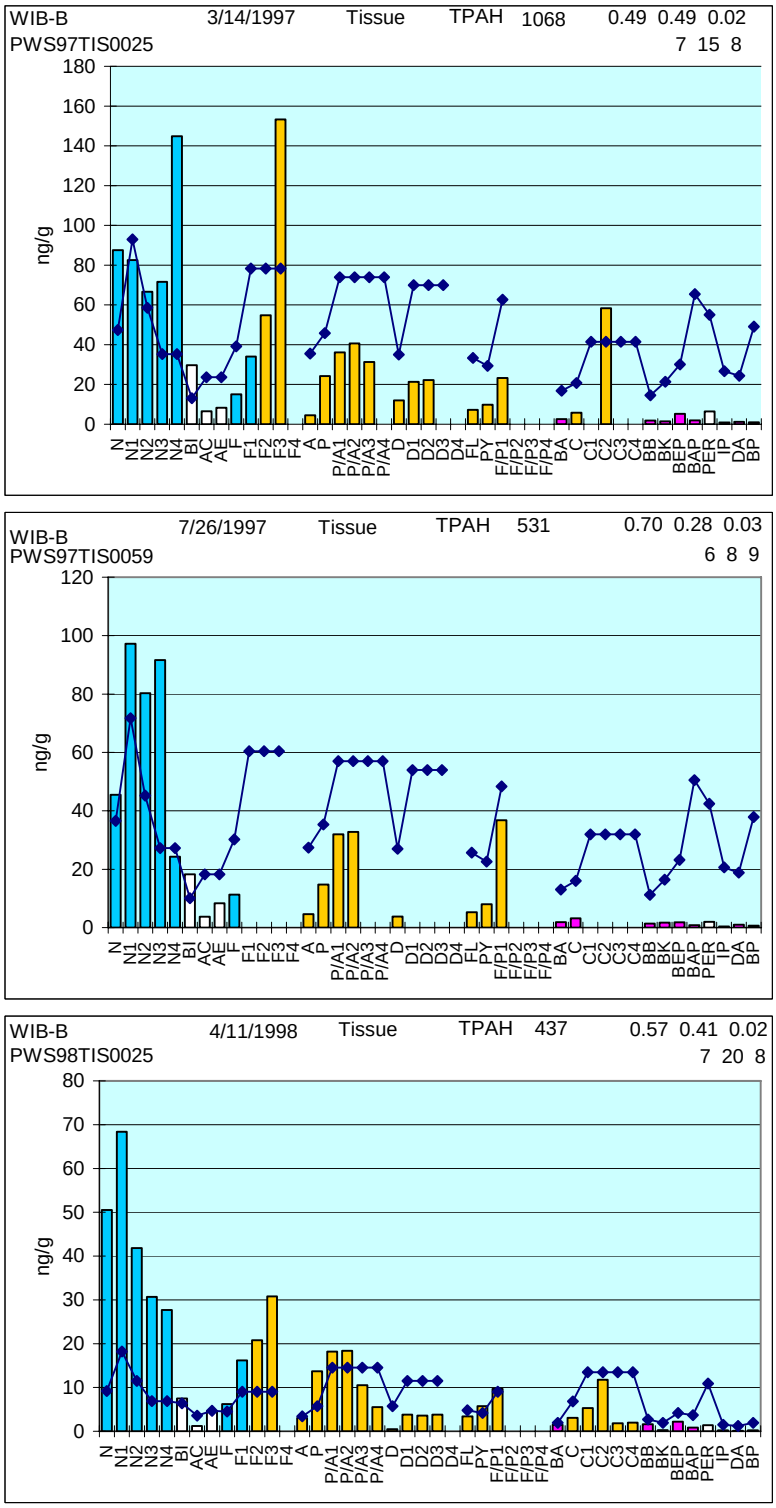

Figure 60 Representative PAH profiles of Windy Bay Mytilus tissue extracts from the three elevated TPAH samples collected in March and July 1997 and April 1998. Phase coding: turquoise = dissolved, gold = particulate/oil-phase, fuchsia = pyrogenic.

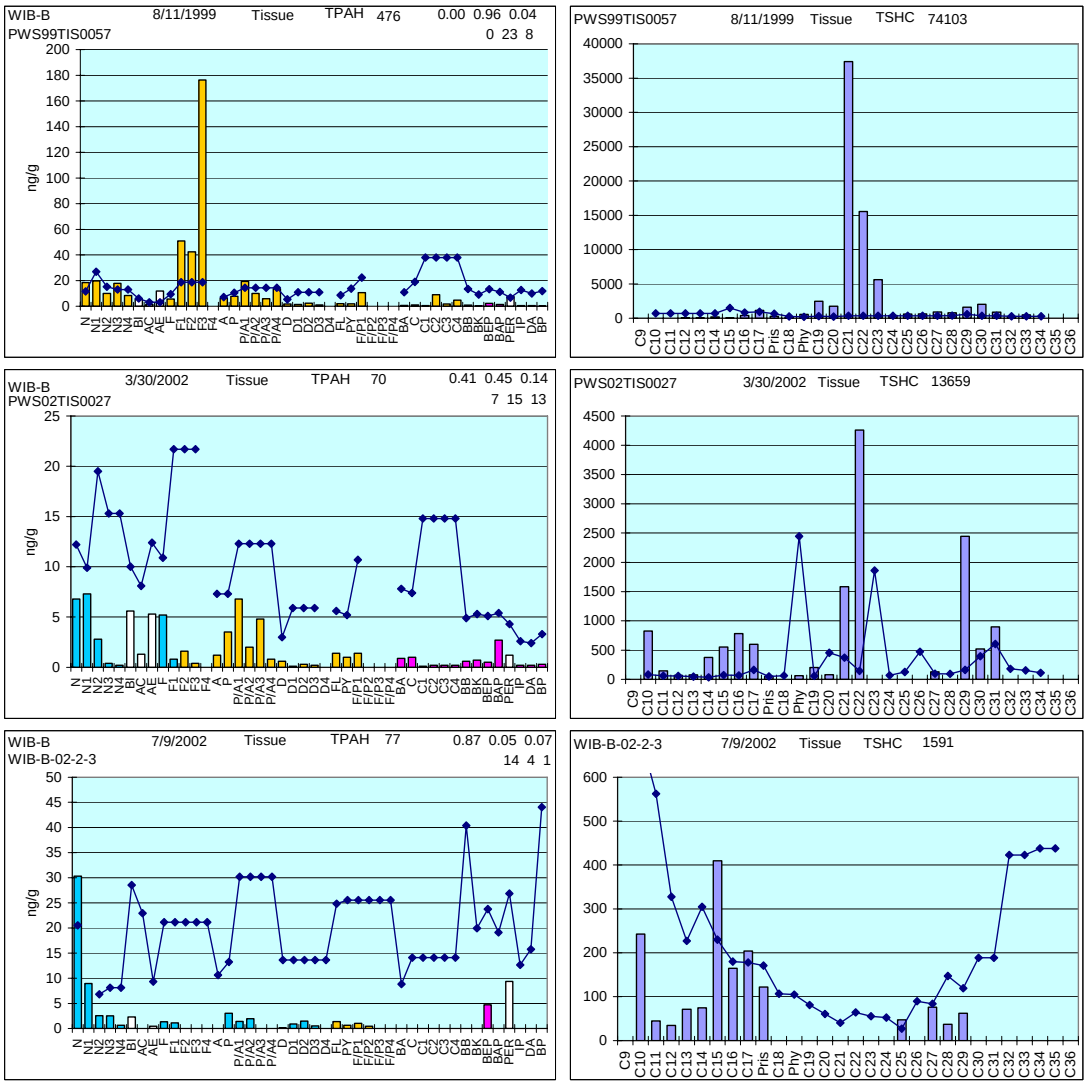

Figure 61 Representative profiles of *Mytilus* tissue extracts from Windy Bay in August 1999, March 2002, and July 2002. The elevated fluorene components in August 1999 are not included in the TPAH value shown in Figure 59. Phase coding: turquoise = dissolved, gold = particulate/oil-phase, fuchsia = pyrogenic.

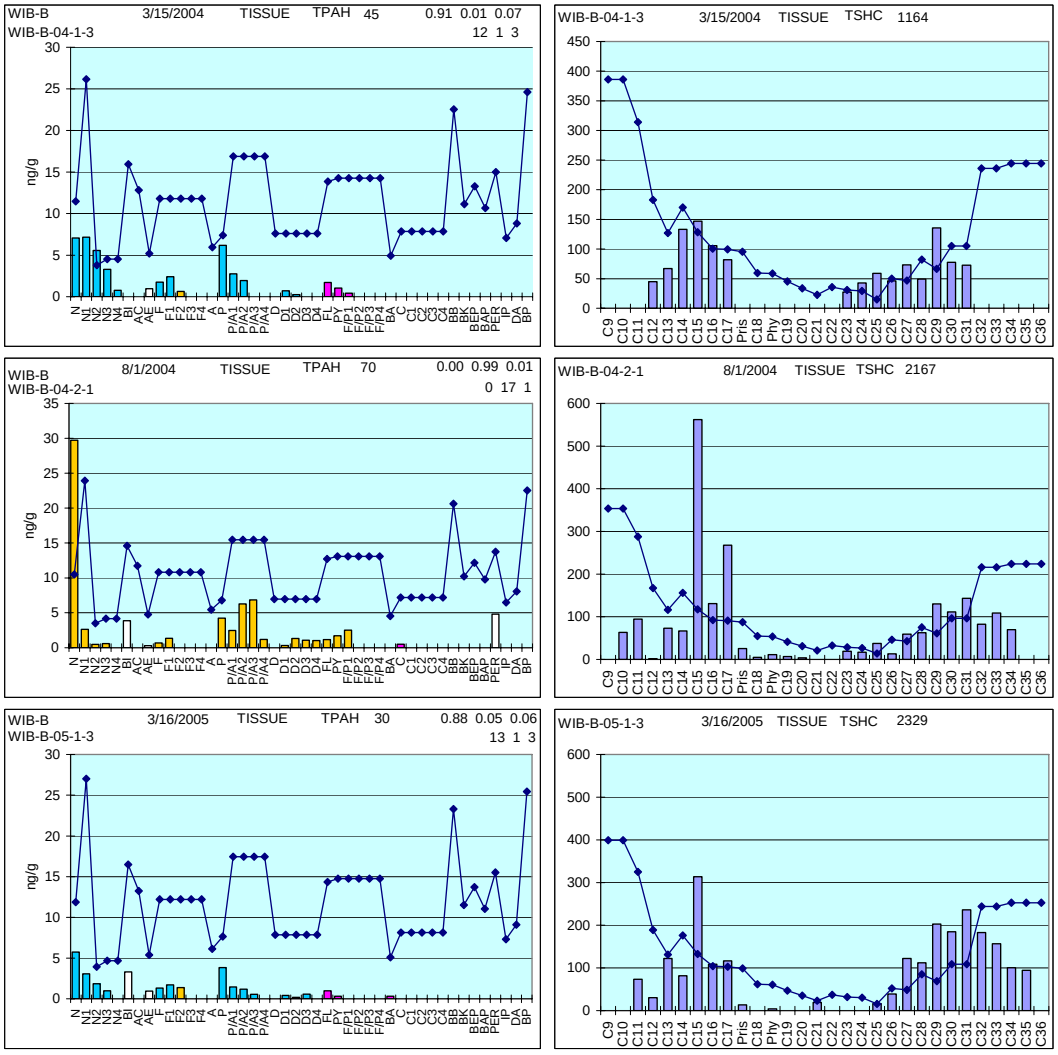

Figure 62 Representative profiles of *Mytilus* tissue extracts from Windy Bay from March and July 2004 and March 2005. Phase coding: turquoise = dissolved, gold = particulate/oil-phase, fuchsia = pyrogenic.

5.3.5 Summary of Tissue Results

With the development of new PAH component indices, it became obvious that the compromised early data must be resolved in order to meaningfully interpret the indices' trends. For example, the early years of the program (March 1993-March 1996) generated data mostly unusable for current needs. Due to the laboratory's GC/MS peak integration procedures, low-level-TPAH samples did not report reliable values to use in trend analyses (section 4.7.2). Only the samples with higher TPAH levels adequately quantified the full suite of analytes. For this report, the low-level samples and any other obviously unreliable data are graphically identified by dashed lines in TPAH Index plots

and ignored. Likewise, the July 1994, July 1996, and July 1999 samples with anomalous fluorene data have been used with the fluorene analytes zeroed. TPAH spikes in July 1999, March 2001 and 2002 and July 2002, which were previously questionable as laboratory artifacts were determined to be acceptable data with significant regional patterns. The resulting adjusted data set without the known anomalies was used for interpretations.

The two Port Valdez stations, being mainly influenced by the treated ballast water discharge from the Alyeska Marine Terminal, are trending independently of the regional sites. Remarkably, the mussels adjacent to the Alyeska Marine Terminal reflected very low and invariable TPAH values, in line with the more remote and pristine stations, which likely reflects changes in the Terminal's treated ballast water discharges. The October 2004 and March 2005 samples from Gold Creek detected an unreported diesel spill that probably occurred sometime in August or early September 2004.

Outside of Port Valdez, TPAH levels have been decreasing in mussel tissues since 1999 and are now at all-time lows for the LTEMP sites. Most stations are now showing mussel tissues with less than 100 ng/g TPAH (and many with less than 50 ng/g). Also, with the exception of the July/August 2004 samples, most reflect a dissolved–phase hydrocarbon signal from an unknown source(s). The July/August 2004 samples exhibited a low-level particulate/oil-phase pattern at both the regional stations within Prince William Sound and the outer Gulf of Alaska coast. Beyond this single event, the synchrony of TPAH highs and lows plus the similarity of signatures suggests that usually the inner Prince William Sound sites are collectively experiencing one low-level source of hydrocarbons while the outer coastal stations are exposed to a possibly different common source(s).

In an effort to determine if the regional Gulf of Alaska stations were simply picking up a background signal from suspended particulate material (SPM) transported by the Alaska Coastal Current (Saupe pers comm, 2004), we examined the 2002 EMAP sediment PAH profiles from the Copper River Delta, Nuka Bay, and Shelikof Strait (Figure 63). The Nuka Bay and Shelikof Strait EMAP stations are the closest available sites to Aialik Bay and Shuyak Harbor LTEMP stations, and the Copper River represents one of several potential sources of the PAH-laden SPM that is transported into PWS and along the outer Kenai coast by the Alaska Coastal Current. Clearly, the PAH profiles from the three respective sediments are nearly identical and reflect the region-wide deposition of a common particulate source(s) of PAH. This pattern is not observed, however, in the mussel tissue samples from the coastal LTEMP stations (which mostly reflect a dissolved-phase signal) nor does it match the particulate/oil-phase signal observed in the July/August 2004 collections from either the PWS or outer coastal regional sites. We therefore conclude that the observed PAH patterns from these regions reflect some other sources or series of events not related to transport of the coastal-current's suspended sediments and their ubiquitous PAH profile.

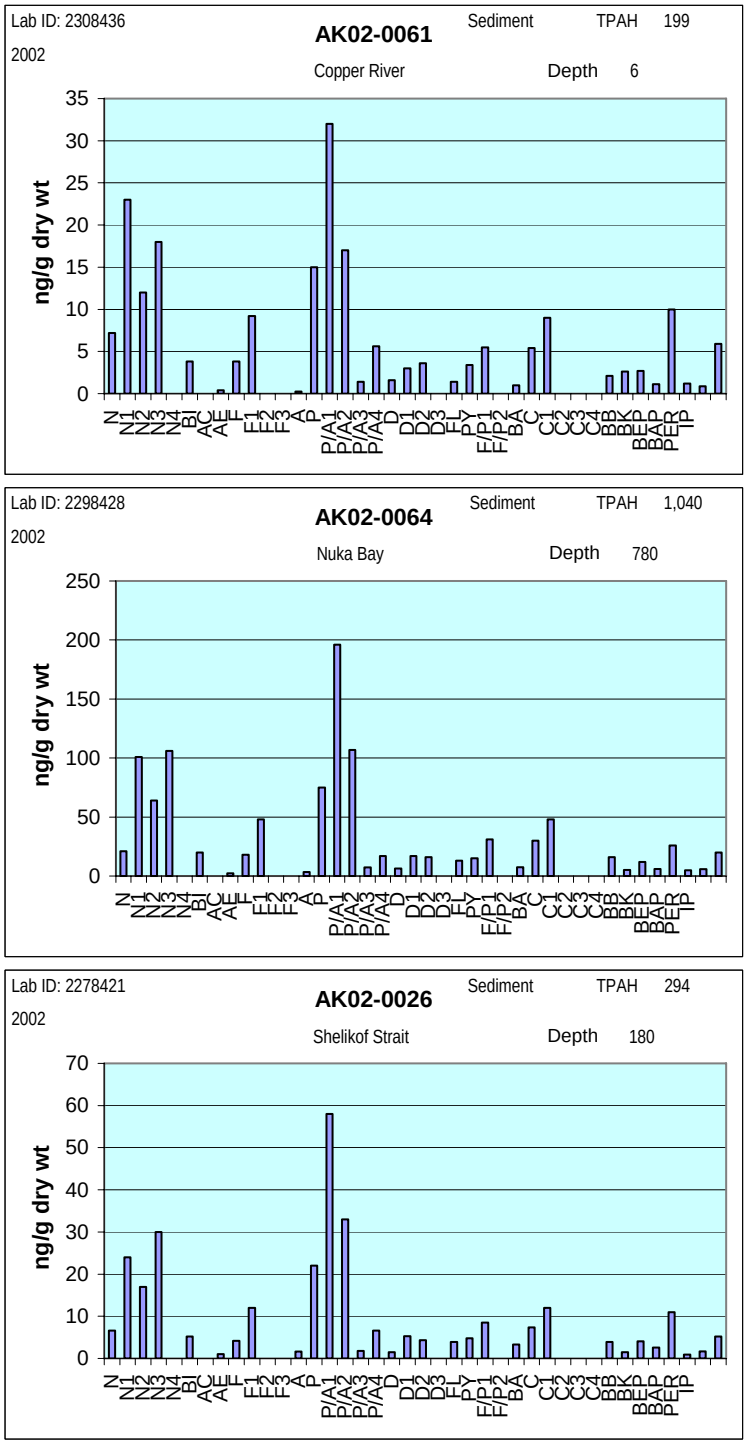

Figure 63 Representative PAH profiles in sediment samples from the Copper River Delta, Nuka Bay, and Shelikof Strait (data from the EPA EMAP program).

Power regressions of log transformed average TPAH time series from the five PWS and three GOA stations show parallel trends (Figure 64). TPAH levels in both regions are dropping at nearly identical rates. This parallelism suggests the decreases are influenced by similar (oceanographic-scale?) processes but the occasional asynchrony of peak events (Figure 19) suggests regional variation in the dynamics. So what broad-scale sources might appear as an ambient background dissolved signal? Suggestions include atmospheric deposits, forest fires, leaching from the pervasive source-rock (oil shale or coal), some upwelling/climate-driven events, a combination of these or some novel mechanism relating to decadal oscillations and/or global warming. There are few data to support or refute any of these concepts, but we are currently favoring atmospheric adsorption and deposition mechanisms (NRC 2003). Also, while most of the PAH profiles reflect a predominantly dissolved-phase signal, what event/mechanism might explain the low-level particulate/oil-phase area-wide pattern both within Prince William Sound and the outer coastal stations observed in July/August 2004?

Another question is how low will this generally declining trend in TPAH values continue? Follow-up sampling in 2004 for residues from the 1997 *M/V Kuroshima* grounding in Summer Bay (near Dutch Harbor) found TPAH levels between 25 and 85 ng/g dry wt, with an average of 57 ng/g dry wt (Helton et al. 2004). This compares favorably with LTEMP's March 2004 range of 32-61 ng/g inside the Sound and 24-37 ng/g at the Gulf sites. These data suggest a natural background TPAH somewhere below 50 ng/g—a range in which analytical sensitivity is highly susceptible to procedural artifacts. It might easily be the case that the LTEMP data are currently tracking variations in the background PAH.

For further comparisons, data from the Federal Mussel Watch program report the average PAH concentration in mussels for the remainder of the West Coast is nearly 30 times higher, 1,982 ng/g dry wt (summing only 24 of the 44 LTEMP analytes). The highest site on the west coast was 46,700 ng/g dry wt at a site in Elliot Bay near Seattle. The lowest, with 41 ng/g, was from mussels collected on Santa Cruz Island, a National Park 20 miles offshore of Santa Barbara in Southern California. Nationwide from 1986-1996, the 15th, 50th, and 85th percentiles were at 77, 230 and 1,100 ng/g dry wt (O'Connor 2002). In 2001, the state-wide average total PAH concentrations in mussels from the five Alaskan Mussel Watch sites (Ketchikan, Skagway, Port Valdez, Unakwik Inlet, and Cook Inlet) was 86.6 ng/g dry wt with levels ranging from 52.5 to 144 ng/g dry wt.

Contrary to suggestions from other corporately-funded studies, the extremely low concentrations and predominantly dissolved-phase nature of the signal in each of the regions does not support the hypothesis that broad areas of Prince William Sound are subject to extensive hydrocarbon contamination from ongoing or past anthropogenic activities (Boehm et al., 2003). Also, there is currently no signal of significant contamination from current Alyeska Marine Terminal or tanker activities. Even sites that were known to be heavily impacted by EVOS are reflecting TPAH levels and phase-signatures that are similar to unaffected areas. While there may be localized increases in

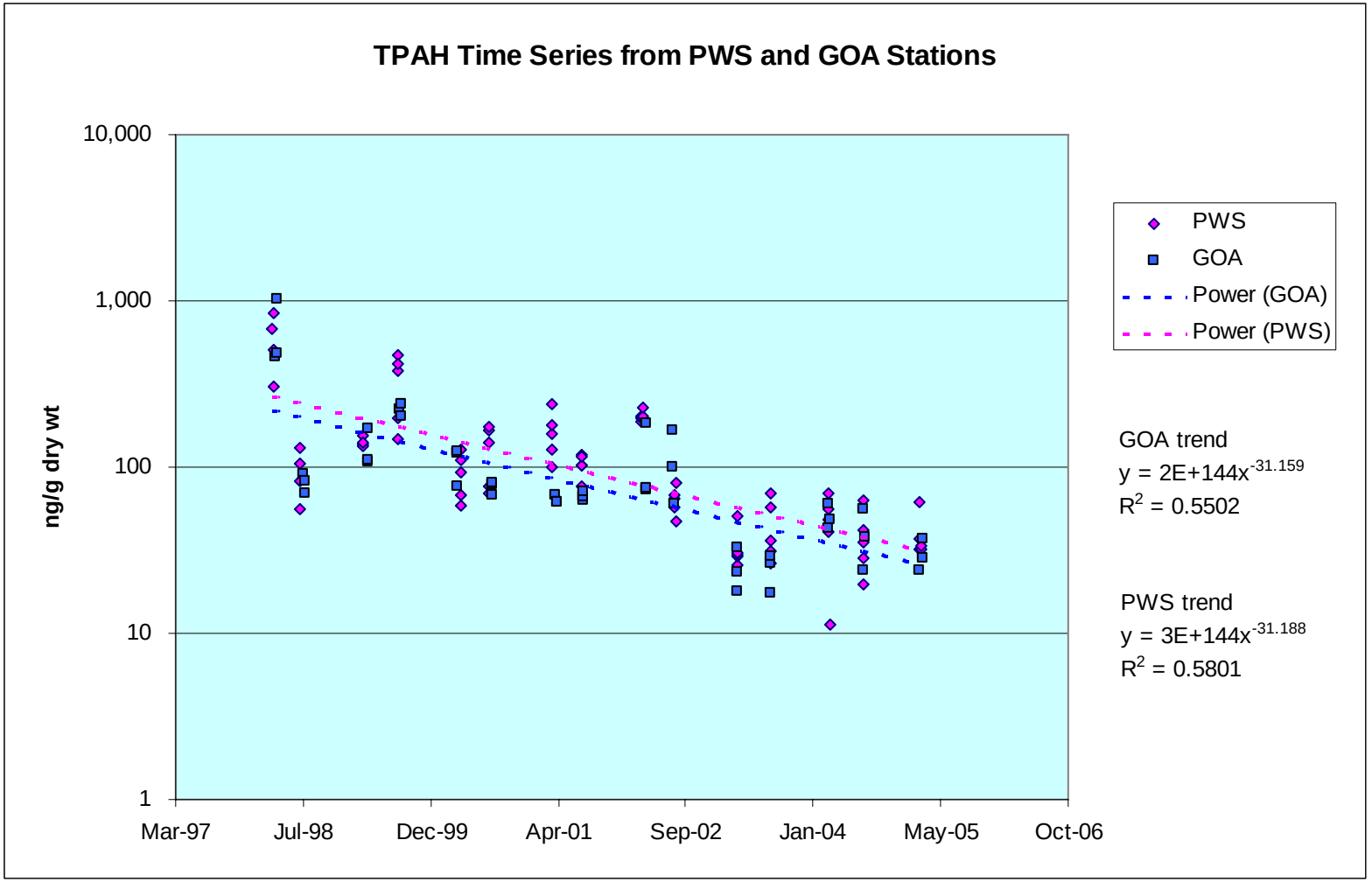

Figure 64 Average *Mytilus* TPAH time series and trend lines comparing Prince William Sound and Gulf of Alaska stations' trends.

TPAH burdens in harbors and bays currently utilized for fishing, camping, logging, mining and other human activities, the contaminants are not reflected in region-wide signals and do not support a extensive chronic-contamination scenario.

6 Conclusions

Focusing on the reliable data, the station trends suggest that TPAH levels have been decreasing in mussel tissues since 1999 and are now at all-time lows for the LTEMP sites outside of Port Valdez. Most stations are now showing mussel tissues with less than 100 ng/g (ppb) TPAH (many with <50 ng/g) and primarily as a dissolved–phase hydrocarbon signal from an unknown source(s). The development of the new PAH phase-assignment indices have, for the first time, allowed us insight into the regional trends in the LTEMP data. We are now able to distinguish temporal and compositional signals that characterize three separate regions encompassing Port Valdez, central Prince William Sound, and the outer-coastal Gulf of Alaska stations.

The synchrony of TPAH highs and lows plus the similarity of signatures also tell us that the inner Prince William Sound sites are collectively experiencing one low-level source of hydrocarbons while the outer coastal stations are exposed to a possibly different common dissolved-phase source. In July/August 2004, both regions showed a common low-level, particulate-PAH source. The two Port Valdez stations, being mainly influenced by the treated ballast water discharge from the Alyeska Marine Terminal, are trending independently of the regional sites.

The extremely low concentrations and dissolved-phase nature of the signal in each of the regions does not support the hypothesis that broad areas of Prince William Sound are subject to extensive hydrocarbon contamination from ongoing or past anthropogenic activities. Also, there is no hydrocarbon signal suggesting environmentally significant contamination from Alyeska Marine Terminal or oil-tanker shipping activities within Port Valdez or Prince William Sound during the 2004-2005 monitoring period.

At the Alyeska Terminal site, conditions are improving; after a prior two-year plateau at already low TPAH levels, subtidal sediments have dropped to even lower levels but still show the weathered ballast oil signature plus combustion products (which may or may not be related to terminal activities), and the usual biogenic marine and terrestrial components. For the mussels, tissue loads from Alyeska Marine Terminal and Gold Creek continue to indicate the accumulation of dissolved and particulate/oil-phase PAH components from the BWTF that are seasonally controlled by water-column stratification. At the Terminal, TPAH dropped and then maintained steady within a range of 55-70 ng/g for the last three years. These trends most likely reflect the decreased ballast-water throughput for the facility (currently down to 9 MGD) as double-hulled tankers (carrying segregated ballast not requiring treatment) come into use and Alaska North Slope crude oil flow through the pipeline drops in volume. The results from Alyeska's EMP complement the LTEMP findings. Among their findings, the UAF contractors report that the BWTF discharge results in local impacts around the diffuser

but not further afield, and also that analysis of sterane/triterpanes (not currently done with LTEMP samples) confirm the BWTF discharge is discernable at low levels in sediments throughout the port.

One significant event in the past year was the detection of an unreported diesel spill at Gold Creek within Port Valdez. Mussels at the site were contaminated by diesel fuel sometime in late summer 2004 with residues still detected at the site in March 2005. Not surprisingly, the diesel was not seen in the subtidal sediments. The same lack of transference was seen during EVOS; surface contamination seldom reached below nearshore subtidal depths. But the bottom line is that LTEMP monitoring works. The program has, to its success, previously documented a tanker-loading spill at the terminal, a sheening incident and a probable increased discharge event from the ballast-water treatment system, and beach-cleaning events in the Sound. And now, the program has picked up an unreported diesel spill.

In summary, the LTEMP program is in a very interesting phase; most stations are showing extremely clean results. With the current highly-sensitive methods, even slight deviations in what now appear to be the ambient background amounts of hydrocarbons can be detected, fingerprinted, and perhaps identified to source. For example, at the current levels of sensitivity and under near-pristine conditions, the Gold Creek diesel spill appears as a monumental spike in the trend line, a jump from 42 to 835 ng/g and a shift to a strong particulate/oil-phase signal. For perspective, in Mussel Watch data from some major urban harbors, this spike would barely rise above background levels.

And finally, there is the dissolved background signal itself; what is the source(s) and what drives the regional similarities, and what oceanographic–scale process would make the stations all peak and fall together? Also, what event or process might explain the apparent relative increase in the low-level particulate/oil-phase signal observed within Prince William Sound and at the outer Gulf of Alaska coastal stations in July/August 2004? There is little additional information within the LTEMP data set with which to answer these questions. We are currently seeking collaboration with atmospheric and oceanographic researchers to help understand the process(es).

7 References

Baumard, P. H. Budzinski, and P. Garrigues. 1998. Polycyclic aromatic hydrocarbons in sediments and mussels of the Western Mediterranean Sea. *Environmental Toxicology and Chemistry* 17(5):765-776.

Blanchard, Arny L., Howard M. Feder, and David G. Shaw. 2003. Variations in benthic fauna underneath an effluent mixing zone at a marine oil terminal in Port Valdez, Alaska. *Marine Pollution Bulletin* 46:1583-1589.

Blanchard, A. L., H. M. Feder, and D. G. Shaw. 2005. Environmental Studies in Port Valdez, Alaska: 2004. Final Report to Alyeska Pipeline Service Co., Inst. Of Marine Science, Univ. Alaska Fairbanks, 221 pp.

Blumer, M., M. Mullin, and D.W. Thomas. 1964. Pristane in the Marine Environment, *Helgolander Wissenshcaftliche Meeresuntersuchungen* 10:187-201.

Boehm, P.D., D.S. Page, W.A. Burns, A.E. Bence, P.J. Mankiewicz and J.S. Brown, 2001. Resolving the Origin of the Petrogenic Hydrocarbon Background in Prince William Sound, Alaska, *Environmental Science and Technology*, 35(3):471-479.

Boehm, P.D., and J.W. Farrington. 1984. Aspects of the polycyclic aromatic hydrocarbon geochemistry of recent sediments in the Georges Bank Region. *Environmental Science and Technology* 18:840-845.

Boehm, P.D., J.S. Brown, and T.C. Sauer. 1989. Physical and chemical characterization of San Joaquin Valley crude oil. Final report prepared for ENTRIX, In., Walnut Creek, California.

Boehm, P.D., J.S. Brown, J.M. Neff, D.S. Page, A.W. Maki, W.A. Burns, and A.E. Bence. 2003. The chemical baseline as a key to defining continuing injury and recovery of Prince William Sound. In Proceedings of the 2003 International Oil Spill Conference. API, Washington, D.C. pp 275-283.

Brown, D.W., L.S. Ramos, M.Y. Friedman, and W.D. MacLeod, Jr. 1980. Ambient temperature extraction of hydrocarbons from marine sediment -- Comparison with boiling solvent extractions. Pages 313-326 in Petroleum in the Marine Environment, L. Petrakis and F.T. Weiss, eds. Advances in Chemistry Series No. 185. American Chemical Society, Washington, D.C.

Brown, J.S. and P.D. Boehm. 1993. The use of double ratio plots of polynuclear aromatic hydrocarbon (PAH) alkyl homologues for petroleum source identification. Pages 799-801 in Proceedings 1993 Oil Spill Conference. American Petroleum Institute, Washington, D.C.

Carls, M.G. 2006. Nonparametric identification of petrogenic and pyrogenic hydrocarbons in aquatic ecosystems. *Environmental Science and Technology* 40:4233-4239.

Colonell, J.M. 1980a. "Ballast Water Dispersal." In *Port Valdez, Alaska: Environmental Studies 1976-1979,* J.M. Colonell (Ed.), Institute of Marine Science, University of Alaska, Fairbanks, Occasional Publication No. 5. 373 p.

Colonell, J.M. 1980b. "Physical Oceanography". In *Port Valdez, Alaska: Environmental Studies 1976-1979,* J.M. Colonell (Ed.), Institute of Marine Science, University of Alaska, Fairbanks, Occasional Publication No. 5. 373 p.

Cross, J.N., J.T. Hardy, J.E. Hose, G.P. Hershelman, L.D. Antrim, R.W. Gossett and E.A. Crecelius. 1987. "Contaminant Concentrations and Toxicity of Sea-Surface Microlayer near Los Angeles, California," *Marine Environmental Research* 23: pp. 307-323.

Davis, J.B. 1968, Paraffinic hydrocarbons in the sulfate-reducing bacterium, *Desulfovibrio desulfuricaus*. Chem. Geol. 3:155-160.

Douglas, G.S., A.E. Bence, R.C. Prince, S.J. McMillen, and E.L. Butler. 1996. Environmental stability of selected petroleum hydrocarbon source and weathering ratios. Environmental Science & Technology 30(7): 2332-2339.

Driskell, W.B., J.R. Payne, and G. Shigenaka. 2005. Revisiting Source Identification, Weathering Models, and Phase Discrimination for *Exxon Valdez* Oil. Proceedings of Arctic Marine Oil Spill Conference 2005, Calgary, Alberta, Canada. pp 33-58.

Farrington, J.W., and B.W. Tripp. 1977. Hydrocarbons in western North Atlantic surface sediments. Geochim. Cosmochim. Acta 41:1627-1641.

Federal Register. 1986. Code of Federal Regulations, Title 40, Part 136, Protection of the Environment. (40 CFR 136). U.S. Government Printing Office, Washington, D.C.

Han, J. and M. Calvin. 1969. Hydrocarbon distribution of algae and bacteria and microbiological activity in sediments, pages 436-443. In Proceedings, National Academy of Sciences. Volume 64. Washington, D.C.; NRC 1985).

Hardy, J.T. 1982. "The Sea-Surface Microlayer: Biology, Chemistry and Anthropogenic Enrichment," *Progress in Oceanography* 11: pp. 307-328.

Hardy, J., S. Kiesser, L. Antrim, A. Stubin, R. Kocan and J.A. Strand. 1987a. "The Sea-Surface Microlayer of Puget Sound: Part I. Toxic Effects on Fish Eggs and Larvae," *Marine Environmental Research* 23: pp. 227-249.

Hardy, J.T., E.A. Crecelius, L.D. Antrim, V.L. Broadhurst, C.W. Apts, J.M. Gurtisen, and T.J. Fortman. 1987b. "The Sea-Surface Microlayer of Puget Sound: Part 2. Concentrations of Contaminants and Relation to Toxicity," *Marine Environmental Research* 23: pp. 251-271.

Hardy, J.T., E.A. Crecelius, L.D. Antrim, S.L. Kiesser, V.L. Broadhurst, P.D. Boehm, and W.G. Steinhauer. 1990. "Aquatic Surface Contamination in Chesapeake Bay," *Marine Chemistry* 28: pp. 333-351.

Helton, Doug, Adam Moles, Jeff Short, Jeep Rice 2004. Results of the *M/V KUroshima* Oil Spill Shellfish Tissue Analysis 1999, 2000 and 2004. Report to the *M/V Kuroshima* Trustee Council. Prepared by NOAA Office of Response and Restoration, Seattle, Washington and NOAA Auke Bay Laboratory, Juneau, Alaska. December 2004, 7 pp.

Kinnetic Laboratories, Inc. (KLI), 2002. 2000-2002 LTEMP Monitoring Report. Prepared for the Prince William Sound Regional Citizens' Advisory Council Long-Term Environmental Monitoring Program. 94 pp. and appendices.

Larsen, M.L. and L.G. Holland 2004. Standard operating procedure for the determination of particle grain size in marine sediments analyzed at the Auke Bay Laboratory. Auke Bay Laboratory, Alaska Fisheries Science Center, National Marine Fisheries Service, NOAA. Juneau, Alaska.

National Research Council (NRC) 1985. *Oil in the Sea: Inputs, Fates, and Effects.* National Academy Press, Washington, D.C. 601 pp.

National Research Council (NRC) 2003. *Oil in the Sea III: Inputs, Fates, and Effects.* National Academy Press, Washington, D.C. 265 pp.

National Research Council (NRC) 2005. *Oil Spill Dispersants: Efficacy and Effects.* National Academy Press, Washington, D.C. 377 pp.

O'Connor, T.P. 2002. National Distribution of Chemical Concentrations in Mussels and Oysters in the USA. /Marine Environmental Research. 53: 117-143

Overton, E.B., J.A. McFall, S.W. Mascarella, C.F. Steele, S.A. Antoine, I.R. Politzer, and J.L. Laseter. 1981. Identification of petroleum residue sources after a fire and oil spill. Pages 541-546 in Proceedings 1981 Oil Spill Conference. American Petroleum Institute, Washington, D.C.

Page, D., P.D. Boehm, G.S. Douglas, and A.E. Bence. 1993. The natural petroleum hydrocarbon background in subtidal sediments of Prince William Sound, Alaska. Abstract #089 in Ecological Risk Assessment: Lessons Learned. 14th Annual Meeting, Society of Environmental Toxicology and Chemistry (SETAC) 14-18 November 1993, Houston, TX.

Page, D.S., P.D. Boehm, G.S. Douglas, and A.E. Bence. 1995. Identification of hydrocarbon sources in the benthic sediments of Prince William Sound and the Gulf of Alaska following the Exxon Valdez oil spill. Pages 41- 83 in Exxon Valdez Oil Spill: Fate and Effects in Alaskan Waters, ASTM STP 1219, Peter G. Wells, James N. Butler, and Jane S. Hughes, Eds., American Society for Testing and Materials, Philadelphia.

Payne, J.R., B.E. Kirstein, G.D. McNabb, Jr., J.L. Lambach, R. Redding, R.E. Jordan, W. Hom, C. de Oliveira, G.S. Smith, D.M. Baxter, and R. Geagel. 1984. Multivariate analysis of petroleum weathering in the marine environment - subarctic. Volume I, Technical Results; Volume II, Appendices. In: Final Reports of Principal Investigators, Vol. 21 and 22. February 1984, U.S. Department of Commerce, National Oceanic and Atmospheric Administration, Ocean Assessment Division, Juneau, Alaska. 690 pp. Volume 21 NTIS Accession Number PB85-215796; Volume 22 NTIS Accession Number PB85-215739.

Payne, J.R., J.R. Clayton, Jr., G.D. McNabb, Jr., B.E. Kirstein, C.L. Clary, R.T. Redding, J.S. Evans, E. Reimnitz, and E. Kempema. 1989. Oil-ice sediment interactions during freezeup and breakup. Final Reports of Principal Investigators, U.S. Dept. Commer., NOAA, OCEAP Final Rep. 64, 1-382 (1989). NTIS Accession Number PB-90-156217.

Payne, J.R., W.B. Driskell, and D.C. Lees. 1998. Long Term Environmental Monitoring Program Data Analysis of Hydrocarbons in Intertidal Mussels and Marine Sediments, 1993-1996. Final Report prepared for the Prince William Sound Regional Citizens Advisory Council, Anchorage, Alaska 99501. (PWS RCAC Contract No. 611.98.1). March 16, 1998. 97 pp plus appendices.

Payne, J.R., W.B. Driskell, M.G. Barron, D.C. Lees. 2001. Assessing transport and exposure pathways and potential petroleum toxicity to marine resources in Port Valdez, Alaska. Final Report Prepared for Prince William Sound Regional Citizens' Advisory Council Contract No. 956.02.1. Prepared by Payne Environmental Consultants, Inc., Encinitas, CA. December 21, 2001. 64 pp plus appendices.

Payne, J.R., W.B. Driskell, and J.W. Short. 2003a. 2002-2003 LTEMP Monitoring Report. Final Report prepared to the Prince William Sound Regional Citizens' Advisory Council, Anchorage, Alaska 99051. PWSRCAC Contract No. 951.03.1. Prepared by Payne Environmental Consultants, Inc., Encinitas, CA. Nov. 6, 2003. 107 pp.

Payne, J.R., J.R. Clayton, Jr., and B.E. Kirstein. 2003b. Oil/suspended particulate material interactions and sedimentation. Spill Science & Technology Bulletin, Vol. 8(2), pp 201-221.

Payne, J.R., W.B. Driskell, M.G. Barron, J. A. Kalmar, and D.C. Lees. 2003c. Public comment regarding the Draft NPDES Permit for BWTF at Alyeska Marine Terminal. Final Report prepared for the Prince William Sound Regional Citizens' Advisory Council, Anchorage, Alaska 99051. PWSRCAC Contract No. 551.02.01. Prepared by Payne Environmental Consultants, Inc., Encinitas, CA. June 2, 2003, 21 p.

Payne, J.R., W.B. Driskell, M.G. Barron, D.C. Lees, L. Ka'aihue, and J.W. Short. 2003d. Assessing transport and exposure pathways and potential petroleum toxicity to marine resources in Port Valdez, Alaska. Poster No. PT214 presented at the SETAC 24th Annual Meeting in North America. November 9-13, 2003, Austin, Texas.

Payne, J.R., W.B. Driskell, and J.W. Short. 2005a. 2003-2004 LTEMP Monitoring Report. Final Report prepared for the Prince William Sound Regional Citizens' Advisory Council, Anchorage, Alaska 99051. PWSRCAC Contract No. 951.04.1. Prepared by Payne Environmental Consultants, Inc., Encinitas, CA. April 18, 2005. 123 pp.

Payne, J.R., W.B. Driskell, J.F. Braddock, J. Bailey. 2005b. Hydrocarbon biodegradation in the Ballast Water Treatment Facility, Alyeska Marine Terminal. Final Report prepared for the Prince William Sound Regional Citizens' Advisory Council, Anchorage, Alaska 99051. PWSRCAC Contract Numbers 558.04.01 and 560.2004.01. Prepared by Payne Environmental Consultants, Inc., Encinitas, CA. May 2, 2005. 48 pp.

Payne, J.R., W.B. Driskell, J.F. Braddock, J. Bailey, J.W. Short, L. Ka'aihue, T.H. Kuckertz 2005c. From Tankers to Tissues – Tracking the Degradation and Fate of Oil Discharges in Port Valdez, Alaska. Proceedings of Arctic Marine Oil Spill Conference 2005, Calgary, Alberta, Canada. pp 959-991.

Payne, J.R. and W.B. Driskell, M.R. Lindeberg, W. Fournier, M.L. Larsen, J.W. Short, S.D. Rice, and D. Janka. 2005d. Dissolved- and Particulate-Phase Hydrocarbons in Interstitial Water from Prince William Sound Beaches Containing Buried Oil Thirteen Years After the *Exxon Valdez* Oil Spill, Proceedings of the 2005 International Oil Spill Conference, American Petroleum Institute, Washington, D.C., pp. 83-88.

Payne, J.R. and W.B. Driskell. 2001. Source characterization and identification of *New Carissa* oil in NRDA environmental samples using a combined statistical and fingerprinting approach. Proceedings of the 2001 Oil Spill Conference, American Petroleum Institute, Washington, D.C., pp. 1403-1409.

Payne, J.R. and W.B. Driskell. 2003. The importance of distinguishing dissolved- versus oil-droplet phases in assessing the fate, transport, and toxic effects of marine oil pollution. Proceedings of the 2003 Oil Spill Conference, American Petroleum Institute, Washington, D.C., pp 771-778.

Salazar, M., J.W. Short, S.M. Salazar, and J.R. Payne. 2002. Port Valdez Monitoring Report. Prince William Sound Regional Citizens' Advisory Council Contract No. 633.01.1. February 7, 2002. 109 pp plus appendices.

Sauer, T. and P. Boehm. 1991. The use of defensible analytical chemical measurements for oil spill natural resource damage assessment. Proceedings of the 1991 Oil Spill Conference. American Petroleum Institute, Washington, D.C., pp 363-369.

Saupe, Susan 2004. Alaska EMAP coordinator, personal communication.

Short, J.W. 2005. Seasonal variability of pristane in mussels (*Mytilus Trossulus*) in Prince William Sound, Alaska. Ph.D. Thesis. University of Alaska, Fairbanks. 204 pp.

Short, J.W., K.A. Kvenvolden, P.R. Carlson, F.D. Hostettler, R.J. Rosenbauer and B.A. Wright, "Natural Hydrocarbon Background in Benthic Sediments of Prince William Sound, Alaska: Oil vs. Coal", *Environmental Science and Technology*, Vol. 33, No. 1, pp. 34-42, 1999.

Woodward-Clyde Consultants and ENTRIX, Inc. 1987. *Ballast water treatment facility effluent plume behavior. A Synthesis of Findings*. Prepared for Alyeska Pipeline Service Company. Walnut Creek, California. March 1987.

8 Appendices

Appendix A LTEMP Oil Primer

Appendix B- 1 TPAH and TSHC summary table for all Alyeska Marine Terminal and Gold Creek sediment samples.

Appendix B-2 Summary of Sediment TPAH and Component Fractions for all Alyeska Marine Terminal and Gold Creek Sediment Grabs

Appendix C Summary of tissue TPAH and TSHC for 2004-2005 program.

Appendix D Interpretation of Samples from Jack Bay Diesel Spill

Appendix A LTEMP Oil Primer

This section is included as background material for those readers unfamiliar with oil chemistry or the oil contaminants found in Prince William Sound and central Alaskan coastal regions.

A.1 Regional Sources

In the LTEMP regional environment, oil hydrocarbons arrive from numerous and varied sources. Topping the list would be Alaskan North Slope (ANS) crude including lingering residues from the *Exxon Valdez* oil spill (EVOS); oil products from the Alyeska Marine Terminal (not necessarily ANS); coal, peat and organic-rich shales from vast local and regional deposits; Cook Inlet crude oil; and refined petroleum products that have made their way into the marine environment.

Of primary interest to LTEMP is, of course, ANS crude oil. This crude actually consists of a blend of petroleum from the production fields on the Alaskan North Slope, including Prudhoe Bay, Kuparuk, Endicott, and Lisburne, that together exhibit a chemical fingerprint that is quite distinct from that of oil found in other geographic areas. The EVOS of March 1989 consisted of ANS crude, which over time has weathered to produce a significantly different fingerprint than that of fresh ANS crude. Petroleum that originates from organic-rich shales (or hydrocarbon "source rock") and coal deposits in the Gulf of Alaska also contribute significantly to the natural (or “background") hydrocarbons in the study area, and these also exhibit a distinctly different fingerprint. Recent work shows the source rock signature to be particularly widespread in the deep sediments of PWS, and indeed, appears unchanged in coastal sediments from upstream of the Copper River past the Outer Kenai and through Shelikof Straits (unpublished data, Susan Saupe). Fortunately, animals exposed to these sediments do not seem to accumulate hydrocarbons because these contaminants are not bioavailable. Natural terrestrial oil seeps have also been invoked as hydrocarbon sources, but recent work indicates input from these seeps is insignificant compared with the other sources.

Other petroleum products that may have been introduced into the marine environment in Prince William Sound (PWS) include oil products from source locations other than Alaska. For example, the Great Alaskan Earthquake of 1964 and the resultant tsunamis washed fuel oil and asphalt made from California source oils into Port Valdez, and subsequently into PWS (Kvenvolden et al. 1995). These authors noted that tarballs from these California-sourced products have been found throughout the northern and western parts of PWS. Most recently, hydrocarbons from historic anthropogenic activities (long-abandoned mines, logging operations, camp sites, and fish canneries) in addition to current settlements within PWS have been hypothesized as being additional sources of background hydrocarbon signals (Boehm et al. 2003).

A.2 Oil Chemistry, Source Allocations, and Weathering Behavior

Chemically, oil is a complex mixture of decayed ancient organic matter broken down and modified under geologic heat and pressure. Each deposit is a unique blend but there are commonalities. Hydrocarbons are by far the most abundant compounds in crude oil,

accounting for 50-98% of the volume. And in various proportions, all crude blends contain "lighter fractions" of hydrocarbons (similar to gasoline), "intermediate fractions" like diesel or fuel oil, heavier tars and wax-like hydrocarbons, and ultimately residual materials like asphalt. For purposes of the LTEMP chemical analyses, crude oil is identified by its signature blend of just two compositional hydrocarbon groups, the polycyclic aromatic hydrocarbons (PAH) and the saturated (or aliphatic) hydrocarbons (SHC), also referred to as n-alkanes. These two compositional groups encompass the intermediate, heavier tars, and wax-like fractions. As shown by the plots in Figure 1, we work with approximately 40 PAH compounds and 26 SHC components to identify a hydrocarbon source. (Names and abbreviations of the individual analytes shown in this and all following figures are presented in Table 2 in Section 4.2 - Analytic Methods.) These PAH typically account for 2-5% of petroleum by weight (and about 3% of ANS crude).

For source identifications, it is useful to distinguish between five main families of PAH components. In order from light to heavy (left to right in the plots), they are: naphthalenes (N), fluorenes (F), phenanthrenes/anthracenes (P/A), dibenzothiophenes (D), and chrysenes (C).

The naphthalenes are two-ring aromatics (i.e., two 6-carbon rings linked together) and are less persistent in the environment compared to the other higher-molecular-weight groups. They typically disappear from spilled oil by evaporation and dissolution weathering and as such, they may or may not be present in the plots of oil residues or oil-contaminated mussel and sediment samples. Because they dissolve slowly and to a limited extent in water, they can also be detected moving directly from the water column into exposed organisms. The fluorenes, anthracenes, and phenanthrenes (which are all three-ring aromatics) are each more persistent in the environment, and as such, they can act as markers to help differentiate among different oil sources. The dibenzothiophenes (another three-ring compound that also contains sulfur) are important, because they are substantially more abundant in Alaskan North Slope crude oil than in other oil deposits in the region such as Cook Inlet or Katalla crude oil. Finally, the heavier four- and five-ring aromatics (including, the chrysenes (C) through benzo(g,h,i)perylene (BP)) are important because: 1) they can help distinguish between crude oils and refined products (such as diesel oil) that may have been produced from a particular crude oil; and 2) they are also representative of combustion by-products.

Chemists have developed a nomenclature to distinguish the various members of each family. The simple parent compounds in each of the five PAH families are referred to as "C_0" (e.g., C_0-naphthalene, here abbreviated simply as "N"). Their other family members, known to chemists as alkyl-substituted homologues, are adorned with an alkyl molecule (-CH_3) in a named position around the margin of the PAH ring. These homologues thus become known by their sequence name, e.g., C1-naphthalene (abbreviated as N1), C2-naphthalene (N2), and so on (N3 and N4) (see Figure 1).

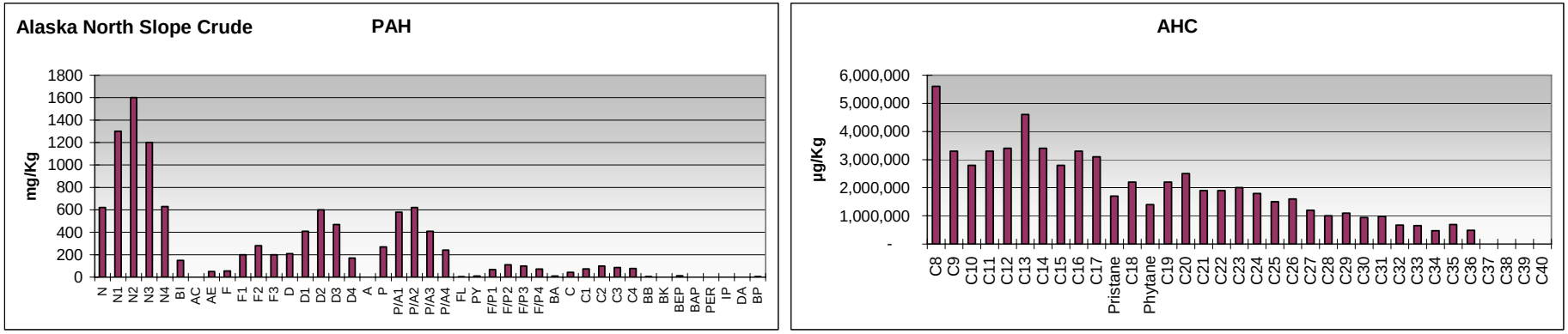

Appendix Figure 1 Example plots of ANS PAH and SHC (also referred to as AHC) components.

Regarding the family structure, it is important to note that petrogenic (petroleum-derived) PAHs have a characteristic fingerprint whereby the parent compounds in each of the five PAH families (e.g., the parent C_0-naphthalene, abbreviated as "N") are usually at lower concentrations than their other family members (see Figure 1). With evaporation/dissolution weathering, these lower-molecular-weight components are more easily eliminated, thus generating a characteristic "water-washed profile" with the levels of $C_0<C_1<C_2<C_3$ within each PAH group. Eventually, with continued weathering, only the most persistent alkylated phenanthrenes/anthracenes, dibenzothiophenes, and chrysenes are seen, and typically at very characteristic, source-specific ratios in the remaining oil residues (Figure 2).

Likewise, in the SHC fraction, the n-alkanes also clearly show the effects of evaporation weathering with losses of all components with molecular weights below n-C_{14} apparent after several weeks (Figure 2). With continued microbial degradation, the remaining n-alkanes will be selectively removed leaving only the branched compounds, pristane and phytane, which are also removed but at a much slower rate over time. Incidentally, phytoplankton make n-C_{15} and n-C_{17} which mussels can accumulate by feeding on the phytoplankton. Substantial concentrations of pristane are also naturally present in some zooplankton; they biosynthesize it from chlorophyll ingested with the phytoplankton they eat. Therefore, all three compounds can show up in mussel and sediment samples as a result of marine biogenic input. In a spring plankton bloom, these natural aliphatic hydrocarbons can easily dominate the SHC fraction. Phytane, on the other hand, is almost exclusively associated with oil, so its presence in samples can also be used as another indicator of petroleum contamination.

Pyrogenic PAHs come from combustion sources including atmospheric fallout and surface runoff from the burning of fossil fuels (diesel, heating oil, gasoline, etc.) and from other pyrogenic sources such as forest fires and camp fires. Creosote, which is used to preserve wood pilings, is also usually included in this category because of a similar PAH profile. Pyrogenic PAHs are characterized by high molecular weight PAHs greater than C_3-dibenzothiophene (D3), and by high concentrations of the parent compounds compared to their alkyl homologues. A typical pattern for pyrogenic PAHs is decreasing concentration with increasing alkyl substitution and molecular weight within a group, i.e., $C_0>C_1>C_2>C_3>C_4$, opposite the trend seen in crude oil and distillate products.

For the aliphatic hydrocarbons, the nomenclature strategy changes. The abbreviation for the aliphatic compound, n-C_{10}, now refers to 10 carbon atoms linked in a straight chain (no cyclic rings). In contrast to the PAHs, aliphatic hydrocarbons can account for more than 70 percent of petroleum by weight. Also, as noted above, aliphatic hydrocarbons can be synthesized by organisms (both planktonic and terrestrial), and may be present as degradation products in some bacteria. As shown in Figure 1, crude petroleum contains a homologous series of n-alkanes ranging from one to more than 30 carbons with odd- and even-numbered n-alkanes present in nearly equal amounts. In contrast, biogenic hydrocarbons (produced by living organisms) preferentially contain specific suites of

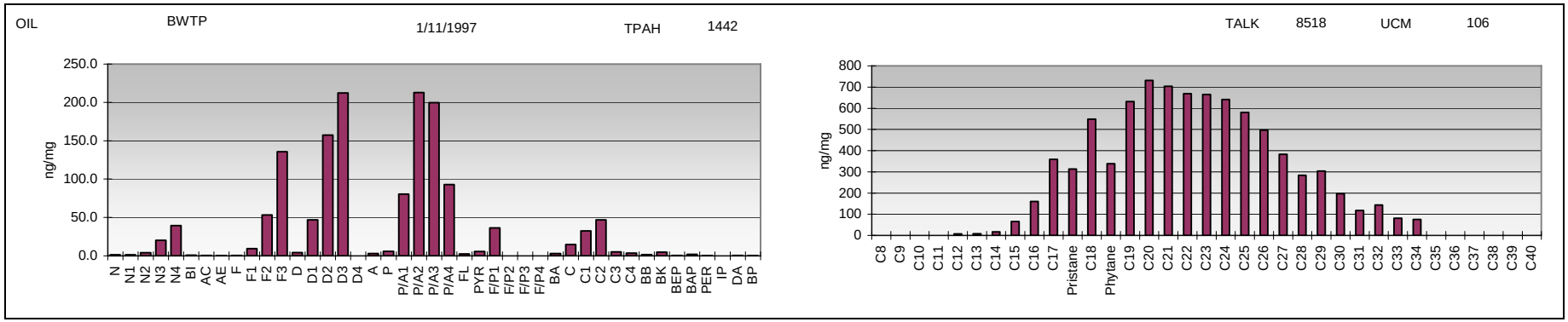

Appendix Figure 2. Plot of weathered ANS from LTEMP 11/97.

normal alkanes with mainly odd-numbered carbons between n-C_{15} and n-C_{33}. In addition to the example of n-C_{15}, n-C_{17}, and pristane from marine plankton cited above, terrestrial plants contribute a predominant odd-numbered carbon pattern including n-C_{25}, n-C_{27}, n-C_{29}, n-C_{31}, and n-C_{33}. These so-called "plant waxes" are commonly observed in marine sediments in depositional areas receiving significant amounts of terrestrial runoff.

Petroleum also contains a complex mixture of branched and cyclic compounds generally not found in organisms. This complex mixture can include oxygenated compounds that produce an "unresolved complex mixture" of compounds (the UCM) on the gas chromatographic chart. The UCM appears proportionally more prominent in analyses as additional oxygenated compounds are introduced to oil by bacterial and photochemical processes. Thus, the presence and amount of the UCM can be a diagnostic indicator of heavily-weathered petroleum contamination.

Once in water, a crude oil signature can be modified by several processes including evaporation and dissolution weathering, and microbial degradation. We've recently identified another twist in tracking an oil source, the dissolved versus particulate fractions. As a droplet of oil enters water, the more readily-dissolvable components, particularly the naphthalenes, are removed from the droplet thus leaving behind a particulate (or oil droplet) fraction with the "water-washed pattern" mentioned above (low on the parent stock). The receiving water then has the dissolved components signature. In essence, one source produces two signatures in water. This process is readily apparent in the discharge into Port Valdez from the Ballast Water Treatment Facility (BWTF) at the Alyeska Marine Terminal.

Figure 3 presents plots of the PAH and SHC associated with this discharge (Payne et al. 2001; Salazar et al. 2002). In this case, the PAH pattern associated with the colloidal/particulate (oil-droplet) phase shows the depletion of naphthalene (N) and methylnaphthalenes (N1) compared to higher alkylated homologues (N2, N3, and N4), and, to a lesser extent, this same "water-washed pattern" is observed for the fluorenes (F's), dibenzothiophenes (D's), and phenanthrenes/anthracenes (P/A's). The SHC (n-alkane) distribution from the BWTF discharge still shows the presence of minute oil droplets (the water insoluble components that do not dissolve). In addition to evaporation weathering, there is evidence of enhanced microbial degradation from the biological treatment tanks at the BWTF as shown by the depleted concentrations of the n-alkanes compared to pristane and phytane (compare the SHC patterns in Figures 1 and 3).

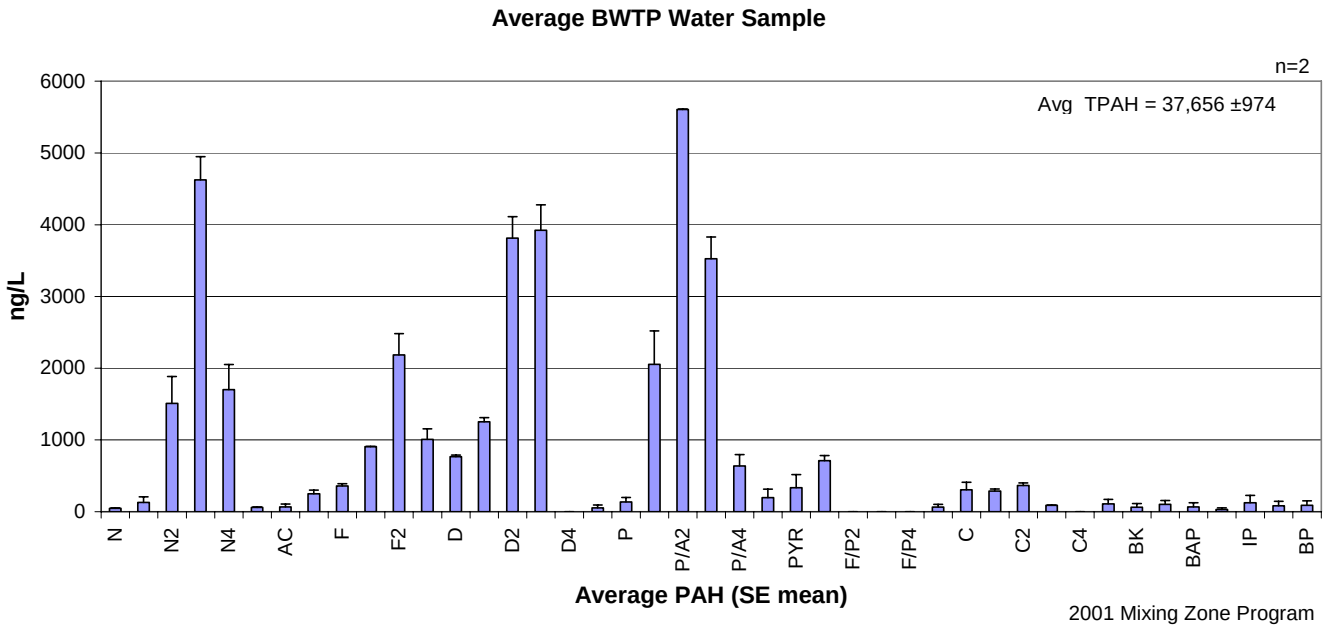

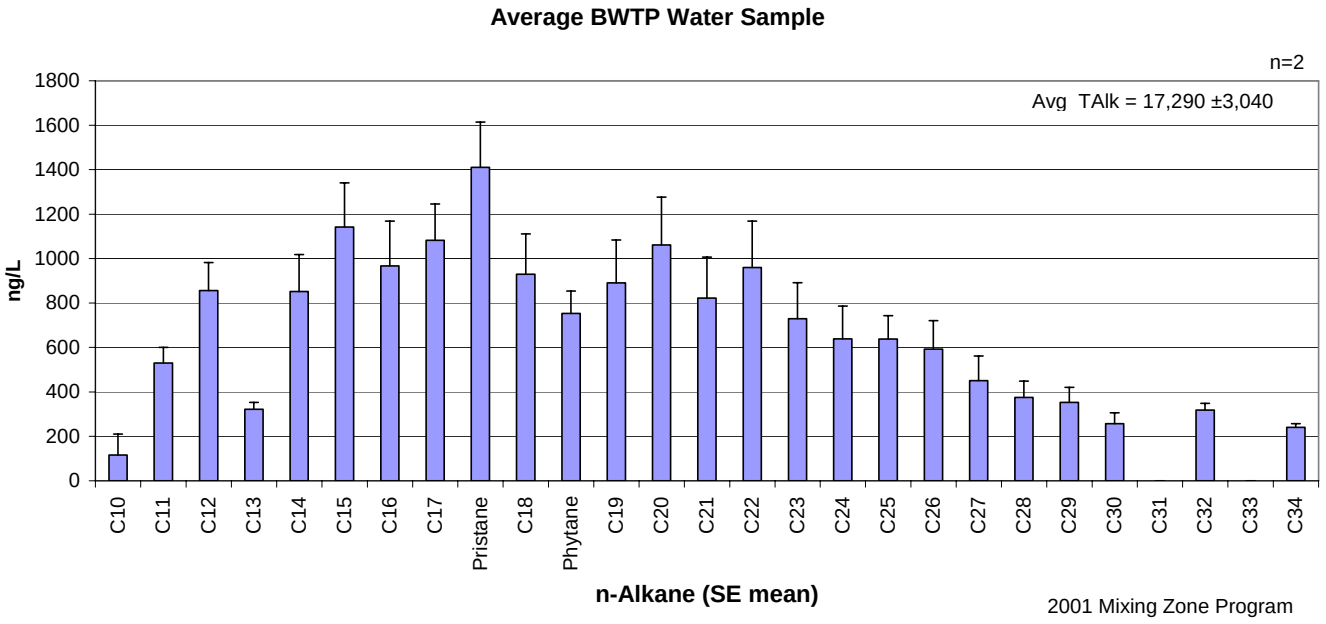

Appendix Figure 3. PAH and SHC plots of effluent from the Alyeska Marine Terminal BWTF (from Salazar et al. 2002).

A.3 Mussels as Indicator Organisms

When analyzing the mussel tissue samples collected as part of LTEMP, it is important to recognize that as filter feeders, mussels can accumulate oil from both the dissolved and particulate/oil-droplet phases. Figure 4 (from Payne et al. 2001) presents examples of mussels collected from oiled areas of Cabin Bay, Naked Island in Prince William Sound in May 1989 immediately after the *Exxon Valdez* oil spill and again in May/June in 1990 and 1991. In 1989, the mussels clearly accumulated PAH and aliphatic hydrocarbons from both the dissolved and particulate phases to which they were exposed; however, the particulate (dispersed oil droplet phase) was the predominant source for the accumulated higher-molecular-weight PAH (C_2-dibenzothiophenes (D2) through higher alkylated homologues of the phenanthrenes/anthracenes and chrysenes) and the aliphatics (phytane plus the even distribution of n-alkanes from n-C_{19} through n-C_{34}). As noted above, these higher-molecular-weight components have only limited water solubilities and have long been associated with the whole oil (droplet) phase. In the post-spill 1990 and 1991 data, the mussels accumulated primarily dissolved-phase PAH (at significantly reduced overall concentrations) from the more water-soluble hydrocarbons still leaching from the contaminated intertidal zone. This is manifest in the plots at the bottom of Figure 4 by the predominant naphthalene and alkyl-substituted naphthalene homologues in greater relative abundance compared to the other PAH. Likewise, the SHC profile for the mussel samples in 1990-1991 is characterized primarily by lower molecular weight biogenic components (n-C_{15}, n-C_{17}, and pristane) with little or no contribution of phytane and higher molecular weight n-alkanes from dispersed oil droplets.

These plots are presented as examples of what should be considered in this report and specifically kept in mind when reviewing the data generated during the past 13 years of the LTEMP. The profiles in Figure 4 are particularly important, because they also illustrate typical patterns of oil contamination (from both particulate and dissolved phases) in the absence of other confounding factors, such as lipid interference.

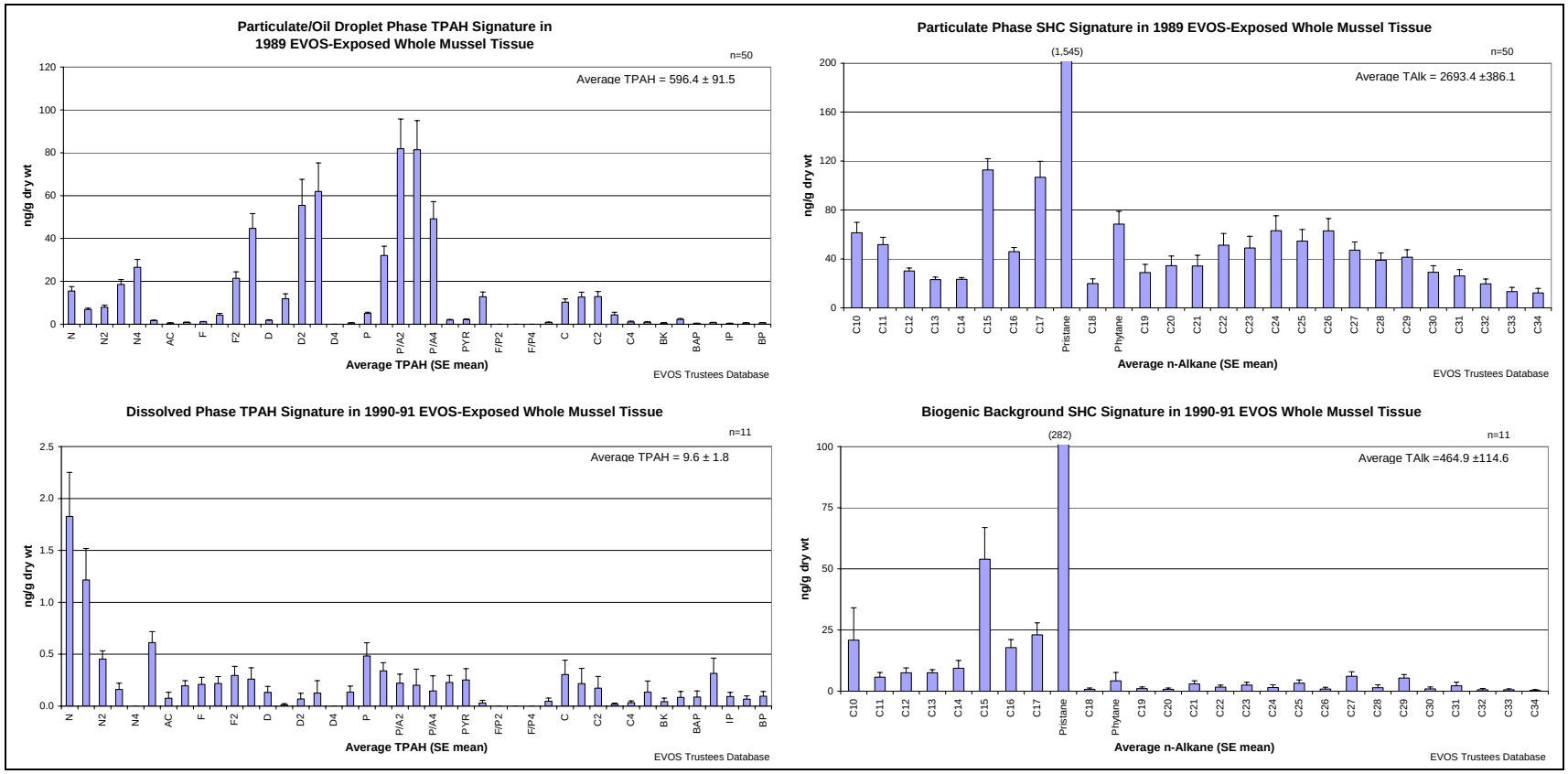

Appendix Figure 4. Average PAH and SHC plots of whole mussel extracts from samples collected from oiled areas of Cabin Bay, Naked Island in Prince William Sound in May 1989 after the Exxon Valdez oil spill (EVOS) and again in May/June 1990 and 1991. The number of samples contributing to each composite is denoted by "n" (from Payne et al. 2001; data from NOAA EVTHD database).

Appendix B-1 TPAH and TSHC summary table for Alyeska Marine Terminal and Gold Creek sediment samples, 1993-2005.

Date	Sample ID	Total SHC	Mean	Std Dev	CV	Total PAH	Mean	Std Dev	CV
Alyeska Marine Terminal Subtidal Sediments (AMT-S)									
3-Apr-93	PWS93PAT0040	1868				196			
3-Apr-93	PWS93PAT0041	2533				341			
3-Apr-93	PWS93PAT0042	1873	2091	383	18.3	191	243	85	35.1
16-Jul-93	PWS93PAT0043	1164				146			
16-Jul-93	PWS93PAT0044	3183				198			
16-Jul-93	PWS93PAT0045	1707	2018	1045	51.8	394	246	131	53.2
26-Mar-94	PWS94PAT0025	1047				202			
26-Mar-94	PWS94PAT0026	1698				167			
26-Mar-94	PWS94PAT0027	1675	1473	369	25.1	239	203	36	17.8
20-Jul-94	PWS94PAT0031	1425				174			
20-Jul-94	PWS94PAT0032	1242				230			
20-Jul-94	PWS94PAT0033	1922	1530	352	23.0	389	264	112	42.2
3-Apr-95	PWS95PAT0022	1291				206			
3-Apr-95	PWS95PAT0023	1093				244			
3-Apr-95	PWS95PAT0024	1785	1390	356	25.6	186	212	29	13.9
11-Jul-95	PWS95PAT0028	2189				1650			
11-Jul-95	PWS95PAT0029	1872				362			
11-Jul-95	PWS95PAT0030	2763	2275	452	19.9	629	880	680	77.2
16-Mar-96	PWS96PAT0004	1109				160			
16-Mar-96	PWS96PAT0005	1578				311			
16-Mar-96	PWS96PAT0006	1100	1262	273	21.7	135	202	95	47.1
12-Jul-96	PWS96PAT0025	2265				326			
12-Jul-96	PWS96PAT0026	1782				201			
12-Jul-96	PWS96PAT0027	1602	1883	343	18.2	381	303	92	30.5
6-Mar-97	PWS97PAT0001	2203				417			
6-Mar-97	PWS97PAT0002	1980				449			
6-Mar-97	PWS97PAT0003	2929	2371	496	20.9	388	418	31	7.3
17-Jul-97	PWS97PAT0029	1124				246			
17-Jul-97	PWS97PAT0030	1477				377			
17-Jul-97	PWS97PAT0031	1892	1498	384	25.7	288	303	67	22.0
29-Mar-98	PWS98PAT0016	1112				120			
29-Mar-98	PWS98PAT0017	1668				451			
29-Mar-98	PWS98PAT0018	972	1251	368	29.4	144	238	185	77.6
5-Apr-00	PWS00PAT0004	1465				313			
5-Apr-00	PWS00PAT0005	1575				335			
5-Apr-00	PWS00PAT0006	1568	1536	62	4.0	412	353	52	14.7
21-Jul-00	PWS00PAT0010	2080				392			
21-Jul-00	PWS00PAT0011	3016				452			
21-Jul-00	PWS00PAT0012	2107	2401	533	22.2	571	472	91	19.4
28-Mar-01	PWS01PAT0001	2987				814			
28-Mar-01	PWS01PAT0002	1803				465			

28-Mar-01	PWS01PAT0003	2659	2483	611	24.6	564	614	180	29.3
22-Jul-01	PWS01PAT0010	1044				160			
22-Jul-01	PWS01PAT0011	1276				536			
22-Jul-01	PWS01PAT0012	1969	1429	481	33.7	311	335	189	56.4
15-Mar-02	PWS02PAT0004	2508				10			
15-Mar-02	PWS02PAT0005	2452				68			
15-Mar-02	PWS02PAT0006	3514	2825	598	21.2	149	76	70	92.2
10-Jul-02	AMT-S-02-2-1	473				192			
10-Jul-02	AMT-S-02-2-2	504				158			
10-Jul-02	AMT-S-02-2-3	551	509	39	7.7	1089	480	528	110.2
18-Mar-03	AMT-S-03-1-1	654				134			
18-Mar-03	AMT-S-03-1-2	694				271			
18-Mar-03	AMT-S-03-1-3	594	648	51	7.8	131	179	80	44.7
27-Jul-03	AMT-S-03-2-1P	604				199			
27-Jul-03	AMT-S-03-2-2P	564				132			
27-Jul-03	AMT-S-03-2-3P	522	563	41	7.3	109	147	47	31.7
27-Jul-03	AMT-S-03-2-1A	791				230			
27-Jul-03	AMT-S-03-2-2A	701				286			
27-Jul-03	AMT-S-03-2-3A	496	663	151	22.8	144	220	71	32.4
23-Mar-04	AMT-S-04-1-1	451				128			
23-Mar-04	AMT-S-04-1-2	417				231			
23-Mar-04	AMT-S-04-1-3	352	407	50	12.3	142	167	56	33.6
13-Oct-04	AMT-S-04-2-1	629				93			
13-Oct-04	AMT-S-04-2-2	703				329			
13-Oct-04	AMT-S-04-2-3	402	578	157	27.1	103	175	133	76.3
4-Mar-04	AMT-S-05-1-1	243				65			
4-Mar-04	AMT-S-05-1-2	337				47			
4-Mar-04	AMT-S-05-1-3	350	310	58	18.8	41	51	12	24.5
28-Jul-04	AMT-S-04-2-1	870				93			
28-Jul-04	AMT-S-04-2-2	943				329			
28-Jul-04	AMT-S-04-2-3	608	807	176	0.22	103	175	133	0.76
4-Mar-05	AMT-S-05-1-1	367				65			
4-Mar-05	AMT-S-05-1-2	491				47			
4-Mar-05	AMT-S-05-1-3	455	438	64	0.15	41	51	12	0.24
Alyeska Marine Terminal Intertidal Sediments (AMT-L)									
14-Jul-98	PWS98PAT0043	254				26			
14-Jul-98	PWS98PAT0044	131				38			
14-Jul-98	PWS98PAT0045	2492	959	1329	138.6	123	62	53	84.8
Gold Coast Subtidal Sediments (GOC-S)									
19-Mar-93	PWS93PAT0001	941				47			
19-Mar-93	PWS93PAT0002	436				36			
19-Mar-93	PWS93PAT0003	1460	946	512	54.1	58	47	11	23.4
25-Jul-93	PWS93PAT0071	1036				57			
25-Jul-93	PWS93PAT0072	408				31			
25-Jul-93	PWS93PAT0073	256	567	413	73.0	25	38	17	45.2
26-Mar-94	PWS94PAT0022	1429				60			
26-Mar-94	PWS94PAT0023	571				45			
26-Mar-94	PWS94PAT0024	638	879	477	54.3	106	70	32	45.2
19-Jul-94	PWS94PAT0028	385				47			

19-Jul-94	PWS94PAT0029	378				18			
19-Jul-94	PWS94PAT0030	737	500	205	41.1	68	44	25	56.6
3-Apr-95	PWS95PAT0019	463				57			
3-Apr-95	PWS95PAT0020	322				34			
3-Apr-95	PWS95PAT0021	528	438	105	24.1	31	41	14	35.0
11-Jul-95	PWS95PAT0025	750				67			
11-Jul-95	PWS95PAT0026	598				59			
11-Jul-95	PWS95PAT0027	444	597	153	25.6	31	52	19	36.1
16-Mar-96	PWS96PAT0001	588				78			
16-Mar-96	PWS96PAT0002	470				156			
16-Mar-96	PWS96PAT0003	523	527	59	11.2	33	89	62	69.9
12-Jul-96	PWS96PAT0028	541				56			
12-Jul-96	PWS96PAT0029	440				45			
12-Jul-96	PWS96PAT0030	629	537	95	17.6	52	51	6	10.9
6-Mar-97	PWS97PAT0004	624				54			
6-Mar-97	PWS97PAT0005	431				39			
6-Mar-97	PWS97PAT0006	441	499	109	21.8	40	44	8	18.9
17-Jul-97	PWS97PAT0026	514				53			
17-Jul-97	PWS97PAT0027	788				55			
17-Jul-97	PWS97PAT0028	552	618	148	24.0	60	56	3	5.7
29-Mar-98	PWS98PAT0013	341				42			
29-Mar-98	PWS98PAT0014	301				48			
29-Mar-98	PWS98PAT0015	352	331	27	8.1	38	43	5	11.6
5-Apr-00	PWS00PAT0001	590				126			
5-Apr-00	PWS00PAT0002	668				81			
5-Apr-00	PWS00PAT0003	918	725	171	23.6	126	111	26	23.4
20-Jul-00	PWS00PAT0007	966				105			
20-Jul-00	PWS00PAT0008	753				111			
21-Jul-00	PWS00PAT0009	912	877	111	12.7	92	103	10	9.3
28-Mar-01	PWS01PAT0004	904				125			
28-Mar-01	PWS01PAT0005	833				131			
28-Mar-01	PWS01PAT0006	901	879	40	4.6	120	126	5	4.2
21-Jul-01	PWS01PAT0007	311				40			
21-Jul-01	PWS01PAT0008	506				59			
21-Jul-01	PWS01PAT0009	2993	1270	1495	117.8	108	69	35	50.8
15-Mar-02	PWS02PAT0002	1568				91			
15-Mar-02	PWS02PAT0003	1165				33			
15-Mar-02	PWS02PAT0007	1407	1380	203	14.7	134	86	51	59.1
10-Jul-02	GOC-S-02-2-1	188				42			
10-Jul-02	GOC-S-02-2-2	147				46			
10-Jul-02	GOC-S-02-2-3	117	151	36	23.9	29	39	9	22.4
18-Mar-03	GOC-S-03-1-1	291				31			
18-Mar-03	GOC-S-03-1-2	368				52			
18-Mar-03	GOC-S-03-1-3	280	313	48	15.4	45	43	11	24.7
27-Jul-03	GOC-S-03-2-1P	203				31			
27-Jul-03	GOC-S-03-2-2P	179				26			
27-Jul-03	GOC-S-03-2-3P	225	202	23	11.4	115	57	50	87.9
27-Jul-03	GOC-S-03-2-1A	283				32			

27-Jul-03	GOC-S-03-2-2A	306				31			
27-Jul-03	GOC-S-03-2-3A	219	269	45	16.8	33	32	1.0	2.1
23-Mar-04	GOC-S-04-1-1	193				33			
23-Mar-04	GOC-S-04-1-2	316				16			
23-Mar-04	GOC-S-04-1-3	132	214	94	43.8	36	28	11	38.7
28-Jul-04	GOC-S-04-2-1	353				22			
28-Jul-04	GOC-S-04-2-2	261				28			
28-Jul-04	GOC-S-04-2-3	150	254	102	0.40	22	24	3	0.14
4-Mar-05	GOC-S-05-1-1	189				17			
4-Mar-05	GOC-S-05-1-2	224				22			
4-Mar-05	GOC-S-05-1-3	271	228	41	0.18	18	19	3	0.13
Gold Creek Intertidal Sediments (GOC-L)									
13-Jul-98	PWS98PAT0040	52				12			
13-Jul-98	PWS98PAT0041	14				5			
13-Jul-98	PWS98PAT0042	26	31	19	63.3	12	10	4	41.8

Appendix B-2 Summary of Sediment TPAH and component fractions, 1993-2005.

			Particulate		Dissolved		Pyrogenic			TPAH	
Sample ID	Sample Date	TPAH ng/g dw	ng/g	portion	ng/g	portion	ng/g	portion	Analytic Lab	Mean	Std Err mean
Alyeska Marine Terminal Sediments (AMT-S)											
PWS93PAT0040	4/3/1993	196	0.0	0.00	171.2	0.88	22.5	0.12	GERG		
PWS93PAT0041	4/3/1993	341	43.6	0.13	269.5	0.80	23.9	0.07	GERG		
PWS93PAT0042	4/3/1993	191	0.0	0.00	175.3	0.93	13.9	0.07	GERG	243	49
PWS93PAT0043	7/16/1993	145	0.0	0.00	125.9	0.87	18.2	0.13	GERG		
PWS93PAT0044	7/16/1993	198	0.0	0.00	179.9	0.92	16.3	0.08	GERG		
PWS93PAT0045	7/16/1993	394	33.4	0.09	49.5	0.13	305.4	0.79	GERG	246	76
PWS94PAT0025	3/26/1994	202	0.0	0.00	142.8	0.71	57.3	0.29	GERG		
PWS94PAT0026	3/26/1994	167	0.0	0.00	151.1	0.92	13.9	0.08	GERG		
PWS94PAT0027	3/26/1994	239	0.0	0.00	174.3	0.74	62.6	0.26	GERG	203	21
PWS94PAT0031	7/20/1994	175	0.0	0.00	156.2	0.90	16.8	0.10	GERG		
PWS94PAT0032	7/20/1994	230	0.0	0.00	204.2	0.90	23.4	0.10	GERG		
PWS94PAT0033	7/20/1994	389	0.0	0.00	336.7	0.87	50.2	0.13	GERG	265	64
PWS95PAT0022	4/3/1995	206	0.0	0.00	162.2	0.80	41.7	0.20	GERG		
PWS95PAT0023	4/3/1995	244	0.0	0.00	193.3	0.80	48.9	0.20	GERG		
PWS95PAT0024	4/3/1995	187	0.0	0.00	164.5	0.89	20.4	0.11	GERG	212	17
PWS95PAT0028	7/11/1995	1,650	0.0	0.00	526.9	0.32	1108.8	0.68	GERG		
PWS95PAT0029	7/11/1995	362	0.0	0.00	339.6	0.95	18.8	0.05	GERG		
PWS95PAT0030	7/11/1995	630	0.0	0.00	607.6	0.97	19.5	0.03	GERG	881	392
PWS96PAT0004	3/16/1996	160	0.0	0.00	136.8	0.86	21.5	0.14	GERG		
PWS96PAT0005	3/16/1996	311	0.0	0.00	297.4	0.96	11.7	0.04	GERG		
PWS96PAT0006	3/16/1996	135	0.0	0.00	119.9	0.90	13.6	0.10	GERG	202	55
PWS96PAT0025	7/12/1996	326	0.0	0.00	305.2	0.94	19.0	0.06	GERG		
PWS96PAT0026	7/12/1996	201	0.0	0.00	188.3	0.94	11.4	0.06	GERG		
PWS96PAT0027	7/12/1996	381	0.0	0.00	110.7	0.31	251.2	0.69	GERG	303	53
PWS97PAT0001	3/6/1997	417	0.0	0.00	377.0	0.91	36.4	0.09	GERG		
PWS97PAT0002	3/6/1997	449	0.0	0.00	416.2	0.93	29.3	0.07	GERG		

			Particulate		Dissolved		Pyrogenic			TPAH	
Sample ID	Sample Date	TPAH ng/g dw	ng/g	portion	ng/g	portion	ng/g	portion	Analytic Lab	Mean	Std Err mean
PWS97PAT0003	3/6/1997	388	0.0	0.00	342.4	0.89	43.2	0.11	GERG	418	18
PWS97PAT0029	7/17/1997	246	0.0	0.00	223.5	0.92	18.8	0.08	GERG		
PWS97PAT0030	7/17/1997	377	0.0	0.00	341.1	0.92	31.6	0.08	GERG		
PWS97PAT0031	7/17/1997	288	0.0	0.00	268.5	0.95	15.4	0.05	GERG	303	39
PWS98PAT0016	3/29/1998	120	0.0	0.00	108.9	0.93	8.8	0.07	GERG		
PWS98PAT0017	3/29/1998	451	0.0	0.00	210.8	0.47	233.6	0.53	GERG		
PWS98PAT0018	3/29/1998	144	0.0	0.00	129.1	0.91	12.1	0.09	GERG	238	107
PWS00PAT0004	4/5/2000	313	0.0	0.00	222.7	0.72	86.8	0.28	GERG		
PWS00PAT0005	4/5/2000	335	0.0	0.00	303.3	0.91	28.5	0.09	GERG		
PWS00PAT0006	4/5/2000	412	0.0	0.00	374.9	0.92	34.2	0.08	GERG	353	30
PWS00PAT0010	7/21/2000	392	0.0	0.00	333.5	0.86	54.1	0.14	GERG		
PWS00PAT0011	7/21/2000	452	0.0	0.00	397.3	0.89	50.8	0.11	GERG		
PWS00PAT0012	7/21/2000	571	54.5	0.10	147.8	0.26	356.4	0.64	GERG	472	53
PWS01PAT0001	3/28/2001	814	0.0	0.00	725.8	0.90	79.0	0.10	GERG		
PWS01PAT0002	3/28/2001	465	0.0	0.00	406.1	0.88	53.9	0.12	GERG		
PWS01PAT0003	3/28/2001	564	43.5	0.08	445.5	0.80	66.9	0.12	GERG	614	104
PWS01PAT0010	7/22/2001	160	20.5	0.13	74.2	0.48	61.5	0.39	GERG		
PWS01PAT0011	7/22/2001	536	51.2	0.10	58.1	0.11	408.9	0.79	GERG		
PWS01PAT0012	7/22/2001	311	0.0	0.00	287.0	0.94	19.4	0.06	GERG	335	109
PWS02PAT0004	3/15/2002	10	4.9	0.53	2.4	0.26	2.0	0.22	GERG		
PWS02PAT0005	3/15/2002	68	0.0	0.00	59.0	0.88	8.0	0.12	GERG		
PWS02PAT0006	3/15/2002	149	0.0	0.00	94.0	0.65	51.4	0.35	GERG	76	40
AMT-S-02-2-2	7/10/2002	1,068	0.0	0.00	1033.0	0.98	25.2	0.02	GERG		
AMT-S-02-2-3	7/10/2002	183	23.0	0.13	98.6	0.55	58.7	0.33	GERG		
AMT-S-02-2-1	7/10/2002	148	21.4	0.15	84.9	0.58	39.8	0.27	GERG	466	301
AMT-S-03-1-1	3/18/2003	127	0.0	0.00	94.1	0.75	31.7	0.25	GERG		
AMT-S-03-1-2	3/18/2003	260	0.0	0.00	171.7	0.66	87.2	0.34	GERG		
AMT-S-03-1-3	3/18/2003	123	0.0	0.00	114.6	0.94	7.2	0.06	GERG	170	45
AMT-S-03-2-1P	7/27/2003	165	14.5	0.09	133.8	0.82	14.1	0.09	GERG		

			Particulate		Dissolved		Pyrogenic			TPAH	
Sample ID	Sample Date	TPAH ng/g dw	ng/g	portion	ng/g	portion	ng/g	portion	Analytic Lab	Mean	Std Err mean
AMT-S-03-2-2P	7/27/2003	118	12.0	0.10	58.3	0.50	45.3	0.39	GERG		
AMT-S-03-2-3P	7/27/2003	93	10.1	0.11	75.1	0.82	6.2	0.07	GERG	125	21
AMT-S-03-2-1A	7/27/2003	195	23.0	0.12	157.6	0.82	11.2	0.06	ABL		
AMT-S-03-2-2A	7/27/2003	265	23.9	0.09	2.9	0.01	232.3	0.90	ABL		
AMT-S-03-2-3A	7/27/2003	126	16.9	0.14	95.0	0.77	11.2	0.09	ABL	195	40
AMT-S-04-1-1	3/23/2004	121	0.0	0.00	21.2	0.18	98.1	0.82	ABL		
AMT-S-04-1-2	3/23/2004	225	30.6	0.14	3.6	0.02	185.0	0.84	ABL		
AMT-S-04-1-3	3/23/2004	134	0.0	0.00	44.9	0.34	85.8	0.66	ABL	160	33
AMT-S-04-2-1	7/28/2004	89	0.0	0.00	12.4	0.14	74.7	0.86	ABL		
AMT-S-04-2-2	7/28/2004	321	28.7	0.09	3.4	0.01	280.3	0.90	ABL		
AMT-S-04-2-3	7/28/2004	91	0.0	0.00	44.4	0.50	44.7	0.50	ABL	167	77
AMT-S-05-1-1	3/4/2005	61	7.8	0.13	1.1	0.02	50.5	0.85	ABL		
AMT-S-05-1-2	3/4/2005	42	7.6	0.18	23.1	0.56	10.7	0.26	ABL		
AMT-S-05-1-3	3/4/2005	37	0.0	0.00	25.5	0.73	9.7	0.27	ABL	47	7
Gold Creek Sediments (GOC-S)											
PWS93PAT0001	3/19/1993	47	0.0	0.00	16.3	0.35	29.8	0.65	ABL		
PWS93PAT0002	3/19/1993	36	0.0	0.00	12.5	0.35	23.0	0.65	ABL		
PWS93PAT0003	3/19/1993	58	0.0	0.00	25.0	0.44	31.8	0.56	ABL	47	6
PWS93PAT0071	7/25/1993	57	0.0	0.00	15.4	0.28	40.5	0.72	ABL		
PWS93PAT0072	7/25/1993	31	0.0	0.00	8.3	0.27	22.0	0.73	ABL		
PWS93PAT0073	7/25/1993	25	0.0	0.00	8.7	0.35	15.9	0.65	ABL	38	10
PWS94PAT0022	3/26/1994	61	0.0	0.00	49.1	0.83	10.2	0.17	GERG		
PWS94PAT0023	3/26/1994	46	0.0	0.00	27.9	0.63	16.4	0.37	GERG		
PWS94PAT0024	3/26/1994	106	0.0	0.00	19.9	0.19	84.9	0.81	GERG	71	18
PWS94PAT0028	7/19/1994	47	0.0	0.00	26.7	0.59	18.9	0.41	GERG		
PWS94PAT0029	7/19/1994	18	0.0	0.00	12.3	0.70	5.2	0.30	GERG		
PWS94PAT0030	7/19/1994	69	0.0	0.00	13.6	0.20	53.6	0.80	GERG	44	15
PWS95PAT0019	4/3/1995	57	8.2	0.15	2.6	0.05	45.3	0.81	GERG		
PWS95PAT0020	4/3/1995	34	0.0	0.00	10.9	0.33	22.4	0.67	GERG		

			Particulate		Dissolved		Pyrogenic		Analytic Lab	TPAH	
Sample ID	Sample Date	TPAH ng/g dw	ng/g	portion	ng/g	portion	ng/g	portion		Mean	Std Err mean
PWS95PAT0021	4/3/1995	31	0.0	0.00	13.5	0.45	16.8	0.55	GERG	41	8
PWS95PAT0025	7/11/1995	67	0.0	0.00	45.6	0.70	19.9	0.30	GERG		
PWS95PAT0026	7/11/1995	59	0.0	0.00	28.9	0.51	28.1	0.49	GERG		
PWS95PAT0027	7/11/1995	31	0.0	0.00	23.0	0.79	6.2	0.21	GERG	52	11
PWS96PAT0001	3/16/1996	78	0.0	0.00	12.2	0.16	63.7	0.84	GERG		
PWS96PAT0002	3/16/1996	156	11.8	0.08	0.0	0.00	140.5	0.92	GERG		
PWS96PAT0003	3/16/1996	33	9.7	0.31	9.1	0.29	12.8	0.41	GERG	89	36
PWS96PAT0028	7/12/1996	56	0.0	0.00	26.0	0.48	28.6	0.52	GERG		
PWS96PAT0029	7/12/1996	46	0.0	0.00	23.0	0.52	21.4	0.48	GERG		
PWS96PAT0030	7/12/1996	53	0.0	0.00	25.9	0.50	25.4	0.50	GERG	51	3
PWS97PAT0004	3/6/1997	54	0.0	0.00	24.3	0.46	28.1	0.54	GERG		
PWS97PAT0005	3/6/1997	39	0.0	0.00	23.8	0.63	14.2	0.37	GERG		
PWS97PAT0006	3/6/1997	40	0.0	0.00	17.0	0.43	22.3	0.57	GERG	44	5
PWS97PAT0026	7/17/1997	53	14.3	0.28	9.7	0.19	27.8	0.54	GERG		
PWS97PAT0027	7/17/1997	55	12.6	0.24	11.4	0.22	28.7	0.54	GERG		
PWS97PAT0028	7/17/1997	60	13.0	0.23	11.6	0.20	32.8	0.57	GERG	56	2
PWS98PAT0013	3/29/1998	42	14.3	0.35	23.3	0.58	2.8	0.07	GERG		
PWS98PAT0014	3/29/1998	48	0.0	0.00	24.8	0.54	20.9	0.46	GERG		
PWS98PAT0015	3/29/1998	38	14.9	0.41	19.4	0.53	2.1	0.06	GERG	43	3
PWS00PAT0001	4/5/2000	127	0.0	0.00	32.9	0.27	90.8	0.73	GERG		
PWS00PAT0002	4/5/2000	81	0.0	0.00	29.9	0.38	48.5	0.62	GERG		
PWS00PAT0003	4/5/2000	126	0.0	0.00	44.0	0.36	79.1	0.64	GERG	111	15
PWS00PAT0007	7/20/2000	105	26.4	0.26	7.5	0.07	68.1	0.67	GERG		
PWS00PAT0008	7/20/2000	111	32.0	0.30	10.5	0.10	65.2	0.61	GERG		
PWS00PAT0009	7/21/2000	92	24.8	0.28	8.5	0.10	55.9	0.63	GERG	103	6
PWS01PAT0004	3/28/2001	125	25.2	0.21	10.4	0.09	86.0	0.71	GERG		
PWS01PAT0005	3/28/2001	131	30.7	0.24	10.8	0.09	84.8	0.67	GERG		
PWS01PAT0006	3/28/2001	120	28.6	0.25	11.8	0.10	76.0	0.65	GERG	126	3
PWS01PAT0007	7/21/2001	40	0.0	0.00	15.7	0.42	21.6	0.58	GERG		

			Particulate		Dissolved		Pyrogenic			TPAH	
Sample ID	Sample Date	TPAH ng/g dw	ng/g	portion	ng/g	portion	ng/g	portion	Analytic Lab	Mean	Std Err mean
PWS01PAT0008	7/21/2001	59	21.7	0.39	3.1	0.06	31.3	0.56	GERG		
PWS01PAT0009	7/21/2001	108	17.5	0.17	3.1	0.03	83.9	0.80	GERG	69	20
PWS02PAT0002	3/15/2002	91	0.0	0.00	38.2	0.43	50.3	0.57	GERG		
PWS02PAT0003	3/15/2002	33	12.3	0.40	1.5	0.05	17.2	0.55	GERG		
PWS02PAT0007	3/15/2002	134	0.0	0.00	36.4	0.28	95.2	0.72	GERG	86	29
GOC-S-02-2-1	7/10/2002	42	0.0	0.00	19.2	0.48	20.9	0.52	GERG		
GOC-S-02-2-2	7/10/2002	46	16.7	0.38	1.5	0.03	26.2	0.59	GERG		
GOC-S-02-2-3	7/10/2002	29	13.9	0.50	0.7	0.02	13.1	0.47	GERG	39	5
GOC-S-03-1-1	3/18/2003	31	0.0	0.00	13.9	0.46	16.4	0.54	GERG		
GOC-S-03-1-2	3/18/2003	52	0.0	0.00	23.0	0.46	27.2	0.54	GERG		
GOC-S-03-1-3	3/18/2003	45	0.0	0.00	20.2	0.47	22.5	0.53	GERG	43	6
GOC-S-03-2-1A	7/27/2003	32	13.9	0.47	3.4	0.11	12.5	0.42	GERG		
GOC-S-03-2-2A	7/27/2003	31	11.3	0.38	0.8	0.03	17.6	0.59	GERG		
GOC-S-03-2-3A	7/27/2003	33	12.3	0.41	4.4	0.15	13.4	0.44	GERG	32	0
GOC-S-03-2-1P	7/27/2003	31	13.2	0.46	3.5	0.12	12.0	0.42	GERG		
GOC-S-03-2-2P	7/27/2003	26	10.6	0.45	2.4	0.10	10.4	0.44	GERG		
GOC-S-03-2-3P	7/27/2003	115	0.0	0.00	22.0	0.19	91.2	0.81	GERG	57	29
GOC-S-04-1-1	3/23/2004	33	14.3	0.45	1.1	0.03	16.1	0.51	GERG		
GOC-S-04-1-2	3/23/2004	16	7.2	0.49	0.6	0.04	7.0	0.47	GERG		
GOC-S-04-1-3	3/23/2004	36	14.5	0.43	1.0	0.03	18.2	0.54	GERG	28	6
GOC-S-04-2-1	7/28/2004	22	0.0	0.00	8.4	0.41	11.9	0.59	GERG		
GOC-S-04-2-2	7/28/2004	28	0.0	0.00	7.5	0.29	18.1	0.71	GERG		
GOC-S-04-2-3	7/28/2004	22	7.5	0.37	0.2	0.01	12.7	0.62	GERG	24	2
GOC-S-05-1-1	3/4/2005	17	0.0	0.00	6.8	0.44	8.6	0.56	GERG		
GOC-S-05-1-2	3/4/2005	22	8.8	0.42	0.4	0.02	11.8	0.56	GERG		
GOC-S-05-1-3	3/4/2005	18	7.1	0.41	0.3	0.02	9.7	0.57	GERG	19	2

Appendix C Tissue TPAH and TSHC summary for LTEMP 2004-2005.

Station	Samp Date	Samp ID	TPAH	average	SE mean	TSHC	average	SE mean
AIB-B	7/30/2004	AIB-B-04-2-1-R2	29			#N/A[2]		
	7/30/2004	AIB-B-04-2-2-R2	20			#N/A		
	7/30/2004	AIB-B-04-2-3-R2	24	24	2.71	#N/A	#N/A	#N/A
	3/7/2005	AIB-B-05-1-1	19			1161		
	3/7/2005	AIB-B-05-1-2-R2	12			915		
	3/7/2005	AIB-B-05-1-3	41	24	8.69	1371	1149	131.88
AMT-B	7/28/2004	AMT-B-04-2-1	69			4020		
	7/28/2004	AMT-B-04-2-2	40			1896		
	7/28/2004	AMT-B-04-2-3	72	60	12.34	2076	2664	832.80
	10/13/2004	AMT-B-04-3-1	59			2010		
	10/13/2004	AMT-B-04-3-2	52			1436		
	10/13/2004	AMT-B-04-3-3	55	55	1.96	2271	1906	246.46
	3/4/2005	AMT-B-05-1-1-R2	42			2189		
	3/4/2005	AMT-B-05-1-2-R2	100			1603		
	3/4/2005	AMT-B-05-1-3-R2	40	61	19.68	2078	1956	179.78
DII-B	7/30/2004	DII-B-04-2-1-R2	22			#N/A		
	7/30/2004	DII-B-04-2-2	28			937		
	7/30/2004	DII-B-04-2-3	35	29	3.76	1912	1424	487.21
	3/7/2005	DII-B-05-1-1	32			1606		
	3/7/2005	DII-B-05-1-2	44			1851		
	3/7/2005	DII-B-05-1-3	35	37	3.63	2409	1956	237.66
GOC-B	7/28/2004	GOC-B-04-2-1-R2	33			1744		
	7/28/2004	GOC-B-04-2-2-R2	57			1970		
	7/28/2004	GOC-B-04-2-3-R2	36	42	7.63	2248	1987	145.76
	10/13/2004	GOC-B-04-3-1	504			3999		
	10/13/2004	GOC-B-04-3-2	1026			6607		
	10/13/2004	GOC-B-04-3-3-R2	975	835	166.25	7788	6132	1119.28
	3/4/2005	GOC-B-05-1-1	167			4387		
	3/4/2005	GOC-B-05-1-2-R2	185			1236		
	3/4/2005	GOC-B-05-1-3	138	163	13.65	2104	2576	939.77
KNH-B	7/29/2004	KNH-B-04-2-1-R2	12			865		
	7/29/2004	KNH-B-04-2-2-R2	83			#N/A		
	7/29/2004	KNH-B-04-2-3-R2	12	36	23.65	#N/A	865	#N/A
	3/14/2005	KNH-B-05-1-1	28			785		
	3/14/2005	KNH-B-05-1-2	24			5784		
	3/14/2005	KNH-B-05-1-3	49	34	7.63	1317	2629	1585.18
SHB-B	7/29/2004	SHB-B-04-2-1-R2	11			1208		
	7/29/2004	SHB-B-04-2-2-R2	31			549		
	7/29/2004	SHB-B-04-2-3	17	20	6.05	1019	925	195.82
	3/7/2005	SHB-B-05-1-1	48			1068		
	3/7/2005	SHB-B-05-1-2	27			1123		
	3/7/2005	SHB-B-05-1-3-R2	21	32	8.15	607	933	163.48
SHH-B	8/2/2004	SHH-B-04-2-1	32			1309		
	8/2/2004	SHH-B-04-2-2	61			2371		
	8/2/2004	SHH-B-04-2-3-R2	20	38	12.27	1519	1733	324.84
	3/16/2005	SHH-B-05-1-1	24			2093		

Station	Samp Date	Samp ID	TPAH	average	SE mean	TSHC	average	SE mean
	3/16/2005	SHH-B-05-1-2	31			2177		
	3/16/2005	SHH-B-05-1-3	30	28	2.43	4885	3052	916.80
SLB-B	7/30/2004	SLB-B-04-2-1	67			2414		
	7/30/2004	SLB-B-04-2-2	#N/A[1]			#N/A		
	7/30/2004	SLB-B-04-2-3	60	63	3.52	1175	1794	619.62
	3/14/2005	SLB-B-05-1-1	27			2863		
	3/14/2005	SLB-B-05-1-2	33			8068		
	3/14/2005	SLB-B-05-1-3	35	32	2.25	7245	6059	1615.38
WIB-B	8/1/2004	WIB-B-04-2-1	69			2167		
	8/1/2004	WIB-B-04-2-2	59			1283		
	8/1/2004	WIB-B-04-2-3	42	57	7.96	1510	1654	264.95
	3/16/2005	WIB-B-05-1-1	33			3697		
	3/16/2005	WIB-B-05-1-2	48			2871		
	3/16/2005	WIB-B-05-1-3	30	37	5.66	2329	2966	397.80
ZAB-B	7/30/2004	ZAB-B-04-2-1	40			1992		
	7/30/2004	ZAB-B-04-2-2	44			1541		
	7/30/2004	ZAB-B-04-2-3	40	42	1.49	2120	1885	175.60
	3/7/2005	ZAB-B-05-1-1	52			2752		
	3/7/2005	ZAB-B-05-1-2	66			1221		
	3/7/2005	ZAB-B-05-1-3	64	61	4.29	1200	1724	514.00

Notes:

1 A number of tissue samples were re-extracted and re-analyzed due to an anomalous PAH spike discovered during internal data analysis and QC review. In one instance, there was not sufficient tissue to allow re-extraction so PAH data for one of three replicates at SLB are not available.

2. SHC analyses were not completed on certain re-extracted samples, so in several instances SHC data are not available. This affected the July 2004 samples from AIB, and individual replicates from July 2004 samples at DII, KNH, and SLB.

Appendix D Jack Bay Diesel Spill

During a "spill drill" exercise in Jack Bay, Prince William Sound on April 29, 2004, a SERVS vessel had an accidental diesel spill which came ashore near Tongue Point just inside Jack Bay (Figure 1 – reproduced from field notes and information provided by PWS RCAC and ADEC). Three sets of field samples (intertidal sediments and mussels) were taken. This report interprets the data from the first two samplings (Figures 2 and 3). The third set of samples, taken two-and-one-half months after the spill on July 15, 2004, is still pending analysis at the Auke Bay Laboratory.

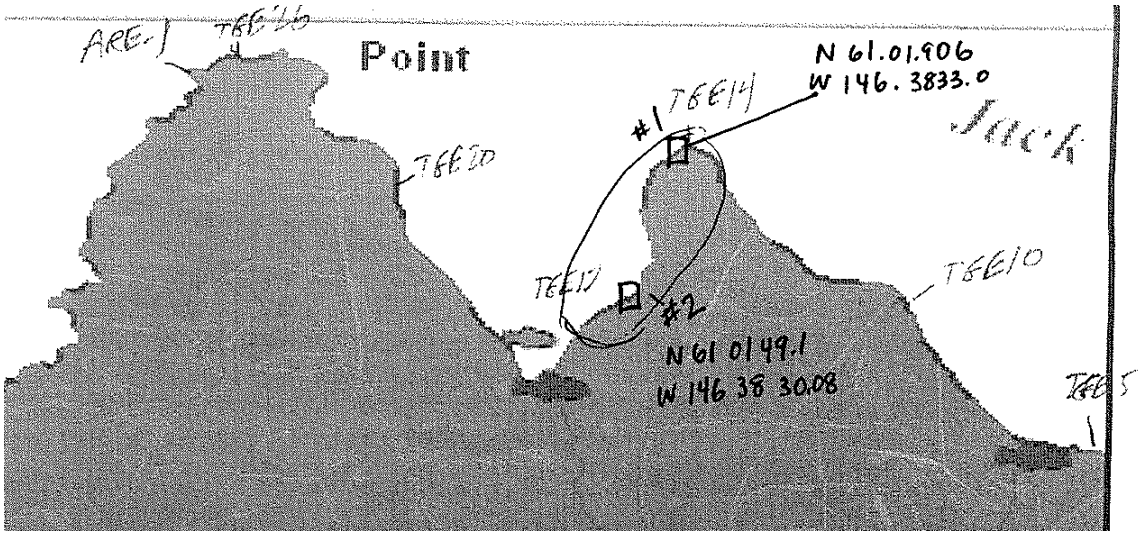

Figure 1. Field Map of Tongue Point, Jack Bay sampling locations.

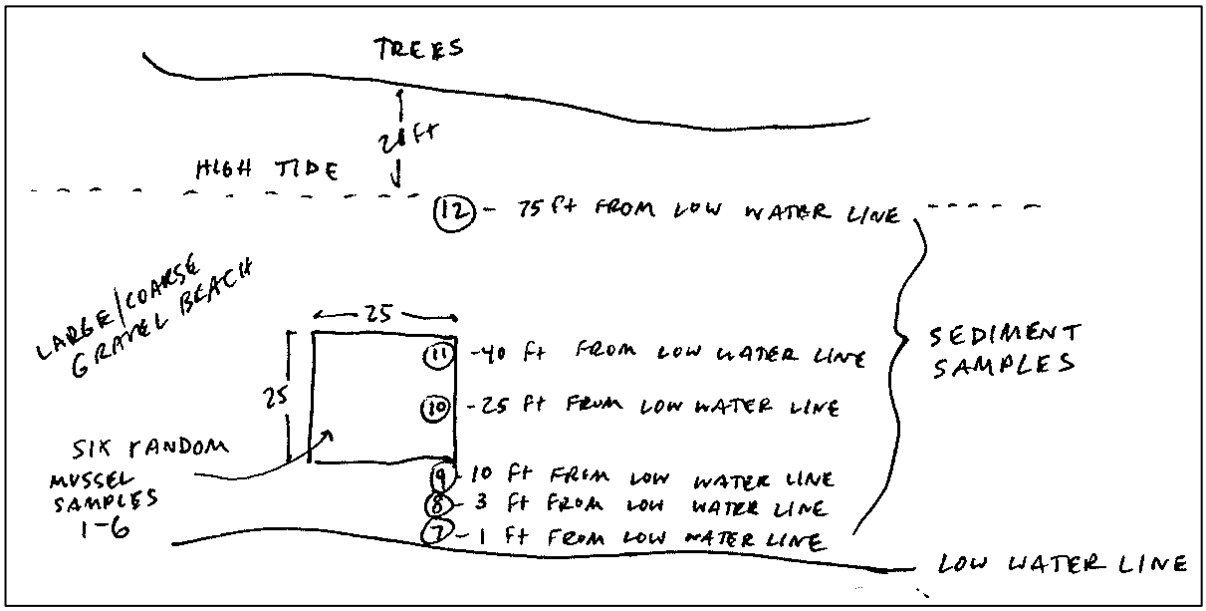

Figure 2. Notes on location of samples from east of Tongue Pt on gravel beach, segment TGE14 collected on 4 May 2004.

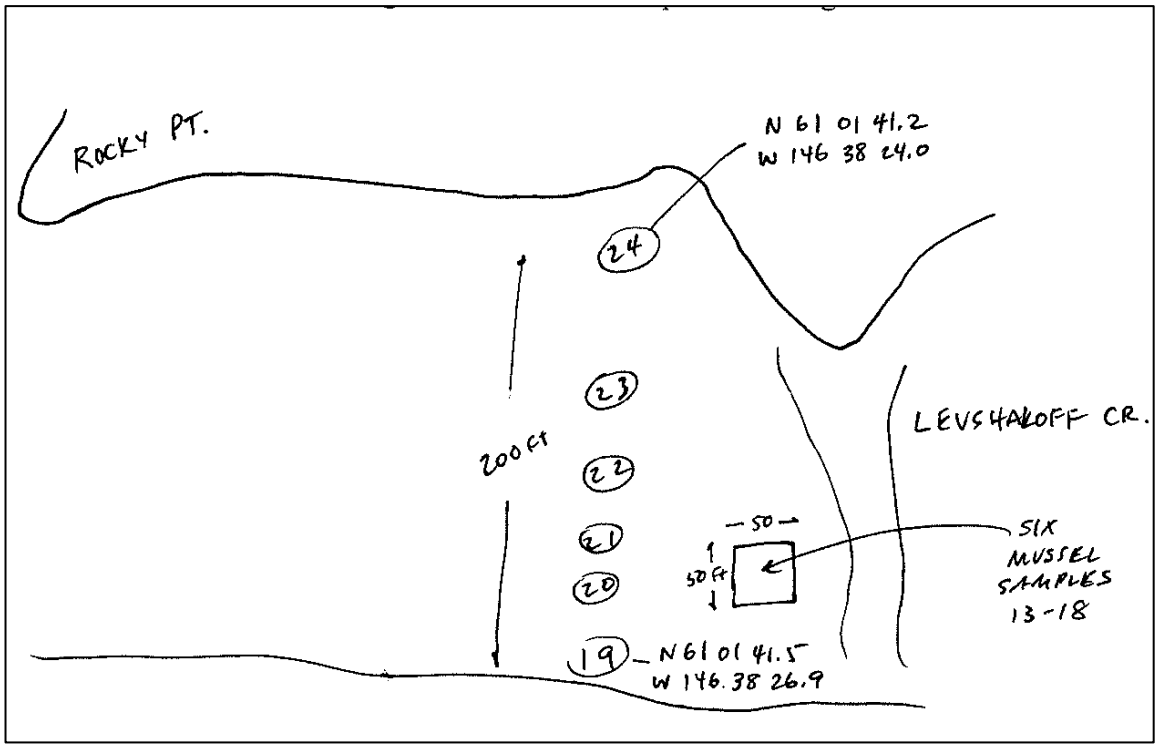

Figure 3. Notes on location of samples from north of Levshakoff Creek on sandy flat, segment TGE16 collected on 13 May 2004.

Unfortunately, no samples of the source diesel were collected for chemical characterization at the time of the spill, but the PAH and SHC profiles for a fairly typical marine diesel oil (Figure 4) show a fairly limited range of components. Because diesel oils represent a distillate cut within a defined boiling-point range, most of the higher-molecular-weight four- and five-ring PAH are missing, and the PAH fraction is characterized by predominant naphthalenes and lesser amounts of fluorenes, phenanthrenes/anthracenes, and dibenzothiophenes. The n-alkanes also usually show a narrow range (typically from n-C12 through n-C23), although the sample shown in Figure 4 includes additional n-alkanes down to n-C9 and up to n-C26. In fresh diesel, however, the distribution ratio of even and odd carbon-number n-alkanes is usually close to one, and changes in the predominance of the straight-chain n-alkanes over the branched isoprenoids (pristane and phytane) can be used to track biodegradation.

The first set of field samples was taken by Dan Gilson (PWS RCAC) and John Engels (ADEC) on May 4th at shoreline segment TGE14, a coarse gravel beach (Figure 2). The six PAH plots of mussel tissue samples show a fresh diesel signature with TPAH values ranging from 1,014 to 1,854 ng/g dry wt (Figure 5). Freshness is evident from the predominant naphthalenes in a particulate/oil-phase signal where the C3- and C4-naphthalenes have not yet been lost to evaporation and/or dissolution processes. Also, from the PAH patterns, the mussels accumulated the diesel from discrete oil droplets as opposed to the dissolved phase. This is also supported by the high levels of phytane (an insoluble component associated only with oil and refined petroleum products) that was also observed in the mussel tissues (see below).

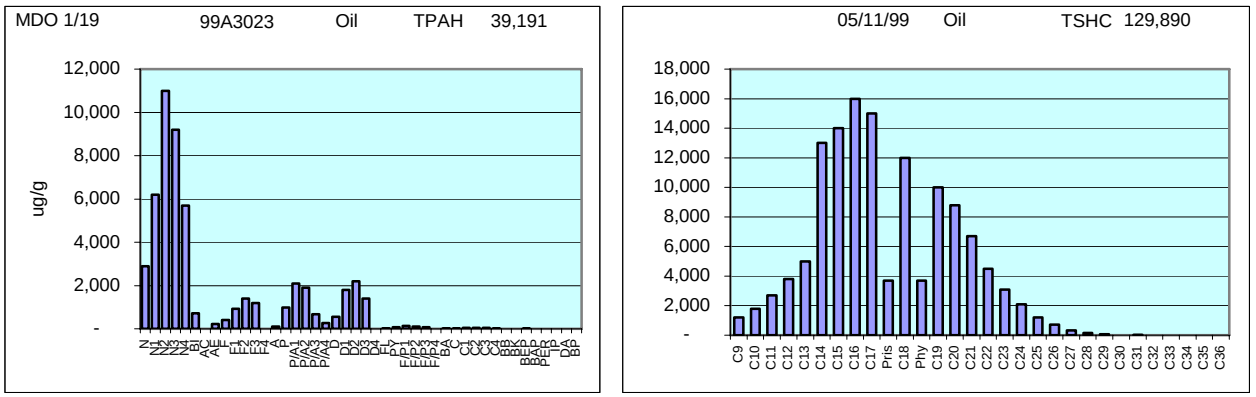

Figure 4. Typical PAH and SHC profiles of a fresh diesel oil (MDO 1/19 from the *T/V New Carissa* spill.

The accompanying PAH data from the sediments (Figure 6) are generated in sequence from the waterline to the upper intertidal of the coarse gravel beach. The PAH levels in these samples are all below laboratory method detection limits, which adds uncertainty to the results but the patterns clearly show a progression from trace amounts of diesel (less fresh than in the tissue samples) to a full-blown signal, albeit miniscule (2-14 ng/g dry wt), midway up the shore nearer the mussel collection sites. Clearly, the mussels are much more effective at retaining higher concentrations of PAH in their tissues than the nearby coarse grained sediments. There are no sediment particle grain size data provided but one might assume that the sediments under the mussel beds may have contained slightly higher amounts of fines and organic detritus which could adsorb and retain the diesel signal. This would retard physical washing of the diesel from the shoreline at that tidal elevation. Alternatively, the diesel may have simply come ashore at a single tide height (near the mussel beds), and that could explain the gradient in TPAH levels and weathering patterns up and down the beach. Also, in a coarse gravel matrix there would be less surface area (relative to a finer mud sediment) onto which a diesel droplet might penetrate and adhere, so, lower amounts of weathered diesel residues might be expected. Gravel beaches are also usually more wave/current exposed than a depositional mud beach so physical washing from the sediments would also be more prevalent. Thus, the low TPAH values along with evidence of dissolution and evaporation weathering (selectively removing the naphthalenes compared to the higher-molecular-weight PAH) typifies this early post-spill scenario.

The tissue SHC data from the first site show a highly biodegraded diesel signal relative to the sediment SHC values (Figure 7 versus 8). Compare the elevated pristane and phytane values in tissues to less degraded signal in the sediment samples. The suite of n-C14 to n-C22 n-alkanes in the sediments is very typical of fresh arctic diesel, and its selective removal from the mussel tissues in as little as five days (where only pristane and phytane remain) suggests the presence of aliphatic hydrocarbon degrading bacteria within the mussels themselves. If the mussels were somehow depurating the less soluble n-alkanes as whole oil droplets, then we would also expect to see much lower levels of phytane. Based on the SHC pattern and the relative abundance of n-C17/pristane and n-C18/phytane in the sediments near the mussels, it does not appear as if much biological degradation has

occurred. Also note again that the sediment TSHC values are roughly 100 times less than the tissues' despite the advanced microbial degradation that has occurred. At the upper intertidal levels, the odd-carbon-numbered, longer-chain plant terrestrial plant waxes begin to appear (n-C27, n-C29 and n-C31) in the sediments (Figure 8). The sparse sediment sample 12 was apparently from above the intertidal spill zone.

A second set of samples was taken by Tony Parkin and Dan Gilson (both PWS RCAC) on May 13, roughly two weeks after the spill. This sampling occurred on a large sandy flat (segment TGE16), which was observed to be exposed to grounded diesel to similar degree as the previous site (Figure 3). Mussel samples from this site showed a similar very fresh diesel signal at even higher TPAH values (1,307-2,668 ng/g dry wt) than the first site (Figure 9). The sediments (Figure 10) likewise show very low TPAH levels (7-12 ng/g dry wt) with evidence of selective water-washing and evaporation weathering (removal) of the more water-soluble naphthalenes compared to the higher-molecular-weight PAH..

The tissue SHC data from the second site again show extremely high levels of pristane and phytane. While the pristane can be attributed to ingestion of copepods and phytoplankton, the phytane indicates a residual signal from highly-weathered diesel (Figure 11). Compared to the fresh diesel signal observed in the sediments collected only five days after the spill, most of the n-alkanes have been microbially degraded in the mussel tissues leaving only large spikes of pristane and phytane. Since phytane only occurs in oil, the phytane spikes imply that these mussels have received some very high doses of diesel (21-45 thousand ng/g). For sediments, the diesel SHC signal is slightly more uniform across the gradient of the sand flats than up the gravel beach at the first site. The TSHC levels are so low (again 100 fold less than in the tissues), that it is difficult to accurately assess the degree of abiotic versus microbial degradation. The relative abundance of pristane and phytane compared to the other n-alkanes in sample JB Sed 20 (Figure 12) suggests, however, that microbial processes may have started in the sediments by this time, The SHC data also show spatially-variable amounts of longer-chain plant waxes in samples collected higher in the intertidal zone.

Rate of Weathering

It is difficult to extract a reliable weathering rate from these data because the samples were not collected from the same locations over time. That is, variability from the different sites, sediment grain size, and exposure regimes would confound any time-series analysis. Clearly, however, the PAH pattern in the mussel samples was still very evident and showed few compound-specific changes over the two weeks between the initial sampling events. Expected rate of weathering may be estimated from the third set of samples if they were collected from the same locations.

Depending on the results from the July 2004 sample collections, it may be prudent to re-occupy the site to evaluate the longer-term weathering and persistence of diesel spilled into the subarctic marine environment. Diesel spills quickly disperse into the water column, and they are difficult to visually detect in the intertidal after only a few days (leaving only occasional sheens but no tarballs or oil-coated rocks). As a result, they are not believed to be very persistent, and they are often written off as not having a long-term environmental

effect. It is impossible to obtain a permit for an intentional oil spill in US waters for research purposes, and it might be prudent to pursue the weathering trends of the diesel spill at Jack Bay since we know exactly when it occurred, and may be able to track its behavior over time.

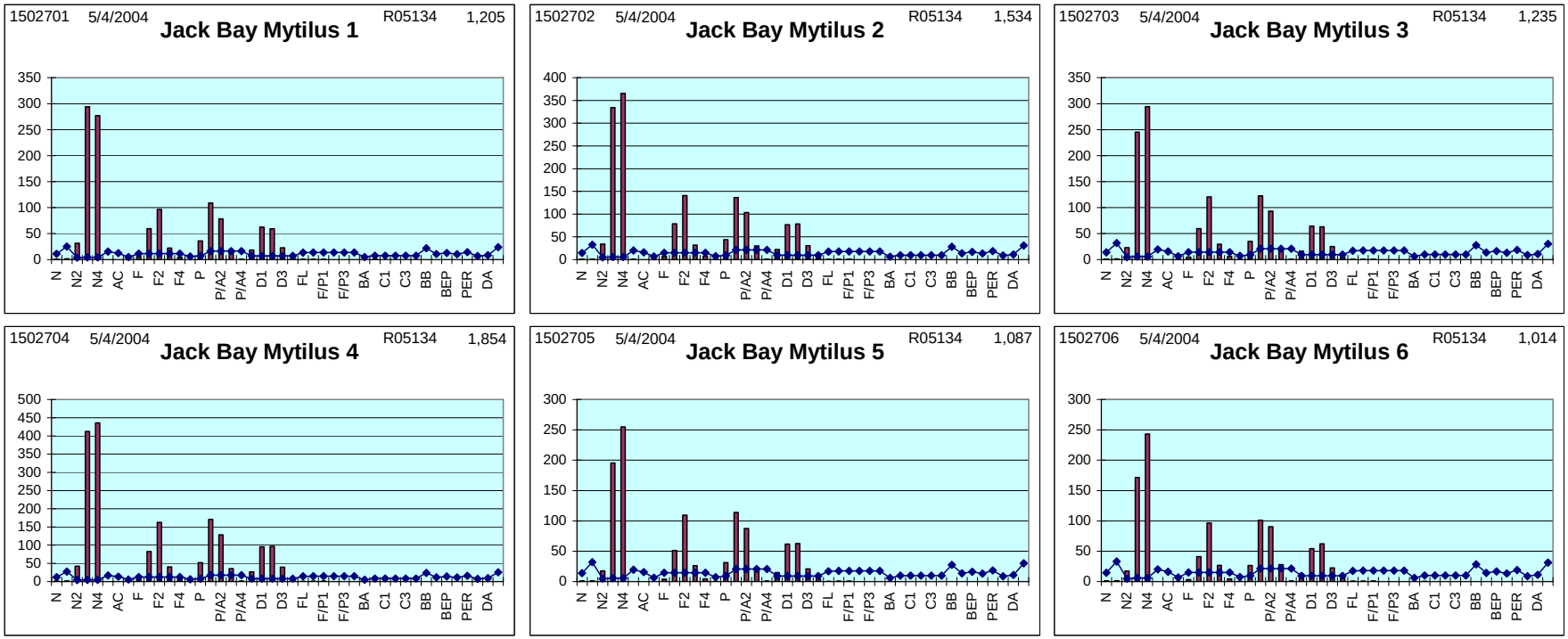

Figure 5. PAH plots of Jack Bay *Mytilus* from segment TGE14 showing fresh diesel signatures, 4 May 2004.

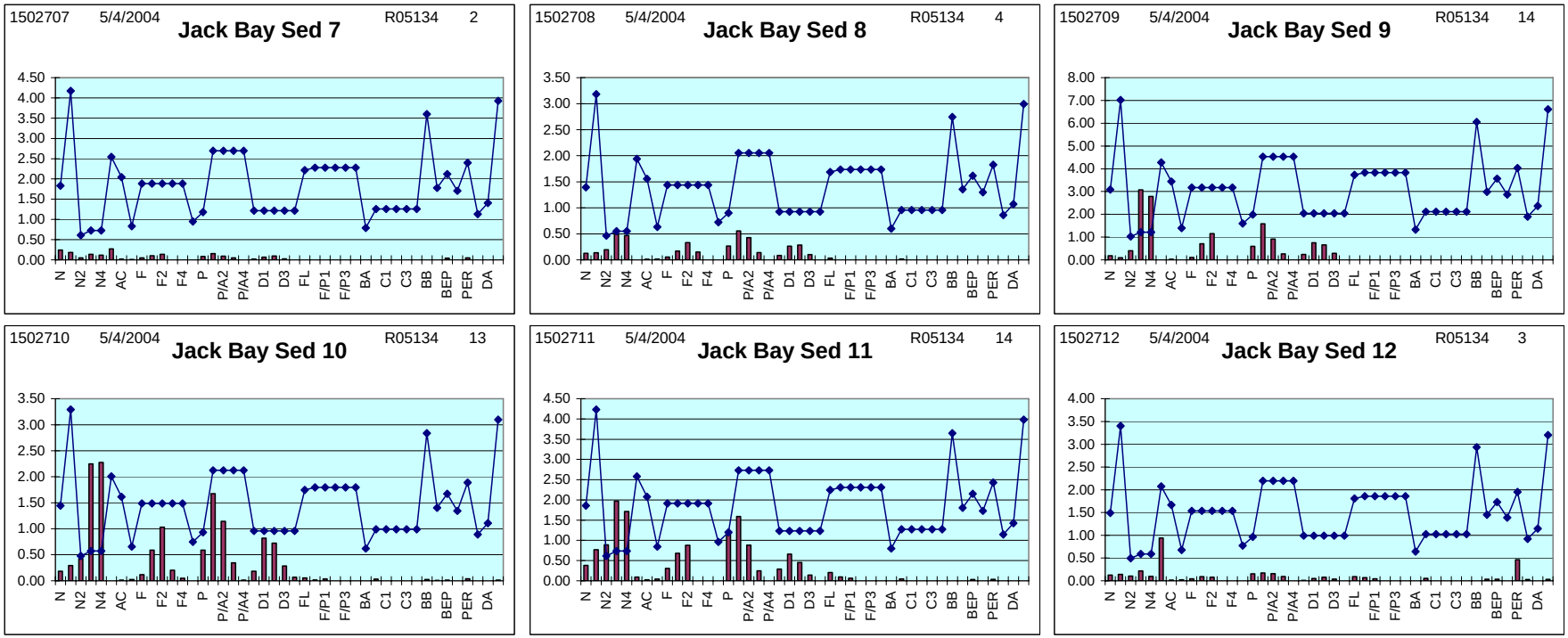

Figure 6. PAH plots of Jack Bay sediments from segment TGE14 showing low and variable concentrations of fresh diesel signatures, 4 May 2004. Samples Jack Bay Sed 10 and Jack Bay Sed 11 were collected in the vicinity of the mussel beds (see Figure 2).

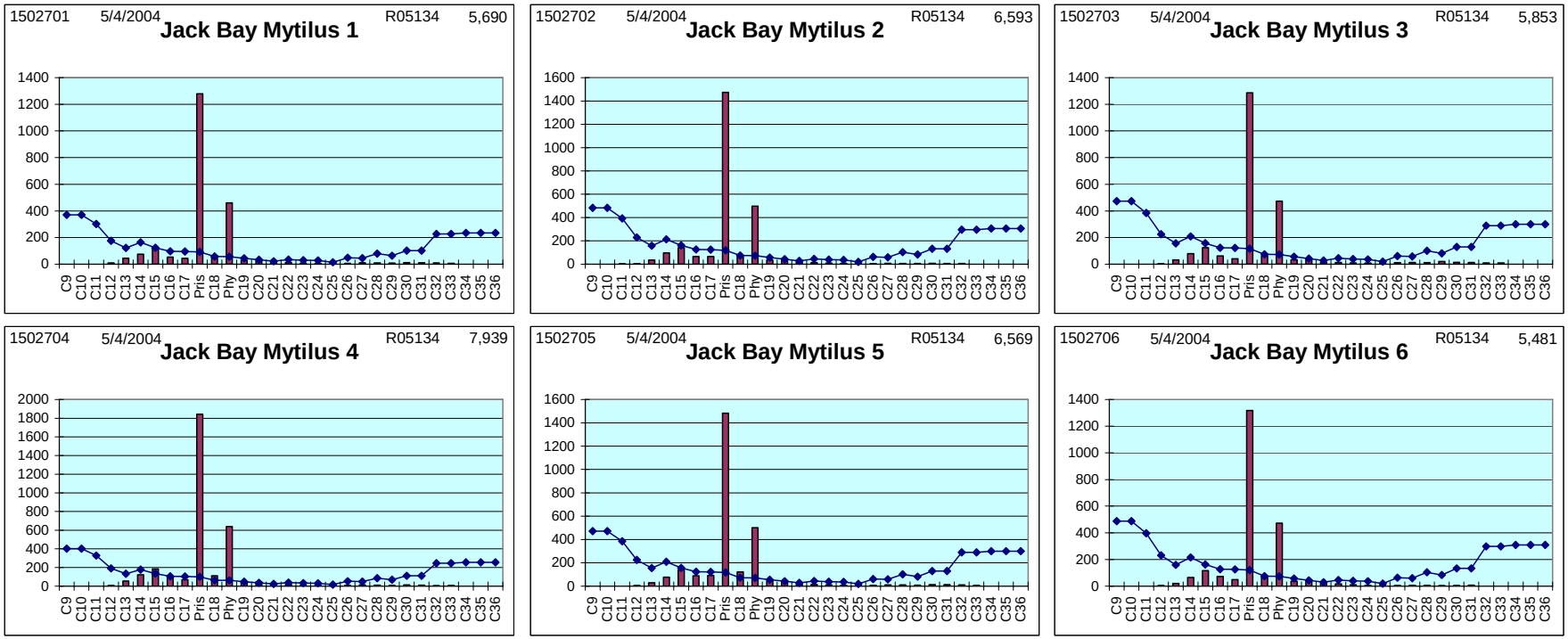

Figure 7. SHC plots of Jack Bay *Mytilus* from segment TGE14 showing microbially degraded diesel signatures, 4 May 2004. Because mussels do not have the enzyme systems to promote this selective n-alkane loss (leaving only the pristane and phytane behind), this pattern most likely reflects microbial degradation of the oil droplets after ingestion by the mussels. Interestingly, the SHC profiles from the sediments near the mussel beds (Figure 8) do not show this same degree of microbial degradation.

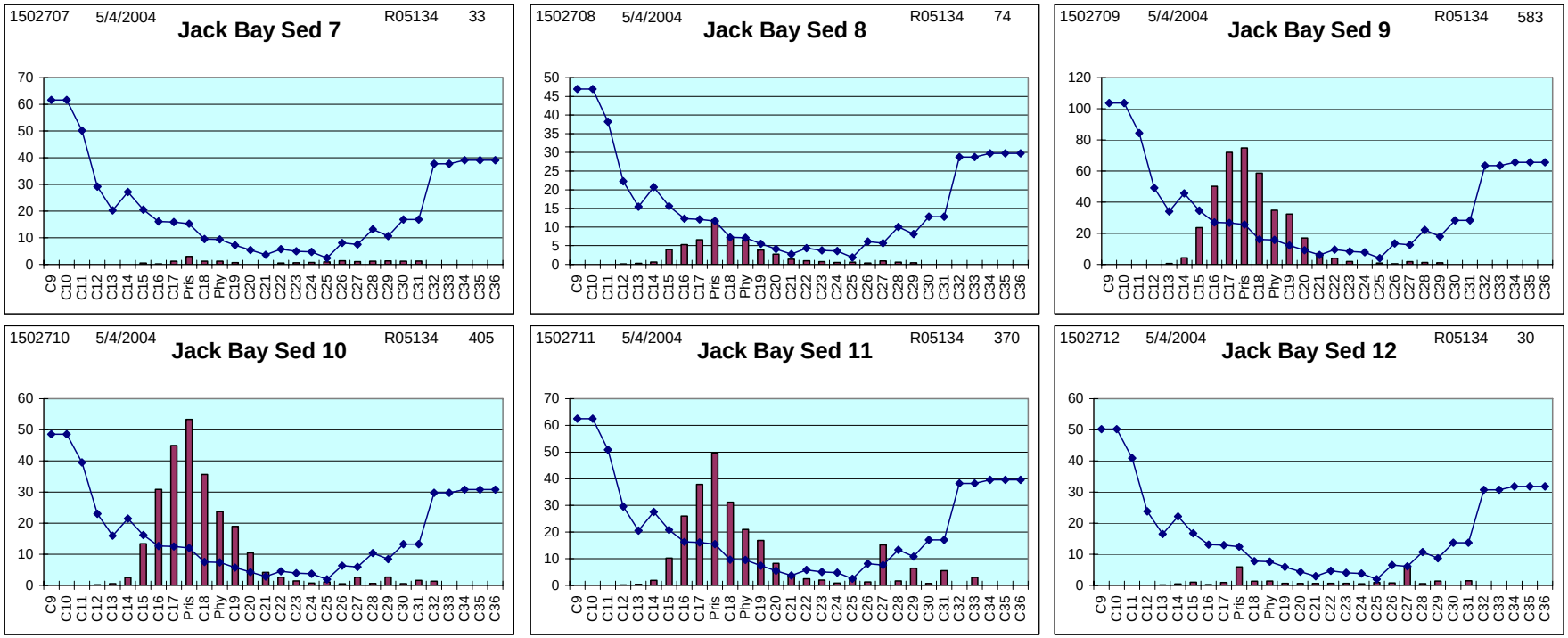

Figure 8. SHC plots of Jack Bay sediments from segment TGE14 showing fresh diesel signatures, 4 May 2004.

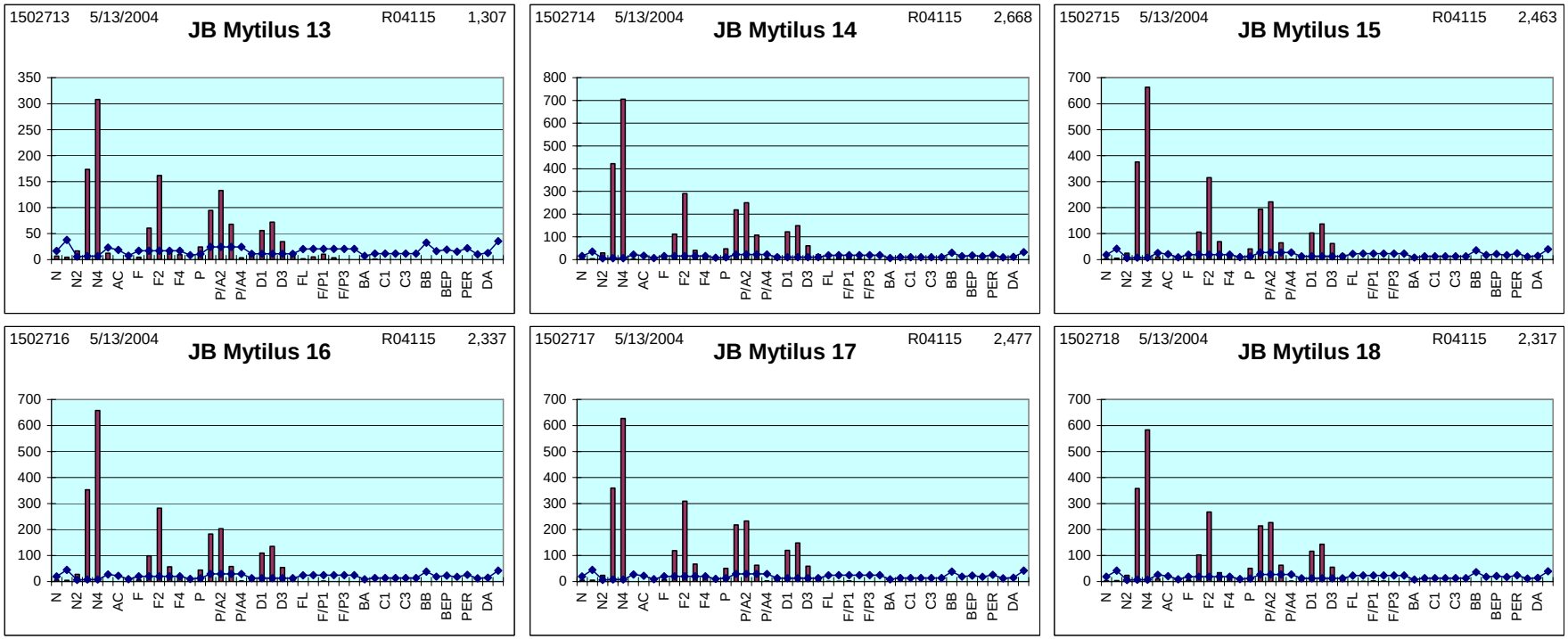

Figure 9. PAH plots of Jack Bay *Mytilus* from segment TGE16 showing the relatively persistent fresh diesel PAH signatures, 13 May 2004. The sediment samples collected at the same time showed a more weathered and water washed pattern with significantly lower concentrations of naphthalenes relative to the other PAH (Figure 10).

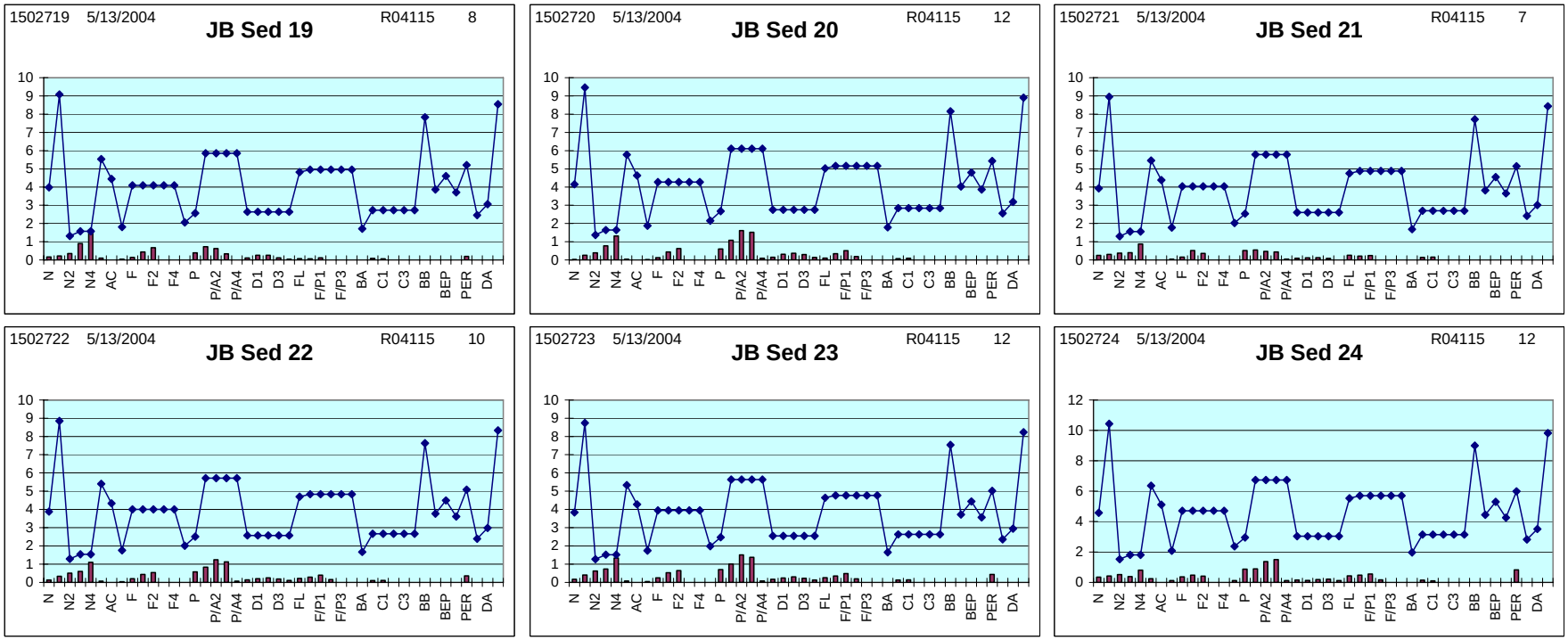

Figure 10. PAH plots of Jack Bay sediments from segment TGE16 showing a water-washed and heavily degraded diesel signatures, 13 May 2004.

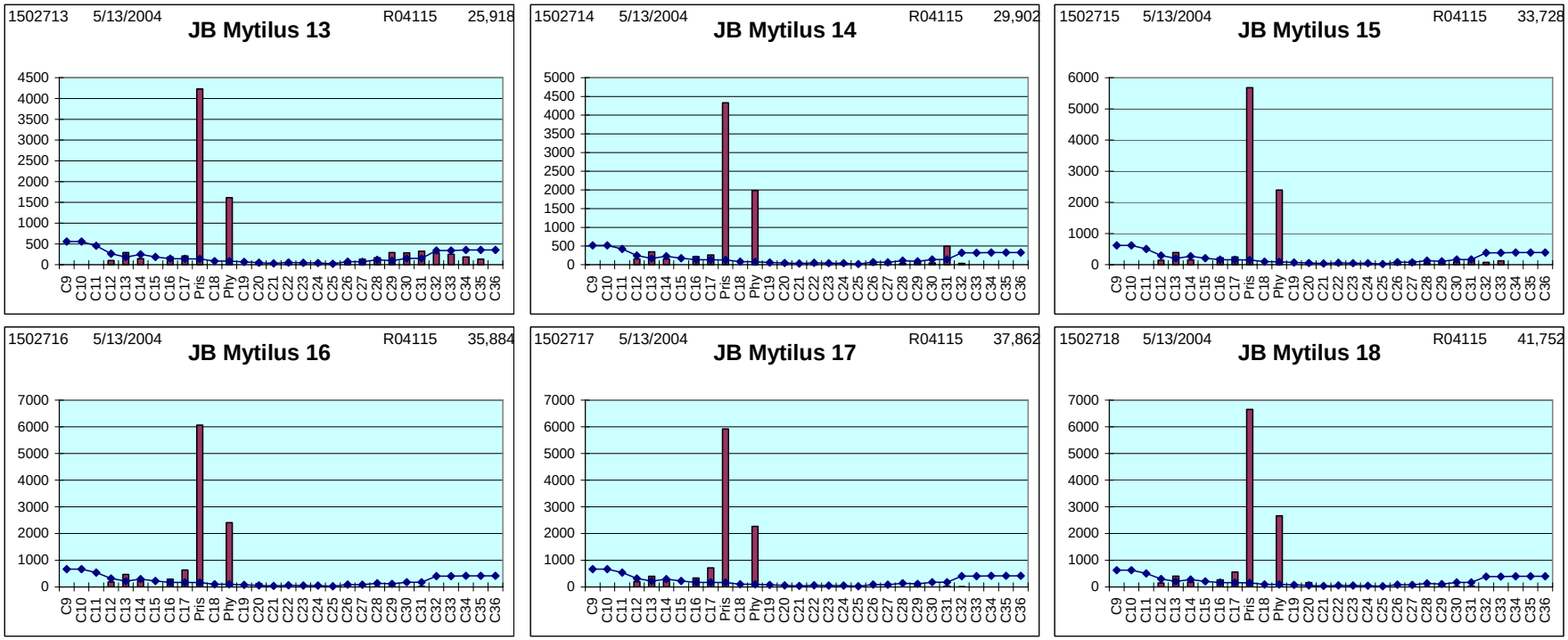

Figure 11. SHC plots of Jack Bay *Mytilus* from segment TGE16 showing microbially degraded diesel signatures, 13 May 2004.

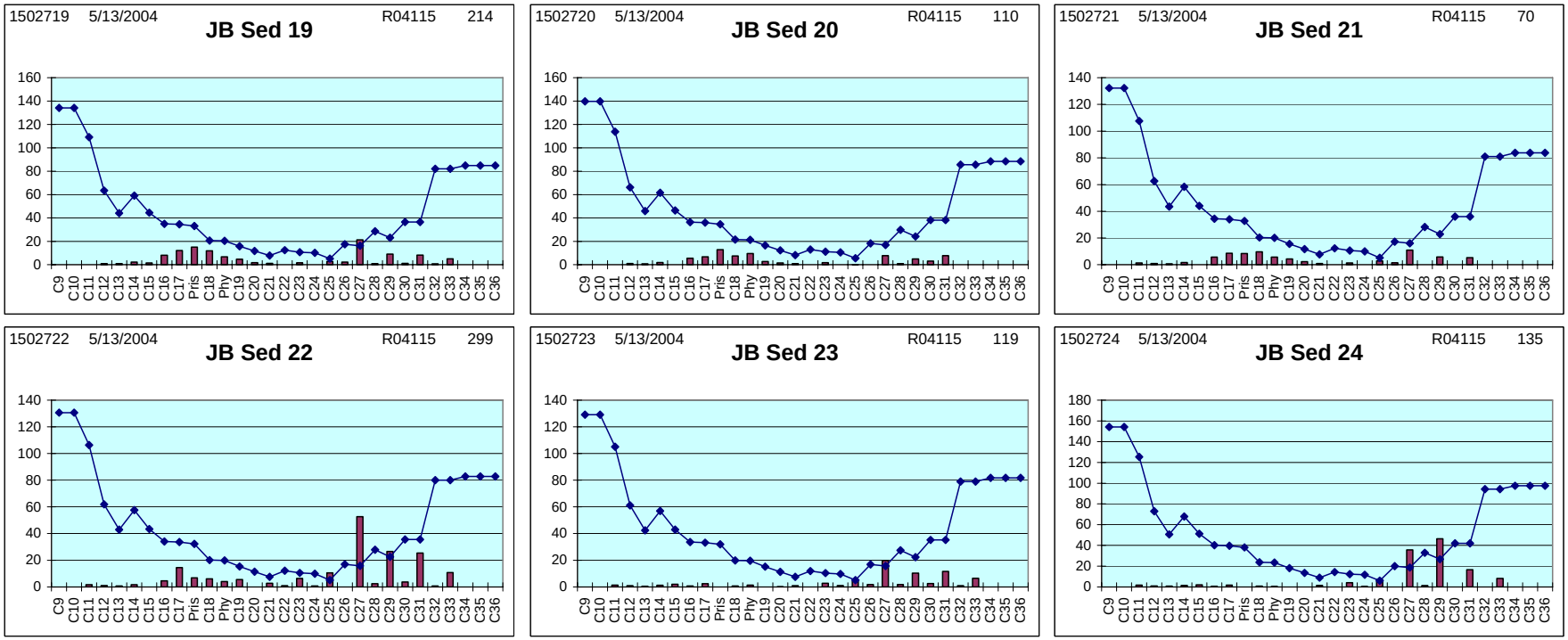

Figure 12 SHC plots of Jack Bay sediments from segment TGE16 showing low-level and partially degraded diesel signatures plus terrestrial plant waxes in the higher intertidal samples (JB Sed 22, JB Sed 23, and JB Sed 24), 13 May 2004.